GENOME-WIDE SCREEN OF GENES THAT REGULATE LIPID DROPLET DYNAMICS IN *SACCHAROMYCES CEREVISIAE*

Identification of Ylr404wp, an Ortholog of Seipin Implicated in Human Congential Generalized Lipodystrophy, As a Regulator of the Morphology of Lipid Droplets

FEI WEIHUA

(*Master of Medicine, Zhejiang University, China*)

HUMBLY

DEDICATED TO

THE GLORY AND HONOR OF

JESUS

Hope deferred makes the heart sick,

But when the desire comes, it is a tree of life.

(Proverbs 13:12)

Acknowledgement

TABLE OF CONTENTS

    Abstracts of two published papers

Summary

Lipid droplets which consist of a highly hydrophobic core of neutral lipids and are surrounded by a monolayer of phospholipids are ubiquitously found in eukaryotic cells. Importantly, changes in cellular dynamics of lipid droplets are associated with many devastating diseases, such as obesity, diabetes, and atherosclerosis. Despite the obvious physiological and pathological importance of lipid droplets, the mechanism underlying the biogenesis of lipid droplets is largely obscure. Several mammalian proteins have been found to have an important role in lipid droplet biosynthesis, but many remain unidentified.

The yeast *Saccharomyces cerevisiae* is a powerful model genetic system, and has proven invaluable to the understanding of many cellular processes, including lipid metabolism. In an effort to identify genes that regulate lipid droplet dynamics, I screened the entire collection of viable single-gene deletion yeast strains, and found 16 mutants with markedly reduced accumulation of lipid droplets and 117 mutants with increased accumulation of lipid droplets. The scope of the functions of identified genes is very broad. The finding that some mutants defective in protein glycosylation or ER-associated degradation displayed elevated synthesis of lipid droplets suggests that a link between ER stress and lipid droplet synthesis likely exists.

A major discovery of this study is that yeast cells accumulate morphologically distinct lipid droplets due to the deletion of *YLR404W*. 3 classes of lipid droplets could be observed in *ylr404w* cells cultured in YPD medium: supersized lipid droplets with a diameter of 0.5 to 1.5 μm, amorphous aggregation of small/intermediate-sized lipid

droplets, loosely scattered and weakly stained tiny lipid droplets with a diameter of less than 0.1 μm. The lipid droplets of *ylr404w* cells demonstrated enhanced fusion both *in vivo* and *in vitro*, suggesting that the formation of supersized lipid droplets is very likely the result of fusion of small lipid droplets.

Sequence homology search, prediction of secondary structure, and expression of human and mouse seipin in *ylr404w* cells indicate that Ylr404wp is an ortholog of seipin. Seipin mutations are implicated in human congenital generalized lipodystrophy, but the mechanism is unknown. In this dissertation, I present that there is a shift from long-chain (18:1) to medium/short-chain (16:0, 14:0, 12:0) in acyl chain pattern of phospholipids in *ylr404w* cells. This result may indicate that aberrant phopholipid metabolism is the unifying theme of lipodystrophy, considering that mutations of AGPAT2 and lipin also lead to lipodystrophy.

This dissertation for the first time presents evidence that Ylr404wp regulates the size and morphology of lipid droplets. In addition, the functional domain of Ylr404wp appears to reside in the ER lumen. Our finding that *YLR404W* deletion results in a shift from long-chain to medium/short-chain fatty acid incorporation into phospholipids should open up new avenues of research into the role of seipin in adipogenesis. It is possible that seipin, AGPAT2, and lipin control adipogenesis through modulation of phospholipid metabolism.

For future studies, whether there is a cause-effect relationship between the phenotypic acyl chain pattern of phospholipids and TAG of *ylr404w* cells and fusion of lipid droplets requires further investigation. Experiments are also needed to establish the role of

Ylr404wp/seipin in metabolism of phospholipids. Moreover, genetic seipin-knockout animal model or cell line is mandatory for understanding the role of seipin in the assembly of lipid droplets and adipogenesis.

List of Tables

List of Figures

Chapter 1

Introduction

Obesity, specifically referring to having an abnormally high proportion of body fat, is now a global public health crisis because of its health complications which include diabetes, heart diseases, stroke, and cancer. Not only developed countries face this exploding health issue, but developing nations also show patterns of emerging obesity as well. In the United States, 17.1% of children and adolescents were overweight (overweight is specifically used for children and adolescents) and 32.2% of adults were obese in 2003-2004; moreover, the prevalence of overweight among children and adolescents and obesity among men increased significantly during the 6-year period from 1999 to 2004 (Ogden et al., 2006). In China, the results of the National Health and Nutrition Examination Survey (NHANES) of year 2002 by Chinese Center for Disease Control and Prevention indicated that 7.1% adults were obese and 8.1% children were overweight (CDC annual report, 2002).

Although how obesity leads to diabetes, heart disease, and cancer at the molecular level is still under intensive study, epidemiological investigations and statistical analysis have unambiguously linked being overweight to increased risk for the above-mentioned diseases. Obesity brings a very heavy financial burden to the citizens and government. United States spends more than $70 billion annually on overweight both in direct health care costs and in indirect costs such as lost productivity (Kopelman, 2000). Therefore obesity study has become increasingly important in biomedical research.

It is known that the deposition of excessive amounts of energy leads to obesity. To be precise, extra energy is stored by mammalian adipocytes mainly as triacylglycerols (TAG) and/or sterol esters (SE) in the form of lipid-rich droplets which we now term *lipid droplets* (LDs) (Mersmann et al., 1975; Traber and Kayden, 1987; Ramirez-Zacarias et al., 1992; Martin and Parton, 2006). As a result, obesity research necessarily involves the study of LDs.

Nevertheless, LD research was largely neglected before the early 1990's. In the past, research of LDs was mainly carried out in the tissues that play a role in lipid storage or transport in animals or plants, such as adipose tissue and liver of animals or seeds and fruits of plants, or microorganisms in response to environment stress. However, as more and more cell types were examined, LDs have been virtually found ubiquitous. Moreover, the importance of LDs as a cellular component has been increasingly recognized. They are no longer reckoned as simple storage compartments; rather LDs have become an emerging cellular organelle widely involved in various physiological and pathophysiological cellular processes.
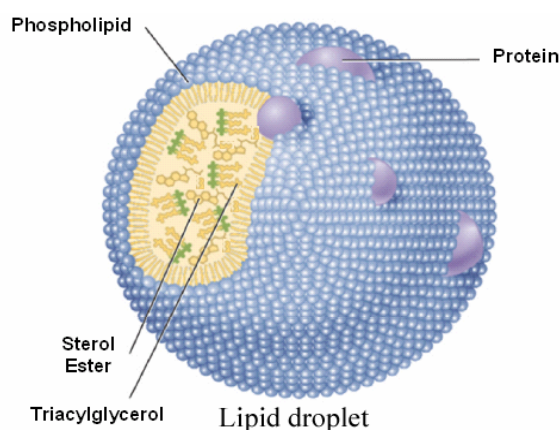
Figure 1-1. Model of LD structure

1.1 The unique structure and general compositions of LDs

LDs consist of a highly hydrophobic core of neutral lipids, mainly TAG and/or SE, and are surrounded by a monolayer of phospholipids with proteins embedded (Murphy and Vance 1999; Zweytick et al., 2000) (Figure 1-1). The structure of LDs is unique in that they are enclosed by a monolayer of phospholipids, which is totally different from other cellular organelles since they are limited by a phospholipid bilayer. In addition, the phospholipid monolayer and the core of LDs have unique compositions as well. Furthermore, LDs have their own characteristic protein compositions. I will present the compositions of the phospholipid monolayer and the contents of the LD core in Section 1.1.1, and discuss the protein compositions of LDs in Section 1.1.2l.

1.1.1 Lipid Compositions of LDs

LDs are covered by a phospholipid monolayer, or a hemi-membrane (Yatsu and Jacks, 1972; Tauchi-Sato et al., 2002). Most, if not all, types of phospholipids, including phosphatidylcholine, phosphatidylethanolamine, phosphatidylinositol, and phosphatidylserine, can be found in the LD phospholipid monolayer. Their relative ratio differs between cells and tissues. For instance, the major phospholipids of the bovine heart LDs are phosphotidylcholine with ~50% and phosphotidylethanolamine with ~40% of total phospholipids (Christiansen and Jensen, 1972). Whereas LDs of the budding yeast *Saccharomyces cerevisiae* contains ~40% phosphatidylcholine, ~20% phosphatidylethanolamine, ~30% phosphatidylinositol, and other phospholipids (Leber et

al., 1994). In HepG2 cells the surface of LDs appears to have a unique property: lysophosphatidylcholine in LDs contains a high proportion of unsaturated acyl chains. In addition, free cholesterol is also contained in the LDs. The content of free cholesterol may vary in different cells, and in adipocytes it was estimated ~30% of the total cellular pool.

The LD core is made of TAG and SE, and their relative ratio is also variable depending on the cell type. For instance, TAG predominates in adipocytes, whereas SE is enriched in steroidogenic cells. In some specialized cells, other esters such as retinyl esters are stored in a large amount (Yamada et al., 1987).

1.1.2 Protein Compositions of LDs

1.1.2.1 Proteins of Mammalian LDs

Recent studies have revealed that dozens of proteins are associated with mammalian LDs and/or are contained in LD-rich fractions. Among them, most studied are PAT proteins, named after perilipin, adipocyte differentiation-related protein (ADRP; also called as adipophilin), and TIP47 (tail-interacting protein of 47 kDa), which share sequence similarities. Perilipin, which is best characterized among the PAT proteins, is a key component of LDs in adipocytes and steroidogenic cells (Blanchette-Mackie et al., 1995; Servetnick et al., 1995). Perilipin knockout studies done by Chan's group (Martinez-Botas et al., 2000) and Londos' group (Tansey et al., 2001) revealed that perilipin null mice were lean, exhibited elevated basal lipolysis and dramatically attenuated catecholamine-stimulated lipolytic activity. These results suggest that on one hand perilipin have a protective function in basal lypolysis, while on the other hand

perilipin are required for stimulated lipolysis. Parallel with these two studies, Clifford et al. (2000) discovered that perilipin and homone-sensitive lipase (HSL) were phosphorylated upon lipolytic stimulation in rat adipocytes and phosphorylated HSL was translocated from the cytosol to the surface of LDs, where it executes lipolysis. Later Sztalryd et al. (2003) and Miyoshi et al. (2006) showed that stimulated lipolysis was dependent on the phosphorylation of perilipin.

ADRP was isolated because of its strong expression in adipose tissue and early induction during adipocyte differentiation (Jiang and Serrero, 1992). Later it was discovered that ADRP is ubiquitously expressed and localizes to LDs (Brasaemle et al., 1997). But its molecular function has not been defined clearly. Gao and Serrero (1999) reported that expressed ADRP in transfected COS-7 cells selectively facilitates uptake of long chain fatty acids. Later, it was found that recombinant histidine-tagged murine ADRP expressed in E. coli is capable of binding fatty acids (Serrero et al., 2000). Taken together, ADRP might function as a fatty acid transporter. However, this is not conclusive.

Chan and colleagues (Chang et al., 2005) showed that in ADRP-null mice uptake of free fatty acids was not compromised. Additionally they reported that adipogenesis was not affected at all in the ADRP-null mice and the LDs in white adipose tissue and brown adipose tissue of mutants and wild type mice were similar in size. However, they discovered that the ADRP-null mice markedly displayed a 60% reduction in hepatic TAG, while maintained a similar rate of VLDL secretion. After further analyzing the TAG content in the hepatic microsomes, they found a twofold increase of microsomal TAG in ADRP$^{-/-}$ mice compared with the wild type. More recently, Magnusson et al. (2006)

reported that overexpression of ADRP increased the accumulation of LDs and reduced the secretion of VLDL, but ADRP RNAi had an opposite effect. These two studies suggest that ADRP may play an important in sorting TAG into storage or secretion.

TIP47, which selectively binds to the cytoplasmic domains of mannose 6-phosphate receptors (MRPs) and is required for MPR transport from endosomes to the *trans*–Golgi network, is 40% identical to the sequence of the mouse ADRP (Diaz and Pfeffer, 1998). Unlike ADRP, the majority of TIP47 is cytosolic when cells are grown in low lipid-containing culture medium, although the presence of TIP47 on the surface of LDs can be detected; upon addition of fatty acids, TIP47 is rapidly recruited to the LDs (Wolins et al., 2000). Currently the role of TIP47 on the surface of LDs is even less defined than ADRP and perilipin.

Other than perilipin, ADRP, and TIP47, several other proteins containing the PAT domain also localize to LDs. Among them are the LSDP1 (Patel et al. 2005) and LSD2 (Gronke et al., 2003) in the insect fat body, S3-12 of the adipocytes (Wolins et al., 2003), and myocardial lipid droplet protein (MLDP, Yamaguchi et al., 2006). The identification of these proteins can eventually help us understand the role of PAT proteins.

Besides PAT proteins, another exciting discovery is the association of caveolin and Rab proteins with the LDs. The caveolins which have three isoforms, caveolin-1 (Cav-1), caveolin-2 (Cav-2), and caveolin-3 (Cav-3), are major proteins of cell surface caveolae (Kurzchalia and Parton, 1999).   In recent years several studies have identified LD as a possible target organelle of caveolins (Pol et al., 2001; Ostermeyer et al., 2001; Fujimoto et al., 2001; Liu et al., 2004; Brasaemle et al., 2004). The association of caveolins with

LDs was first described after the finding that the mutant caveolin protein, Cav-3^{DVG} specifically associated with LDs; subsequently full-length caveolins were also detected in the LDs, particularly when their concentration at the ER is elevated by overexpression (Pol et al., 2001). This discovery leads to speculation that LD can have an important role in lipid trafficking because caveolins have been suggested a role in cholesterol transport (van Meer, 2001).

Unlike caveolin, the association of Rab proteins with LDs was inferred from the proteomic analysis of LD-enriched fraction (Fujimoto et al., 2004; Liu et al., 2004; Umlauf et al., 2004). Among these proteins, the targeting of Rab18 to LDs was confirmed by colocalization studies (Ozeki et al., 2005; Martin et al., 2005). The role of Rab proteins on the LDs has not been defined. One possibility is that they are involved in LD lipolysis, which might also be true for caveolins. The reason for this speculation is that Rab proteins and caveolin-1 which were present in the LD-enriched fraction isolated from lipolytically stimulated 3T3-L1 adipocytes were absent in the LDs under basal condition (Brasaemle et al., 2004).

Besides the above-mentioned proteins, mammalian LDs could harbor many other proteins which were identified by proteomics of LD-rich fractions. However, results from these proteomic studies show a diverse nature of protein compositions of LDs, which is likely to reflect differences between cell types.

1.1.2.2 Proteins of Plant LDs

The protein components of plant LDs (also called oil bodies) have not been studied as

intensively as those of mammalian LDs with the exception of oleosins. Oleosin proteins and genes have been characterized at the biochemical, cellular, molecular levels in numerous desiccation-tolerant plant species (Tzen et al., 1990; Roberts et al., 1993; Millichip et al., 1996; Chen et al., 1997). Oleosins continuously wrap around the LDs of these plants. In addition, plant oleosin is correctly targeted to yeast LDs in transformed yeast strains (Ting et al., 1996). Evidence suggests that the targeting of oleosin to LDs is regulated by the protein's characteristic hydrophobic central domain (Li et al., 1992), and in particular, by a triple-proline knot motif (Abell et al., 1997). It should be noted, however, that oleosins are absent from lipid-rich tissues of fruits and many tropical oilseeds which normally do not undergo desiccation (Murphy, 1993). This suggests that oleosins are unlikely to play a major role in LD biogenesis *per se*.

1.1.2.3 Proteins of Yeast LDs

In the yeast *S. cerevisiae*, proteins associated with LDs are predominantly involved in the synthesis and activation of fatty acids and sterols (Athenstaedt et al., 1999). Among them are Erg1p, Erg6p, and Erg7p (ergosterol biosynthesis), Faa1p, Faa4p, and Fat1p (fatty acid metabolism), and Tgl1p, Tgl3p, and Tgl4p (neutral lipids degradation). A similar result was also found in the yeast *Yarrowia lipolytica* (Athenstaedt et al., 2006). In addition, the same group found that Rab proteins were also detected in the LD-rich fraction when *Y. lipolytica* was grown in oleic acid-supplemented medium to induce LD formation.

In summary, LDs have their own unique lipid and protein compositions, suggesting that LDs are an independent organelle. In addition, their association with proteins of various cell functions implies that LDs are engaged in a variety of cellular activities.

1.2 Intracellular Localization of LDs

Results from electron microscopy studies have indicated that the ER encases the surfaces of LDs to varying degrees (Novikoff et al., 1980; Bozzola and Russell, 1992; Prattes et al., 2000; Martin et al., 2005; Ozeki et al., 2005). Figure 1-2 shows an illustration. This finding is consistent with the result of colocalization studies using fluorescence microscopy which suggests that a portion of LDs accumulate at subcompartments of the ER (Figure 1-3). Taken together, these results lead to speculation that LDs are synthesized by the ER; they may be associated with the ER closely after formation before their eventual detachment.

Other than their intimate relationship with the ER, LDs have also been found to have association with mitochondria (Blanchette-Mackie et al., 1995; Cohen et al., 2004) and peroxisomes (Blanchette-Mackie et al., 1995; Schrader, 2001; Binns et al., 2006). In addition, LDs, the ER, mitochondria, and peroxisomes were found to form constellations in differentiating 3T3-L1 cells, suggesting the interplay of these organelles in lipid metabolism (Novikoff et al., 1980).
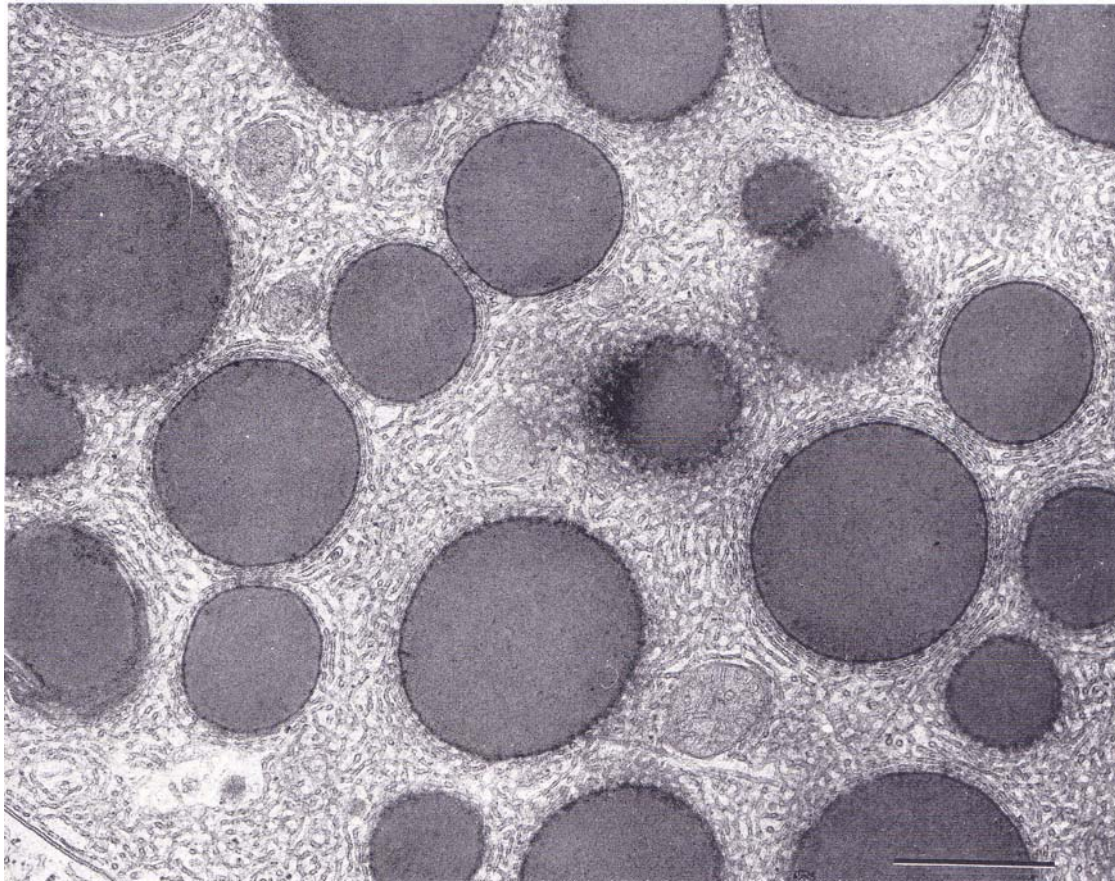
Figure 1-2. LDs are found among smooth ER. Thin membrane cisternae of the smooth ER wrap around the surface of LDs. Bozzola and Russell, Electron microscopy, principles and techniques for biologists, 1992: Jones and Bartlett Publishers, Sudbury, MA. WWW.jbpub.com. Reprinted with permission.
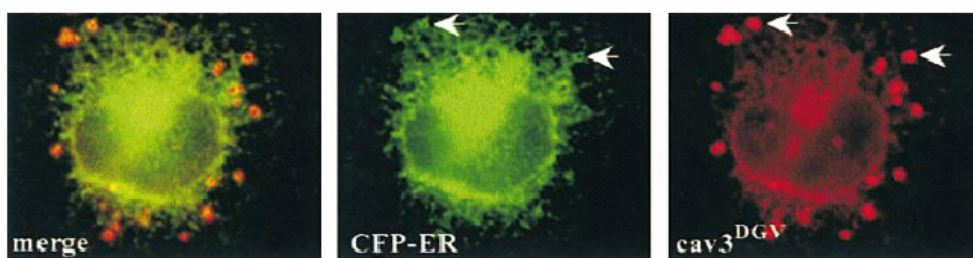
Figure 1-3. Colocalization of LDs and the ER marker (green, middle panel). BHK cells were transfected with an HA-tagged Cav-3 mutant protein which localizes to LDs. LDs were labeled with a mAb to HA tag (right panel). Reproduced from **Journal of Cell Biology**, **2001, 152: 1057-1070**. Copyright 2001, Rockefeller University Press.

1.3 LDs, the emerging cellular organelle

In the past, LDs were regarded only as inert lipid storage depots providing energy

sources and substrates for synthesis of membrane components and some specific lipophilic substances, such as steroid hormone. However, LD studies in the past 10 years have greatly expanded our understanding of this organelle. These studies demonstrate that LDs are associated with many cellular processes, such as immune response, viral diseases, and protein quality control and degradation.

1.3.1 The role of LDs in inflammation and immune response

LDs have a central regulatory role in both innate and acquired immune response (reviewed by Bozza et al., 2007). Increased numbers of LDs in leukocytes and other cells associated with imflammation have been repeatedly reported. In addition, significant correlation between increased LD formation and enhanced LO- and COX-derived eicosanoids has been observed both clinically and experimentally.

Recent studies have also shown that LDs in eosinophils contain arachidonyl-phospholipids and enzymes required to release arachidonic acid from phospholipids, including cytosolic phospholipase A_2 ($cPLA_2$) and mitogen activated protein (MAP) kinase. They also contain all the downstream enzymes needed for eicosanoid synthesis, including lipoxygenase (LO), cyclooxygenase (COX), and leukotriene (LT) C_4 synthase. Moreover, direct evidence has been demonstrated more recently that LDs are the main formation sites of eicosanoid within stimulated leukocytes. Thus LDs function as a key feature of leukocyte activation and a critical regulator of inflammatory disease and become a target for novel anti-inflammatory therapies.

1.3.2 LDs and Hepatitis C virus infection

The Hepatitis C virus is the major causative agent of non-A/non-B hepatitis (Choo et al., 1989). The majority of acutely infected individuals subsequently develop chronic infection; liver cirrhosis and hepatocellular carcinoma are well-recognized late complications of chronic hepatitis C (Saito et al., 1990). HCV is a positive-stranded RNA virus of about 10kb nucleotides. The viral genome encodes a precursor polyprotein of about 3000 amino acids, which is then cleaved into structural and nonstructural proteins. The structural proteins are located at the N-terminal end of the polyprotein and consist of the core protein, which forms the viral capsid, and two envelope glycoproteins, E1 and E2. The nonstructural proteins include NS2, NS3, NS4A, NS4B, NS5A, and NS5B, which are involved in polyprotein processing and viral replication (reviewed by De Francesco, 1999).

The HCV core protein which has a regulatory effect on cellular gene expression and on the viral cycle was detected on the ER membrane and on the surface of LDs as well (Moradpour et al., 1996; Barba et al., 1997), suggesting that LDs may play an important role in HCV infection. Later it was found that a central hydrophobic domain (AA 125-144) is required for its association with LDs (Hope and McLauchlan, 2000) and this motif has sequence similarity with the central hydrophobic domain of plant oleosin and they are interchangeable (Hope et al., 2002). Very recently, three published papers presented evidence that the association of core protein with LDs through this LD binding domain is critical for virus assembly, indicating that LDs are involved in the production of infectious HCV particles. Among them, one discussed that the disruption of the association of HCV core protein with LDs reduces the production of infectious virus (Boulant et al., 2007). Another showed that the central domain of core protein is a major determinant for efficient virus assembly (Shavinskaya et al., 2007). The third paper

provided data that core protein recruits nonstructural proteins and replication complexes to LD-associated ER membranes, and this recruitment is critical for producing infectious particles (Miyanari et al., 2007). Considered together, accumulated evidence undoubtedly points to LDs as an important factor in HCV infection.

1.3.3 The role of LDs in protein storage and degradation

The idea that LDs may serve as a transient storage depot for proteins which are either destined for degradation or for future use when conditions change was inspired by several independent findings that histones were abundant in LDs of early *Drosophila* embryos and that apolipoprotein B (ApoB) accumulated on the surface of LDs in cultured mammalian cells (reviewed by Brasaemle and Hansen, 2006; Fujimoto and Ohsaki, 2006; Welte, 2007).

Early *Drosophila* embryogenesis is characterized by rapid nuclear division which is not accompanied by cell division. Twelve nuclear divisions generate more than 4,000 nuclei, the assembly of which requires quite a number of histone proteins to package thousands of copies of *Drosophila* genome into chromatin. Since histones of early *Drosophila* embryos are derived from maternal histones deposited in oocytes, and from translation of maternal mRNAs, in order to prevent excessive free histones which are potentially toxic from causing harm during early embryogenesis, these histones should be stored somewhere. In a proteomic study of LDs of *Drosophila* embryos, Cermelli et al. (2006) found that abundant histones 2A, 2Av, and 2B (H2A, H2Av, and H2B) were bound to LDs, suggesting that LDs appear to provide a safe haven for embryonic histones. In addition, their finding that the copies of histones on LDs decreased during the first six

hours of embryogenesis further supported this hypothesis.

ApoB, the primary protein of very low-density lipoproteins (VLDL), was found to be highly concentrated around LDs of HuH7 cells, particularly after proteasomal or autophagic inhibition. In addition, ApoB associated with LDs was poly-ubiquinated and surrounded by autophagic vacuoles, suggesting that it is destined for destruction (Ohsaki et al., 2006). Given that ApoB has the propensity to form aggregates in aqueous environment which are considered toxic, its association with LDs suggests that LDs may serve as a temporal storage place.

In addition to histones and ApoB, various other proteins were found to be associated with LDs under certain conditions, such as overproduced HMG-CoA reductase in the fission yeast *Schizosaccharomyces pombe* (Lum and Wright, 1995), the Parkinson's disease protein α-synuclein and the peripheral membrane protein Nir2 after lipid loading (Cole et al., 2002; Litvak et al., 2002), as well as Hsp70 after heat shock (Jiang et al., 2007). These findings indicate that LDs play an active role in protein management.

1.4 Biosynthesis of LDs

The involvement of LDs in cellular processes and diseases helps LDs gain attention. However, little is known about the exact mechanism of LD biogenesis at the molecular level. The pathways and enzymes involved in these pathways leading to the synthesis of TAG and SE, the core components of the LDs, have been largely defined. These data point to ER as the site for the synthesis of LD core components. But LDs are a unique

structure because they are encapsulated by a phospholipid monolayer. It is still unknown how LDs acquire this limiting monolayer.

1.4.1 Biosynthesis of LD Core Components

It has been established that eukaryotic organisms are equipped with several pathways for TAG and SE synthesis. In addition, multiple isoforms of the enzymes in the lipid synthetic pathway catalyze the same chemical reaction. The focus of this section is on the last step of TAG and SE biosynthesis.

In eukaryotic organisms, TAG is primarily synthesized by acylation of diacylglycerol (DAG) via the phosphatidic acid pathway or via the monoacylglycerol pathway, which are both acyl-CoA dependent (Lehner and Kuksis, 1996) although TAG synthesis can also be catalyzed by phospholipid diacylglycerol acyltransferase (Oelkers et al., 2000; Dahlqvist et al., 2000) or diacylglycerol transacylase (Lehner and Kuksis, 1993). Figure 1-4 presents an illustration of the phosphatidic acid pathway and Figure 1-5 the monoacylglycerol pathway.
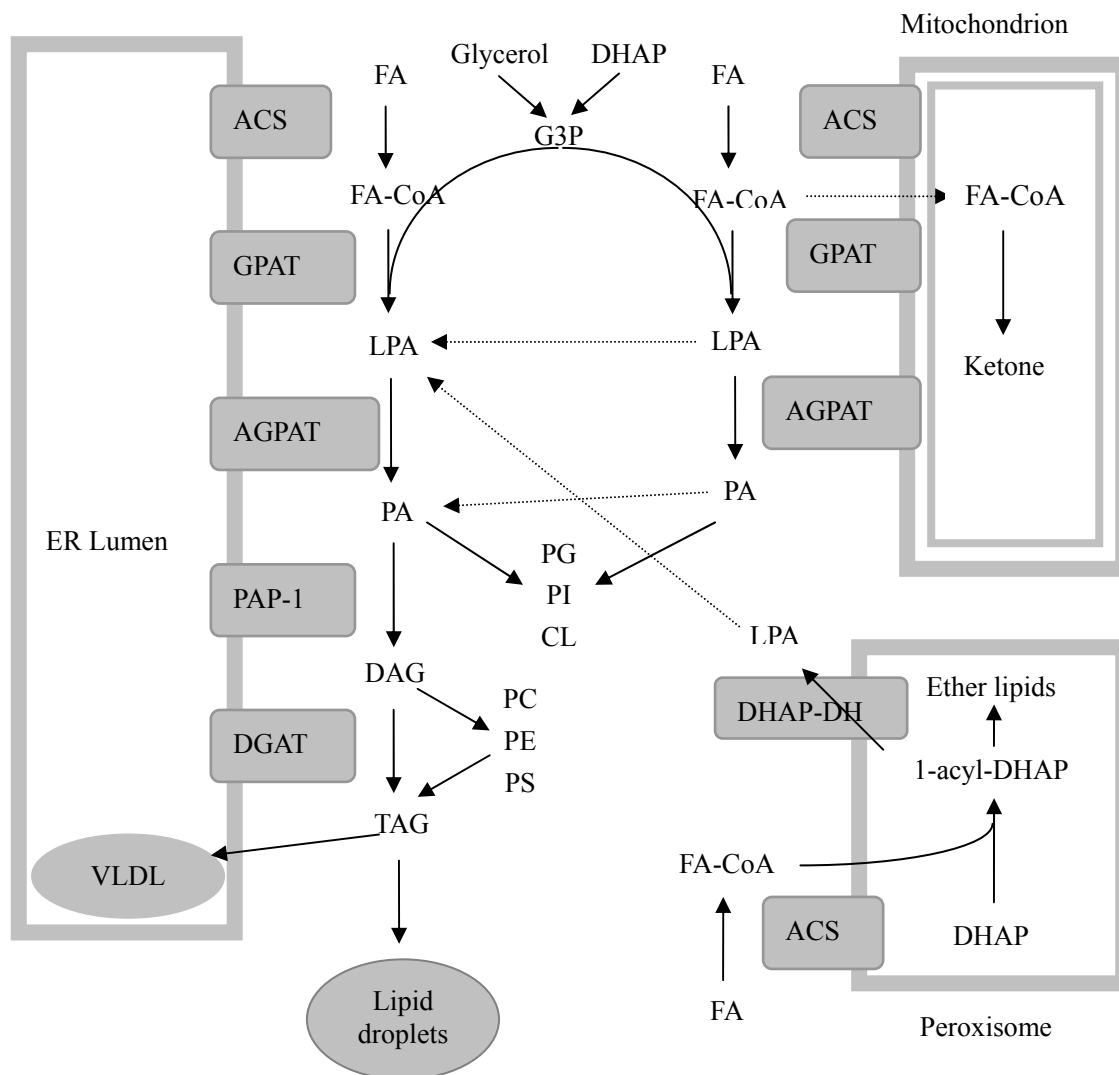
Figure 1-4. TAG biosynthesis in liver via the phosphatidic acid pathway. ACS, acyl-CoA synthetase; AGPAT, acylglycerolphosphate acyltransferase; CL, cardiolipin; DAG, diacylglycerol; DGAT, diacylglycerol acyltransferase; DHAP, dihydroxyacetone phosphate; DHAP-DH, DHAP dehydrogenase; ER, endoplasmic reticulum; FA, fatty acid; G3P, glycerol-3-phosphate; GPAT, glycerol-3-phosphate acyltransferase; LPA, lysophosphatidic acid; PA, phosphatidic acid; PAP, phosphatidic acid phosphatase; PC, phosphatidylcholine; PE, phosphatidylethanolamine; PG, phosphatidylglycerol; PI, phosphatidylinositol; PS, phosphatidylserine; TAG, triacylglycerol; VLDL, very low density lipoprotein. Adapted from Coleman and Lee (2004). Prog Lipid Res. 43, 134-176

   The phosphatidic acid pathway mainly associated with the microsomal fraction represents the *de novo* route to TAG formation. It involves a stepwise acylation of sn-glycerol-3-phosphate or of dihydroxyacetone phosphate to phosphatidic acid. The hydrolysis of the phosphatidic acid results in sn-1,2-diacylglycerol, which is further

acylated to TAG. The monoacylglycerol pathway of TAG biosynthesis forms a major route in enterocytes. 2-monoacylglycerols are derived from the hydrolysis of TAG in the intestinal lumen by pancreatic lipase. Sequential acylation of monoacylglycerol by monoacylglycerol acyltransferase and diacylglycerol acyltransferase (DGAT) ultimately leads to the formation of TAG.
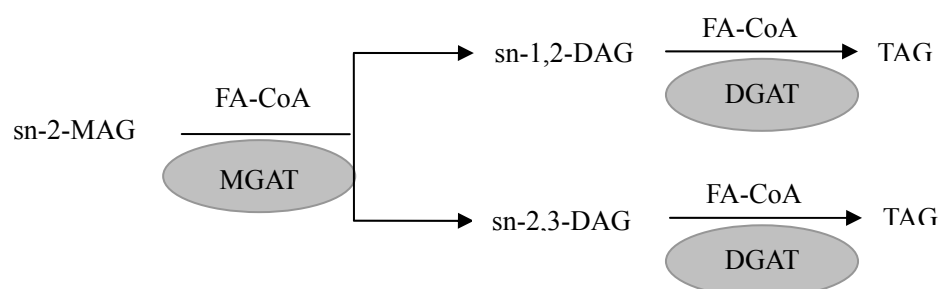
Figure 1-5. TAG biosynthesis via the monoacylglycerol pathway. MAG, monoacylglyccrol; MGAT, monoacylglycerol acyltransferase; DAG, diacylglycerol; DGAT, diacylglycerol acyltransferase; TAG, triacylglycerol.

The terminal step of TAG synthesis is catalyzed by DGAT both in the phosphatidic acid pathway and in the monoacylglycerol pathway as well. DGAT activity predominantly localizes to microsomal subcellular fraction (Coleman and Bell, 1976). Precise identification of DGAT had been hampered by the extreme difficulty in purifying the protein (Lehner and Kuksis, 1996) because it is an integral membrane protein. DGAT1 was cloned based on its homology to acyl-CoA:cholesterol acyltransferase (ACAT) (Cases $et\ al.$, 1998; Oelkers $et\ al.$, 1998). The existence of DGAT2 was anticipated because DGAT1$^{-/-}$ mice have normal plasma TAG levels, store TAG in fat cells, and maintain some DGAT activity in most tissues. When two novel DGAT isoforms without sequence homology to DGAT1 were purified and cloned from the oleaginous

fungus *Mortierella rammaniana* (Lardizabal *et al.*, 2001), the mouse and human homologs were sought. DGAT2 was cloned because of its identity with this fungal DGAT (Cases *et al.*, 2001).

DGAT in *S. cerevisiae* was also characterized through its sequence homology to DGAT2 of *M. rammaniana* (Sorger and Daum, 2001; Oelkers *et al.*, 2002) and the gene was termed *DGA1* corresponding to the yeast ORF *YOR245C*. Unexpectedly, localization studies by Sorger and Daum (2001) suggested that the enzyme activity of Dga1p is mainly localized in the LDs, although the ER is also the localization site. Incorporation assay using C^{14}-labeled DAG and acyl-CoA revealed a 70-90 fold enrichment of DGAT activity in LDs over the homogenenate, but also a 2-3 fold enrichment in microsomal fraction.

Apart from the acylation of DAG, TAG is also synthesized using phospholipids as acyl donor and DAG as acceptor; the reaction is catalyzed by the enzyme called phospholipid diacylglycerol acyltransferase (PDAT) (Dahlqvist *et al.*, 2000; Oelkers *et al.*, 2000). PDAT was unveiled in microsomal preparations from plant oil seeds and its activity was also noticed in yeast microsomes. Sequence homology search revealed that the gene *LRO1* corresponding to ORF *YNR008W* has significant similarity to lecithin cholesterol acyltransferase (LCAT), which transfers an acyl group from phosphatidylcholine to cholesterol.

The formation of SE is catalyzed by the enzymes either from the acyl-CoA cholesterol acyltransferase (ACAT) family or from the lecithin cholesterol acyltransferase (LCAT)

family. ACAT is capable of catalyzing the synthesis of cholesterol esters in the crude rat liver homogenate (Goodman *et al.*, 1964). Subcellular fractionation studies suggested that ACAT enzyme activity resides in the rough ER (Hashimoto and Fogelman, 1980; Reinhart *et al.*, 1987; Lange *et al.*, 1993) and detergent treatment indicated that ACAT is an integral membrane protein (Doolittle and Chang, 1982). However, due to its sparse presence and its susceptibility to inactivation by detergents, little progress had been made towards purifying the enzyme to homogeneity before the cloning and functional expression of ACAT cDNA. Human *ACAT1* gene was cloned by functional complementation of mutant cells lacking ACAT activity (Chang *et al.*, 1993). The cloning and expression of two sterol esterification genes in yeast was also reported and the genes were named *ARE1* and *ARE2*, respectively (Yang *et al.*, 1996). Both genes share strong sequence homology with the human *ACAT1* gene near the C-terminal region.

The discovery of *ACAT2* was preceded by several findings which led to the expectation for a second mammalian cholesterol esterification enzyme (Buhman *et al.*, 2000). Human ACAT2 cDNA was identified through homology search of sequence database and cloned; it has over 40% identity with human ACAT1 (Cases *et al.*, 1998).

Contrary to ACAT which is membrane bound, LCAT is a soluble enzyme. It converts cholesterol and phosphatidylcholines (lecithins) to cholesteryl esters and lysophosphatidylcholines on the surface of HDL, and LCAT, thus, determines the removal of cholesterol from tissues. LCAT was identified as a unique plasma enzyme by Glomset (1962). The gene and cDNA for human LCAT were first cloned and sequenced by Mclean *et al.* (1986). Sequence homology search for LCAT led to the identification of DGAT1

and PDAT, which do not catalyze the formation of cholesteryl esters, but TAG instead. Lro1p in yeast is a member of PDAT family.

The identification of these enzymes and the localization of most of them to the ER (except mammalian LCAT which are cytosolic and yeast Dga1p which also localizes to LDs in addition to the ER) unequivocally show that the ER is the site of TAG and SE synthesis. However, how the synthesized TAG and SE reach their final destination ─the LDs is yet to be elucidated. Currently there are several models hypothesized for this process. These models will be briefly introduced in the next section.

1.4.2 Models of the Biogenesis of LD

The prevailing model of LD biogenesis is budding of nascent LDs from the ER (Murphy and Vance, 1999). Figure 1-6 shows this model for LD formation. In this model, neutral lipids are synthesized between the two leaflets of the ER bilayer. Subsequently the mature LD buds from the cytoplasmic leaflet of the
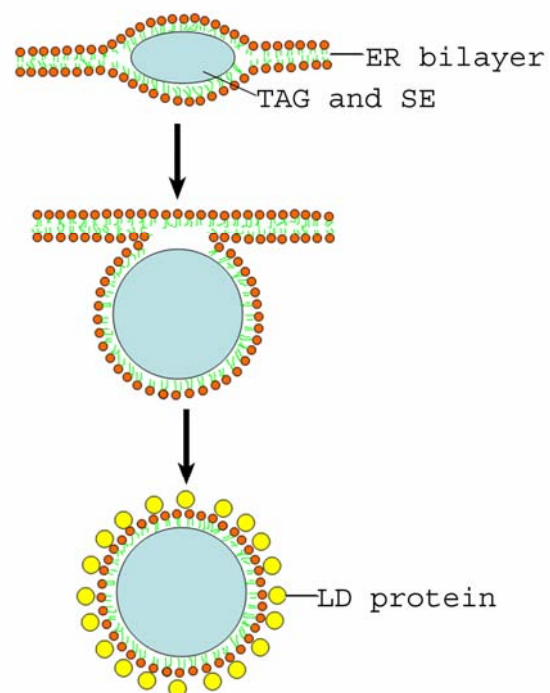
Figure 1-6. The budding model of LD formation. According to this model, neutral lipids are synthesized between the leaflets of the ER. The mature LD is speculated to subsequently bud off from the cytoplasmic leaflet of the ER membrane to form an organelle which is bound by a limiting monolayer of phospholipids and LD-associated proteins.

ER membrane to form an organelle which is contained within a limiting monolayer of phospholipids and associated LD proteins. Although this model is widely accepted, it is more hypothetical than based on firm evidence. To date, neutral lipids accumulation has never been observed within the leaflets of the ER bilayer. Blanchette-Mackie *et al.* (1995) claimed that they observed sites of continuity between membrane surface of LDs and the outer membrane leaflet of ER using freeze-fracture electron microscopy, the resolution of their image, however, is not sufficient to make this argument stand firm.
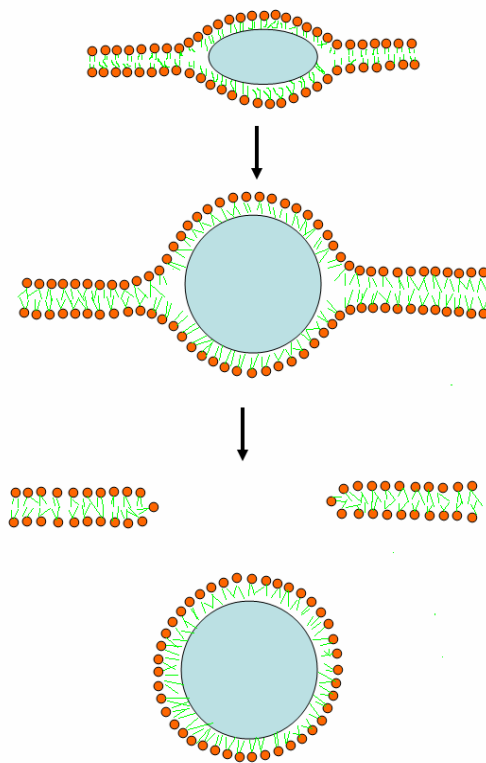
Figure 1-7. An alternative budding model according to Ploegh. Neutral lipids are also synthesized between the leaflets of the ER. But unlike the first model, a portion of phospholipids monolayer is taken from the ER luminal leaflets, together with its inserted proteins.

More recently, Ploegh proposed an alternative budding model (2007). Based on the presence of Bip and Calnexin in isolated LD fraction, he considered that LD formation involves the formation of transient bicellar structures, created by fusion of the luminal and cytoplasmic leaflets of the ER membrane (Figure 1-7). However, the presence of

Calnexin and Bip could be an isolation artifact, particularly in view of the propensity of the ER enwrap LDs, although he argued that the absence of other abundant ER-resident proteins might rule out this possibility.

Besides, it is noteworthy to mention that a "delivery" model was proposed by Robenek *et al.* (2006) based on results obtained through freeze-fracture electron microscopy. This model is shown in Figure 1-8. Based on this model, LDs closely appose to domains of the cytoplasmic leaflet of the ER membrane, where lipids and proteins are delivered from the ER membrane to the LDs. This model takes the spatial relations of the ER and LDs into consideration and may account for the enlargement and maturation of LDs, but it fails to explain how the nascent LDs are generated.
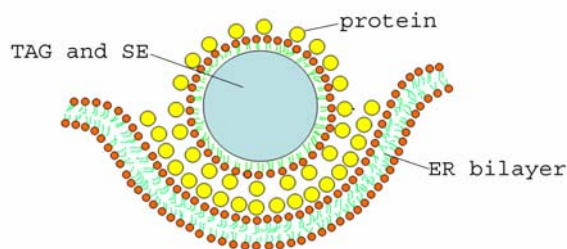
Figure 1-8. The delivery model of LD formation. According to this model, LDs closely appose to the cytoplasmic leaflet of the ER membrane. Neutral lipids and phospholipids are synthesized at the ER and transferred from the ER to the nascent LDs. This process may occur in specialized domains of the ER.

In addition to the aforesaid three models, another hypothesis for LD biogenesis is the post-encasement model (Zweytick *et al.*, 2000). Based on ultrastructural studies of developing seeds of mustard (Bergfeld *et al.*, 1978) and crambe (Smith, 1974), this model proposes that LD may arise from a membranous matrix contained within the cytoplasm.

Lipids released naked from the ER form droplets in the cytoplasm and subsequently associate with proteins synthesized by free ribosomes (Stobart *et al.*, 1986). Apparently this model does not explain clearly the formation of surface phospholipid monolayer.

At present, none of these models can be definitely confirmed. Many questions remain to be answered. Thus concerted effort is needed in order to determine how LDs are generated by the ER.

1.5 The search for factors that affect LD biogenesis

Attempts have been made in the past 10 years to identify factors that affect LD biogenesis. Neutral lipids synthesis has been identified as an essential determinant in LD formation. In addition, quite a number of proteins are actively involved in LD synthesis.

1.5.1 No neutral lipids, no LDs

The core of LDs consists of TAG and/or SE. As previously stated, TAG synthesis in yeast is primarily catalyzed by Dga1p and Lro1p, and SE synthesis by Are1p and Are2p. Reduced LD formation was observed in yeast cells deficient in TAG synthesis due to deletion of *DGA1* and *LRO1* genes (Oelkers et al., 2002), and also in cells deficient in SE synthesis due to mutation in *ARE1* and *ARE2* genes (Yang et al., 1996). Moreover, yeast cells in which all the four genes implicated in neutral lipids synthesis were knocked out could no longer synthesize LDs (Oelkers et al., 2002; Sandager et al., 2002). These data

show that impaired neutral lipids synthesis affects the synthesis of cytoplasmic LDs. When neutral lipids synthesis is completely disrupted, no LD formation occurs. This indicates that neutral lipids synthesis is essential for LD formation.

1.5.2 The role of LD-associated proteins in LD biosynthesis

1.5.2.1 PAT proteins and fat packaging

Based on the nature of their association with LDs, PAT proteins can be divided into two classes: those that constitutively associate with LDs, such as perilipin and ADRP (class 1); and those that move from the cytosol to coat nascent LDs during rapid LD synthesis, such as TIP47, S3-12, and MLDP (class 2). An emerging concept is that class 1 proteins control access of metabolic enzymes to stored neutral lipids, thereby regulating lipolysis, while class 2 proteins sequester newly synthesized neutral lipids and facilitate their delivery to mature LDs (Wolins et al., 2006).

The hydrophobicity of neutral lipids such as TAG and SE necessitates elaborate mechanisms to emulsify these molecules before their transport between aqueous compartments of organisms. Consistent with this purpose, an elongated helix formed by 11-mer repeats was identified in many LD binding proteins, including perilipin, ADRP, TIP47, S3-12, as well as apolipoproteins (Bussell and Eliezer, 2004). It was proposed that the 11-mer repeats form unusual right-handed helices with 3 turns per repeat, thereby generating a TAG miscible face and a water miscible face. Notably, approximately two-thirds of the amino acid sequence of the 160 kDa S3−12 consists of these 11-mer repeats.

Furthermore, TIP47, S3-12, and MLDP also contain a 4-helix bundle (Hickenbottom et al., 2003). This domain has significant structure similarity to an amphipathic 4-helix bundle present in exchangeable apolipoprotein apoE which allows apoE to coat the lipoprotein surface in TAG-rich lipoproteins and to release from the particle as TAG is hydrolyzed and the lipoprotein particle shrinks. Given that class 2 PAT proteins primarily associate with LDs during rapid LD synthesis, this structure similarity suggests that they and apoE function in a similar manner. Consistent with the structure prediction, Wollins et al. (2005) found that under basal condition, all of the TAG is in large, centrally located perilipin-coated LDs and class 2 PAT proteins are cytosolic. However, when adipocytes are cultured in the presence of long-chain fatty acid, within 10 min, small LDs emerge that are uniform in size and have a uniform coat composed of TIP47, S3-12, and ADRP. Over the next hour of long-chain fatty acid treatment, TIP47 and S3–12 are concentrated on the smallest, most peripheral LDs. ADRP is concentrated on LDs intermediate in size and location between the smaller, peripheral TIP47/S3–12 coated LDs and the large, central perilipin coated LDs. When long-chain fatty acid is removed from the adipocyte media, adipocytes return readily over 30–180 min to their homeostatic LD architecture, with S3–12 in the cytosol and all of the TAG packaged in perilipin-coated LDs.

1.5.2.2 Caveolin and LD synthesis

Following the finding that caveolins associate with LDs under some experimental conditions, Pol et al. (2004) went on to examine whether this association has physiological relevance. In their study, caveolin-1 and caveolin-2 redistributed from

plasma membrane and/or Golgi apparatus to LDs in A431 and FRT cells upon lipid loading. In addition, removal of oleic acid from the culture medium rapidly reversed the redistribution, suggesting a bidirectional caveolin trafficking pathway. Strikingly, during the first hours of liver regeneration after partial hepatectomy, caveolins show a dramatic redistribution from cell surface to newly synthesized LDs. At later stages of liver regeneration, the level of caveolins in LDs suddenly decreased, even when LDs were still abundant. More strikingly, residual hepatocytes after partial hepatectomy in caveolin-1 gene-disrupted mice (cav1$^{-/-}$) failed to accumulate LDs and cell divisions stalled, which led to impaired liver regeneration and low survival. Given that during liver regeneration fatty acids released by adipocytes are taken up by hepatocytes where they are esterified and stored as TAG in large LDs before ultimately being metabolized (Farrell, 2004), the function of caveolins may be mainly to transport fatty acids for its deposition into LDs as TAG.

1.5.2.3 Phospholipase D and LD formation

Phospholipase D (PLD) catalyzes the hydrolysis of membrane glycerophospholipids to form phosphatidic acid (PA). Mammalian PLD exists in two isoforms, PLD1 and PLD2. PLD1 uses phosphatidylcholine as substrate. PLD1 is regulated by phosphatidylinositol-4,5-bisphosphate, protein kinase C and ADP Ribosylation Factor (ARF) and Rho family GTPases (Jenkins and Frohman, 2005). In a recent study, ADRP was shown to interact with ARF1, preferentially in the GDP-bound form, and evidence suggested that GDP-bound ARF1 induces dissociation of ADRP from the LD surface

(Nakamura et al., 2004). More recently, it was found that oleic acid-induced LD formation in NIH3T3 cells was accompanied by an increase in PLD activity; the activation of PLD1 appeared to be ARF1-dependent since Brefeldin A suppressed both PLD activation and LD formation in oleic acid-treated cells. In addition, co-existence of PLD1 with ADRP and Arf1 in LD-enriched subcellular fractions prepared from oleic acid-treated cells was observed in this study (Nakamura et al., 2005). In another study, PLD1 overexpression induced TAG synthesis and LD formation, whereas PLD1 siRNA inhibited oleic acid-induced LD formation (Andersson et al., 2006). Based on these studies, PLD1 is suggested to have an important role in LD biosynthesis. However, PLD1 may not be essential for LD formation. A yeast strain *spo14* in which the yeast PLD1 gene *SPO14* was removed from the chromosome still synthesizes a significant number of LDs (our unpublished data).

In summary, a number of LD-associated proteins have been shown to be implicated in neutral lipids synthesis and LD formation. Besides the above-mentioned proteins, there are also prp19 (Cho et al., 2007), and Fat specific protein 27 (Puri et al., 2007). Given that energy storage and metabolism is a highly orchestrated event, we hypothesize that more genes and their protein products are required to modulate LD dynamics, including their synthesis and degradation. For instance, *snf2* mutant lacking Snf2p, the catalytic subunit of the SWI/SNF chromatin remodeling complex displayed hyperaccumulation of LDs (Kamisaka et al., 2006), indicating that transcriptional regulation plays a critical role in LD synthesis. To identify these genes and protein products, more effort is needed.

1.6 *Saccharomyces cerevisiae* as a model to study LD biosynthesis

The budding yeast *Saccharomyces cerevisiae* is a unicellular eukaryotic microorganism. It is extremely important as a model organism in modern cell biology research, and is one of the most thoroughly studied eukaryotic microorganisms. It is easy to culture, and being a eukaryote, it shares the complex internal cell structure of plants and animals. Therefore, it becomes a very important tool for developing basic knowledge about the function and organization of eukaryotic cell genetics and physiology. Over the past several decades, *S. cerevisiae* has been used for studying mechanisms underlying many cellular activities, such as cell cycle, vesicular trafficking, ribosome biogenesis, and so on.

S. cerevisiae is the first eukaryotic genome that is completely sequenced (Goffeau et al., 1996). Based on that, a whole collection of gene deletion strains have been constructed (Winzeler et al., 1999). With this advancement, it is more convenient to use *S. cerevisiae* as a tool to identify genes and proteins involved in a specific cellular activity, particularly when "reverse genetics" is employed.

The budding yeast *S. cerevisiae*, like other eukaryotic organisms, synthesizes cytosolic LDs as well. LDs can be found in this unicellular eukaryote throughout the life cycle. Proliferation of LDs can be observed when cells enter stationary phase, or when cells are limited to nitrogen supply (Willison and Johnston, 1985), or when the culture media are supplemented with free fatty acids such as oleic acid (Binns et al., 2006).

Yeast LDs share many common features with the animal and plant LDs. First, yeast LDs also consist of a hydrophobic core of neutral lipids encircled by a monolayer of amphipathic phospholipids with a specific population of proteins associated with the phospholipid monolayer. Second, lipid biosynthesis enzymes essential for the formation of neutral lipids are closely associated with the ER in yeast cells as in animals and plants. Thus it is reasonable to imagine that the mechanism of LD biogenesis in yeast should have some degree of similarity with that of animal and plant cells. In this study, we used *S. cerevisiae* as a tool to identify novel gene products that may play a role in LD formation by screening ~4700 single deletion mutants for abnormalities in the number and morphology of LDs.

Chapter 2

Materials and Methods

2.1 Reagents and antibodies

Reagents:

From *Amersham Biosciences*: [4-^{14}C]cholesterol, Ficoll^{TM} PM400, and [9,10(n)-^{3}H]oleic acid.

From *BD*: peptone, tryptone, yeast extract, and yeast nitrogen base (without amino acids).

From *BDH*: PMSF, and potassium chloride.

From *Bio 101*: yeast nitrogen base (without ammonium sulfate, amino acids and dextrose).

From *BioRad*: dithiothreitol, Bradford protein assay reagent, sodium dodecyl sulfate, sucrose, Tween 20, Triton X-100, urea, and X-Gal.

From *Duchefa*: EDTA.

From *Electron Microscopy Sciences*: 25% (v/v) glutaraldehyde and 4% (w/v) osmium tetroxide.

From *J.T.Baker*: Tris (Base).

From *Merck*: acetic acid, chloroform, diethyl ether, hexane, potassium acetate (KAcO), and sodium hydroxide.

From *Invitrogen*: BODIPY 493/503, DiOC6$_{(3)}$, rhodamine phalloidin; and MS-compatible silver stain kit.

From *Sigma*: adenine, all the essential amino acid components, ampicilin, aprotinin, ATP, Brefeldin A, Brij58, BSA, creatine phosphate, creatine phosphate kinase, cycloheximide, 1,2-dioctanoyl-sn-glycerol (DAG), DMSO, doxycycline, formaldehyde, galactose, glucose, GMP-PNP, GTP, GTP-γ-S-Li$_4$, HEPES, IPTG, latrunculin A, lithium acetate, lyticase, magnesium acetate (MgAcO), manganese chloride tetrahydrate, mannitol, Nile red, nocodazole, NP-40, oleic acid, oleoyl coenzyme A, pepstatin A , polyethylene glycol, raffinose, sodium azide, sodium fluoride, sorbitol, trichloroacetic acid, tunicamycin, tyloxapol, and uracil.

From *US Biological*: zymolase 20T.

Antibodies:

From *Biorad*: Goat anti-rabbit IgG (H+L)-HRP conjugate and goat anti-mouse IgG (H+L)-HRP conjugate.

From *Molecular probes*: anti-Dpm1 mouse monoclonal, anti-GFP rabbit polyclonal, anti-tubulin mouse monoclonal, and rhodamine-conjugated goat anti-mouse antibodies.

From *Santa Cruz Biotechnology*: anti-GST Mouse Monoclonal

Anti-Vti1 rabbit polyclonal was a gift from Dr Wanjin Hong, Institute of molecular and cell biology, Singapore (Coe et al., 1999).

2.2 Strains

Wild type BY4741 and a collection of approximately 4700 haploid saccharomyces

cerevisiae deletion strains developed by the Saccharomyces Genome Deletion Project (Winzeler *et al.*, 1999) is available at EUROSCARF (<u>EURO</u>pean <u>S</u>accharomyces <u>C</u>erevisiae <u>AR</u>chives for <u>F</u>unctional analysis) collection center (http://web.uni-frankfurt.de/fb15/mikro/euroscarf/). The collection was made by polymerase chain reaction-mediated start- to stop- codon disruption of each of the open reading frames (ORFs) larger than 100 codons in the BY4741 wild-type strain. The genotype of the wide-type strain is: *MATa his3Δ1 leu2Δ0 met15Δ0 ura3Δ0*. Because 18.7% of the genes are essential for growth on rich media, only non-essential genes are represented in this collection.

In addition, w303 (MATa *leu2-3,112 trp1-1 can1-100 ura3-1 ade2-1 his3-11,15*) and

its derivative *are1Δare2Δdga1Δlro1Δ*

(*are1Δ*::HIS3*are2Δ*::LEU2*dga1Δ*::URA3*lro1Δ*::URA3) were also used in this study.

The *E. Coli* DH5α strain used for plasmid construction was purchased from *Invitrogen*. The BL21 strain used for protein expression was also from *Invitrogen*.

2.3 Culture and media

Unless otherwise stated yeast cells were grown with rotary shaking at 30°C in liquid YPD medium (1% yeast extract, 2% bacto peptone, 2% dextrose). Alternatively, cells were grown in synthetic complete medium (0.67% nitrogen base, 2% dextrose with all amino acids supplemented), or in YPO medium (1% yeast extract, 2% bacto peptone, 0.1% oleic acid in 1% Brij58), or in YPDO medium (1% yeast extract, 2% bacto peptone,

2% dextrose, 0.1% oleic acid in 1% Brij58). Plasmid-carrying strains were grown on synthetic medium with appropriate selection as described by Kaiser et al. (1994). Cell growth was monitored by OD_{600} of yeast in suspension.

Bacteria were grown in LB medium (Ausubel et al., 2005) at 37°C.

2.4 Fluorescence microscopy

Fluorescence imaging was performed on a Leica DMLB microscope (Wetzlar, Germany) with a Curtis ebq 100 fluorescent lamp. Samples were viewed using a ×100/1.30 oil immersion objective lens. Images were taken with a DFC480 digital camera and a Leica FW4000 software.

LD staining— Nile red (Sigma) is a specific and excellent vital dye for intracellular LDs. Because Nile red has broad excitation and emission fluorescence spectra, one of the following two UV-filter sets was used in this study based on the resolution. First, a 436/7-nm bandpass excitation filter, a 455-nm dichromatic mirror, and a 470-nm longpass emission filter (Leica filter cube E4); second, a 450-490-nm bandpass excitation filter, a 510 dichromatic mirror, and a 515-nm longpass emission filter (Leica filter cube I3).

To record the process of LD fusion in the *ylr404w* mutant, 3 μl of mid-log phase cells (OD_{600}~1.5) stained with Nile red were spotted on a slide and covered with a coverslip. Under the microscope, cells in which two or several LDs lay close together were selected. Images were collected at a one-second interval until the fusion process completed. The

images were edited with Macromedia Flash MX 2004 into movie format.

Actin staining— Actin staining by Rhodamine-conjugated phalloidin was done according to the procedure described previously by Pringle et al. (1989). Briefly, cells were fixed with 3.7% formaldehyde for 1 h, washed for three times and resuspended in PBS, and stained with Rhodamine phalloidin for 1 h. Cells were washed for another three times, resuspended in PBS and processed with fluorescence microscopy. Rhodamine fluorescence was visualized with a 515-560-nm bandpass excitation filter, a 580-nm dichromatic mirror, and a 590-nm long-pass emission filter (Leica filter cube N2.1).

Microtubule staining— Tubulin-containing structures were visualized by indirect immunofluorescence as described previously (Adams and Pringle, 1984) except that 50 U/ml lyticase was used instead of Glusulase. Essentially, Microtubules were labeled with mouse α-tubulin mAbs and visualized using rhodamine-conjugated goat α-mouse antibodies.

Green fluorescence protein— GFP signal was visualized with a 470/40-nm bandpass excitation filter, a 500-nm dichromatic mirror, and a 525/50-nm bandpass emission filter (Leica filter cube GFP).

DAPI staining of nucleus— Cells fixed with 3.7% formaldehyde for 15 min were stained with 5 µg/ml DAPI. DAPI fluorescence was observed with a 340-380-nm

bandpass excitation filter, a 400-nm dichromatic mirror, and a 425-nm longpass emission filter (Leica filter cube A).

2.5 Lipid analysis

Neutral lipids analysis

Lipid extraction— Lipid extraction from lyophilized yeast cells was done as previously described (Zhang et al., 2003). Briefly, cells were grown in appropriate medium until required growth phase (determined by OD_{600}), harvested, washed twice with 0.5% Nonidet P-40, once with dH2O, and lyophilized. The dried cell pellets were resuspended in 50μl of lyticase (Sigma) solution (1700 units/ml in 10% glycerol) and incubated at 37°C for 15 min, at -70°C for 1 h and at 37°C for 15 min. Lipids were extracted with hexane, blown dry and kept for further characterization.

Thin layer chromatography— Quantitation of neutral lipids was as described by Zweytick et al. (2000) with modifications. Samples were dissolved in 100 μl of chloroform/methanol (2:1, v/v) and applied to Silica gel 60 F_{254} plates (Merck) and chromatograms were developed in hexane:diethyl ether:acetic acid (85:15:1) with triolein and cholesteryl ester as the standard. For quantitation of SE and TAG, plates were dipped into methanolic $MnCl_2$ solution (0.63g $MnCl_2·4H_2O$, 60mL water, 60mL methanol and 4mL concentrated sulfuric acid), dried and heated at 120°C for 15 min. Densitometric scanning was performed at 500nm with a CAMAG TLC scanner. For each assay, at least

three independent tests were done; average and standard deviation were calculated.

Oleic acid incorporation— The in vivo assay of incorporation of [^{3}H]oleic acid into SE and TAG was done as described previously (Zhang et al., 2003). 5mL of cells at OD_{600}~0.6-0.8 were pulsed with 5µCi of [^{3}H]oleic acid at 30°C for 30 min with shaking. Lipid extraction and TLC were done as mentioned above except that the plates were stained with iodine vapor. Incorporation of label into neutral lipids was determined after scintillation counting (Beckman) and normalization to a [^{14}C]cholesterol internal standard and cell dry weight. For each assay, at least three independent tests were done; average and standard deviation were calculated.

Phospholipids and fatty acyl profile analysis

Lipid extraction— Extraction of total lipids was done essentially as described elsewhere (Bligh and Dyer, 1959). Briefly, cell pellets were resuspended in 900 µL of ice clod chlorofom:methanol (1:2) and incubated under vacuum with shaking at 900 RPM inside a 4°C cold dark room. Then 400 µL of ice-cold water and 300 µL of chloroform were added, mixed, and centrifuged at 12000rpm for 3 min at 4°C. After the lower organic phase was collected, 50 µL of 1M HCl and 500 µL of chloroform were added to the aqueous phase for a second lipid extraction. The lower organice phase was collected and combined with the first extract. The combined lipid extract was dried.

Analysis of lipids using high performance liquid chromatography/mass

spectrometry — An Agilent high performance liquid chromatography (HPLC) system coupled with an Applied Biosystem Triple Quadrupole/Ion Trap mass spectrometer (4000Qtrap) was used for quantification of individual lipids. Samples were introduced into the mass spectrometer by loop injections with chloroform:methanol:300mM piperidine (1:1:0.1) as a mobile phase at a flow of $200\mu L.min^{-1}$ (Shui et al., 2007). Based on product ion and precursor ion analysis of head groups and fatty aclys, two comprehensive sets of multiple reaction monitoring (MRM) transitions were set up for quantitative analysis of various lipids (Guan et al., 2006), and results are expressed as normalized intensities.

Fatty acyl profiles of polar lipids were acquired using a Waters Micromass Q-Tof micro mass spectrometer in the negative electrospray ionization (ESI) ion mode. Piperidine (final concentration 15 µM) was added into lipid extracts to enhance ionization. Samples were infused into the mass spectrometer at a flow rate of $15\mu L.min^{-1}$. High collision energy (state how much) was applied to fragment polar lipid parent ions to generate fatty acyl profiles. The operation parameters for mass spectrometer are: sample cone temperature, 250°C; sample cone voltage, 70 V; collision energy, 55 V. Mass spectra were recorded from m/z 140 to 900.

Calculation of Lipid Levels — Precursor ion (PIS) or neutral loss (NL) scans of phospholipids headgroup fragments (Han et al, 2005) were used to obtain information on yeast phospholipid compositions. Based on this information, a comprehensive list of multiple reaction monitoring (MRM) transitions was next setup to follow fatty acyl

compositions of these lipids (parent _fatty acyl fragment transitions). The signal intensity of each MRM value was normalized using Eqn (1).

$$\text{Normalized intensity of lipid 1} = \frac{\textit{Signal intensity of lipid 1}}{\sum \textit{Signal intensity of all MRM transition measured}} \qquad (1)$$

Fatty acyl profiles of neutral lipids were analyzed using a sensitive HPLC/ESI/MS method. Briefly, separation of TAG from polar lipids was carried out on an Agilent Zorbax Eclipse XDB-C18 column (i.d. 4.6X150mm). HPLC conditions were (1) chloroform:Methanol:0.1M NH$_4$OAc (100:100:4) as a mobile phase at a flow rate of 0.25 mL. min^{-1}; (2) column temperature: 30°C; (3) injection volume: 30 μL. An Applied Biosystem Triple Quadrupole/Ion Trap mass spectrometer (3200Qtrap) was used to record mass spectra in both positive and negative ESI modes in enhanced MS (EMS) scan mode. Turbo spray source voltage, 5000 and -4500 volts for positive and negative, respectively; source temperature, 250 °C. A total run time of 30 min was utilized to elute both polar lipids and TAGs. Selective ion monitoring (SIM) was used to record major TAGs and phospholipids and intensities of individual TAG ions were normalized to total polar lipids for comparison.

2.6 Yeast genetic manipulations

S. Cerevisiae gene sequence and genome information could be retrieved from NCBI or from Yeast Genome Database (http://www.yeastgenome.org/). Standard DNA manipulations were performed according to Ausubel et al. (2003). DNA fragments were

purified from agarose gel using GFX Gel Band Purification kit (Amersham Biosciences).

DNA sequencing was done by standard method (Sanger et al., 1977) to check some of the

constructions. DH5α cells were transformed according to the manufacturer's instruction.

Transformation of yeast using lithium acetate was done as described by Gietz and Woods

(2002).

Vectors used for subcloning are shown in Figure 2-1.
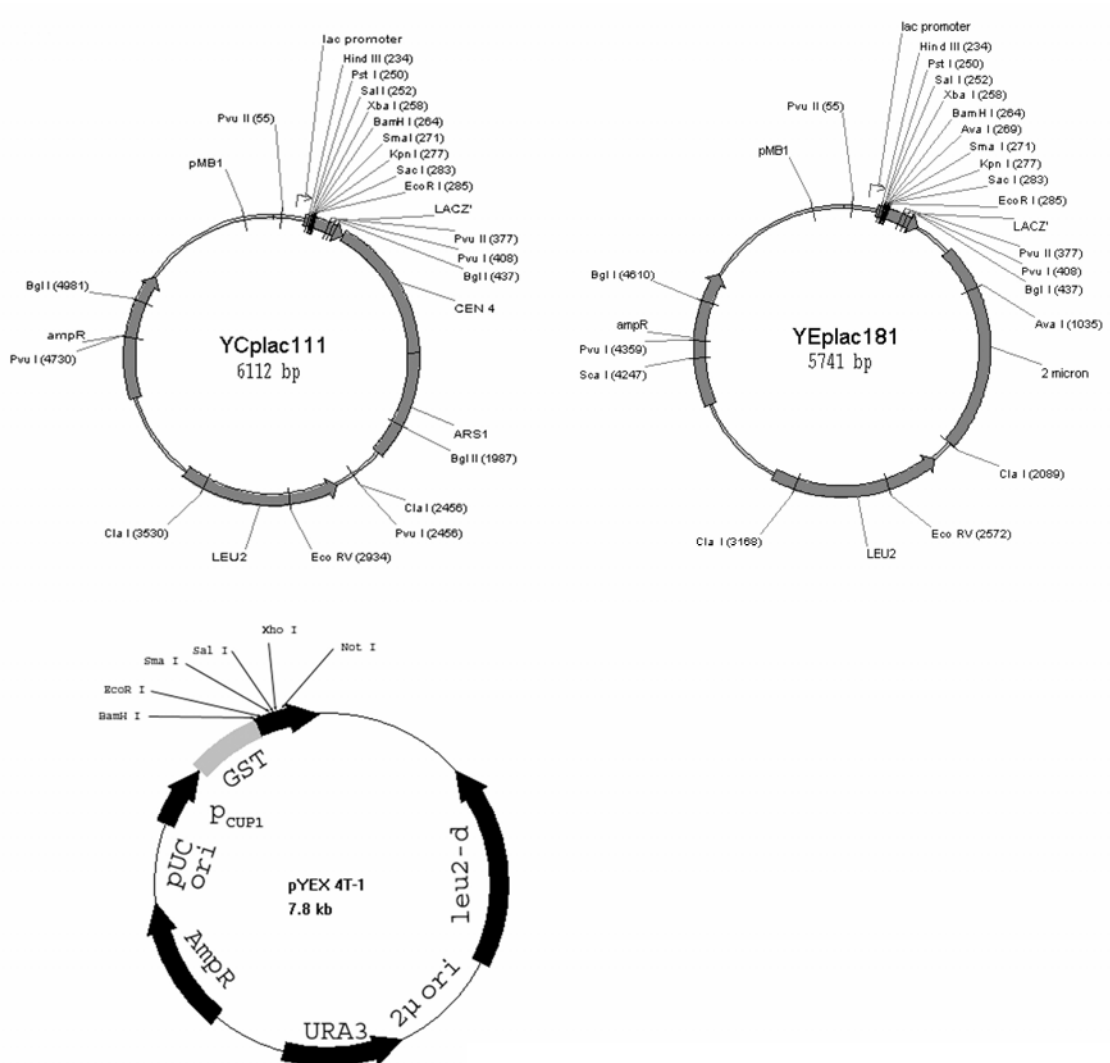
Figure 2-1. Diagrams of vectors used for subcloning.

Construction of a vector expressing GFP-tagged YLR404wp: A 1.4 Kb fragment

containing the natural promoter and the coding sequence before the stop codon of *YLR404W* was amplified by PCR, using a 5' primer, 5'-*HindIII*-TTACCATGCACGTTGTCG, and a 3' primer, 5'-*BamHI*-GCTATGTTTCTTGGATT. This fragment was then subcloned into the *HindIII*- and *BamHI*-cleaved YCplac111-GFP plasmid in which the GFP coding sequence was inserted between the *BamHI* and *EcoRI* restriction sites.

Construction of GST-tagged Ylr404wp overexpression vector: An 858-bp fragment containing the coding sequence of *YLR404W* was amplified by PCR, using a 5' primer, 5'-*BamHI*-ATGAAAATCAATGTATCC, and a 3' primer, 5'-*EcoRI*-TCAGCTATGTTTCTTGG. The fragment was then subcloned into the *BamHI*- and *EcoRI*-cleaved pYEX 4T-1 plasmid.

Construction of Ylr404wp protein segments: DNA sequences that code for Ylr404wp1-253, Ylr404wp1-274, Ylr404wp12-285, and Ylr404wp37-285 were amplified by PCR, using primers containing *BamHI* and *EcoRI* restriction sites added to the 5' and the 3' end of these fragments. The PCR products were then subcloned into the *BamHI* and *EcoRI* cleaved pYEX 4T-1 plasmid.

Construction of a vector expressing GFP-tagged Tgl3p: A 2.7 Kb fragment containing the natural promoter and the coding sequence before the stop codon of *TGL3* was amplified by PCR, using a 5' primer, 5'ACGGC-*HindIII*-TCTGTT, and a 3' primer,

5'-*BamHI*-CCTACTCCGTCTTGCTCTT. This fragment was then subcloned into the *HindIII*- and *BamHI*-cleaved YCplac111-GFP plasmid in which the GFP coding sequence was inserted between the *BamHI* and *EcoRI* restriction sites.

Construction of vectors expressing GFP-tagged seipins: The coding sequences of human seipin and mouse seipin were amplified by PCR, using a 5' primer, 5'-*SphI*-ATGGTCAACGACCCTCCAGTACCTGC, and a 3' primer, 5'-*BamHI*-GGAACTAGAGCAGGTGGGGCGCTGTC from human cDNA BC009866 or BC012140; a 5' primer, 5'-*SphI*- ATGTCTACAGAAAAGGTAGACCAAAAGG, and a 3' primer, 5'-*BamHI*- GGAACTAGAGCAGGTGGGGCGCTGTC from human cDNA AF052149; a 5' primer, 5'-*SphI*- ATGATACATCAAAGAAGAGAAGCTGG, and a 3' primer, 5'-*XbaI*- GGAACTGGAGCAGGTCGGGCGTTGC from mouse cDNA BC061689. The fragments were subcloned into *SphI*- and *BamHI*- cleaved or SphI- and XbaI- cleaved YCplac111-MET3-GFP plasmid in which the MET3 promoter was inserted between *HindIII*- and *SphI*- restriction sites and the GFP coding sequence inserted between the *BamHI*- and *EcoRI*- sites.

Gene deletions: PCR-based gene deletion strategy was as described by Baudin et al. (1993). The *IRE1* gene in the *anp1*, *mnn10*, *mnn11*, *pmr1*, and *doa10* strains were replaced by a HIS3 marker amplified from pFA6-His3MX6 with primers containing flanking sequences for the genes of interest. The primers are shown in Table 2-1.

Table 2-1. Primers used to replace *IRE1* by HIS3 marker amplified from pFA6-His3MX6. Letters in bold are the flanking sequences.

gene		primers
IRE1	5'	**CTCCATATCACCCTTCATACACATTAAAAAAACAGCATATCTGAGGAAT TAATA**CGTACGCTGCAGGTCGAC
	3'	**GGTTACTACTAATGATCAAAGTAACATTAATGCAATAATCAACCAAGAA GAAGA**TCGATGAATTCGAGCTCG

Site-directed mutagenesis: Site-directed mutagenesis was performed using a Stratagene Quickchange II XL kit according to the manufacturer's instruction.

Table 2-2. Primer sequence used for reverse transcription PCR to determine the mRNA levels of *ARE1*, *ARE2*, *DGA1*, and *LRO1*. *ACT1* serves as a loading control.

Gene		Sequence
ARE1	forward	5'TACGTGTTCGCATGGATGTT
	reverse	5'ACCCAGTCCACTTCCAGTTG
ARE2	forward	5'TCATCCCAGGAACTGCTACC
	reverse	5'GTGACCACCGTTTCTGAGGT
DGA1	forward	5'AGCGTTTGCAACAGAAGGTT
	reverse	5'CAAATGCAAACACAGGCACT
LRO1	forward	5'AGTGAAAATTTTGCCGTTGG
	reverse	5'TGCACGTAGCGTAAAGTTCG
ACT1	forward	5'TGTCACCAACTGGGACGATA
	reverse	5'AACCAGCGTAAATTGGAACG

RNA isolation and RT-PCR— Total RNA was extracted using the RNeazy kit (Qiagen). On-column Dnase digestion (Qiagen) was done for all RNA samples. RNA concentrations were determined by measuring absorbance at 260 nm and 280 nm. RNA purity and integrity was assessed by gel electrophoresis. RT-PCR was performed using an Access RT-PCR kit (Promega). 1 μg total RNA for each sample was used in a 50 μl system. Both ribosomal RNA and ACT1 which encodes yeast actin were used as loading controls. Primers are shown in Table 2-2. PCRs were performed for 25 cycles. 10 μl final products were used to run gel electrophoresis and the intensity of the bands under the UV

light was compared. 25-cycle PCR was still in the exponential phase, because for all samples the intensity of the PCR product after 30-cycle amplification was significantly stronger than that after 25-cycle amplification.

2.7 Antibody preparation and protein immunoblotting

Preparation of antisera: Antibodies against Are1p and Lro1p were raised by immunizing the rabbits with GST-fused Are1p-12-190 and Lro1p-440-661 corresponding to the 179 near N-terminal amino acids of Are1p and 222 C-terminal amino acids of Lro1p, respectively. DNA sequence encoding Are1p-12-190 was amplified by PCR using a 5' primer, 5'-*BamHI*-GTAGATCCCTGAAAAGTTC, and a 3' primer, 5' -*XhoI*-GAGTTTCTTAAGATCCGC. DNA sequence encoding Lro1p-440-661 was amplified by PCR using 5'-*BamHI*-ACTGACACATACGGCAAT, and 5' -*XhoI*-TCAATGTCGGTCATT. Both segments were inserted into *BamHI*- and *XhoI*- cleaved pGEX 4T-1 vector (Figure 2-2). GST-fused peptides were expressed in the BL21 bacteria strain.

Protein immunoblotting: Bradford protein assay (Bradford, 1976) was performed with 1-20 μl samples in a microtiter plate using Bio-Rad protein assay reagent. BSA was used as a protein standard. SDS-PAGE was performed according to Laemmli (1970) using 10% or 8% acrylamide. Electrophoresed proteins were visualized by staining with Coomassie blue (Ausubel et al., 2005). For immunoblotting, electrophoresed proteins were transferred to nitrocellulose filters as previously described (Towbin et al., 1979).

Filters were blocked and antibody incubations were performed with 5% nonfat dry milk in 20 mM Tris·Cl, pH7.4, 150 mM NaCl (TBS) with 0.05% Tween 20. Detection of filter-bound antibodies was performed using the ECL detection system (Pierce).

2.8 Subcellular fractionation and Isolation of organelles

Preparation of spheroplasts— Spheroplasts from yeast cells were prepared according to Daum et al. (1982). Cells were harvested by centrifugation at 3,000g for 5 min, washed once with ddH$_2$O, suspended to 0.5g, wet weight/ml in 0.1M Tris·Cl, PH9.4, 10mM DTT, and incubated at 30°C for 10min. Afterwards they were washed once with 1.2M sorbitol and suspended in 1.2M sorbitol, 20mM K$_3$PO$_4$, PH7.4, to 0.15g, wet weight/ml. Zymolase 20T was added to 2mg/g wet weight cells. The suspension was incubated at 30°C with gentle shaking for 30 to 60 min. Conversion of spheroplasts was checked as described (Schatz and Kovac, 1974). Spheroplasts were harvested by centrifugation for 5min at 1,500g, washed twice with 1.2M sorbitol, and suspended in appropriate buffer for homogenization.

Isolation of LDs— LDs were purified as described by Leber et al. (1994) with modifications. Briefly, spheroplasts were suspended 0.15 g/ml in *breaking buffer* (10mM Tris·Cl, PH6.9, 0.2 mM EDTA, 12% (w/w) Ficoll 400) and chilled on ice. Protease inhibitors were added in buffers as such: 1 mM PMSF, 2 μg/ml aprotinin, 0.5 μg/ml leupeptine, 1 μg/ml pepstatin A. Spheroplasts were homogenized with a Dounce

homogenizer applying 10-20 strokes using a loose fitting pistil and the homogenate was transferred into 13.5 ml Ultra clear centrifuge tubes (Beckman) and overlaid with an equal volume of breaking buffer. Centrifugation was performed for 60 min at 28 000 rpm in an SW-41 swing bucket rotor (Beckman). A floating layer which consists mainly of lipid droplets and vacuoles was collected and suspended gently in breaking buffer using a Dounce homogenizer with a loose fitting pistil. The suspension was again transferred into 13.5 ml Ultra clear tubes, overlaid with an equal volume of 10mM Tris·Cl, PH7.4, 0.2mM EDTA, 8% (w/w) Ficoll 400, and centrifuged as described above. The floating layer was recovered, suspended gently in 10 mM Tris·Cl, 0.2 mM EDTA, 0.6 M sorbitol, 8% (w/w) Ficoll 400 in 13.5 ml Ultra clear tubes, and overlaid with 10 mM Tris·Cl, 0.2 mM EDTA, 0.25 M sorbitol. After centrifugation at 28 000 rpm for 30 min, the floating layer consists of highly enriched lipid droplets separated from vacuoles.

To solubilize LD-associated proteins, isolated LDs were mixed with 1 vol of 10% SDS and incubated for 1 h at 37°C in a sonicating water bath. During the incubation, samples were removed every 10 min and agitated on a vortex mixer before returning to the bath. Then samples were centrifuged for 10 min at 15 000g, room temperature. The infranatant containing the solubilized proteins beneath the floating lipid layer was collected (Ausubel et al., 2003).

To extract lipids, isolated LD-rich fractions were mixed with 10 vol of hexane. The mixtures were vigorously agitated on a vortex mixer for 5 min. After centrifugation at 2,000 g for 5 min, the organic supernatant was collected and hexane was blown dry.

Fractionation of whole cell extract－ To fractionate whole cell extract, a continuous sucrose density gradient fractionation procedure was used as described (Kolling and Hollenberg, 1994) except that only 13 fractions were taken from top to bottom. Briefly, cells were lysed in STED10 (10% w/w sucrose, 10 mM Tris PH7.4, 1 mM EDTA, 1 mM DTT) using a glass-bead beater, and spun at 500 g for 5 min to remove cell debris. 950 μl of cleared cell extracted was loaded onto a sucrose density prepared as such: In 13 ml SW41 centrifuge tubes 3.8 ml of STED53 (53% sucrose), STED35 (35% sucrose) and STED20 (20% sucrose) were loaded on top of each other. Centrifugation was performed at 30,000 rpm for 13-17 h for membranes to reach their equilibrium density. 950 μl fractions were collected from the top of gradient. Dpm1p was used as the ER marker.

Preparation of lipid droplet-free cytosol－ The strain *are1Δare2Δdga1Δlro1Δ* which is deficient in neutral lipids synthesis, hence devoid of lipid droplets, was used to prepare lipid droplet-free cytosol. Cytosol was prepared by differential centrifugation principally as described by Allan and Balch (2005). Spheroplasts were suspended 0.15 g/ml in *lysis buffer*, and homogenized with a Dounce homogenizer. After the homogenate was centrifuged at 1,500 g for 5 min, the supernatant was further clarified by centrifugation at 27,000 g for 10 min and at 150,000 g for 90 min at 4ºC.

2.9 Transmission electron microscopy

Cell cultures were centrifuged at 2,000 g for 3 min to pellet the cells. Subsequently

cells were fixed with 2·5% (v/v) glutaraldehyde (Electron Microscopy Sciences) and postfixed with 2% (w/v) osmium tetroxide (Electron Microscopy Sciences). Samples were further dehydrated in an ethanol series and embedded in Spurr's Resin. 80-nm ultrathin sections were stained with uranyl acetate and lead citrate and examined under a JEM-1230 Joel electron microscope.

Chapter 3

Biochemical characterization of LD synthesis

As mentioned in Chapter 1, LD is ubiquitously found in eukaryotic cells. The only known eukaryotic cell type that does not contain cellular LDs is the *are1Δare2Δdga1Δlro1Δ* yeast strain in which all the four enzymes catalyzing the synthesis of neutral lipids, i.e., Are1p, Are2p, Dga1p, and Lro1p, were deleted (Sandager et al., 2002). Given that our understanding of the mechanism underlying LD biogenesis is rather limited, it has not been determined whether other factors besides neutral lipids synthesis are essential for LD formation. In this chapter, evidence is presented that cytoskeleton and ER-to-Golgi transport are not required for LD synthesis. More intriguingly, energy poisons do not block LD formation either.

3.1 Biosynthesis of LDs does not necessarily require cytoskeleton

In NIH 3T3 cells, newly formed LDs were observed to form complexes with one another, and this process is microtubule-dependent (Bostrom et al., 2005). In *Drosophila*, controlled transport and distribution of LDs requires the perilipin homolog LSD2, which is a regulator of microtubule motor activity (Welte et al., 2005). These data might suggest microtubule play a role in LD maturation and trafficking, however, whether microtubule is required in LD biogenesis is not conclusive. In this study, nocodazole was used to disrupt the microtubule structure (Jacobs et al., 1988) and the disruption was confirmed by visualization of tubulin-containing structure (Adams and Pringle, 1984). As shown in

Figure 3-1C, after 1 h incubation in the presence of 15 μg/ml nocodazole, microtubules

were disassembled completely, whereas the microtubule structure remained intact in the
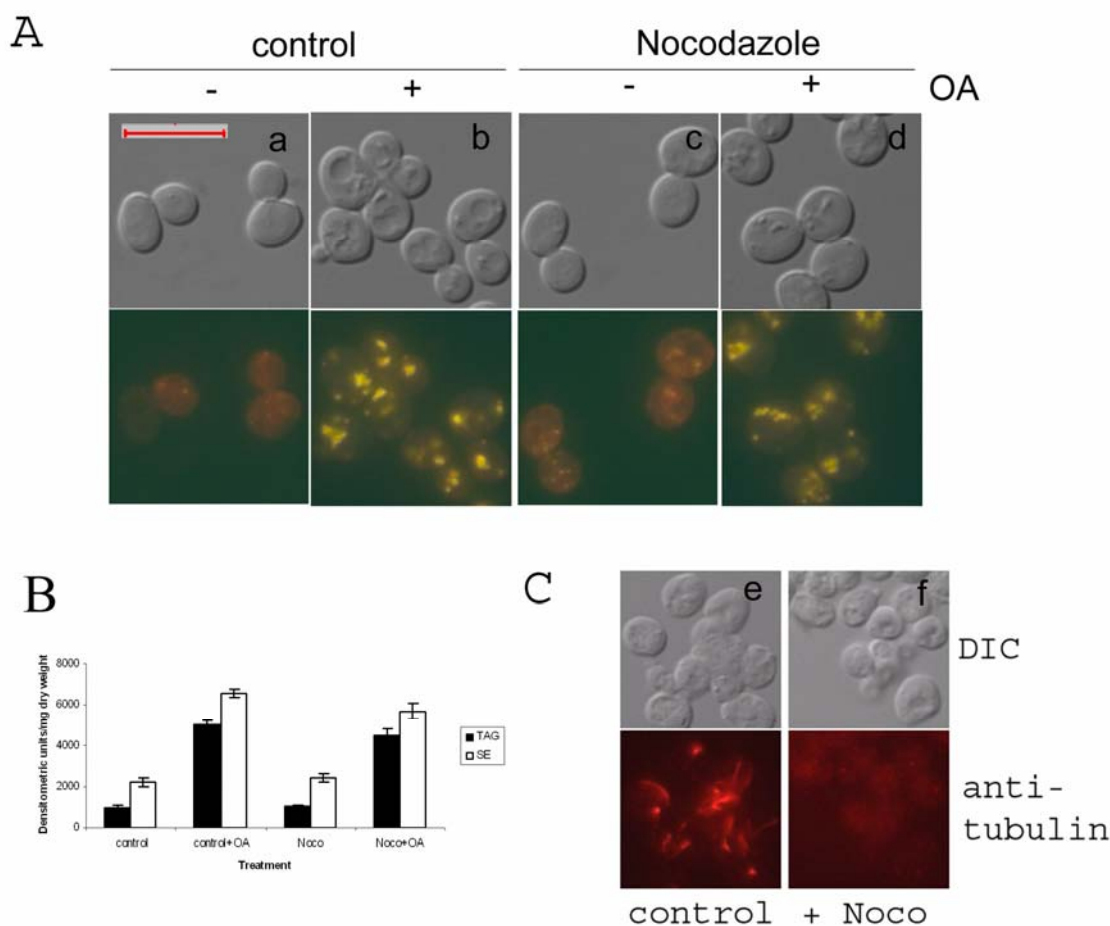
Figure 3-1. LD biogenesis does not depend on microtubule. Cells were refreshed in YPD and grown for ~6 h at 30°C till OD_{600} ~0.5. Subsequently cells were treated with 15 μg/ml nocodazole (c&d) or an equivalent volume of DMSO (control, a&b). After 1 h incubation, cells were either harvested (a&c) or treated with 0.5 mM oleate for another 1 h (b&d). Fluorescence microscopy and lipid analysis were performed afterwards. A. Nile red staining of LDs. Bar, 10 μm. B. Quantitation of intracellular TAG and SE. C. Indirect antitubulin immunofluorescence micrograph of cells fixed after 1 h of incubation in medium containing DMSO (e) or DMSO plus nocodazole (f). OA, oleate; Noco, nocodazole.

control group. Subsequently the cells were treated with 0.5 mM oleate for 1 h. Similar to

the control group, cells pretreated with nocodazole increased LD synthesis as well (Figure

3-1A). Neutral lipids quantitation revealed that TAG and SE synthesis was only slightly

affected after the disassembly of microtubule, about 10% less than the control group

(Fgiure 3-1B).

Similarly, Latrunculin A was used to disrupt the F-actin (Ayscough et al., 1997) and
the disruption was confirmed by rhodamine phalloidin staining (Pringle et al., 1989).
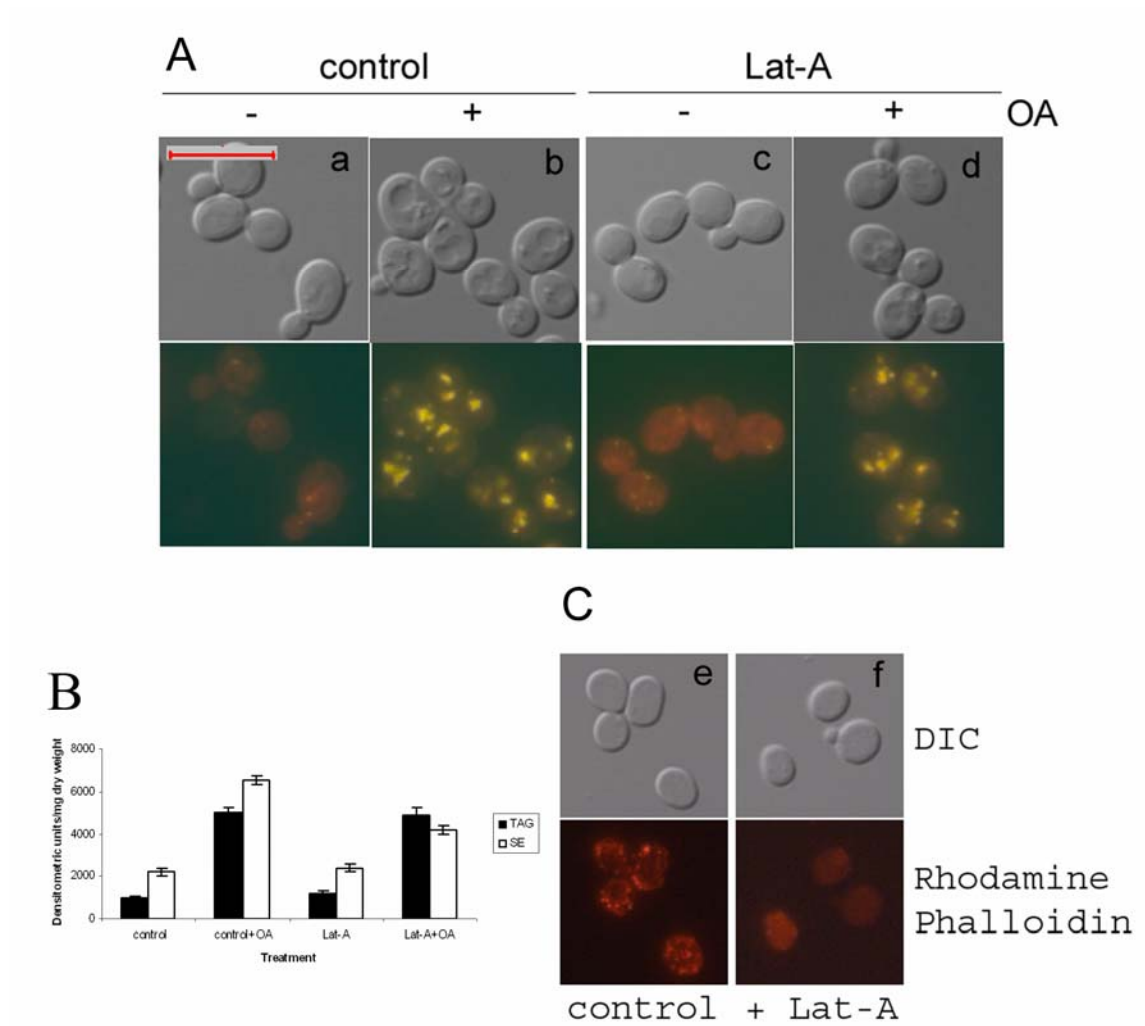
Figure 3-2. LD biogenesis does not require F-actin. Cells were refreshed in YPD and grown for ~6
h at 30°C till OD$_{600}$ ~0.5. Subsequently cells were treated with 100 μM Latrunculin A (c&d) or an
equivalent volume of DMSO (control, a&b). After 1 h incubation, cells were either harvested (a&c) or
treated with 0.5 mM oleate for another 1 h (b&d). Fluorescence microscopy and lipid analysis were
performed afterwards. A. Nile red staining of LDs. Bar, 10 μm. B. Quantitation of intracellular TAG and
SE. C. Rhodamine phalloidin staining of cells fixed after 1 h of incubation in medium containing
DMSO (e) or DMSO plus Latrunculin A (f). OA, oleate; Lat-A, Latrunculin A.

After 1-h treatment with Lat-A, the actin patch disappeared (Figure 3-2C). Then the cells
were incubated in the presence of 0.5 mM oleate for 1 h, followed by microscopic

examination and lipid analysis. After the disruption of actin, lipid analysis revealed that oleate-induced TAG synthesis was at the same level as the control group while SE synthesis was moderately affected, i.e., about 30% reduced (Figure 3-2B), and the formation of LDs was not greatly affected (Figure 3-2A). The data above show that the deposition of TAG and SE into LDs does not require cytoskeleton.

3.2 ER-to-Golgi transport is not essential in LD biogenesis

Generation of a vesicle from a precursor membrane constitutes the initial step of vesicular trafficking, followed by transport of the vesicle to its destination, and finally the fusion of the vesicle with the target compartment. COPII-coated vesicles mediate the export of newly synthesized protein from the ER. In the budding yeast, COPII vesicles are assembled on the surface of the ER by sequential binding of Sar1p GTPase which is activated by Sec12p guanidine nucleotide exchange factor, followed by the Sec23/24p complex and Sec13/31p complex (Barlowe, 2002). The loss of function of any of these proteins blocks the exit of secretory protein from the ER (Nakano and Muramatsu, 1989; Kaiser and Schekman, 1990; Hicke et al., 2002; Salama et al., 1997). After vesicles are synthesized, they are transported to the targeted compartment, eventually dock at the target compartment and fuse with it. The docking of vesicles at the target compartment and the fusion of apposing membranes are mediated by SNAREs (Hong, 2005). NSF and α-SNAP are essential regulators of the SNAREs. Sec18p in yeast is a mammalian NSF ortholog, the loss of function of which results in an inability of the vesicles to fuse with the target membrane (Kaiser and Schekman, 1990). Whether ER-to-Golgi transport is
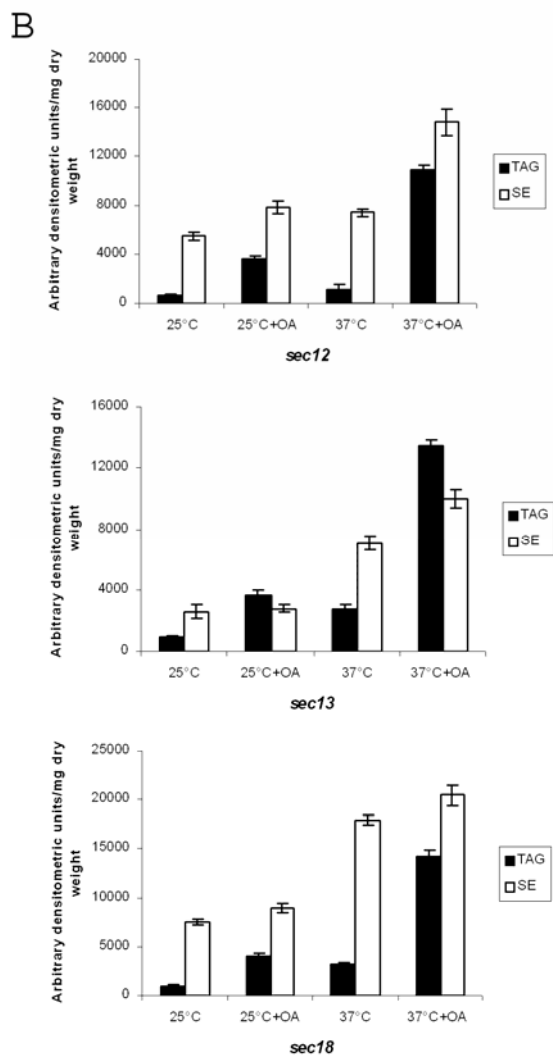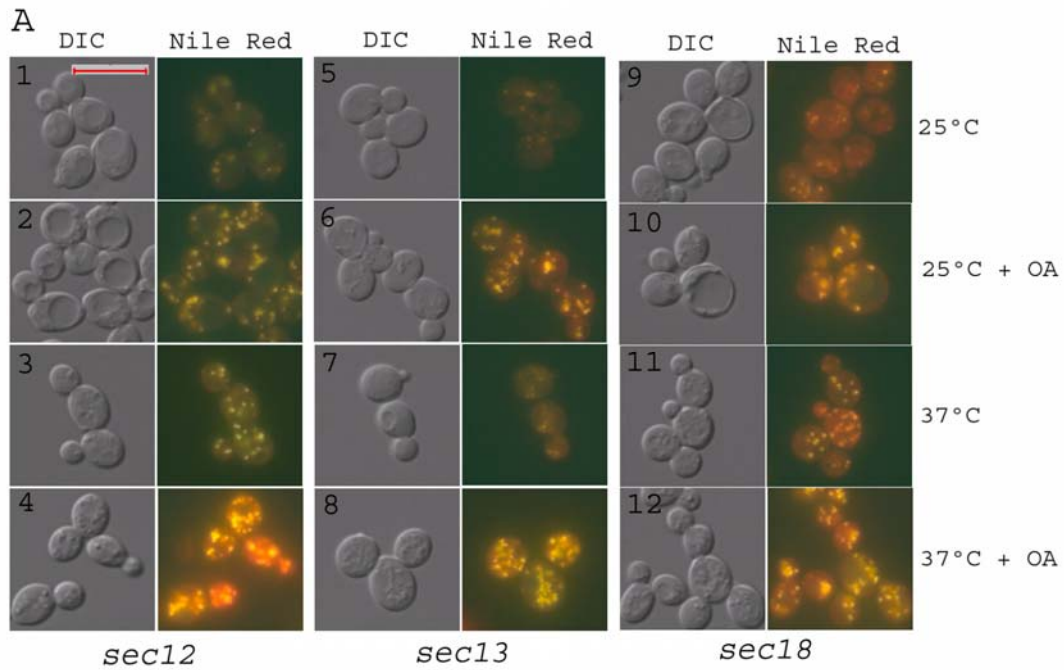
Figure 3-3. ER-to-Golgi transport is not essential in LD synthesis. Cells were grown in YPD at 24°C till OD_{600} ~0.5. Subsequently cells were harvested (1, 5, 9), or incubated in the presence of 0.5 mM oleate (2, 6, 10), or shifted to 37°C (3, 7, 11, and 4, 8, 12). After incubation at 37°C for 1h, cells were either harvested (3, 7, 11) or supplied with 0.5 mM oleate for 1h (4, 8, 12). A. Nile red staining of LDs. Bar, 10 μm. B. Quantitation of intracellular TAG and SE.

essential in LD biogenesis has not been defined yet. To test this possibility, we made use of the *sec12*, *sec13*, and *sec18* temperature-sensitive (ts) mutants.

The mutant strains were grown at the permissive temperature (24°C) and then shifted to the nonpermissive temperature (37°C) and incubated for 1 h. Subsequently, cells were supplied with 0.5 mM oleate and incubated for another 1 h. As shown in Figure 3-3 A, oleate-induced LD synthesis was not impaired when the cells were shifted to the nonpermissive temperature. On the contrary, parallel to the elevated synthesis of neutral lipids at the nonpermissive temperature (Figure 3-3B), these *sec* mutants synthesized more LDs at 37°C than at 25°C (Figure 3-3A). Since Sec12p and Sec13p are indispensable for the formation of COPII, and Sec18p is an essential regulator of SNAREs, this data clearly shows that ER-to-Golgi transport is not essential for LD biogenesis.

3.3 Energy poisons cannot block LD formation

Then I moved forward to test whether energy depletion could inhibit the synthesis of LDs. Wild type cells were incubated in the presence of 10 mM NaF and 10 mM NaN_3 serving as energy poisons to block all ATP production (Vida and Emr, 1995). To my great surprise, energy poisoning failed to block oleate- induced synthesis of LDs. As seen in Figure 3-4B, after the treatment with NaF/NaN_3 for 1 h, cells had an increase of both TAG and SE synthesis, about twofold increase for each. Meanwhile microscopy demonstrated that besides an enlarged vacuole, energy depletion also resulted in a twofold increase of LDs (Figure 3-4A). It suggested that cells sensed the stress caused by energy

depletion and made an immediate storage of TAG and SE into LDs.
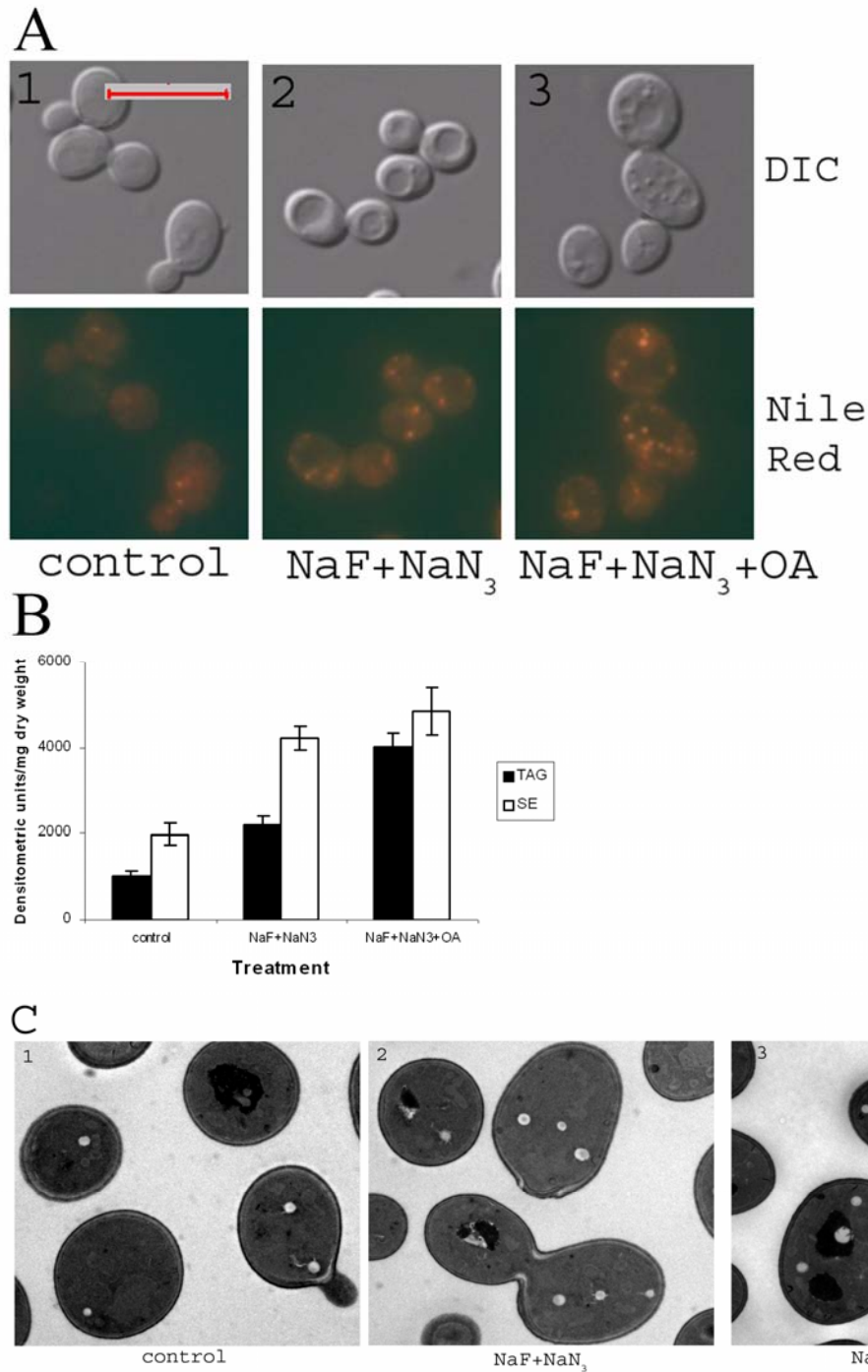
Figure 3-4. Energy poisons cannot block oleate-induced LD formation. Cells were grown in YPD at 30°C till OD_{600} ~0.5. Subsequently cells were either harvested (1), or treated for 1 h with 10 mM NaF and 10 mM NaN_3 (2 &3). After energy depletion, cells were either harvested (2) or incubated with 0.5 mM oleate for 1 h (3). A. Nile red staining of LDs. Bar, 10 μm. B. Quantitation of intracellular TAG and SE. C. Thin-section electron micrograph of cells. Bar, 2 μm.

When the energy-starved cells were further supplied with exogenous oleate, they continued to synthesize more TAG, since lipid analysis discovered another 90% increase of intracellular TAG compared to the energy-depleted group without oleate treatment. SE level also had a 15-20% increase (Figure 3-4B). Moreover, when counted under the fluorescence microscope, intracellular LDs increased as well, from 2.5 ± 1.1 per cell on average (n=223) to 4.3 ± 1.9 per cell on average (n=251) (Figure 3-4A). LD synthesis in response to energy depletion was further confirmed using thin-section electron microscopy, and so was oleate-induced LD synthesis in energy-starved cells (Figure 3-4C). When the wild type cells were grown in YPD medium to $OD_{600}\sim0.5$, almost all cross-sections of the cell contained 0-2 LDs. After the cells were subjected to 1-h NaF/NaN_3 treatment, some cross-sections contained 3-4 LDs. When 0.5 mM oleate was supplied to these energy-starved cells, even more (5-6) LDs could be observed in some cross-sections. Taken together, these data show that NaF/NaN_3 treatment does not block the synthesis of neutral lipids and the deposition of newly-synthesized neutral lipids into LDs. This result also gives additional supporting evidence that vesicular transport is not essential in LD biogenesis, because NaF/NaN_3 has been shown to efficiently block vesicular transport (Vida and Emr, 1995; Hanson et al., 2002;).

3.4 Summary

These results clearly indicate that cytoskeleton and vesicular transport are not essential in LD formation. At this stage, we still cannot draw any conclusion that LD biogenesis is energy-independent, because NaF/NaN_3 treatment may not completely

deplete the intracellular ATP store.

It should be noted, however, that exogenous oleate was supplied to the cells in these experiments to promote the synthesis of LD. It is unknown whether cytoskeleton and/or vesicular transport have a role in LD biogenesis under normal growth conditions when the cells would not have access to an excess of oleate. It is possible that even if they are not directly involved in the deposition of neutral lipids into LDs, they might be required to transport the substrates for TAG and SE synthesis from other membrane compartments to the ER, for instance, DAG, free fatty acids, and sterols.

Chapter 4

Genome-wide screening for yeast genes whose deletions result in defective accumulation of intracellular LDs

The genome of the budding yeast *S. cerevisiae* has been completely sequenced (Goffeau et al., 1996). Based on that, a whole collection of gene deletion strains have been constructed (Winzeler et al., 1999) and are commercially available at the EUROSCARF (EUROpean Saccharomyces Cerevisiae ARchives for Functional analysis collection center. This makes possible the screen for genes whose deletion leads to a specific phenotype of interest by taking an approach of "reverse genetics". Reverse genetics which proceeds in the opposite direction of classical forward genetics aims to identify the possible phenotypes that may result from alteration of a specific genetic sequence. It might be time-consuming and labor-intensive; however, it is a powerful method. In this study, we screened the entire collection of ~4700 haploid deletion strains of *S. cerevisiae* purchased from EUROSCARF to identify genes involved in intracellular LD accumulation.

4.1 Nile red staining of LDs in the wild type yeast (BY4741) cells

Nile red, 9-diethylamino-5H-benzo[α]phenoxazine-5-one, is a specific and excellent vital dye for intracellular LDs. The fluorescent color is dependent on the excitation wavelength, and varies from golden yellow (excitation at 450-500 nm) to orange-red (excitation at 515-560 nm) (Greenspan et al., 1985; Greenspan and Fowler, 1985). In this

study, golden yellow was chosen because it offers a better resolution of LDs in addition to a low background. Figure 4-1A shows the Nile red staining of cytoplasmic LDs in the wild type (hereafter WT) cells grown to early stationary phase. Considering that wide field fluorescence microscope was used in this study, microadjustment of the sample platform was performed whenever necessary to observe the out-of-focus LDs. Due to the same reason, the count of intracellular LDs was performed directly under the microscope. Because yeast cells accumulate LDs when they enter the stationary phase in response to nutrient limitation, WT cells and all the mutants were grown overnight to early stationary phase in this study, immediately followed by Nile red staining and fluorescence microcopy. Early-stationary-phase WT cells contain 5.16±2.18 LDs per cell on average (n=200) and approximately 80% of the cells accumulate 3 to 6 LDs. To be precise, 24% of the cells accumulate 3 LDs, 19% 4 LDs, 19% 5 LDs, and 17% 6 LDs.

4.2 Genome-wide scan for genes whose deletions result in defective accumulation of cytoplasmic LDs

Subsequently we screened the entire collection of ~4700 viable single deletion mutants to identify genes the deletion of which lead to defective accumulation of cytoplasmic LDs. Based on our observation that most mutants have around the same number of LDs as the WT cells, we arbitrarily categorized the strains of which the majority (>50%) cells accumulate less than 3 LDs as fld (few lipid droplets) mutants, and the strains of which the majority cells accumulate more than 7 LDs as mld (many lipid droplets) mutants. Among the mld mutants, some strains of which the majority cells

contain more than 11 LDs were labeled as strong phenotype (Figure 4-1). Genome-wide screening of the entire collection of viable single deletion strains led to a discovery of 16 fld mutants and 117 mld mutants. Obviously, the percentage of fld strains among a total of 4850 viable deletion mutants (0.33%) is much smaller than that of mld strains (2.38%). No LD-null mutant was identified in this study. Table 4-1 summarizes the genes the deletion of which result in reduced accumulation of intracellular LDs, and Table 4-2 summarizes the genes whose deletions result in accumulation of more intracellular LDs. Genes were grouped according to known or presumed function of their products. Genes whose deletions have reduced number of LDs encode: components of glycosylation machinery, enzymes seated on some metabolic pathways, proteins involved in protein biosynthesis, and miscellaneous proteins (Table 4-1). Genes whose deletions lead to increased quantity of LDs include members of the same groups discussed above; besides, genes whose products serve as channels and transporters, most of which belong to the vacuolar ATPase family, genes of cytoskeleton related proteins, genes encoding proteins responsible for DNA maintenance and chromatin structure, genes whose products involved in protein modification and degradation, genes encoding transcription factors, genes whose products implicated in vesicular trafficking, and some hypothetical or uncharacterized ORFs (Table 4-2). The number of intracellular LDs was confirmed at least three times by fluorescence microscopy when stained with Nile red.
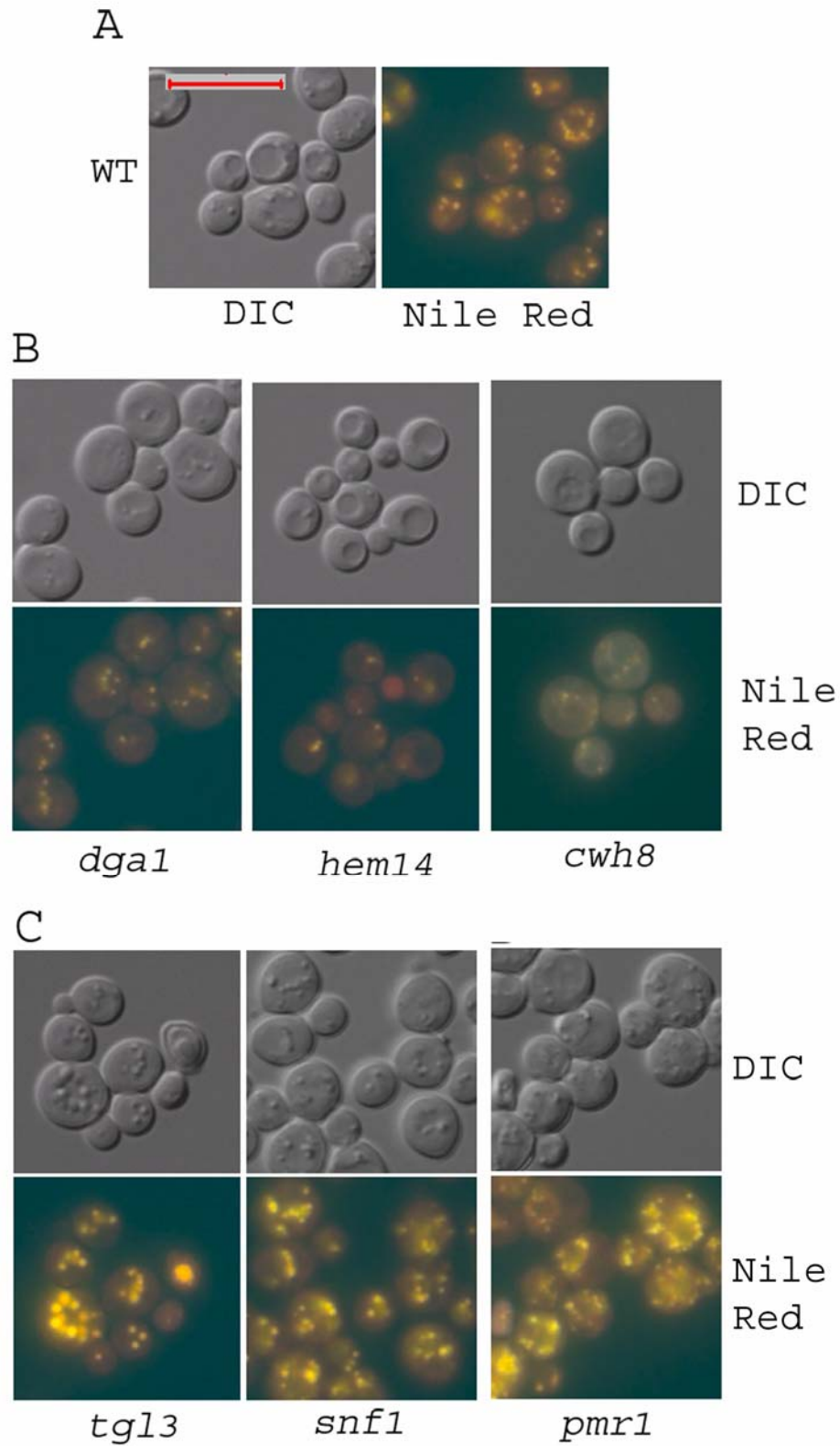
Figure 4-1. Nile red staining of LDs in the WT cells and selected mutants. Bar, 10 μm. A WT cells. B. 3 selected fld strains (*dga1*, *hem14*, and *cwh8*). C. 3 selected mld strains (*tgl3*, *snf1*, and *pmr1*). Among them, *pmr1* gives a strong phenotype.

Table 4-1. Genes identified in genome-wide screening for fld strains (16)
Metabolic enzymes (4)
COX5A, CYS4, DGA1, HEM14
Protein glycosylation (1)
CWH8
Protein biosynthesis (5)
RPP2B, RPL2B, RPL8B, RPL12B, RPL20A
Transcription factors (1)
HMO1
Miscellaneous (5)
BUD25, LTV1, NEM1, SPO7, SSD1

ABOVE: This table lists a total of 16 genes whose deletions result in decreased intracellular LDs. The number of genes in each group was indicated in parenthesis. Some genes may have different designations; our choice was made based on the frequency of their use in literature. Detailed gene information could be found at Saccharomyces Genome Database.

RIGHT: This table lists a total of 117 genes whose deletions demonstrate increased intracellular LDs, among which 14 give strong phenotype (indicated by *).

Table 4-2. Genes identified in genome-wide screening for mld strains (117)
Channels and transporters (5)
FUI1, VMA6, VMA8, VMA13, VMA21
Cytoskeleton organization (6)
ARC18, ARP1, CNM67, NUM1, SPC72*, VRP1
DNA maintenance / chromatin structure (9)
EST1*, EST2*, EST3, POL32, MRE11, RAD27*, RAD50, RTT109, XRS2
Metabolic enzymes (18)
ADE3, ADE4, ADE5,7, ADE6, ADE8, ADE12, ELO3, ERG2, ERG3, ERG4, ERG5, ERG6, KGD1*, MET7, PFK2, RNR4, TGL3, TGL4
Protein glycosylation (7)
ANP1, ERD1, MNN10, MNN11, OCH1, OST4, PMR1*
Protein biosynthesis (3)
RPS12, RPS21B, RPS30B
Protein degradation (4)
DEF1, DOA10, HRD1, UBX1
Protein modification (3)
MAP1, MDM20, PPG1
Protein / RNA transport (1)
APQ12
RNA modification and metabolism (3)
DHH1, KEM1, REF2
Signaling / Transcription factors (18)
HPR1, MFT1, NOT5, PAF1, PGD1, PHO85, RLR1, ROX3*, RPB4, SNF1, SNF2, SNF6, SNF11, SRB2*, SRB5*, SSN3, SWI3, TAF14
Vesicular transport (22)
CHC1, SAC1, SWA2, VAM3, VPS1, VPS11, VPS15, VPS16, VPS18, VPS19, VPS27, VPS31, VPS33, VPS34, VPS39, VPS41, VPS43, VPS45, VPS53*, VPS54, VPS64, VPS66
Hypothetical / uncharacterized ORF (10)
YDL073W , YDR532C , YGL168W*, YKL037W , YJL075C,   YLL030C*, YLR358C, YOR041C, YPL183W-A, YPR087W*
Miscellaneous (8)
ARG82, BUD22, ELM1, GON7*, KRE6, MMS22, SPS1, TPD3

4.3 Electron microscopic examination of the WT cells and selected mutants

Under conventional electron microscope, LDs which appear electron-lucent can be easily identified. To further confirm that the fld mutants identified in this study contain fewer LDs and the mld mutants contain more LDs than the WT cells, we examined 3 fld

mutants, 3 mld mutants, 1 of which displays strong phenotype, together with the WT cells

using transmission electron microscopy (TEM). It is noted that TEM only observe

cross-sections of the yeast cells, and therefore it should not
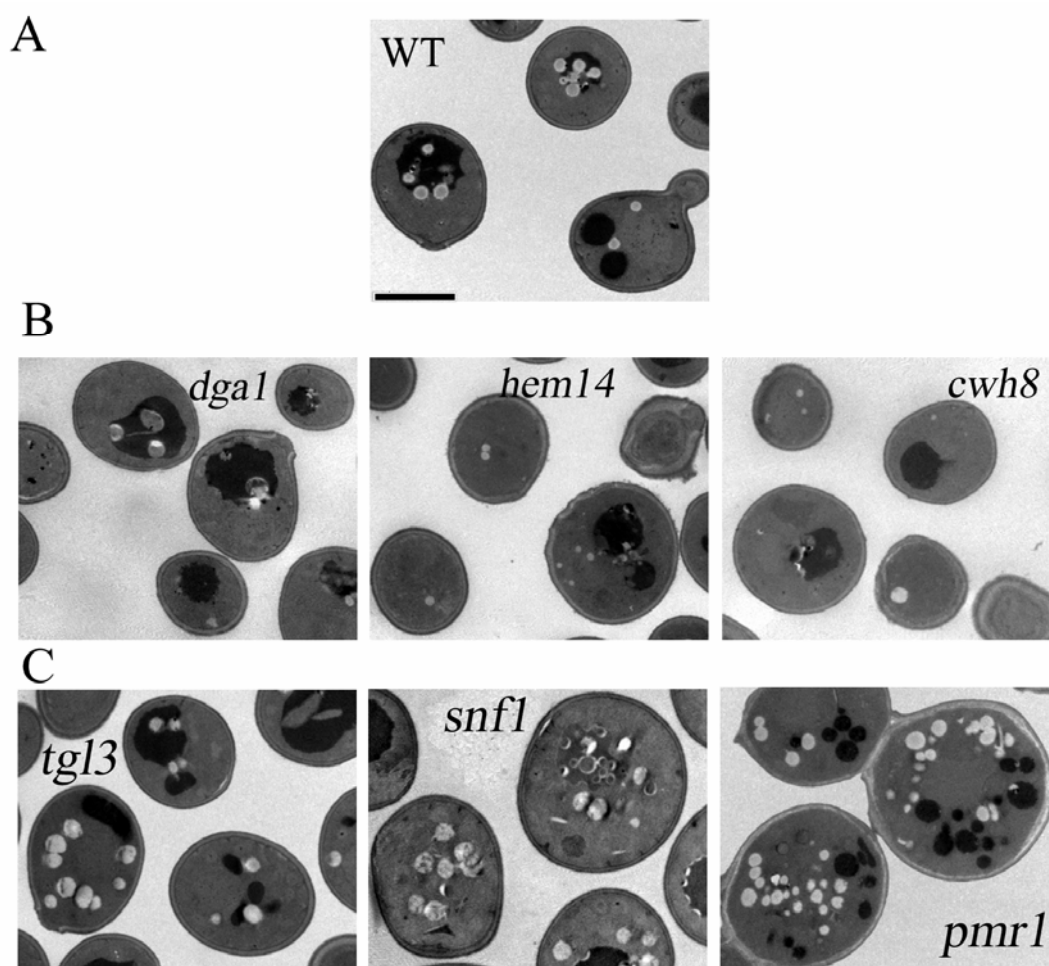
Figure 4-2. Thin-section electron micrograph of WT cells and selected mutants. A WT cells. B. 3 selected fld strains (*dga1*, *hem14*, and *cwh8*). C. 3 selected mld strains (*tgl3*, *snf1*, and *pmr1*). Bar, 2 μm

be used for counting the number of LDs contained in one single cell. However, because

the mld mutants contain more LDs than the WT, the chance of the appearance of LDs in

cross-sections of the mld mutants is higher than those of the WT. In addition, the average

number of LDs per cross-sectioned mld mutant cell is more than that per cross-sectioned

WT cell. The same logic applies to the fld mutants as well.

WT cells and 6 selected mutants were fixed with 2.5% glutaraldehyde and postfixed with 2% (w/v) osmium tetroxide. The samples were subsequently dehydrated in a series of graded ethanol and embedded in Spurr's Resin. 80-nm ultrathin sections were stained with uranyl acetate and lead citrate and examined under a JEM-1230 Joel electron microscope. As shown in Figure 4-2, as many as 4 or 5 LDs could be observed in sections of the WT cells. The majority of sections of the fld strains contained less than 3 LDs and the size of LD could be much smaller than the WT cells. Most of the sections of the mld mutants contain more than 6 LDs. Some sections of the *pmr1* strain even displayed 20 LDs. These results are consistent with the data obtained through fluorescence microscopy.

4.4 Neutral lipids analysis of 16 fld mutants

The synthesis of the core lipids, TAG and SE, so far is known to be the major contributor in LD formation. Little is know about whether other factors/proteins are involved in LD formation. In this study, 16 strains were identified to have fewer LDs than the WT (Table 4-1). In order to see whether these deleted genes directly affect LD assembly without impingement upon neutral lipids synthesis, we quantitated the neutral lipids of these mutants. The result is shown in Figure 4-3. The data shows that 9 strains (*hmo1*, *cox5a*, *dag1*, *hem14*, *cwh8*, *rpp2b*, *rpl8b*, *rpl12b*, and *bud25*) have decreased TAG and SE, 4 strains (*rpl2b*, *rpl20a*, *bud25*, and *nem1*) have decreased TAG only, and 3 strains (*cys4*, *spo7*, and *ssd1*) have decreased SE only. This suggests that reduced LD accumulation in these mutants is very likely the result of decreased neutral lipids synthesis. Therefore, these genes may not be directly involved in LD assembly.
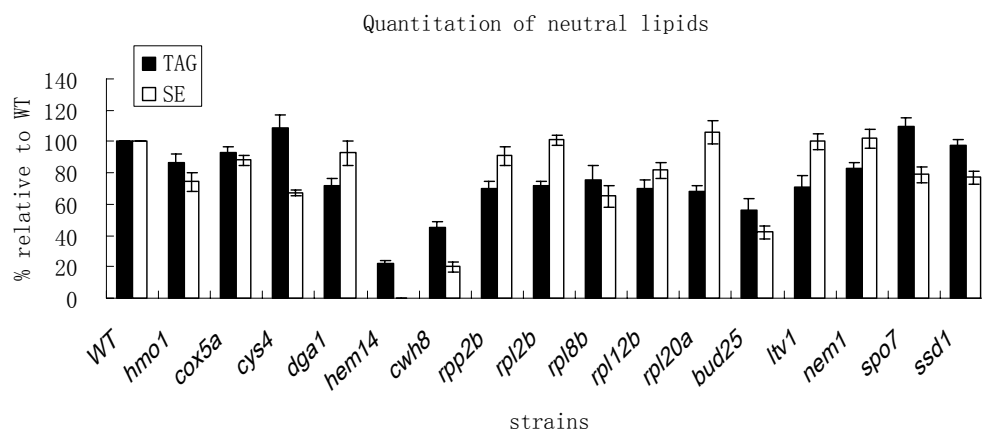
Figure 4-3. Neutral lipids analysis of WT and fld strains.

4.5 Conditions of endoplasmic reticulum stress stimulate LD formation in *S. Cerevisiae*

Cumulative evidence indicates that ER is the site for LD biosynthesis (Murphy and Vance, 1999). However, no ER related signaling pathways have been identified to regulate or associate with the biogenesis of LDs. Through genome-wide screening, 117 mld mutants were identified. Among these mutants, many are involved in endoplasmic reticulum (ER) stress.

4.5.1 Mutants defective in N-linked glycosylation accumulated more LDs

Physiologically ER stress can result from mutations of genes encoding glycosylation enzymes (Zhang and Kaufman, 2006). In this study, we found that seven mutants that affect protein glycosylation, *anp1*, *erd1*, *mnn10*, *mnn11*, *och1*, *ost4*, and *pmr1*, produce more LDs than the WT when cells enter stationary phase (Figure 4-4A). As shown in Table 4-3, these mutants contain significantly more LDs than the WT cells. In addition,

lipid analysis showed that compared with the WT, the mutants had elevated TAG and/or

SE (Figure 4-4B).

A.
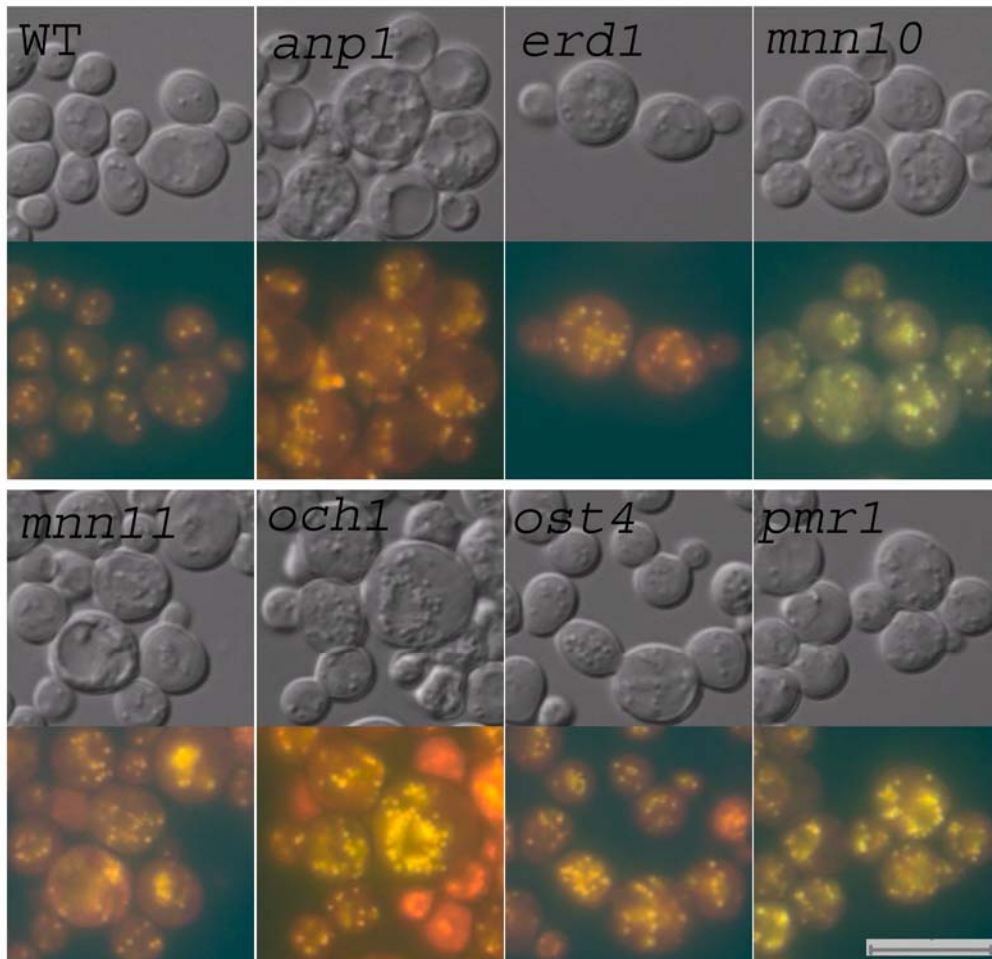
B.
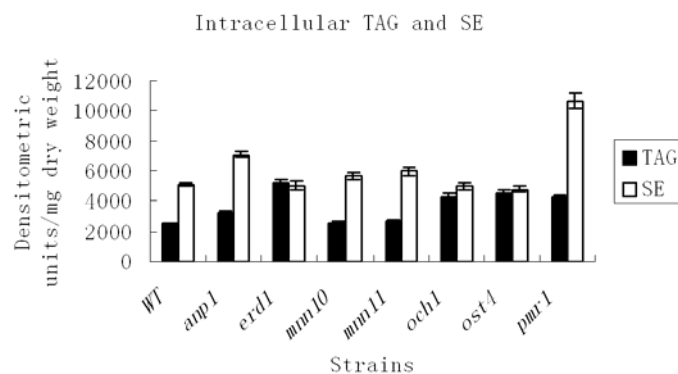
Figure 4-4. Mutants defective in protein glycosylation display more intracellular LDs. Cells were grown in YPD till early stationary phase. A. microscopic examination of LDs of WT, *anp1*, *erd1*, *gas1*, *mnn10*, *mnn11*, *och1*, *ost4*, and *pmr1* cells. Bar, 10 μm. B. Quantitation of intracellular TAG and SE.

Table 4-3. The number of LDs of the WT cells and the mutants defective in protein glycosylation when cells were grown to stationary phase.

Strains	the average number of LDs
WT	5.2±2.2
anp1*	8.3±2.7
erd1**	9.3±2.4
mnn10*	7.9±1.9
mnn11*	8.3±2.5
och1***	10.3±3.7
ost4***	10.2±3.1
pmr1***	11.9±2.8

*, p<0.05; **, p<0.01; ***, P<0.001; all compared with the WT cells (n=100).

4.5.2 Mutations in ERAD components resulted in more LD accumulation

ER-associated protein degradation (ERAD) is responsible for the degradation of misfolded or unassembled proteins from the ER. The ERAD pathway translocates misfolded proteins back into the cytosol, where they are eliminated by the proteasome (Brodsky and McCracken, 1999). Walter and colleagues found that impaired ERAD leads to an accumulation of unfolded proteins in the ER, thus constitutively causing ER stress (Travers *et al*., 2000). In this study we also found that LD biosynthesis was increased when *DOA10* or *HRD1*, nonessential genes required for ERAD, is disrupted (Figure 4-5). The average number of intracellular LDs was 7.3±2.1 and 6.9±1.7 (both p<0.05 compared with the WT 5.2 ± 2.2) for *doa10* and *hrd1*, respectively. Meanwhile, *doa10* displayed a 35% increase of TAG and 60% increase of SE; *hrd1* displayed a 30% increase of TAG and 40% increase of SE, all compared with the WT (Figure 4-5).

A
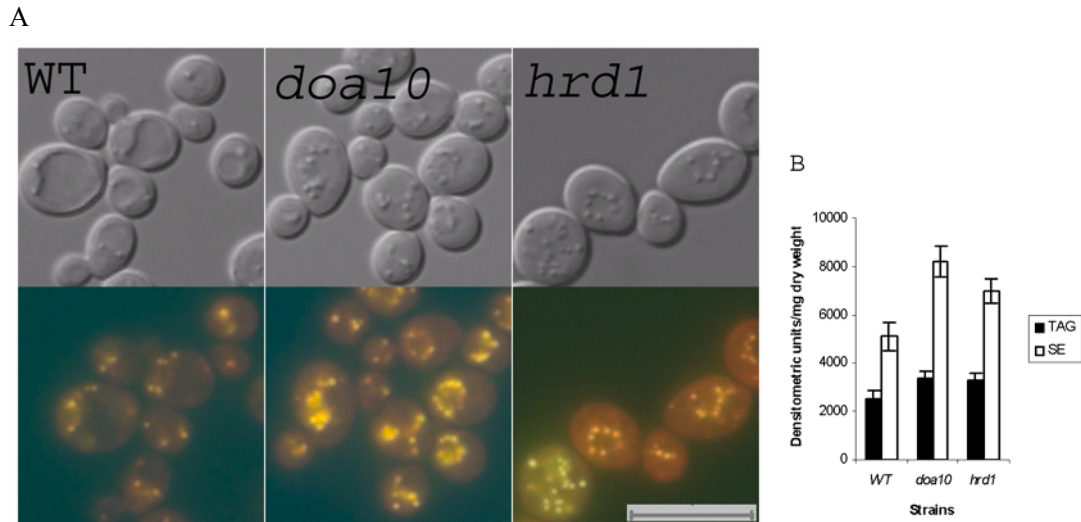
Figure 4-5. ERAD mutants accommodate more LDs. A. Microscopic demonstration of intracellular LDs of WT, *doa10* and *hrd1* cells. Bar, 10 μm. B. Quantitation of TAG and SE of three strains.

4.5.3 Tunicamycin and Brefeldin A treatment induced LD synthesis

To further test whether ER stress causes LD accumulation, we experimentally induced ER stress by treating cells with the drug Tunicamycin (Tm), which inhibits N-linked glycosylation, and found that Tm treatment led to increased intracellular LD production. WT cells, grown to early exponential phase (OD_{600}~0.5), were either harvested immediately or treated with Tm or an equivalent volume of DMSO (final 0.2% v/v). After 1 h of incubation in the presence of Tm cells accumulated more LDs (3.1±1.3) compared with the group receiving no additional treatment (1.5±0.8, p<0.01). DMSO alone had no obvious effect on LD formation (Figure 4-6A). Lipid quantitation analysis showed that Tm treatment increased TAG and SE synthesis by 30% and 130% respectively (Figure 4-6B). Furthermore, Tm treatment enhanced oleate induced LD synthesis. As shown in Figure 4-6, compared with the control group (YPD+DMSO), cells that were treated with Tm beforehand displayed more LDs and also a higher level of TAG and SE after the

addition of oleate. When the control group was incubated in the presence of 0.5 mM oleate for 1 h, the number of LDs per cell on average was 5.2±2.1, intracellular TAG was increased to as much as 6.5 times that of the YPD group, while SE synthesis was only elevated to as much as 1.5 times. In contrast, when the cells were pretreated with Tm for 1 h, the average number of intracellular LDs after supplementation with oleate was 9.1±2.9 (p<0.001), cellular TAG increased eightfold while SE increased fivefold (both compared to the YPD group).

Similarly BFA induced neutral lipids synthesis and LD formation in *erg6* cells as well (Figure 4-6). Since BFA cannot easily penetrate the cell wall of the WT cells, we selected the *erg6* mutant. When the *erg6* cells was incubated in the presence of 75 μg/ml BFA, the number of intracellular LDs per cell on average increased from 2.6±1.1 to 3.6±1.3 (p<0.01), cellular TAG synthesis was elevated by 7 times and SE synthesis by 80%. In addition, when oleate was added into the medium, cells pretreated with BFA also synthesized more LDs compared with the control group (11.3±3.5 versus 6.3±2.8, p<0.001). Likewise, BFA treatment also accelerated oleate-induced intracellular TAG and SE synthesis.

Figure 4-6 (next page). Tm treatment induces LD formation in the WT cells and BFA in *erg6* mutants at early log phase. 5 groups of cells were refreshed in YPD and grown for ~6 h at 30°C till OD_{600} ~0.5. Group 1 was harvested; group 2, 3, 4, 5 were added with 10 μg/ml of Tm (or 75 μg/ml of BFA) or an equivalent volume of DMSO (or ethanol). After 1 h incubation, group 2 and 3 were harvested while group 4 and 5 were treated with 0.5 mM oleate for another 1 h. Fluorescence microscopy and lipid analysis were performed afterwards. A. Microscopic observation of cells and LDs. Bar, 10 μm. OA: oleate. B. Quantitation of intracellular TAG and SE.

A

WT — erg6

1. YPD / YPD
2. YPD+DMSO / YPD+DMSO
3. YPD+Tm / YPD+BFA
4. YPD+DMSO+OA / YPD+DMSO+OA
5. YPD+Tm+OA / YPD+BFA+OA

B

Densitometric Units/mg dry weight

Treatment (WT): YPD, YPD+DMSO, YPD+Tm, YPD+DMSO+OA, YPD+Tm+OA

Treatment (erg6): YPD, YPD+ethanol, YPD+BFA, YPD+ethanol+OA, YPD+BFA+OA

TAG ■ SE □
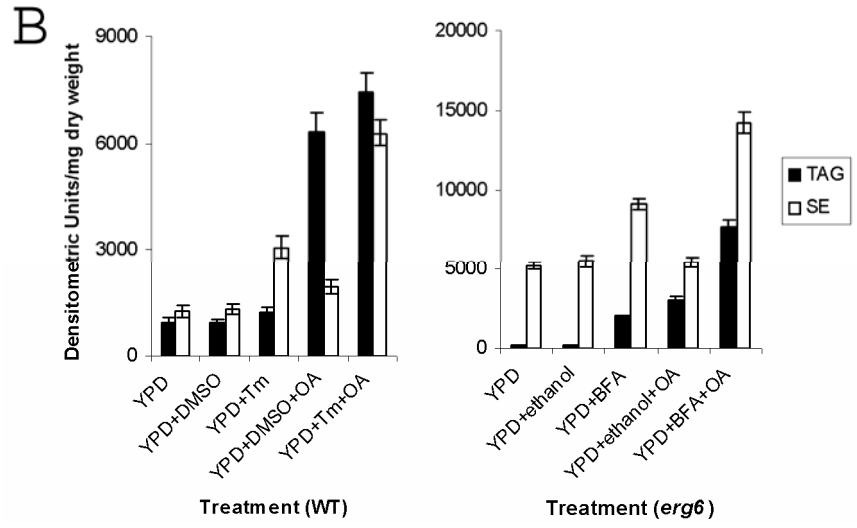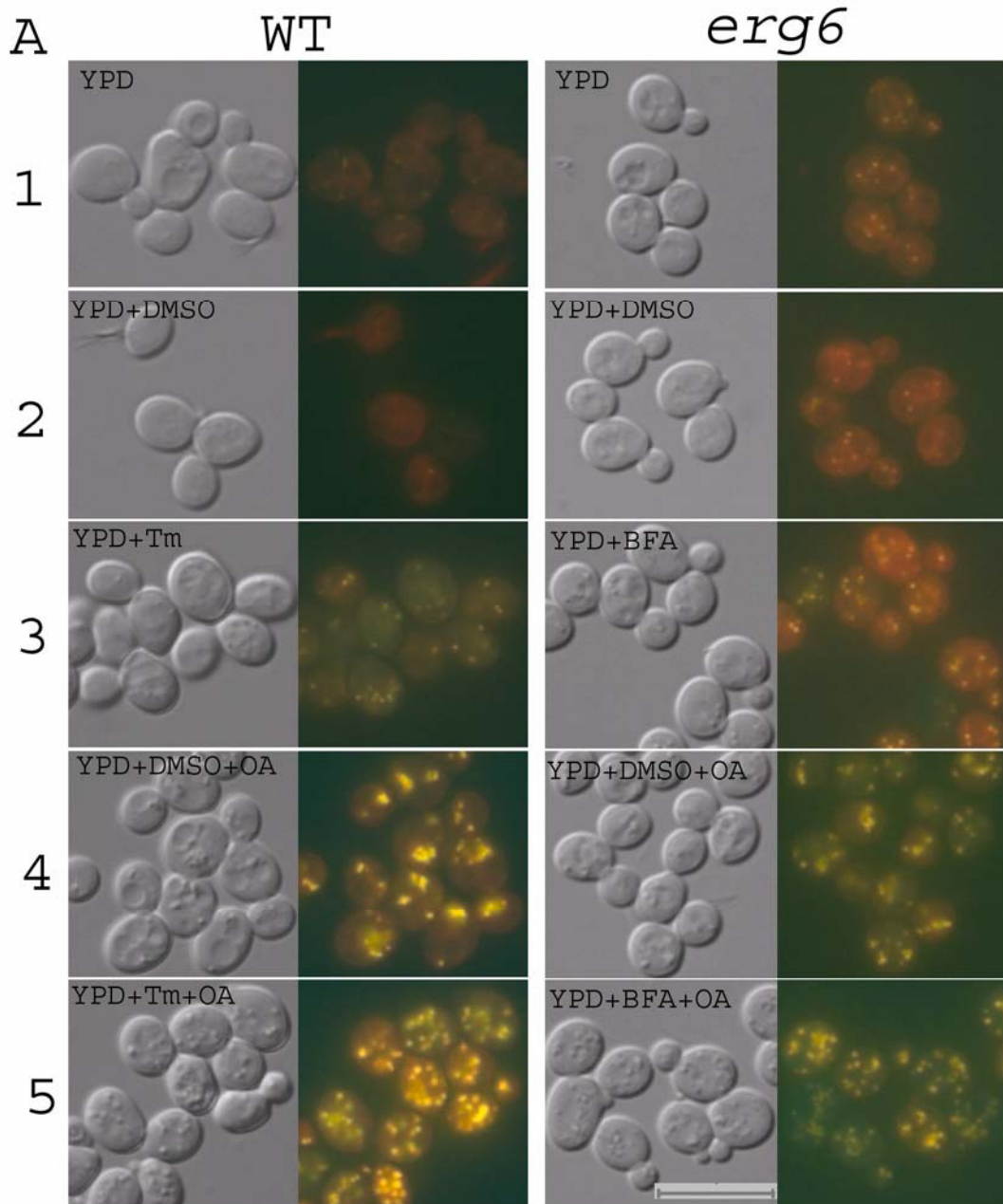
4.5.4 Removal of ER stress condition by restoration of protein glycosylation alleviated the "fatty" phenotype

To further verify our hypothesis that conditions of ER stress induce neutral lipids synthesis and LD formation, we studied whether the removal of ER stress could restore the defective LD accumulation. Pmr1p is a Ca^{2+} ATPase implicated in protein glycosylation; *pmr1* mutants have defects in outer chain glycosylation (Rudolph et al., 1989). Evidence suggested the defect is primarily due to the failure to transport Mn^{2+} into the secretory pathway and addition of Mn^{2+} greatly alleviates the glycosylation defect in *pmr1* cells (Dürr et al., 1998). As expected, supplementation of Mn^{2+} effectively reduced the production of LDs in *pmr1* mutants. As shown in Figure 4-7A and 4-7B, with the addition of gradually increased concentration of Mn^{2+}, *pmr1* cells began to decrease LD formation and synthesis of neutral lipids. When the concentration of Mn^{2+} was increased to 4.5 µM, its effect reached a plateau. Higher level of Mn^{2+} inhibited the growth of *pmr1* cells with 450 µM causing complete growth arrest. In contrast, supplementation of Mn^{2+} of equivalent concentrations to the WT cells did not result in any significant change either in the number of LDs (Figure 4-7C) or in the concentration of intracellular neutral lipids (Figure 4-7D). Nonetheless, 450 µM Mn^{2+} also caused slow growth of the WT cells.

In summary, our data indicate that conditions of ER stress lead to LD formation. 1) Mutants either defective in protein glycosylation or ERAD displayed more LDs than the WT cells; 2) Agents that induce ER stress triggered LD synthesis; 3) Alleviation of ER stress via restoration of glycosylation decreased LD production. To our knowledge, this study offers the first link between a well established ER signaling pathway and LD

formation.

It should be noted that although these mutants all accumulated more LD than the WT, their impact on neutral lipids synthesis varied between strains. *erd1*, *och1*, and *ost4* mainly upregulated TAG synthesis, *anp1*, *mnn10*, and *mnn11* mainly upregulated SE synthesis, while *pmr1*, *hrd1*, and *doa10* upregulated both TAG and SE synthesis (Figure 4-4 and 4-5). In addition, after Tm treatment, the increase of SE synthesis was more prominent than that of TAG synthesis, whereas BFA treatment appeared to have a greater impact on TAG synthesis (Figure 4-6). These results suggest that different types of ER stress may differ in their impact on neutral lipids synthesis.

Figure 4-7 (next page). Addition of Mn^{2+} reduces the "fatness" of *pmr1* cells. Cells were grown in YPD till early stationary phase (OD_{600}~3-4) in the absence or presence of Mn^{2+} ranging from 4.5 nM to 4.5 μM. Then cells were harvested, followed either by microscopic observation or lipid analysis. Addition of gradually increased concentration of Mn^{2+} decreased the neutral lipids synthesis and production of LD formation in *pmr1* cells. However, equivalent concentrations of Mn^{2+} had no obvious effect on the WT cells in terms of neutral lipids synthesis and LD formation. A. Microscopic examination of LDs in *pmr1* cells. Bar, 10 μm. B. Quantitation of intracellular neutral lipids of *pmr1* cells. C. Microscopic examination of LDs in the WT cells. D. Quantitation of intracellular neutral lipids of the WT cells.

A *pmr1*
Mn²⁺
0
4.5 nM
45 nM
450 nM
4.5 µM

C WT
Mn²⁺
0
4.5 nM
45 nM
450 nM
4.5 µM

B

pmr1

Densitometric units/mg dry weight

Mn²⁺ (concentration)

■ TAG
□ SE

D

WT

Densitometric units/mg dry weight

Mn²⁺ (concentration)

■ TAG
□ SE
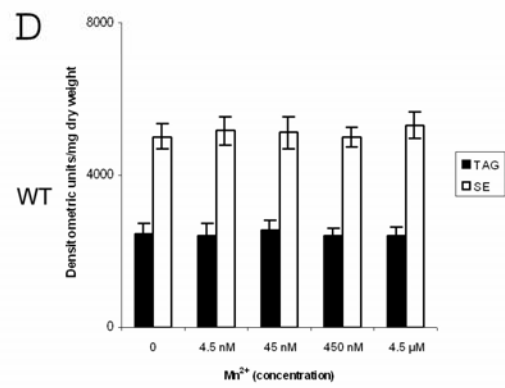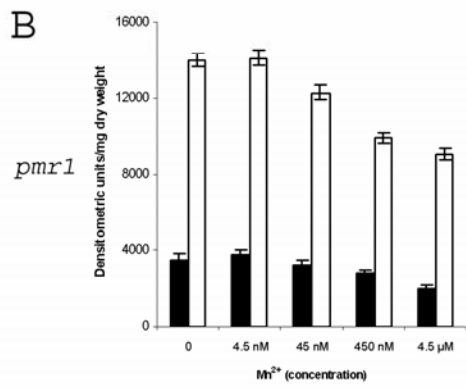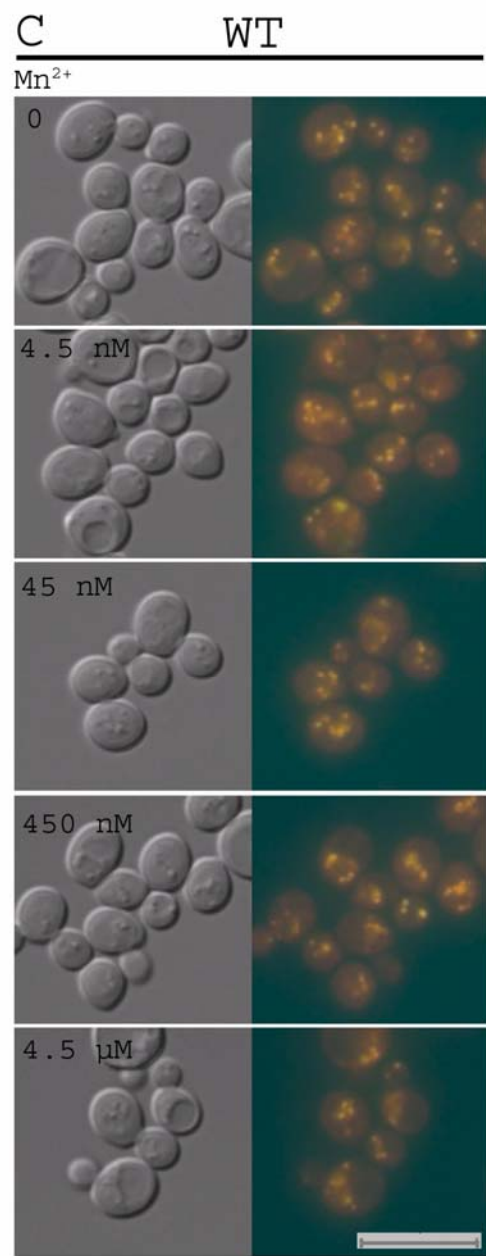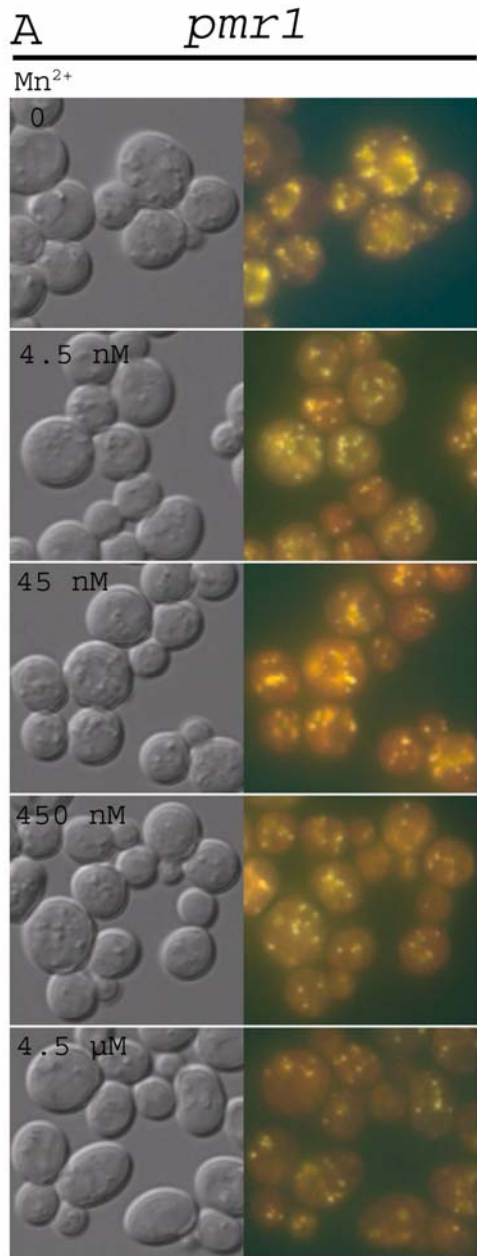
4.5.5 Stimulated LD production in conditions of ER stress was not Ire1p- dependent

Since unfolded protein response (UPR), a signal transduction cascade that allows eukaryotic cells to respond to changing conditions in the ER, is activated whenever protein folding in the ER is compromised, we investigated whether LD formation in conditions of ER stress was part of UPR. Because UPR requires Ire1p, which senses the accumulation of unfolded proteins in the ER lumen and cues the information across the ER membrane (Patil and Walter, 2001), we set out to find out whether Ire1p was essential for LD formation in conditions of ER stress. We knocked out *IRE1* from *anp1*, *mnn10*, *mnn11*, *pmr1*, and *doa10* strains. All the double deletion mutants conveyed hypersensitivity to 0.5 μg/ml Tm (data not shown). However, both the level of neutral lipids and the quantity of intracellular LDs of double deletion mutants showed no significant difference from that of corresponding single deletion strains (Figure 4-8). Moreover, Tm treatment also led to elevated synthesis of neutral lipids and accelerated formation of LDs in *ire1* cells. As seen in Figure 4-9, Tm treatment dramatically increased LD formation in exponentially growing *ire1* cells and the number of LDs increased from 1.6±0.5 to 3.1±1.2 (p<0.01). In addition, TAG synthesis was elevated by 10% and SE by 90%. Based on these two experiments, we conclude that LD formation in conditions of ER stress is not dependent on Ire1p. This shows that stimulated LD biosynthesis in conditions of ER stress is not part of UPR, although the scope of UPR is very broad and many aspects of secretory function are under the regulation of UPR (Travers et al., 2000).
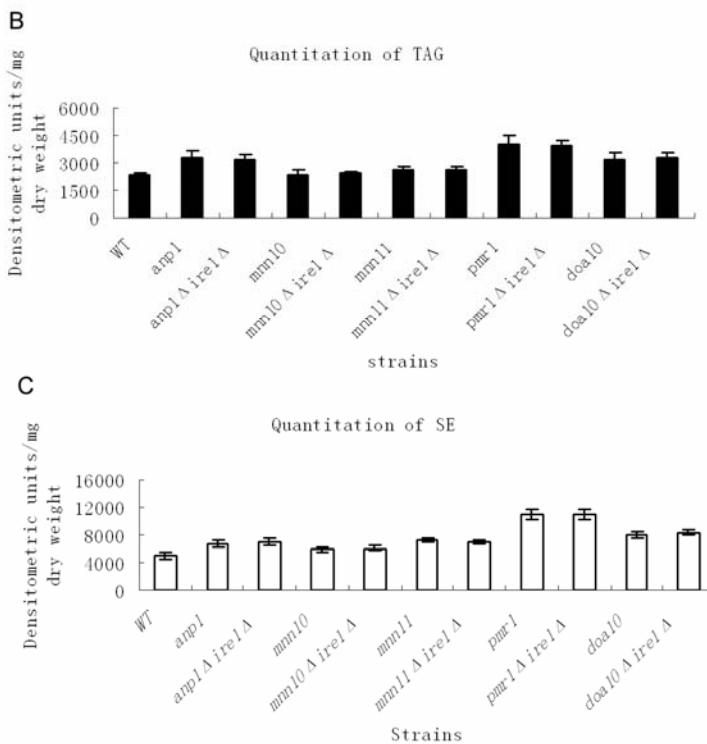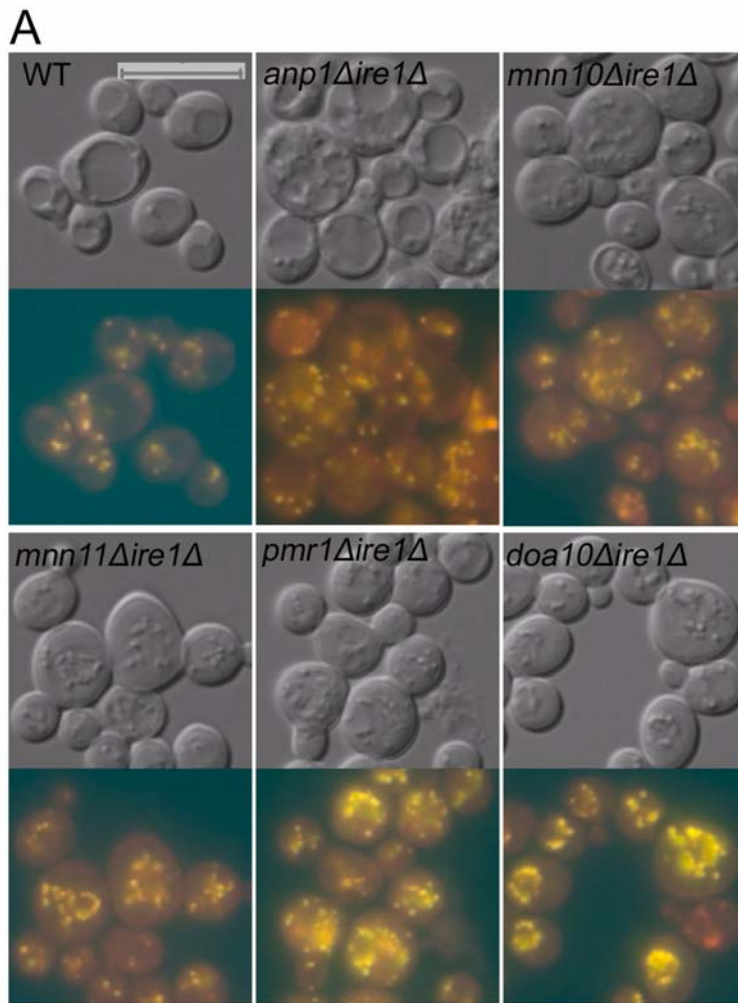
Figure 4-8. Intracellular LDs and neutral lipids synthesis are not reduced after *IRE1* was knocked out in strains defective either in protein glycosylation or ERAD. A. Microscopy of intracellular LDs of the WT and double deletion mutants. Bar, 10 μm. B and C, Analysis of cellular TAG and SE. Double deletion mutants were compared with the WT and their corresponding single deletion mutants.
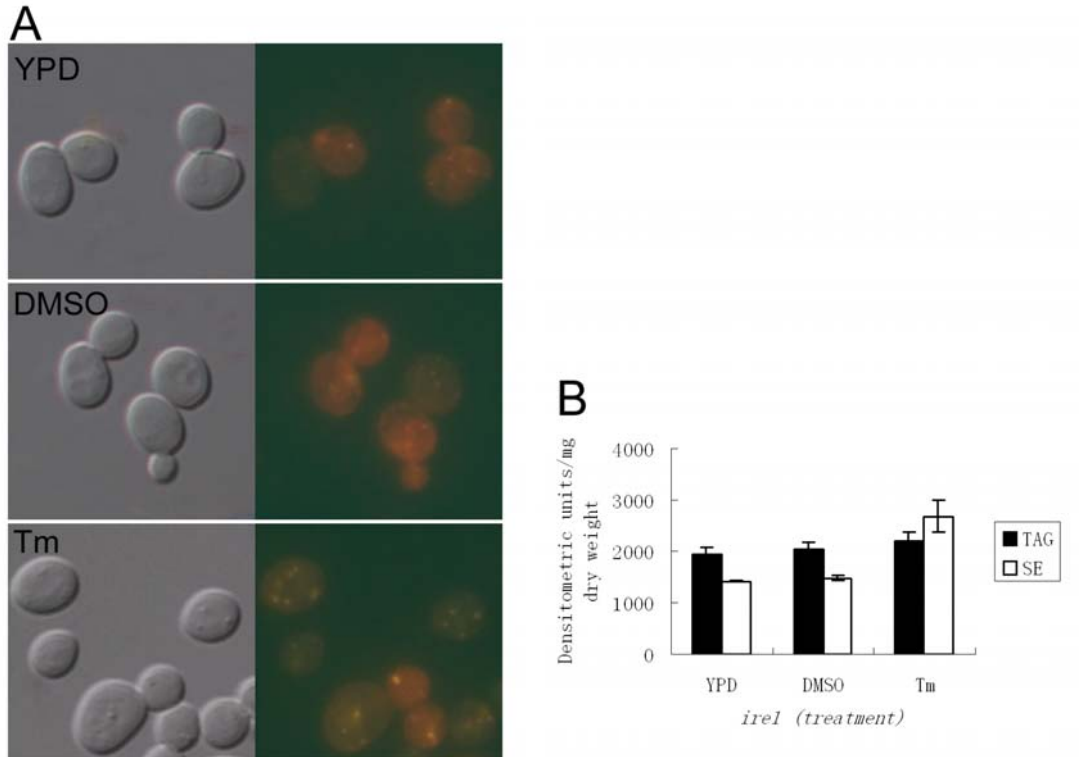
Figure 4-9. Tm treatment induces LD formation in *ire1* cells. Cells were refreshed in YPD and grown for ~6 h at 30°C till OD_{600} ~0.6. Subsequently cells were either harvested or treated with 10 μg/ml of Tm or an equivalent volume of DMSO for 1 h. A. Microscopic observation of cells and LDs. Bar, 10 μm. B. Quantitation of intracellular TAG and SE.

4.5.6. Enzymes catalyzing the synthesis of neutral lipids were not upregulated when LD formation was stimulated in conditions of ER stress.

The stimulated synthesis of neutral lipids and LDs in conditions of ER stress could have many possible causes. Among them, the expression level of the enzymes catalyzing the synthesis of TAG and SE was examined. Are1p, Are2p, Dga1p, and Lro1p are the four enzymes catalyzing the final step of the formation of SE and TAG. To be precise, Are1p and Are2p are responsible for the formation of SE and a minor portion (about 5%) of TAG, while Dga1p and Lro1p are responsible for the majority of TAG synthesis (Mullner and Daum, 2004). In this study, we successfully raised antibodies against Are1p and Lro1p and used them to observe the cellular level of Are1p and Lro1p via immunoblotting when

ER stress was initiated. As indicated in Figure 4-10A, Tm treatment did not upregulate

the level of Are1p and Lro1p. In addition, both ERAD mutants and four selected protein

glycosylation mutants that were found containing significantly more LDs in this study

had a similar (or even lower) level of Are1p and Lro1p to (than) that of the WT cells.

Furthermore, supplementation of Mn^{2+} reduced the "fatness" of *pmr1*, but failed to

change the cellular level of Are1p and Lro1p (Figure 4-10B).
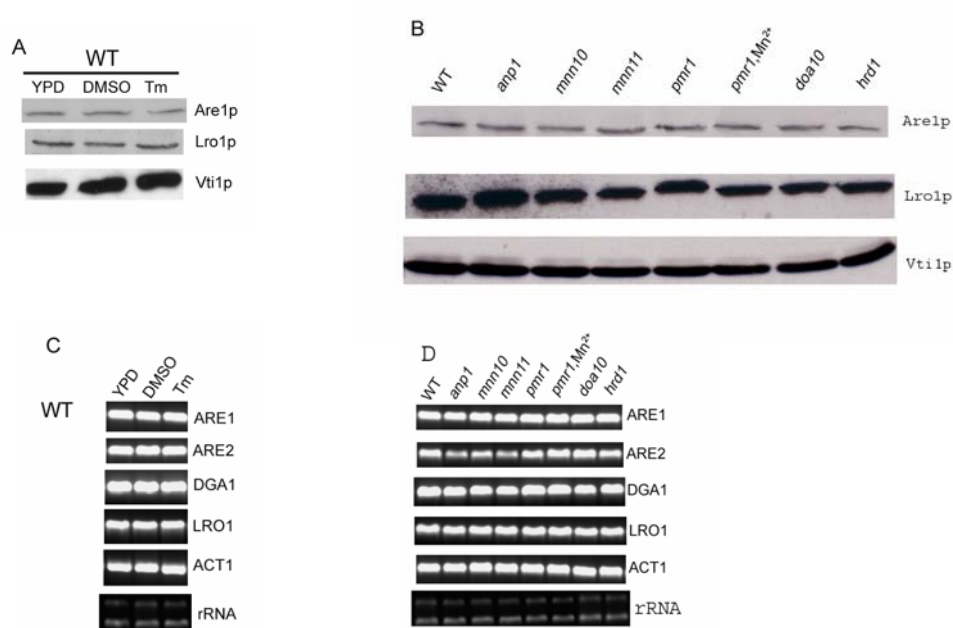
Figure 4-10. Enzymes involved in neutral lipids synthesis are not upregulated in conditions of ER stress. A. Tm treatment did not increase the cellular level of Are1p and Lro1p. Vti1p served as a loading control. B. Strains defective either in protein glycosylation or ERAD had a similar or even lower level of Are1p and Lro1p. Restoration of glycosylation in *pmr1* mutants by supplementation of Mn^{2+} didn't lead to change of Are1p and Lro1p level. C. mRNA level of *ARE1*, *ARE2*, *DGA1*, and *LRO1* were not significantly upregulated after Tm treatment. Total RNA was isolated, followed by RT-PCR analysis. Both ribosomal RNAs and *ACT1* served as loading controls. D. mRNA level of *ARE1*, *ARE2*, *DGA1*, and *LRO1* were not significantly upregulated in strains defective either in protein glycosylation or ERAD.

Besides Are1p and Lro1p, Are2p and Dga1p are the other two enzymes involved in

neutral lipids synthesis. We did not have antibodies against Are2p and Dga1p, and

therefore we chose RT-PCR to compare the mRNA level of *ARE2* and *DGA1*. First, we

compared the mRNA level of the WT cells before and after Tm treatment. As seen in Figure 4-10C, after Tm treatment, the mRNA level of *ARE1* and *LRO1* remained unchanged, which was consistent with our data that Tm treatment did not result in a significant change of Are1p and Lro1p, as shown in Figure 4-10A. Importantly, the mRNA level of *ARE2* and *DGA1* was not upregulated after Tm treatment as well. Furthermore, the mutants defective either in protein glycosylation or ERAD did not express a higher mRNA level of *ARE1*, *ARE2*, *DGA1*, or *LRO1* than the WT cells (Figure 4-10D). On the contrary, the mRNA level of *ARE2* was even obviously lower in *anp1* and *mnn11*. All our results, taken together, clearly demonstrate that enzymes involved in neutral lipids synthesis are not upregulated in conditions of ER stress, although these conditions lead to an elevated synthesis of LDs. This suggests that lipid trafficking from other cellular compartments to the ER and/or lipid synthesis in the ER *per se* is enhanced when the ER is under stress, and cells convert delivered and/or newly synthesized sterol/DAG/fatty acids into SE and TAG.

4.5.7 The interesting cwh8 strain

Interestingly, *cwh8* strain which is also defective in protein glycosylation did not exhibit LD hyperaccumulation; instead this mutant produced significantly fewer LDs than WT cells. It appeared, therefore, that this strain vetoes the association between ER stress and LD synthesis. Is that really the case?

Cwh8p encodes a dolichyl pyrophosphate (Dol-PP) phosphatase located in the ER membrane (Fernandez et al., 2001). Dol-PP phosphatase removes a phosphate from the

Dol-PP generated in the ER lumen by oligosaccharyltransferase that transfers oligosaccharides from Dol-PP onto nascent glycoproteins in the ER. Lack of Cwh8p results in an increase in cellular Dol-PP and a deficiency in Dol-PP-linked oligosaccharides (van Berkel et al., 1999). Since overexpression of Rer2p, a key enzyme catalyzing a rate-limiting step in the *de novo* synthesis of Dol-P, and Sec59, a dolichol kinase, can partially restore the growth defect of *cwh8*, it suggests that Cwh8p plays a role in maintaining sufficient Dol-P levels that are required for efficient protein *N*-glycosylation *in vivo* (Fernandez et al., 2001).

The *cwh8* strain exhibits severe underglycosylation of many glycoproteins. Then why this strain displayed LD hypoaccumulation instead of LD hyperaccumulation? Could it be that the deletion of *CWH8* impairs the expression or function of enzymes involved in neutral lipids synthesis? To test this possibility, I examined the incorporation of [^{3}H]oleate into neutral lipids. As shown in Figure 4-11, *in vivo* incorporation of [^{3}H]oleate into TAG and SE was severely impaired in *cwh8* cells. The rate of [^{3}H]oleate incorporation into neutral lipids of *cwh8* cells was merely about one third that of WT.
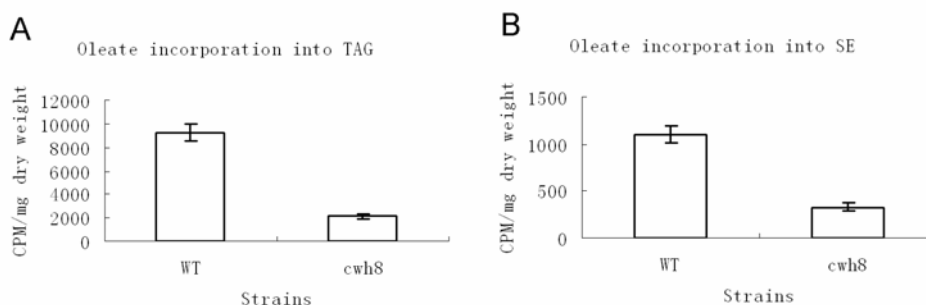
Figure 4-11. [^{3}H]oleate incorporation into neutral lipids of WT and *cwh8* cells. Cells were grown to mid-log phase, and pulsed with 1 μCi/mL of [^{3}H]oleate for 30 min.

Then I checked the expression level of Are1p and Lro1p using antibodies produced in

our laboratory. Remarkably, the expression levels of both Are1p and Lro1p in *cwh8* mutant were greatly reduced, as compared to that in WT cells. Expression of *CWH8* gene inserted into the YCplac111 vector successfully restored the expression of Are1p and Lro1p in *cwh8* cells (Figure 4-12).
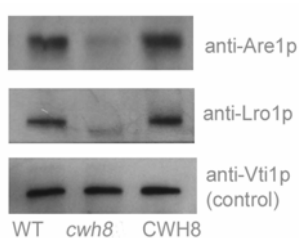
Figure 4-12. Expression level of Are1p and Lro1p in WT strain, *cwh8* strain, and *cwh8* strain transformed with YCplac111-CWH8 vector. Vti1p was a loading control.

Previously I have shown that the expression level of Are1p and Lro1p in the other protein glycosylation mutants identified in this study was comparable to that in the WT cells (Figure 4-10). These data suggest that deletion of *CWH8* gene on one hand causes protein underglycosylation, leading to ER stress which is supposed to induce LD synthesis; on the other hand, this deletion also leads to insufficient expression of enzymes involved in neutral lipids synthesis, which ultimately affects TAG and SE synthesis and blocks ER stress-induced LD synthesis. Therefore, although *cwh8* cells exhibited LD hypoaccumulation, this does not contradict the link between ER stress and LD synthesis.

4.5.8 ER stress may be responsible for LD overaccumulation in vma and vps mutants

4 mutants (*vma6*, *vma8*, *vma13*, and *vma21*) lacking proteins required for the assembly of vacuolar H^+-ATPase accommodate more LDs than the WT cells (Table 4-2).

Vacuolar H^+-ATPase functions to acidify organelles such as Golgi apparatus, endosomes, and vacuoles, and at the same time drives the antiporters for amino acids, Ca^{2+}, and K^+. Consequently, vacuolar H^+-ATPase is involved in a variety of cellular processes such as endocytosis, vacuolar protein sorting and intracellular trafficking (Beyenbach and Wieczorek, 2006). Besides the *vma* strains, another 22 mutants with mutations in genes involved in vesicular protein trafficking displayed increased accumulation of LDs (Table 4-2). Since these mutants inevitably affect the secretory pathway by one degree or another, soluble and membrane proteins which are synthesized on the rough ER and originally destined for secretion or localization to other organelles such as vacuoles may be blocked in the ER lumen, giving rise to increased ER load and ER stress. Therefore, hyperaccumulation of LDs observed in *vma* and *vps* mutants may be due to ER stress as well.

4.6 LD synthesis is under transcriptional control

18 mutants lacking signaling/transcription factors displayed hyperaccumulation of LDs (Table 4-2). Among them, 5 mutants are mutated in *PGD1*, *ROX3*, *SRB2*, *SRB5*, or *TAF14*, subunits of the RNA polymerase II mediator complex. *Rox1*, *srb2*, and *srb5* even displayed strong phenotype. This suggests that this complex is extremely important in maintaining cellular lipid metabolism, although the molecular mechanism is unknown at this stage. Given that mediator is a central link in the enhancer-activator-mediator-pol II-promoter pathway, and the transduction of regulatory signals through this pathway is crucial for transcriptional activation in all eukaryotic organisms (Kornberg, 2005), it can be

concluded that controlled gene expression is indispensable for regulated LD metabolism. This conclusion is further corroborated by our observation that LDs overaccumulate in mutants lacking components of THO complex (*hpr1*, *mft1*, and *rlr1*), mutants lacking components of SWI/SNF complex (*snf2*, *snf6*, *snf11*, and *swi3*), and *snf1*.

THO complex is required for transcription elongation (Chavez et al., 2000) and acts at the interface between transcription and mRNP export (Jimeno et al., 2002). Its disruption leads to transcription elongation impairment and DNA hyperrecombination, indicating that THO complex is a functional unit in gene expression and genome stability (Chavez et al., 2000). SWI/SNF complex, another complex that affects LD accumulation, is an ATP-dependent chromatin remodeling complex (Cote et al., 1994). Chromatin remodeling is mandatory for transcriptional initiation because genomic DNA is packaged into chromatin, producing repressing effect on gene expression. Increasing evidence indicates that gene expression is regulated by means of permitting access of DNA-binding factors to DNA via chromatin remodeling.

Besides the mutants of THO complex and SWI/SNF complex, *snf1* also displayed increased accumulation of LDs. Snf1 is an AMP-activated serine/threonine protein kinase which plays a critical role in the response to glucose depletion. In glucose-grown cells the regulatory domain of Snf1 autoinhibits the catalytic domain, and when glucose becomes limiting, the Snf4 activating subunit binds to the Snf1 regulatory domain and release the catalytic domain, thereby activating the transcription of glucose-repressed genes under conditions of glucose depletion (Jiang and Carlson, 1996; Carlson, 1999). Like its mammalian homolog AMP-activated protein kinase (AMPK) which, once activated,

switches off ATP-consuming anabolic pathways, such as cholesterol and fatty acids biosynthesis, and switches on ATP-producing catabolic pathways, such as fatty acid oxidation, the Snf1 complex acts as a key player in the response to glucose deprivation primarily by inducing expression of genes required for catabolic pathways that generate ATP (Hardie et al., 1998). Since the above-mentioned proteins are all general transcription factors, the fact that LDs hyperaccumulate in these mutants suggests that LD synthesis is under tight control.

LD hyperaccumulation was also observed in *pho85* strain. Pho85, a cyclin-dependent protein kinase (CDK), was initially identified as a transcriptional repressor of *PHO5*, an acid phosphatase gene (Gilliquet et al., 1990), and later studies found that Pho85 is also involved in glycogen metabolism and the deletion of *PHO85* resulted in hyperaccumulation of glycogen (Timblin et al., 1996). The result of this study suggests that Pho85 may also be involved in the regulation of LD synthesis.

Unlike the other transcription factors, the deletion of *HMO1* reduces the LD synthesis. Hmo1p is a family member of the high mobility group (HMG) proteins which associate with chromatin (Lu et al., 1996). Recently, it has been found that Hmo1p belongs to the ribosomal DNA transcription system (Gadal et al., 2002) and associates with promoters of many ribosomal protein genes (Hall et al., 2006). These reports may explain why the deletion of HMO1 leads to reduced accumulation of LDs since many mutants which affect the assembly of the large (60s) ribosomal unit synthesize fewer LDs than the WT (Table 4-1).

4.7 DNA maintenance and LD synthesis

Nine genes whose deletions resulted in increased LD accumulation encode proteins involved in DNA maintenance (Table 4-1 and 4-2). Among these mld mutants, 3 strains, *est1*, *est2*, and *rad27* display strong phenotype. Est1p and Est2p, together with Est3p, are required for telomerase activity *in vivo* (Taggart AK and Zakian, 2003). Rad27p is a 5' to 3' endonuclease required for Okazaki fragment processing (Budd and Campbell, 1997). Among the other genes whose deletions lead to elevated accumulation of LDs, the products of *MRE11*, *RAD50*, and *XRS2* comprise the RMX complex which functions in the repair of DNA damage (D'Amours and Jackson, 2002). Because these mutants affect DNA maintenance/chromatin structure, they might have negative impact on transcription. Thus the increased accumulation of LDs in these mutants is possibly also a result of inadequate modulation of transcription.

4.8 Cell metabolism and LD accumulation

18 genes whose deletions result in increased LD accumulation and 4 genes whose deletions result in reduced LD synthesis encode metabolic enzymes (Table 4-1 and Table 4-2). This result is quite imaginable because LD synthesis is part of the interconnected cellular metabolic pathways, and therefore any perturbation in the other metabolic pathways may impact LD synthesis.

Mutants lacking enzymes seated in the pathway of the *de novo* biosynthesis of purine nucleotides, Ade3p, Ade4p, Ade5,7p, Ade6p, Ade8p, and Ade12p, demonstrated elevated LD synthesis. Neutral lipids analysis revealed that both TAG and SE synthesis were
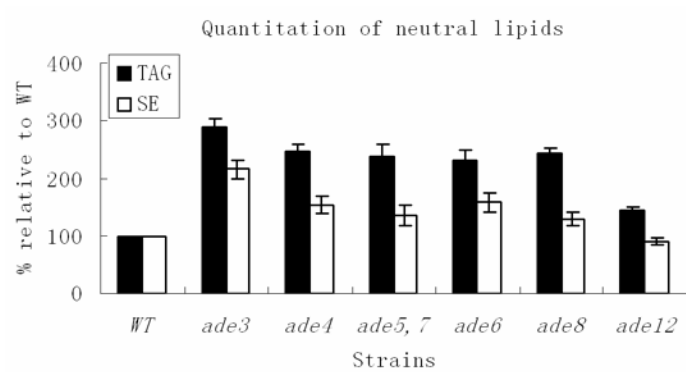
Figure 4-13. Neutral lipids analysis of *ade* strains.

upregulated, and the increase of TAG was more prominent than that of SE (Figure 4-13). The exact reason for this phenotype is not clear yet. One speculation is that these strains affect not only the synthesis of purine nucleotides, but also the relative amounts of ATP and GTP. Because oxidation of fatty acids can only occur after they form acyl-CoA through ATP-dependent acylation, it is possible that the rate of fatty acid oxidation is decreased in these strains. Since excessive fatty acids are harmful to the cell, they are channeled to the synthesis of neutral lipids which are deposited into the LDs.

Five *erg* mutants which affect the synthesis of ergosterol were also found to contain more LDs than the WT. Given that esterified ergosterol and esterified ergosterol precursors comprise one of the two classes of core components of the LDs, defect in ergosterol formation could seriously impact LD synthesis. In one possible way, lack of ergosterol may signal the cell to synthesize more ergosterol precursors which eventually become esterified and stored in LDs. In another possible way, the fact that at least two enzymes (Erg6p and Erg7p) in the ergosterol biosynthetic pathway localize to the LDs (Huh et al., 2003) suggests that LDs play an important role in ergosterol synthesis. Therefore, defect in ergosterol biosynthesis may require the overproduction of LDs.

Among the fld mutants identified were *cox5a* and *hem14*. Cox5a is the subunit Va of cytochrome c oxidase, the terminal member of the mitochondrial inner membrane

electron transport chain (Cumsky et al., 1985). Although Cox5a has one functional isoform, it is predominantly expressed during aerobic growth. Therefore, decreased LD synthesis of *cox5a* suggests that proper function of electron transport chain is required for normal LD synthesis. *HEM14* encodes a protoporphyrinogen oxidase, an enzyme in the heme biosynthetic pathway (Camadro and Labbe, 1996). Since heme is required for the assembly of yeast cytochrome c oxidase (Saltzgaber-Muller and Schatz, 1978), heme deficiency inevitably causes the *hem14* strain unable to assemble cytochrome c oxidase, which eventually affects LD synthesis, similar to the *cox5a* strain. However, lack of heme also affects ergosterol synthesis (Gollub et al., 1977), which may contribute to the decreased LD formation in *hem14* as well, as neutral lipids analysis shows that SE formation is almost completely abolished in this strain (Figure 4-3).

4.9 The assembly of ribosome and LD formation

8 mutants lacking proteins required for ribosome assembly have defective accumulation of LDs. Interestingly, 5 strains which affect the assembly of the large subunit (60S) synthesize fewer LDs (Table 4-1), while 3 strains which affect the assembly of the small subunit (40S) synthesize more LDs (Table 4-2), all compared with the WT. It is known that eukaryotic ribosomes contain approximately 78 different ribosomal proteins, 46 of the large subunit and 32 of the small subunit (Mager *et al*., 1997), but the function of individual proteins has not been clearly understood. Therefore, it remains to be established that how LD synthesis is affected in these mutants.

Chapter 5

Ylr404wp, an endoplasmic reticulum membrane protein, regulates the morphology of lipid droplets

The molecular mechanism underlying LD biogenesis is still elusive. It is known that neutral lipids are synthesized at the ER, but how lipids are finally packaged into LDs and how LDs acquire their protein compositions remains yet to be established. To achieve this goal, search of proteins that are involved in LD assembly is mandatory.

In an effort to identify genes whose product may be involved in LD formation, I screened the entire collection of single gene deletion mutants and found 117 mld mutants and 16 fld mutants. In addition, I also discovered that Ylr404wp, a protein of unknown function, regulates the morphology of LDs.

5.1 The *ylr404w* phenotype

5.1.1 *ylr404w* cells synthesize morphologically distinct LDs

Through genome-wide screening, I identified the *ylr404w* strain whose intracellular LDs are morphologically distinct from those of the WT cells. When grown in rich medium until stationary-phase, WT cells usually accommodated 3 to 6 LDs, which were about 0.2-0.4 μm in diameter and were almost spherical in shape, as shown by Nile red staining and fluorescence microscopy (Figure 5-1a). In contrast, LDs observed in *ylr404w* cells were very irregular in terms of quantity, shape, and size. Based on the quantitative and morphological difference between LDs, *ylr404w* cells could be categorized into 3

classes. The first class took up 20 to 30 percent of the total cell population and contained

one or several LDs that were almost spherical in shape and were about 0.5 to 1.5 μm in

diameter (hereafter termed supersized LDs) (Figure 5-1b, as indicated by arrow), which

means that the volume of the largest LD of the *ylr404w* cells was about 50 times that of

the largest LD of the WT cells. Among this class of cells, 5%-10% of the total population

contained only one observable LD. The second class took up 50 to 70 percent of the cell

population and contained an amorphous aggregation of neutral lipids in addition to

several small LDs which were about 0.1-0.4 μm in diameter (Figure 5-1c&d, amorphous

neutral lipid aggregation as indicated by arrow head). The neutral lipid aggregation was

very likely to be a heap of LDs which were closely apposed to one another. The

remaining 5 to 10 percent of the cells belonged to the third class. This class contained

many loosely scattered and weakly stained tiny LDs which had a diameter of less than 0.1

μm (Figure 5-1e).

This phenotype of *ylr404w* was not only observed in stationary phase cells, but also in

log phase cells. When refreshed in rich medium until log phase, most of the WT cells

contained 2 or 3 LDs, which were smaller than those of stationary phase, about 0.1 μm in

diameter (Figure 5-1a'). As for *ylr404w* cells, they still could be classified into 3 classes

based on the quantity, shape, and size of LDs. The first class usually contained one LD,

which was 0.3 to 0.6 μm in diameter (Figure 5-1b', as indicated by arrow). The second

class contained an amorphous aggregation of neutral lipids. But compared to their

stationary-phase counterpart, this neutral lipid aggregation was smaller and more weakly

stained (Figure 5-1c', as indicated by arrow head). The third class either contained no

observable LDs, or several tiny ones (Figure 5-1b'). The proportion of these 3 classes among the total cell population and their relative ratio varied between batches of cell culture. Generally, the third class took up more than 50 percent, while the other two classes shared the remaining 50 percent.
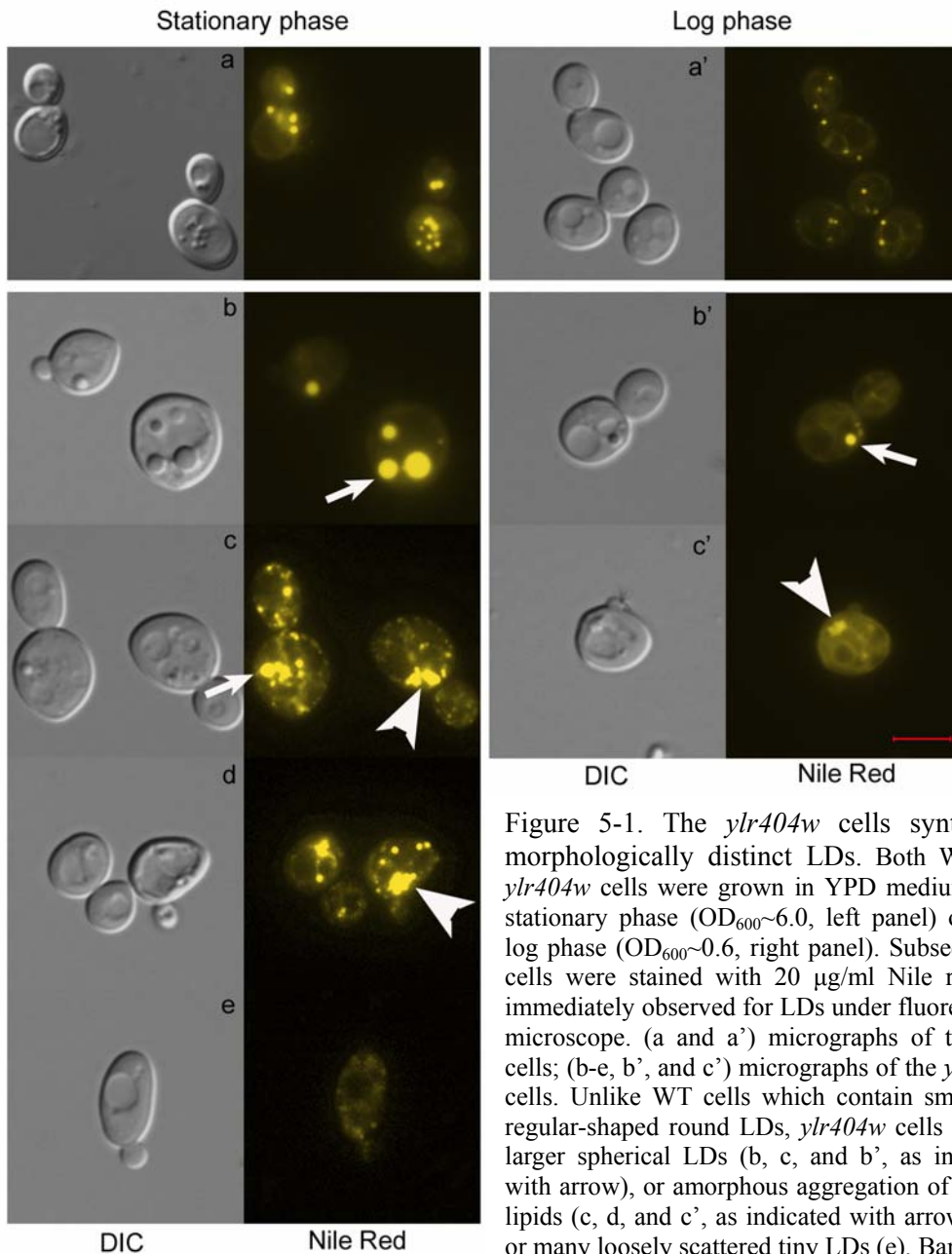
Figure 5-1. The *ylr404w* cells synthesize morphologically distinct LDs. Both WT and *ylr404w* cells were grown in YPD medium until stationary phase (OD_{600}~6.0, left panel) or until log phase (OD_{600}~0.6, right panel). Subsequently cells were stained with 20 μg/ml Nile red and immediately observed for LDs under fluorescence microscope. (a and a') micrographs of the WT cells; (b-e, b', and c') micrographs of the *ylr404w* cells. Unlike WT cells which contain small and regular-shaped round LDs, *ylr404w* cells contain larger spherical LDs (b, c, and b', as indicated with arrow), or amorphous aggregation of neutral lipids (c, d, and c', as indicated with arrowhead), or many loosely scattered tiny LDs (e). Bar, 5 μm.

In order to achieve a better resolution of LDs and to have a better understanding of the nature of the amorphous neutral lipid aggregation observed in some cells, we performed transmission electron microscopy (TEM) for the WT and *ylr404w* strains. Cells were grown in rich medium until stationary phase, harvested, fixed with 2.5% glutaraldehyde, and postfixed with 2% (w/v) osmium tetroxide. The samples were subsequently dehydrated in a series of graded ethanol and embedded in Spurr's Resin. 80-nm ultrathin sections were stained with uranyl acetate and lead citrate and examined under a JEM-1230 Joel electron microscope. Under TEM, LDs appear electron-lucent and thus can be easily identified. As seen in Figure 5-2a, one typical cross-section of a WT cell contained 5 LDs, which were round and were about 0.2 to 0.4 μm in diameter. The cross-sections of *ylr404w* cells could again be divided into 3 classes in the same manner as previously used. Some cross-sections displayed one or several large LDs, which were either round or oval (Figure 5-2, b-e). Consistent with the result of fluorescence microscopy, some LDs could have a diameter of up to 1.5 μm (Figure 5-2d). In sections which displayed several LDs, these LDs very often clumped together and were not clearly demarcated (Figure 5-2, d&e). This phenomenon was further observed in the second class of cross-sections, in which many smaller LDs stayed very close to one another and formed aggregations (Figure 5-2, f&g). These aggregations were reminiscent of the amorphous neutral lipid clump observed under fluorescence microscopy (Figure 5-1, c&d). Class 3 cross-sections contained many tiny LDs, most of which had a diameter of less than 0.1 μm and were loosely scattered. This confirmed our observation of LDs in Figure 5-1e.
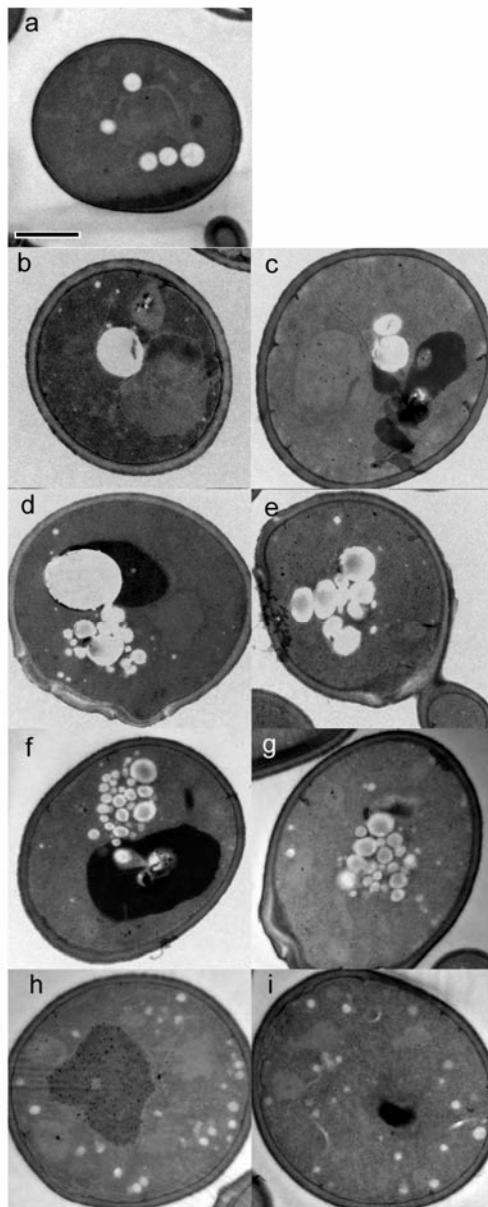
Figure 5-2. Conventional transmission electron microscopy (TEM) of WT and *ylr404w* cells. Cells were grown in YPD to stationary phase, fixed with 2·5% (v/v) glutaraldehyde and 2% (w/v) osmium tetroxide, and subjected to electron microscopy. LDs are seen as electron-transparent droplets. a) TEM of WT cells. This typical cross-section of WT cells contains 5 LDs with a diameter of about 0.2 to 0.4 μm which appear round in shape and clearly demarcated. b-i) TEM of *ylr404w* cells. The cross-sections of *ylr404w* cells either display one or several supersized LDs (b, c, d, e), or an aggregation of small LDs which clump together (f & g), or loosely scattered tiny LDs with a diameter less than 0.1 μm. The tiny LDs can also be observed in other cross-sections (b-g). Bar, 1 μm.
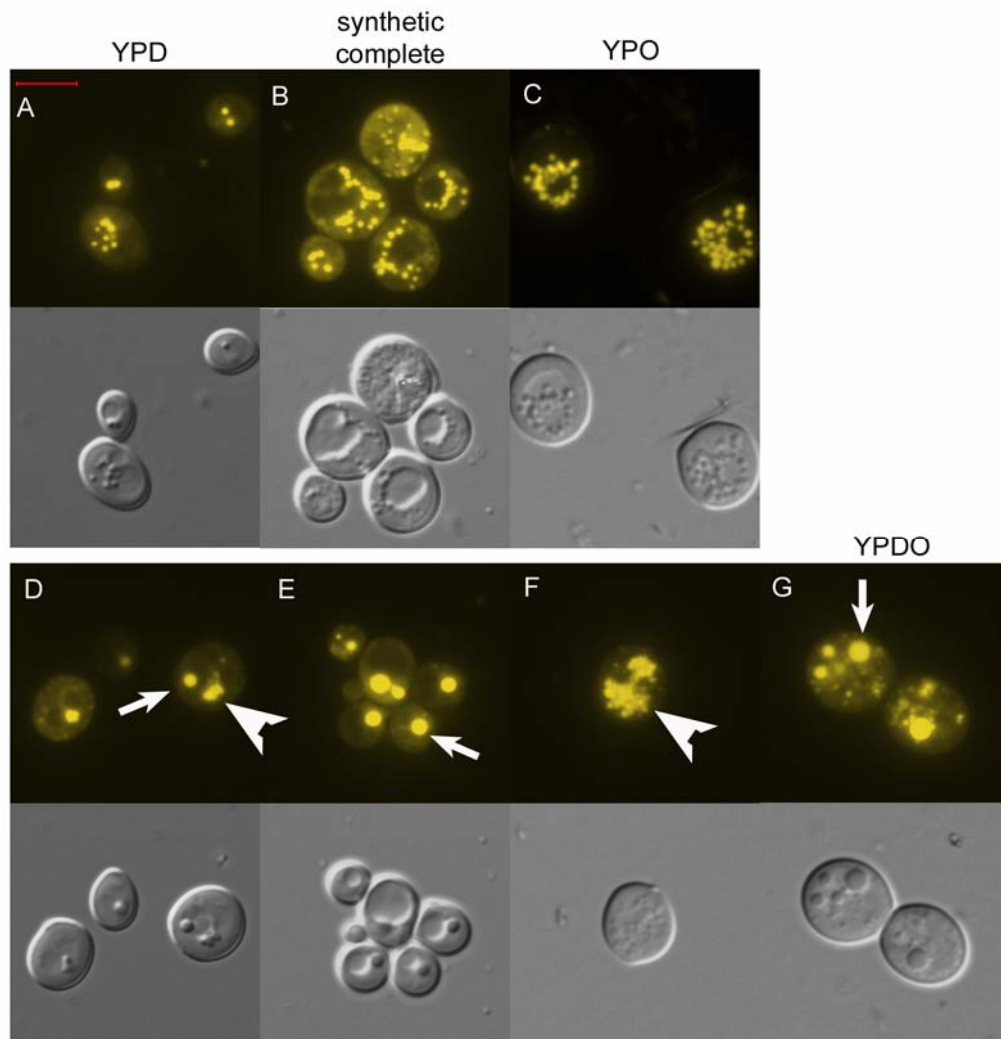
Figure 5-3. Culture media affect LD morphology in *ylr404w* cells. WT and *ylr404w* cells were grown until stationary phase in YPD medium (A&D), synthetic complete medium (B&E), YPO medium (C&F), or YPDO medium (G). The preparation of medium was described in Materials and Methods. Cells were harvested, stained with Nile red, and observed by fluorescence microscopy. A-C) Nile red staining of WT cells. LDs of WT cells hyperaccumulated when the medium was changed from YPD (A) to synthetic complete medium (B), or to YPO medium (C). D-G) Nile red staining of *ylr404w* cells. *ylr404w* cells accumulated supersized LDs (arrow) as well as aggregation of small LDs (arrowhead) when cultured in YPD medium (D). In contrast, more than 80% of the cells accumulated only supersized LDs when grown in synthetic complete medium, whereas more than 95% accumulated only aggregation of small LDs when grown in YPO medium (E). Bar, 5 μm.

5.1.2 LDs of the *ylr404w* cells grown in synthetic complete medium and oleic medium

Images have been shown that *ylr404w* cells synthesize distinctly three types of LDs.

In stationary phase, there are supersized LDs with a diameter of 0.5-1.5 μm, tiny LDs with a diameter of less than 0.1 μm, and amorphous aggregations of intermediate-sized LDs. But how these LDs which differ greatly from one another are produced in the same mutant? Do they represent three stages of LD formation in this mutant? Is there a common mechanism responsible for their formation? With these questions in mind, we subjected the mutant to conditions that lead to the proliferation of LDs, so that we may observe some changes of LDs in different growth conditions.

Yeast cells demonstrated marked proliferation of LDs when they were grown in synthetic medium (an independent observation in this study), or in oleic acid medium (Binns et al., 2006), compared with those cultured in YPD rich medium. As shown in Figure 5-3, A-C, a remarkable increase of LD formation, both in terms of quantity and size, could be observed in WT cells if the culture medium was changed from YPD medium to synthetic complete medium, or to YPO medium. But interestingly, when the *ylr404w* strain was incubated in synthetic complete medium, the average number of LDs did not increase, but rather decreased. As previously stated and also shown in Figure 5-3D, when *ylr404w* cells were grown in YPD medium, they not only accumulated one or several supersized LDs per cell, but also amorphous aggregations of intermediate-sized LDs, which may have a number of more than 20. In addition, less than 10% of the cells contained only one LD. When the culture medium was changed to synthetic complete medium, more than 60% of the cells contained only one large LD, and 20% contained two or several LDs. Accompanying the decrease in their quantity, the average size of the supersized LDs increased: when *ylr404w* cells were grown in YPD medium, the

supersized LDs had an average diameter of 0.81±0.21 μm (n=101); when the cells were cultured in synthetic medium, the average diameter changed to 1.17±0.19 μm (n=99). Moreover, Amorphous LD aggregations were only observed in about 10% of the cells (Figure 5-3E). In contrast, when *ylr404w* cells were cultured in oleic acid medium, more than 95% of the cells accumulated amorphous aggregations of LDs. The supersized LDs observed frequently in YPD medium and more frequently in synthetic complete medium became a rare incidence in YPO medium (Figure 5-3F). However, when the mutant was cultured in YPDO medium, the supersized LDs appeared again (Figure 5-3G), which suggested that the disappearance of these supersized LDs was not a result of the presence of oleic acid, but rather through some unknown mechanism.

5.1.3 LDs of the *ylr404w* cells fuse in vivo

The mechanism underlying the appearance of the supersized LDs observed in the *ylr404w* strain, particularly when the mutant was cultured in the synthetic complete medium, could have four possibilities. First, it may be that many small- or intermediate-sized LDs fuse into one large LD. Second, if the "budding from the ER membrane" is a correct model for LD biosynthesis, LDs that effectively bud from the ER in the WT cells might fail to bud in this mutant. Consequently, many small LDs remain in the two leaflets of the ER membrane and ultimately meet with one another, becoming one large LD. Third, LD biosynthesis might go through the "fission" step in WT cells, by which cells censor the size of LDs and undergo fission if the censored LDs are considered as too large. The *ylr404w* strain might somehow lose this capability. Last, enzymes

catalyzing the synthesis of neutral lipids might be extremely concentrated in one or several domains of the ER in the *ylr404w* strain. According to the delivery model proposed by Robenek *et al*. (2006), newly synthesized neutral lipids are delivered into the nearest LDs. Therefore, concentrated synthesis of neutral lipids might eventually lead to the appearance of the supersized LDs observed in the *ylr404w* strain.

However, the fact that not only did the *ylr404w* cells synthesize supersized LDs, but some of them also synthesized small and tiny LDs, which were either loosely scattered or clumped together, suggests that the last two possibilities are least probable. If there are subdomains of neutral lipids synthesis within the ER membrane, there should not be the third class of *ylr404w* cells in which many tiny LDs are loosely scattered in the cytoplasm. Similarly, inhibition of the fission of LDs also cannot account for the origination of these tiny LDs. In addition, no direct evidence has ever been obtained for LD fission. Therefore, we focused our attention on the first two possibilities.

Could it be that LDs fail to bud from the ER membrane and eventually form the supersized ones? To examine this possibility, we need to have a close look at the spatial relations of the LDs and the ER by means of TEM. If the second possibility is true, we should be able to observe the supersized LDs confined in the two leaflets of the ER membrane. However, under TEM, all the supersized LDs lay outside of the ER. As seen in Figure 5-4, there was no detectable neutral lipids accumulation within the ER membrane leaflets. Between the ER and the supersized LD lay one vacuole. In fact, the LD was so large that it severely compressed this vacuole, resulting in the close apposition of the two opposite ends ($\times$150K). If these supersized LDs should remain between the ER

membrane leaflets, I believe they would greatly reduce the volume of the ER lumen, thereby severely impairing the normal function of the ER.
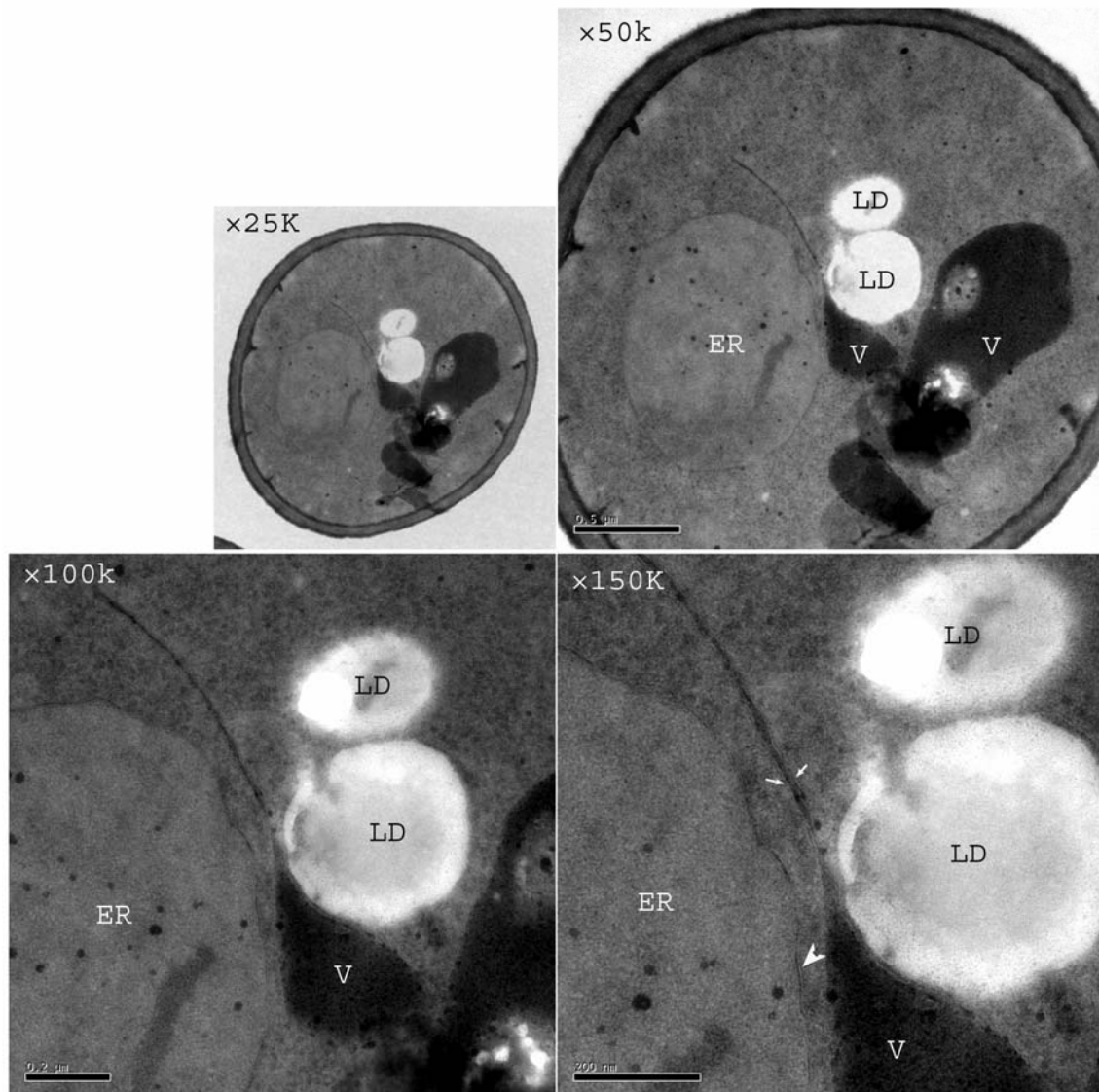
Figure 5-4. The spatial relationship between LDs and the ER in the *ylr404w* cells under TEM. Cells were grown in YPD to stationary phase, fixed with 2·5% (v/v) glutaraldehyde and 2% (w/v) osmium tetroxide, and subjected to electron microscopy. LDs which appear electron-transparent lie outside of the ER. One vacuole lies between the ER and the two LDs. One LD severely compresses the vacuole, leading to the close apposition of the opposite ends of the vacuolar membrane (arrow). No neutral lipids accumulation could be observed between the two leaflets of the ER membrane (arrowhead). V, vacuole.

Then we were left with the only possibility, namely, fusion of small LDs into large ones. Since the appearance of the supersized LDs was more common in the cells grown in the synthetic complete medium than those grown in YPD medium, the *ylr404w* cells were subsequently cultured in the synthetic complete medium until mid-log phase (OD_{600}~1.5), stained with Nile red, and examined for fusion of LDs under microscope. The reason why I chose mid-log phase was that more than 60% of the cells cultured in synthetic complete medium contained only one large LD, which clearly indicated that fusion had already completed in these cells if fusion really occurred. Under fluorescence microscope, cells in which two or several LDs lay close together were targeted. Amazingly, in some of these cells (about 10% of the targeted cells), I did observe the fusion of LDs. It started from the approaching of one LD toward the other, and finished after a new and larger LD appeared. This process was very fast and completed within seconds. To record the fusion of LDs, I collected images at a one-second interval until the fusion process completed. The series of images taken during the fusion of LDs are shown in Figure 5-5A and are also edited into movie format with Macromedia Flash MX 2004 (Movie, in vivo LD fusion). Figure 5-5 B&C show another two examples of LD fusion except that the images were taken before and after the fusion of LDs.
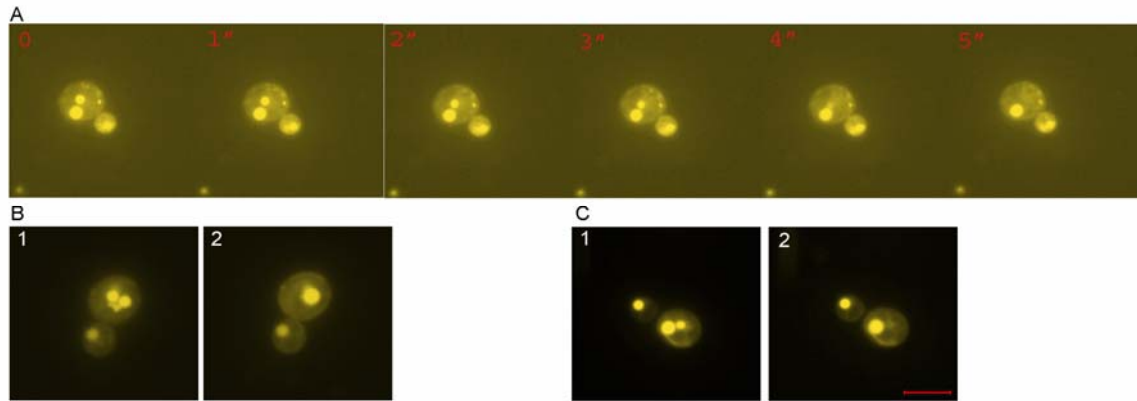
Figure 5-5. Fusion of LDs occurs in *ylr404w* cells and this process requires only several seconds. Cells were grown in synthetic complete medium until mid-log phase (OD$_{600}$~1.5), stained with Nile red, spotted on glass slides and covered with a coverslip. Under the microscope, cells in which two or several LDs lay close together were selected. A) The process of LD fusion in *ylr404w* cells. Images were collected at a one-second interval until the fusion process completed. B and C) another two examples of LD fusion. The images were taken before (1) and after the fusion (2). Bar, 5 μm.

5.1.4 LDs isolated from the *ylr404w* cells fuse in vitro

Based on our observation that fusion of LDs occurred in log-phase *ylr404w* cells, we further supposed that LDs in stationary-phase *ylr404w* cells also possess the ability to fuse with one another. Since over 60% of the cells contained only one LD, there was no chance for this one LD to fuse with another one. Therefore, we need to use the in vitro system.

Tgl3p, a TAG lipase of *S. cerevisiae*, exclusively localizes to LDs (Athenstaedt and Daum, 2003). To mark the LDs, we expressed the GFP-tagged Tgl3p in the WT and *ylr404w* strains. As shown in Figure 5-6A, the Tgl3p-GFP was targeted to the LDs both in the WT and in the *ylr404w* strains. Besides displaying a characteristic ring-like distribution, Tgl3p-GFP in the *ylr404w* cells also demonstrated punctate signals, which were reminiscent of the tiny LDs.
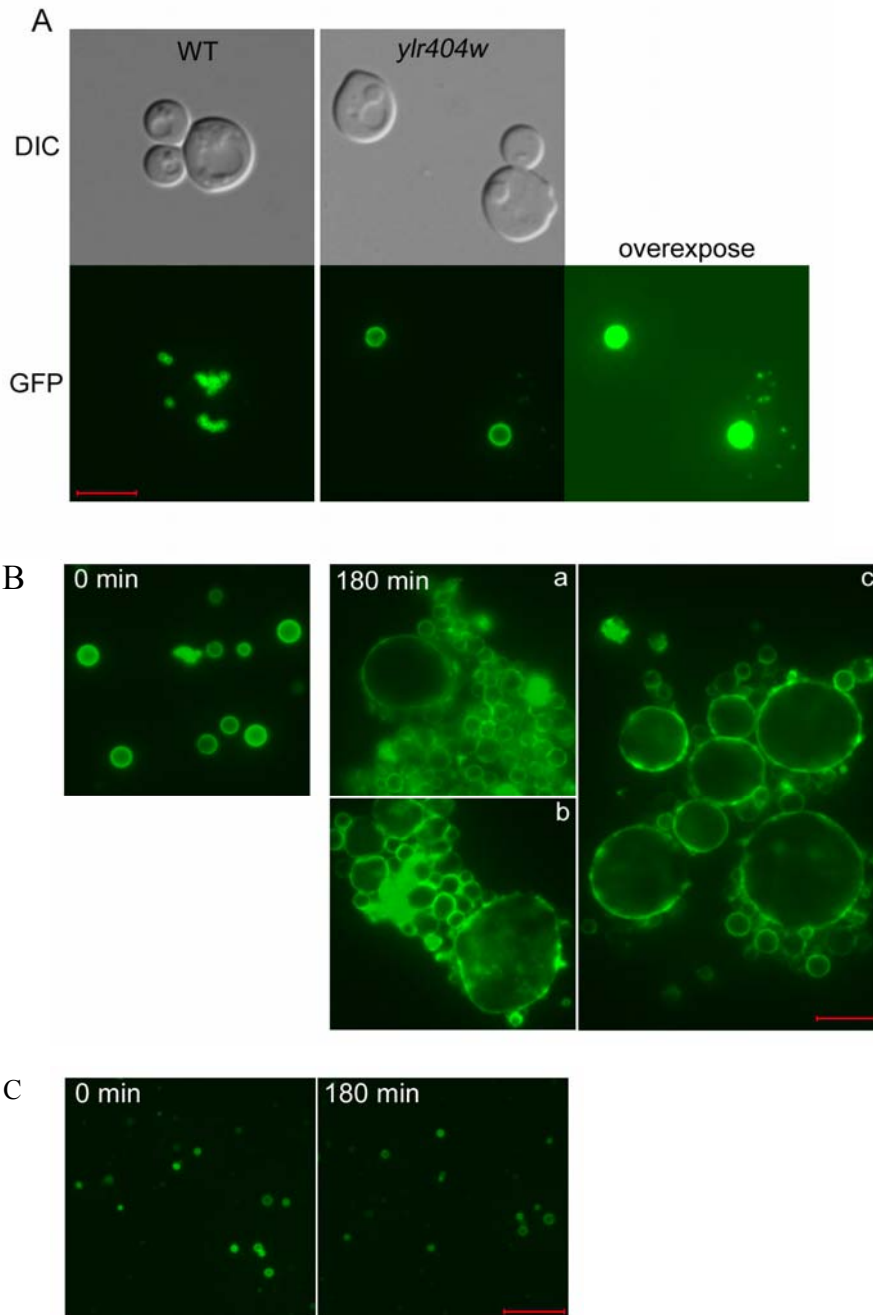
Figure 5-6 LDs isolated from *ylr404w* cells Fuse *in vitro*. A) Tgl3p-GFP exclusively localizes to LDs both in WT and *ylr404w* strains. In order to show tiny LDs in *ylr404w* cell, large LDs were overexposed. B) LDs isolated from *ylr404w* cells Fuse *in vitro*, and this process does not require cytosolic proteins or energy. Tgl3p-GFP tagged LDs were isolated from *ylr404w* cells and resuspended in PBS. Subsequently they were incubated at 30°C for 3 h. The images were taken before (0 min) and after incubation (180 min, a-c). a-c represent different types of fusion. C) LDs isolated from WT cells do not apparently fuse.

WT and *ylr404w* cells harboring the Tgl3p-GFP-expression vector were cultured in

synthetic selection medium until stationary phase (OD$_{600}$~4.5) and were subsequently subjected to isolation of LDs. The detailed procedure was described in Materials and Methods. Isolated LDs were immediately resuspended in cytosol purified from the WT cells, cytosol purified from the *ylr404w* cells, cytosol purified from the LD-deficient QKO strain (*are1Δare2Δdga1Δlro1Δ*), or in PBS buffer. The reaction mixture was incubated at 30°C for 3 h. Before the incubation, LDs isolated from the *ylr404w* cells which had a diameter of 0.5-1.5 μm were evenly distributed in the reaction system, and they did not form aggregations. To our surprise, after 3 h incubation, whatever the LDs were suspended in, many of them clumped to form aggregations. Remarkably, some LDs displayed a diameter of ~10 μm. Obviously these LDs resulted from the fusion of the isolated LDs. Figure 5-6B shows the LDs suspended in PBS before (0 min) and after the incubation (180 min, a-c).

LDs isolated from the WT cells, on the other hand, did not demonstrate obvious fusion (Figure 5-6C). It is noteworthy to mention, however, that this does not prove that isolated wild-type LDs cannot fuse. It is possible that our *in vitro* system was not sensitive enough to detect the fusion of LDs.

5.1.5 In vivo LD fusion in the *ylr404w* cells is filament actin-dependent

It was previously suggested that LDs of NIH3T3 cells undergo microtubule-dependent fusion (Bostrom et al., 2005). To study whether the fusion of LDs of the *ylr404w* cells requires microtubule, I treated the mutant with 15 μg/ml nocodazole or an equivalent amount of DMSO. After 1 h incubation, cells were either subjected to

antitubulin immunofluorescence or Nile red staining, or treated with 0.5 mM oleate for another 1 h, followed by Nile red staining. As seen from Figure 5-7A, microtubule structure was completely disrupted in cells incubated in the presence of nocodazole for 1 h, but remained intact in cells of the control group. Nile red staining before and after oleate treatment showed that cells incubated in the presence of 0.5 mM oleate synthesized much larger LDs. More importantly, microtubule disruption due to nocodazole treatment did not block the formation of supersized LDs, which suggested that the fusion of LDs was not microtubule-dependent.

Subsequently I determined whether actin was required for the fusion of LDs of the *ylr404w* cells. The experimental procedure to study the role of the filament actin (F-actin) in LD fusion was similar to the study of microtubule except that Latrunculin A (Lat-A) was used to disrupt F-actin instead of nocodazole which specifically break microtubule structure. Disruption of F-actin after 1 h treatment of Lat-A was confirmed by Rhodamine phalloidin staining (Figure 5-7B). Subsequently cells were incubated in the presence of 0.5 mM oleate for another 1 h, followed by Nile red staining. It was evident that oleate treatment after F-actin disruption could not lead to the formation of the supersized LDs in the majority of cells. Instead these cells accumulated several small LDs which were loosely distributed and appeared irregular in shape and had a "diameter" of 0.1-0.2 μm. As for cells of the control group, the treatment of an equivalent amount of DMSO did not block the oleate-induced formation of the supersized LDs (Figure 5-7B). Taken together, it is very likely that F-actin is essential for LD fusion in this mutant.

To rule out the probability that F-actin disruption exerts its effect on LD synthesis

instead of on LD fusion, we performed the Lat-A treatment and oleate incubation in the

WT cells. As shown in Figure 5-7C, Lat-A treatment also resulted in disruption of F-actin

in the WT cells, however, it did not lead to significant change of oleate-induced LD

synthesis, both in terms of morphology and quantity. Therefore, it is almost certain that

the inability of the *ylr404w* cells to synthesize the supersized LDs after F-actin disruption

indicates that the fusion of LDs in this mutant is F-actin mediated.
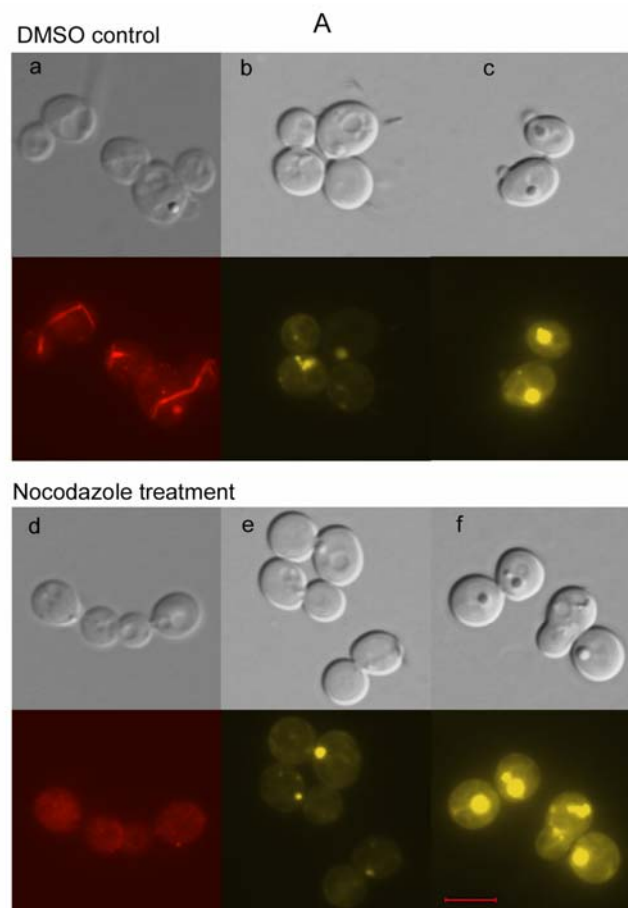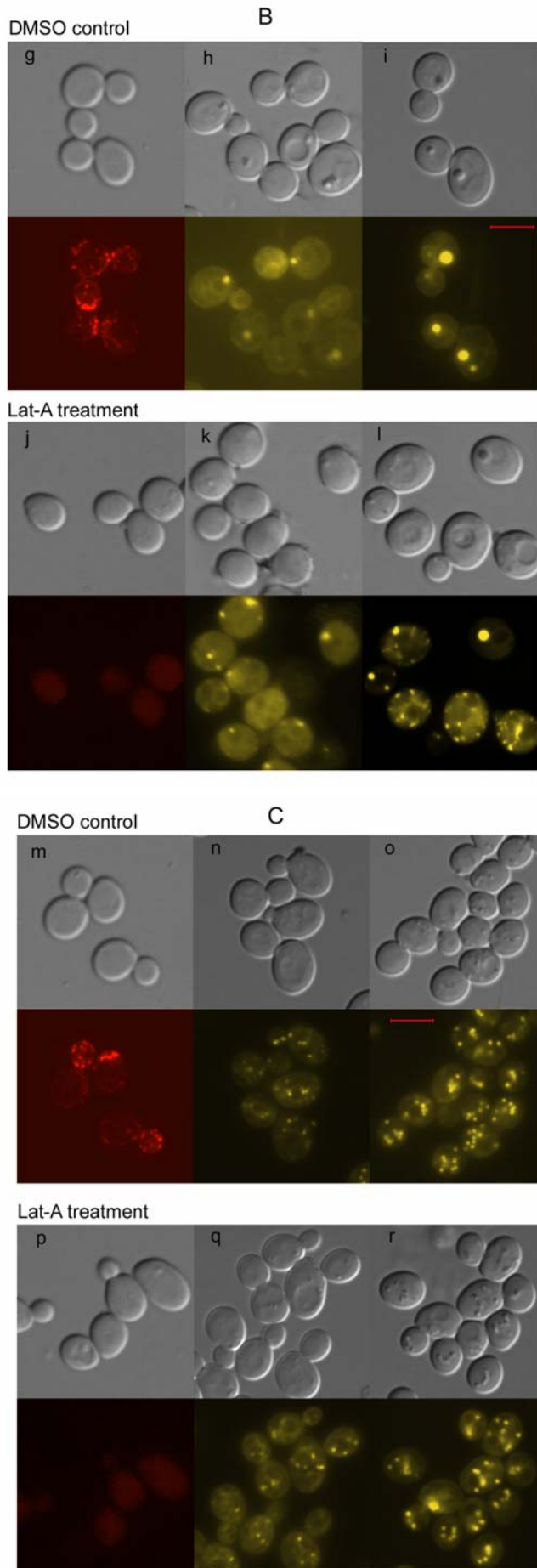
Figure 5-7. Fusion of LDs in the *ylr404w* strain requires filament actin (F-actin), but not microtubule. A) LD Fusion in the *ylr404w* cells is not dependent on microtubule. *ylr404w* cells were grown in YPD until log phase (OD$_{600}$~0.6), and treated with 15 μg/ml nocodazole (d-f) or an equivalent amount of DMSO (0.15% v/v, a-c). After 1 h incubation, cells were either subjected to antitubulin immunofluorescence (a and d) or Nile red staining (b and e), or treated with 0.5 mM oleate for another 1 h, followed by Nile red staining (c and f). B) LD Fusion in the *ylr404w* cells requires intact F-actin. Log-phase *ylr404w* cells were treated with 100 μM Latrunculin A (j-l) or an equivalent amount of DMSO (2% v/v, g-i) for 1h. Subsequently cells were subjected to Rhodamine phalloidin staining (g and j) or Nile red staining (h and k), or treated with 0.5 mM oleate for another 1 h, followed by Nile red staining (i and l). C) Disruption of F-actin by Latrunculin A in WT cells does not greatly affect the synthesis or morphology of LDs. Drug treatment and fluorescence microscopy were the same as in B).

5.2 Functional and structural analysis of Ylr404wp

Why do cells mutated in the ORF *YLR404W* demonstrate LD fusion? What is the function of the protein product of *YLR404W*? How dose Ylr404wp prevent LD fusion in the WT cells? To answer these questions, I carried out functional and structural studies of Ylr404wp.

5.2.1 *YLR404W* complements the *ylr404w* phenotype

```
  1 - ATGAAAATCAATGTATCCCGTCCATTACAGTTTTTACAATGGAGTTCATATATTGTTGTT - 60
  1 - M  K  I  N  V  S  R  P  L  Q  F  L  Q  W  S  S  Y  I  V  V  - 20

 61 - GCATTTCTGATACAATTGCTAATCATTCTTCCTTTATCGATCTTAATATATCACGATTTT - 120
 21 - A  F  L  I  Q  L  L  I  I  L  P  L  S  I  L  I  Y  H  D  F  - 40

121 - TACCTAAGACTATTACCTGCCGATTCCTCTAACGTAGTCCCCCTTAATACGTTCAACATT - 180
 41 - Y  L  R  L  L  P  A  D  S  S  N  V  V  P  L  N  T  F  N  I  - 60

181 - TTAAATGGCGTACAATTTGGTACAAAATTCTTCCAATCTATTAAAAGCATTCCGGTAGGT - 240
 61 - L  N  G  V  Q  F  G  T  K  F  F  Q  S  I  K  S  I  P  V  G  - 80

241 - ACAGATCTGCCGCAAACAATAGACAATGGCTTATCACAGTTAATCCCCATGCGTGACAAC - 300
 81 - T  D  L  P  Q  T  I  D  N  G  L  S  Q  L  I  P  M  R  D  N  - 100

301 - ATGGAATACAAGCTCGATCTAAACCTACAGCTTTATTGCCAGAGCAAAACTGACCATTTA - 360
101 - M  E  Y  K  L  D  L  N  L  Q  L  Y  C  Q  S  K  T  D  H  L  - 120

361 - AATTTAGACAATTTGTTAATTGATGTTTACAGAGGTCCAGGCCCGCTATTGGGTGCTCCT - 420
121 - N  L  D  N  L  L  I  D  V  Y  R  G  P  G  P  L  L  G  A  P  - 140

421 - GGAGGAAGTAACAGCAAAGATGAAAAAAATCTTTCACACTTCTAGACCTATTGTCTGCCTC - 480
141 - G  G  S  N  S  K  D  E  K  I  F  H  T  S  R  P  I  V  C  L  - 160

481 - GCACTGACGGATTCCATGTCGCCTCAGGAGATCGAACAACTAGGCCCATCACGTCTAGAC - 540
161 - A  L  T  D  S  M  S  P  Q  E  I  E  Q  L  G  P  S  R  L  D  - 180

541 - GTTTACGATGAAGAATGGCTAAATACAATAAGAATAGAGGACAAAATATCGTTAGAGTCT - 600
181 - V  Y  D  E  E  W  L  N  T  I  R  I  E  D  K  I  S  L  E  S  - 200

601 - TCATATGAAACAATCTCGGTGTTCTTGAAAACGGAGATTGCCCAAAGAAATCTAATAATA - 660
201 - S  Y  E  T  I  S  V  F  L  K  T  E  I  A  Q  R  N  L  I  I  - 220

661 - CATCCAGAAAGTGGGATTAAGTTTAGGATGAATTTTGAGCAGGGATTAAGAAACTTGATG - 720
221 - H  P  E  S  G  I  K  F  R  M  N  F  E  Q  G  L  R  N  L  M  - 240

721 - CTTCGAAAAAGATTTTTATCTTATATTATTGGCATTTCAATTTTCCATTGCATAATATGT - 780
241 - L  R  K  R  F  L  S  Y  I  I  G  I  S  I  F  H  C  I  I  C  - 260

781 - GTACTTTTTTTTATCACAGGTTGCACTGCATTCATTTTTGTTAGAAAGGGTCAGGAAAAA - 840
261 - V  L  F  F  I  T  G  C  T  A  F  I  F  V  R  K  G  Q  E  K  - 280

841 - TCCAAGAAACATAGCTGA - 858
281 - S  K  K  H  S  *
```

Figure 5-8. Nucleotide sequence and deduced amino acid sequence for *YLR404W*.

YLR404W is located on chromosome 12 of *S. cerevisiae*. Before this study, it was still an uncharacterized ORF encoding a putative 285-amino acid protein (Figure 5-8). In order to confirm that the *ylr404w* phenotype was indeed caused by the deletion of *YLR404W*, I transformed this mutant with vectors expressing Ylr404wp and tested whether the gene *YLR404W* complemented the *ylr404w* phenotype.

Two Ylr404wp-expression vectors were constructed. First, a 1.4 Kb fragment containing the natural promoter and the coding sequence before the stop codon of *YLR404W* was subcloned into the *HindIII*- and *BamHI*-cleaved YCplac111-GFP plasmid in which the GFP coding sequence was inserted between the *BamHI* and *EcoRI* restriction sites, such that Ylr404wp was C-terminally GFP-tagged. Second, The coding sequence of *YLR404W* including the stop codon was inserted between the *BamHI* and *EcoRI* sites of the pYEX 4T-1 plasmid, such that Ylr404wp was N-terminally GST-tagged and was under the control of copper promoter. The *ylr404w* strain was transformed with either one of the two constructs or their corresponding empty vectors, and grown in synthetic selection media until stationary phase. Subsequently cells were stained with Nile red and observed under microscope. As seen in Figure 5-9, *ylr404w* cells transformed with the empty YCplac111 -GFP or pYEX 4T-1 still synthesized supersized LDs, while those transformed with YCplac111-YLR404W-GFP or pYEX 4T-1-YLR404W synthesized several small LDs, resembling the WT cells. Since *YLR404W* complemented the *ylr404w* phenotype, a conclusion was reached that the deletion of *YLR404W* was responsible for the formation of supersized LDs in the *ylr404w* strain.
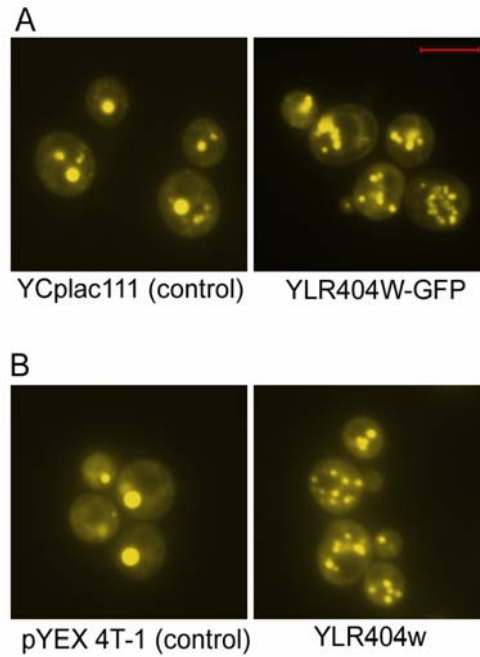
Figure 5-9. Transformation of *YLR404W* gene complements the *ylr404w* phenotype. Transformed *ylr404w* cells were grown in appropriate selection media until stationary phase, followed by Nile red staining and fluorescence microscopy. A) Cells were transformed either with YCplac111 vector alone or with YCplac111-YLR404W-GFP. B) Cells were transformed either with pYEX 4T-1 vector alone or with pYEX 4T-1-YLR404W.

5.2.2 Ylr404wp is an integral ER membrane protein

To understand the molecular function of Ylr404wp, I first examined its subcellular localization. For this purpose, *ylr404w* cells transformed with YCplac111-YLR404W-GFP were used. As shown in Figure 5-10A, these cells expressed a ~60kDa protein recognized by anti-GFP rabbit serum, corresponding to the GFP-tagged Ylr404wp. In contrast, lysate prepared from cells transformed with the empty YCplac111-GFP did not show such a band. To gain insights into the intracellular localization of Ylr404wp, differential centrifugation experiments were performed. Cell extracts prepared from *ylr404w* cells expressing GFP-tagged Ylr404wp were fractionated by centrifugation at 13 000 g for 10 min, resulting in P13 pellet and S13 supernatant fractions, which were further probed with anti-GFP. Immunoblotting analysis showed that similar to ER protein

Dpm1, GFP-tagged Ylr404wp was predominantly found in the P13 fraction, which contains membranes derived from the ER, plasma membrane, vacuoles, mitochondria and nuclei (Figure 5-10B). To better define the subcellular distribution of Ylr404wp, cell extracts were subjected to continuous sucrose density gradient analysis. Thirteen fractions were collected from top to bottom (1-13) and probed for the presence of GFP-tagged Ylr404wp and Dpm1 (ER) by immunoblotting. For Ylr404wp, a distribution pattern coincided with that of Dpm1 was observed, confirming the ER localization of Ylr404wp (Figure 5-10C).

To further examine the localization of Ylr404wp in the ER, we observed by fluorescence microscopy the GFP signal of the Ylr404wp-GFP fusion protein. As shown in Figure 5-10D, Ylr404wp-GFP was found exclusively on the ER membrane. This observation plus the results described above provide strong evidence that Ylr404wp is an ER membrane protein.

Membrane proteins can be classified into two categories: integral and peripheral. To examine the nature of the association of Ylr404wp with the ER membrane, equal aliquots of a P13 fraction were treated with 1% triton X-100, 6 M urea, 0.1M Na_2CO_3 PH 11, 1 M NaCl, or lysis buffer (mock) respetively on ice for 30 min, and then centrifuged at 100,000 g for 45 min resulting in S (supernatants) and P (pellets), which were subsequently probed for the presence of Ylr404wp-GFP. As shown in Figure 5-10E, Ylr404wp-GFP was solubilized by 1% triton, however, it was not affected by treatments with 6 M urea, 1 M NaCl and 0.1 M Na_2CO_3 PH 11, which dissociate peripheral membrane proteins only. Thus, Ylr404wp is an integral ER membrane protein.
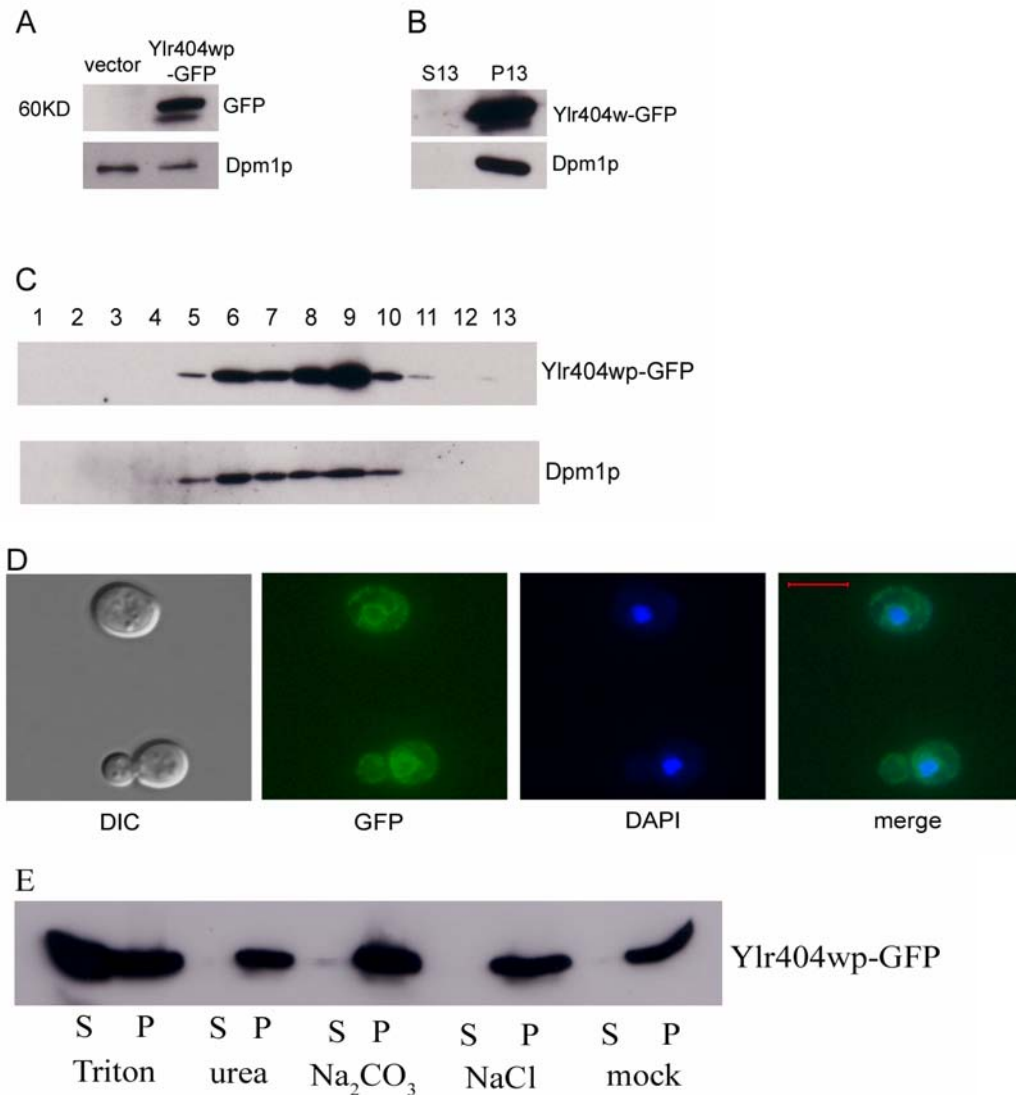
Figure 5-10. Ylr404wp is an integral endoplasmic reticulum (ER) membrane protein. A) *ylr404w* cells transformed either with YCplac111 vector alone or with YCplac111-YLR404W-GFP were lysed and immunoblotted with anti-GFP. The molecular weight of Ylr404wp-GFP is about 60 KD. B) Differential centrifugation fractionation analysis of yeast proteins. Cells expressing Ylr404wp-GFP were spheroplasted and subjected to differential centrifugation as described in Materials and Methods. The 13,000 g pellet (P13) and soluble fraction (S13) were analyzed by immunoblot using anti-GFP and anti-Dpm1. C) Cells expressing Ylr404wp-GFP were lysed in STED buffer using glass beads and a 500 g supernatant was loaded on the top of a continuous sucrose gradient (10-53%) and centrifuged at 100,000 g for 15h. Fractions were collected from the top, separated by SDS-PAGE and immunoblotted with anti-GFP and anti-Dpm1. D) Fluorescence microscopy. GFP signal shows the localization of GFP-tagged Ylr404wp; DAPI shows the nucleus. Bar, 5 μm. E). Membrane extraction. The P13 fraction of Ylr404wp from *ylr404w* cells was treated with the indicated reagents on ice and centrifuged at 150,000g again resulting in pellet (P) and supernatant (S). Mock: treatment with lysis buffer only.

5.2.3 Cytosolic segments are not essential for the function of Ylr404wp in

preventing the formation of supersized LDs

An integral membrane protein always has a unique orientation in the membrane, which determines the protein's function. In this study, we found that yeast strain lacking Ylr404wp, an ER integral membrane protein, accumulated supersized LDs, which almost certainly result from the fusion of many small LDs. In order to better understand the role of Ylr404wp in LD synthesis, I decided to determine its topology.

First, a computer-based approach was taken to identify the transmembrane domains. Specifically, 3 prediction models (TMHMM, HMMTOP, and SOSUI) were used. The result shows that all 3 models agreed that Ylr404wp contains two transmembrane helices (Table 5-1). In addition, according to TMHMM and HMMTOP prediction, both N-terminus and C-terminus are cytosolic.

Table 5-1 Prediction of transmembrane helix in Ylr404wp by TMHMM, HMMTOP, and SOSUI.

Model	Reference	Result		
TMHMM	Krogh et al., 2001	inside	1	12
		TMhelix	13	35
		outside	36	251
		TMhelix	252	274
		inside	275	285
HMMTOP	Tusnady and Simon, 1998	inside	1	16
	Tusnady and Simon, 2001	TMhelix	17	36
		outside	37	248
		TMhelix	249	273
		inside	274	285
SOSUI	Hirokawa et al., 1998	TMhelix	15	37
		TMhelix	248	270

Consistent with this prediction, Kim et al. (2003) previously provided evidence that the C-terminus of Ylr404wp is cytosolically oriented. In their study, they chose a dual Suc2/His4C topology reporter to examine whether a protein's C-terminus is in the cytosol or in the ER lumen. *SUC2* gene of this reporter encodes a segment of invertase containing

eight *N*-glycosylation acceptor sites. When this domain is localized in the ER lumen, the fusion protein becomes heavily glycosylated. The histidinol dehydrogenase activity of the His4C moiety converts histidinol to histidine only when it is localized in cytosol. Thus, only cells expressing fusion proteins with the reporter domain in the cytosol can grow on histidine-free media supplemented with histidinol. Since the yeast strain expressing the Ylr404wp-Suc2/His4C fusion protein could grow on histidine-free media supplemented with histidinol but did not glycosylate the reporter, it indicated that the C-terminus is cytosolic. Given that Ylr404wp is predicted to be a double-pass membrane protein and hence N-terminus and C-terminus have the same orientation, we may reach a conclusion that this protein's N-terminus is also in the cytosol.

LDs lie outside of the ER. It is, therefore, tempting to determine which protein segment, cytosolic termini or luminal domain, is essential for Ylr404wp's function in preventing the fusion of LDs. For this purpose, I made four constructs that expressed different GST-tagged truncated Ylr404wps lacking N-terminus (Ylr404wp-12-285), C-terminus (Ylr404wp-1-274), N-terminus plus the first transmembrane helix (Ylr404wp-37-285), and C-terminus plus the second transmembrane helix (Ylr404wp-1-253), respectively. The schematic diagram of these mutant proteins is shown in Figure 5-11A. The expression of these proteins was confirmed by immunoblotting against GST (Figure 5-11B). As shown in Figure 5-11C, both Ylr404wp lacking N-terminus and that lacking C-terminus could restore the normal LD formation in the *ylr404w* mutant, suggesting that neither N-termial nor C-terminus is essential for this protein's function. In contrast, both transmembrane helices are indispensable for its

normal activity, because constructs expressing GST- Ylr404wp-37-285 and GST-Ylr404wp-1-253 could not rescue the mutant from producing supersized LDs. Considering that transmembrane domains determine a targeted integration of proteins into the membrane, we may conclude that both transmembrane helices of Ylr404wp are required for the correct location of its luminal domain. Therefore, it is possible that Ylr404wp's function depends on the luminal segment. This will be further discussed in section 5.3.
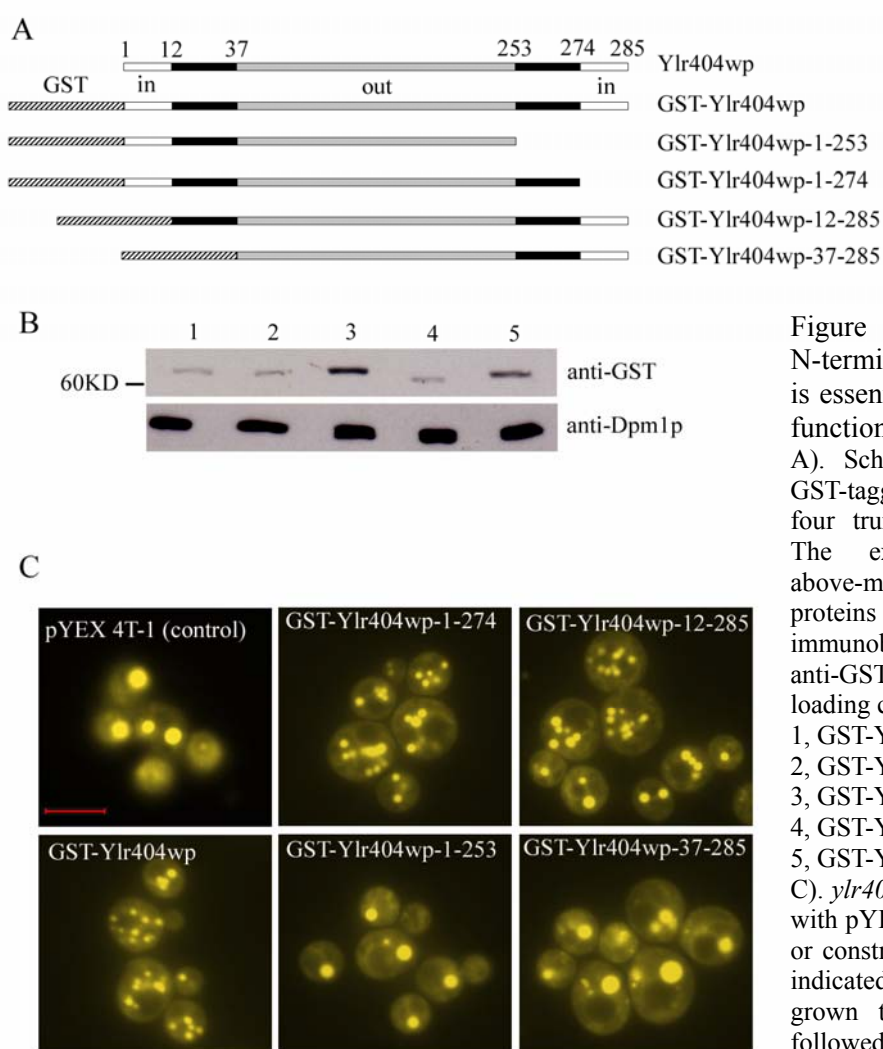
Figure 5-11 Neither N-terminus nor C-terminus is essential for Ylr404wp's function in LD formation. A). Schematic diagrams of GST-tagged Ylr404wp and its four truncated variants. B). The expression of the above-mentioned five proteins as confirmed by immunoblotting against anti-GST. Dpm1 serves as a loading control.
1, GST-Ylr404wp-1-253;
2, GST-Ylr404wp-1-274;
3, GST-Ylr404wp-12-285;
4, GST-Ylr404wp-37-285;
5, GST-Ylr404wp.
C). ylr404w cells transformed with pYEX4T-1 empty vector or constructs that express the indicated proteins were grown to stationary phase, followed by Nile red staining and fluorescence microscopy.

5.2.4 Overexpression of Ylr404wp does not further reduce the size of LDs

Deletion of *YLR404W* resulted in the formation of supersized LDs in the *ylr404w* mutant, indicating that Ylr404wp is implicated in LD formation. But what will become of the size of LDs when this protein is overexpressed? Will the LDs be even smaller? To answer this question, I experimentally induced the overexpression of Ylr404wp. In the construct pYEX 4T-1-YLR404W, the expression of the GST-Ylr404wp fusion protein is under the control of *CUP1* promoter, which can be induced in the presence of copper sulfate. As shown in Figure 5-12B, addition of 100 μM copper sulfate significantly increased the amount of GST-Ylr404wp (Dpm1 was used as a loading control). However, this marked elevation of Ylr404wp's intracellular concentration did not lead to significant change of the size of LDs (Figure 5-12A), suggesting that the overexpression of Ylr404wp could not further reduce the size of LDs.
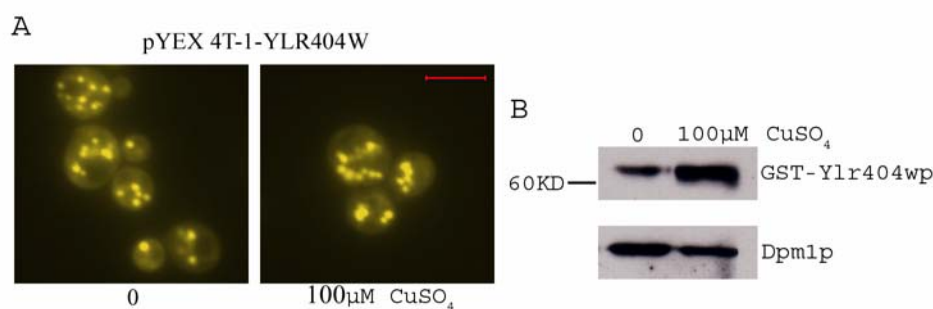
Figure 5-12. Overexpression of Ylr404wp does not lead to morphological change of LDs. To induce the overexpression of Ylr404wp, *ylr404w* cells transformed with pYEX4T-1-YLR404W were cultured in the presence of 100 μM CuSO₄. A) Nile red staining. B) The expression level of GST-Ylr404wp. Dpm1 serves as a loading control.

5.3 Sequence homologs of Ylr404wp

Table 5-2, Prediction of transmembrane helices by TMHMM, HMMTOP, and SOSUI in proteins that exhibit sequence similarity to Ylr404wp. * denotes a weakly predicted transmembrane helix.

protein	Prediction Model	Result		
Kpol_1002p3	TMHMM	inside	1	14
		TMhelix	15	37
		outside	38	240
		TMhelix	241	263
		inside	264	281
	HMMTOP	inside	1	16
		TMhelix	17	36
		outside	37	248
		TMhelix*	194	210
		inside	211	240
		TMhelix	241	261
		outside	262	281
	SOSUI	TMhelix	18	40
		TMhelix	242	264
CAGL0M09933g	TMHMM	inside	1	14
		TMhelix	15	37
		outside	38	240
		TMhelix	241	263
		inside	264	273
	HMMTOP	inside	1	16
		TMhelix	17	37
		outside	38	237
		TMhelix	238	262
		inside	263	273
	SOSUI	TMhelix	16	38
		TMhelix	241	263
AER072Wp	TMHMM	inside	1	14
		TMhelix	15	37
		outside	38	227
		TMhelix	228	250
		inside	251	261
	HMMTOP	inside	1	11
		TMhelix	12	36
		outside	37	226
		TMhelix	227	251
		inside	252	261
	SOSUI	TMhelix	15	37
		TMhelix	228	250
CAH02060	TMHMM	inside	1	14
		TMhelix	15	37
		outside	38	207
		TMhelix	208	230
		inside	231	232
	HMMTOP	inside	1	16
		TMhelix	17	41
		outside	42	204
		TMhelix	205	229
		inside	230	232
	SOSUI	TMhelix	16	38
		TMhelix	206	228

PROMALS alignment

```
Ylr404wp        1   MKINVSRPLQFLQWSSYIVVAFLIQLLIILPLSILIYHDFYLRLLPADSS---NVVPLNTFNI-------  60
Kpol_1002p3     1   MLVNVTRPLQLLQWSSYIAITCLVQLLIILPLSILIFHDFYARLLPPDSS---QWVPLSTSNT-------  60
CAGL0M09933g    1   MKFNLTRPLQIAQWVSYILGVGILQIVVILPLAVLLFHDFYTRLLPSDSS---VWVPLDNFNS-------  60
CAH02060        1   MKINVSIPLQAARWFSYLLILICIEIIFILPLSNLLWIDFINRLIPNNRM---HVIPLSNMAN-------  60
AER072Wp        1   MQINVLGPVQWVPWATYAAVILWVQVVVILPLATVLWQDFYSQLLPSESLFERQLRPVKAPASAAGSVNN  70

Ylr404wp       61   LNGVQFGTKFF--QSIKSIPVGTDLPQTIDNGLSQLIPMRDNMEYKLDLNLQLYCQSKTDHLNLDNLLID  128
Kpol_1002p3    61   FDF----EKFD--QYIDRISIDKPLPPILDNGLSQMIPLRDYILYKMDLDYKFYCLK--DSVNRG-----  117
CAGL0M09933g   61   -NASGLNTRFK--QGIVCVSPDKQLPGLKPNGLSQPIALRCHTNYKLDMKLEFYCHSLD---------A  117
CAH02060       61   SWTV----PFD----LRVIANV---TSTKENEIRSDIPL------DVTLNLGIYCTSH-----------  101
AER072Wp       71   MWSMDLWRRSVSPQDVKSTPPS---AAQEQLAVQSGIR------YLLVIDLQLQCFDQ-----------  119

Ylr404wp      129   VYRGPGPLLGAPGGSNSKDEK---IFH-TSRPIVCLALTDSMSPQEIEQL-G-PSRLDVYDEEWLNTIRI  192
Kpol_1002p3   118   -YKSPLDTLQLRVSVATTDDDVSTVIYRRNIPIVCIRDTDSISTEGLSKI-G-PNRLKVFEKEWQNHIDI  184
CAGL0M09933g  118   IGNSKGTDLQYAVVSLSDDSN---LFYRYRQPVICRNQ-GATNVLEGNNH-A-KSRMEVLRNEWLNSLSL  181
CAH02060      102   ---RPIE-----AVTLSIDDN------PRKLPLVCFDN---LNFLSSRFN-GFDSVSKTVKKDVINDFKF  153
AER072Wp      120   ---EPIH-----VVTVEVTAQ------TESFTVTCFPG---VEHAMRSPWTA-QPLATRIQHEFENRLQL  171

Ylr404wp      193   EDKISLESSYETISVFLKTEIAQRNLIIHPESGIKFRMNFEQGLRNLMLRKRFLSYIIGSIFHCIICVL  262
Kpol_1002p3   185   EDKISIDPDVVKIYYDFIPGSPSMHLKFDPKSGARYRMEFQQGFRNIMLRWRKLTHIFGTLVCYVIISTL  254
CAGL0M09933g  182   EDIADISPQLENIEISIDLPNSNGEILLEPTSGILLRRSFEQGLRNWMLRRWRTTYIIGTAVFYISLSFI  251
CAH02060      154   G--FPVNPDNKRIRIDLKDYTEDYLLSY---INVQFSVKYT-GFRKFLLSWRRTCHLLGTLLFASLISSC  217
AER072Wp      172   PD-ILLSADTRMVNVTIQSTARLRFGHR---SAYSLSMQVG-GIRYAMLHWYRTCHILGTTLFVGVISAW  236

Ylr404wp      263   F--FITGCTAFIFVRKGQ-----E-KSKKHS  285
Kpol_1002p3   255   F--SVTGVLSFYLVNQKELATGTG-TDTKT-  281
CAGL0M09933g  252   F--VITCMATFLIFTKVY-----G-KHQKQ-  273
CAH02060      218   FLLSFTGVFSYIVMA---------------  232
AER072Wp      237   FYISFSIAFMVIGFLRGA-----GAKNTKS-  261
```

Figure 5-13. Sequence alignment of Ylr404wp and its homologs via PROMALS. Amino acids in red are identical and those in blue are highly similar between species. Orange bars represent two transmembrane domains. Black bars are regions selected for mutagenesis study.

To identify the sequence homologs of Ylr404wp, the protein's predicted amino acid sequence was analyzed by BLAST searches of the NCBI database using protein-protein BLAST algorithm (search date, October, 2007). The list of proteins that exhibited a significant (E-values≤1e-4) similarity to Ylr404wp included a hypothetical protein Kpol_1002p3 of *Vanderwaltozyma polyspora* (Score = 192 bits (487), Expect = 2e-47), a hypothetical protein CAGL0M09933g of *Candida glabrata* (Score = 174 bits (442), Expect = 4e-42), AER072Wp of *Ashbya gossypii* (Score = 58.5 bits (140), Expect = 5e-07), an unnamed protein product (accession No., CAH02060) of *Kluyveromyces lactis* (Score = 50.4 bits (119), Expect = 1e-04). Interestingly, all these four proteins were predicted to be double-pass integral membrane proteins, including Kpol_1002p3 which was also very likely a double-pass transmembrane protein based on the prediction by

TMHMM and SOSUI (Table 5-2), indicating it is highly likely that these proteins and Ylr404wp are of the same family.

To further study their sequence relationship, I carried out a multiple sequence alignment for these five proteins using PROMALS (Pei and Grishin, 2007) and the result is shown in Figure 5-13. Apparently, amino acids of the N-terminus and two transmembrane helices display better homology, followed by several residues in the luminal segment. Because both termini seem not essential for Ylr404wp's function in LD synthesis, in order to determine whether the luminal region really accounts for this protein's function, I performed multiple amino acid deletions and single amino acid changes to two of these residues (amino acids 44-46 and 105-113) by site-directed mutagenesis. Among the 14 recombinant variants (44-46D (deleted), L44D, L45D, P46L, 105-113D, L105D, D106A, L107D, N108A, L109D, Q110A, L111D, Y112D, C113T), except N108A and Q110A, the other 12 mutants obliterated the rescue effect of Ylr404wp in the *ylr404w* strain, no matter these mutants were expressed by pYEX 4T-1(Figure 5-14A) or YCPlac111 vector (Figure 5-14B). GFP signals showed that N108A and Q110A maintained Ylr404wp's localization to the ER membrane, while the other variants formed spherical protein bodies whose nature remains to be determined at this stage (Figure 5-14C). This set of data not only implied that the luminal region is essential for the protein's function, but also provided support that the aforesaid four proteins are homologs of Ylr404wp.
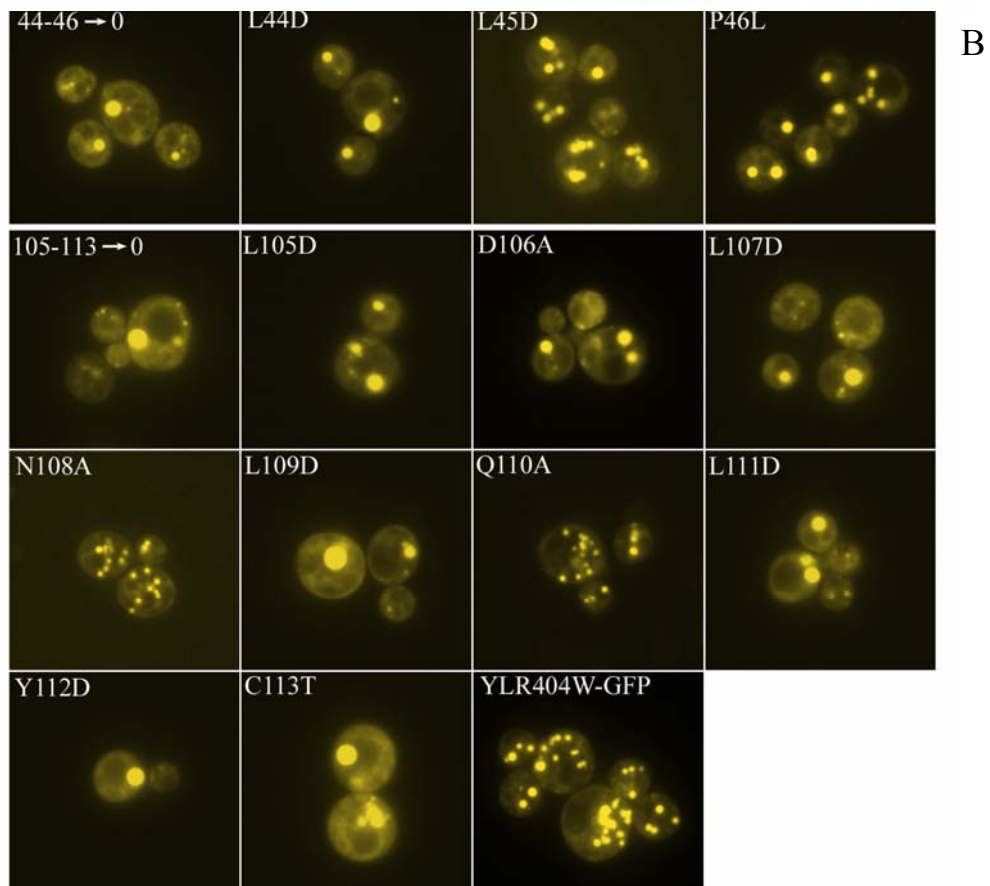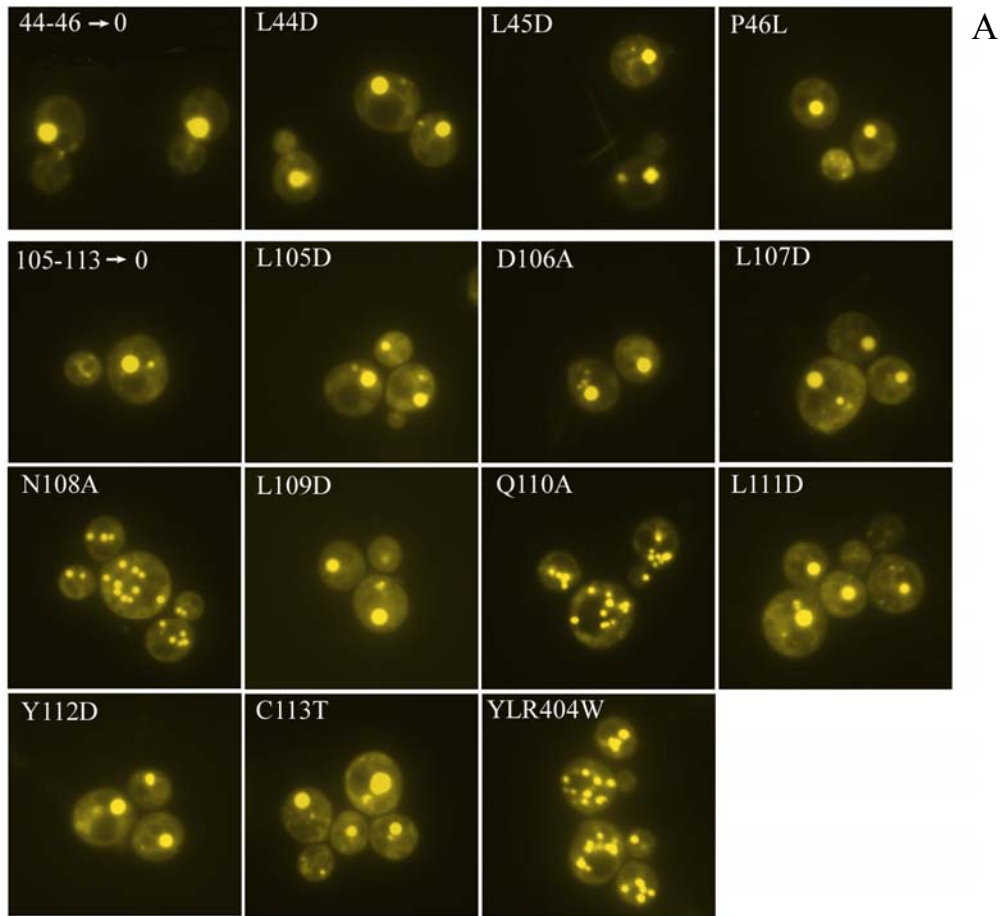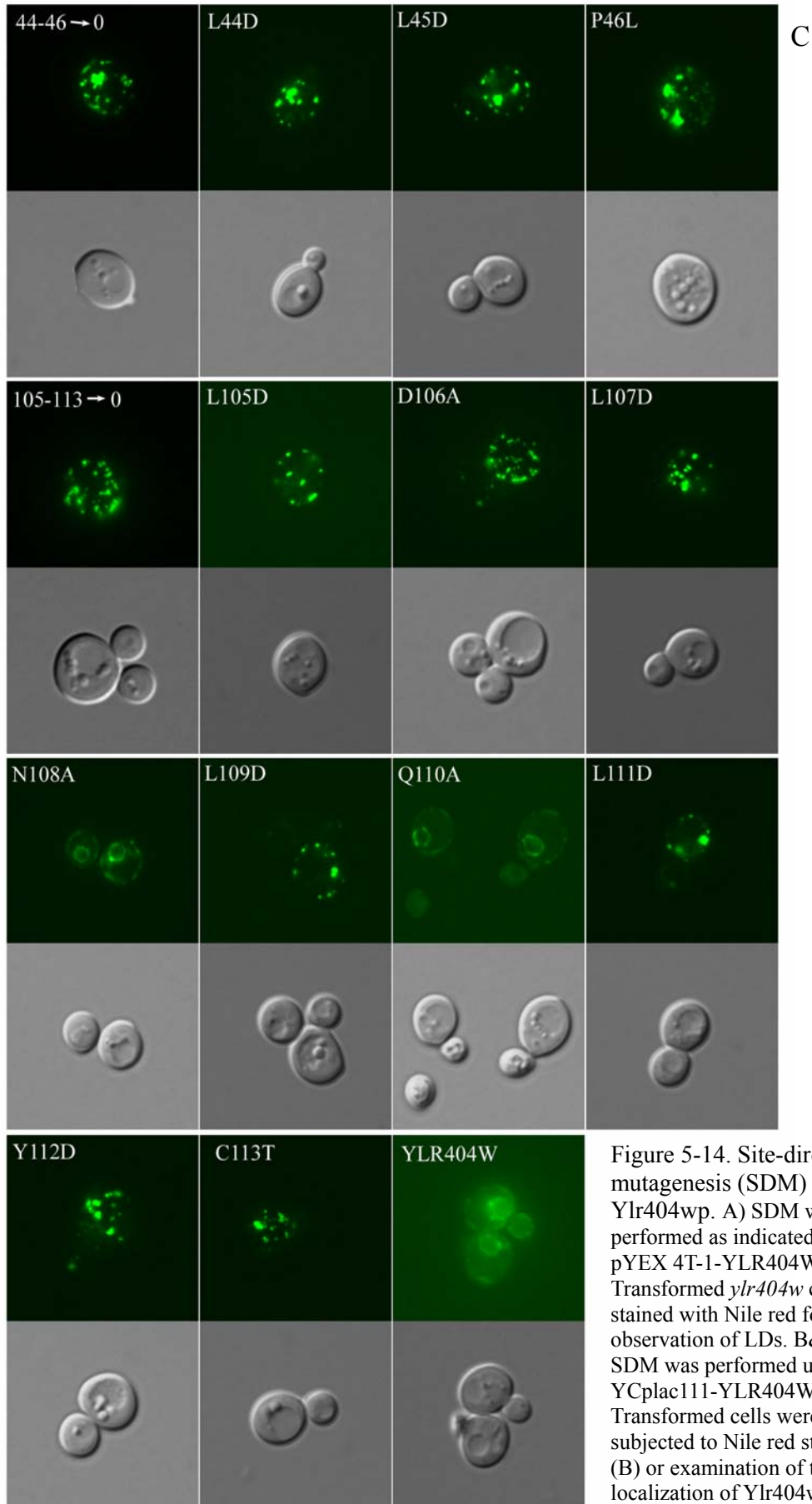
Figure 5-14. Site-directed mutagenesis (SDM) of Ylr404wp. A) SDM was performed as indicated using pYEX 4T-1-YLR404W. Transformed *ylr404w* cells were stained with Nile red for observation of LDs. B&C) SDM was performed using YCplac111-YLR404W-GFP. Transformed cells were subjected to Nile red staining (B) or examination of the localization of Ylr404wp-GFP (C).

However, no mammalian homologs of Ylr404wp were identified via protein-protein BLAST searches. The organisms hosting the above-mentioned five proteins including Ylr404wp are all under the order of Saccharomycetales (Fungi › Dikarya › Ascomycota › Saccharomycotina › Saccharomycetes › Saccharomycetales). Given that these species are far from mammals, it is probable Ylr404wp and its mammalian homologs only share certain motifs. To identify these proteins, I performed Position-Specific Iterated BLAST searches. The result showed that Ylr404wp and several mammalian FOXD4 proteins share the same PGPLLGAP motif (Figure 5-15). However, none of these proteins were predicted to be integral membrane proteins by TMHMM, HMMTOP, and SOSUI. In addition, this PGPLLGAP motif is even not found in the four identified sequence homologs of Ylr404wp. Therefore, these FOXD4 proteins were very unlikely to be of the same family as Ylr404wp. To verify my prediction, I performed multiple amino acid deletions and single amino acid changes to this motif, and found that none of them affected the biological activity of Ylr404wp (Figure 5-16A) or changed its subcellular localization (Figure 5-16B), which indicated that this motif is not essential and these proteins are not Ylr404wp's homologs.

Besides these FOXD4 proteins, human seipin which is responsible for the Berardinelli–Seip congenital lipodystrophy syndrome and its mammalian homologs were also identified by Position-Specific Iterated BLAST query. Is this class of proteins closely related with Ylr404wp? Do they function similarly as Ylr404wp? These questions will be addressed in Chapter 6.

>Ylr404wp [Saccharomyces cerevisiae]   133   PGPLLGAP   140

> FOXD4 protein (Accession No., AAI03887) [Homo sapiens]   228   PGPLLGAP   235

> FOXD4 protein (Accession No., AAQ72341) [Pan troglodytes] 233   PGPLLGAP   240

> FOXD4 protein (Accession No., AAQ72339) [Gorilla gorilla] 233   PGPLLGAP   240

Figure 5-15. An identical motif observed both in Ylr404wp and mammalian FOXD4 proteins.
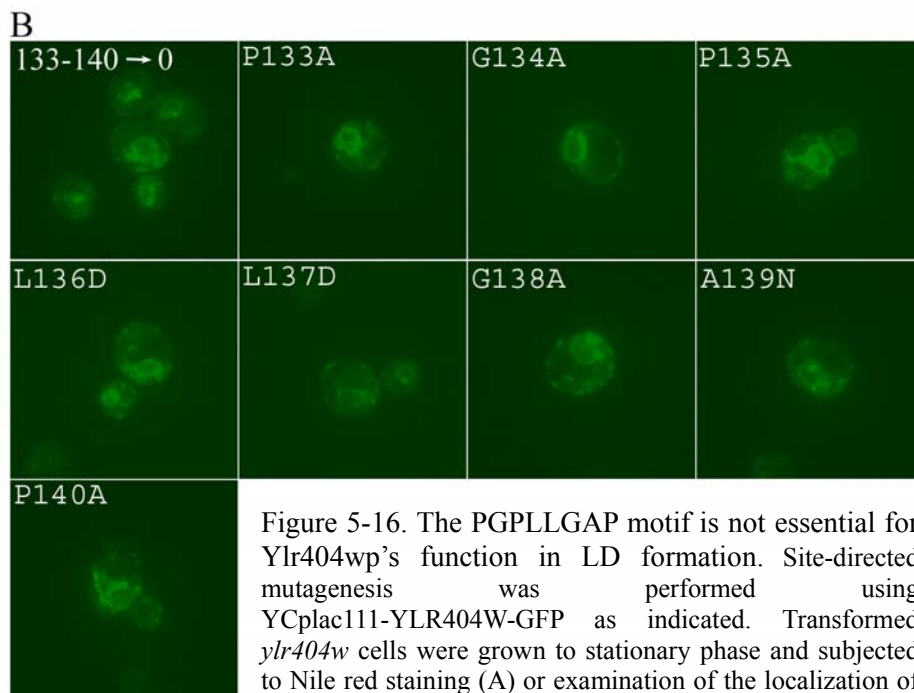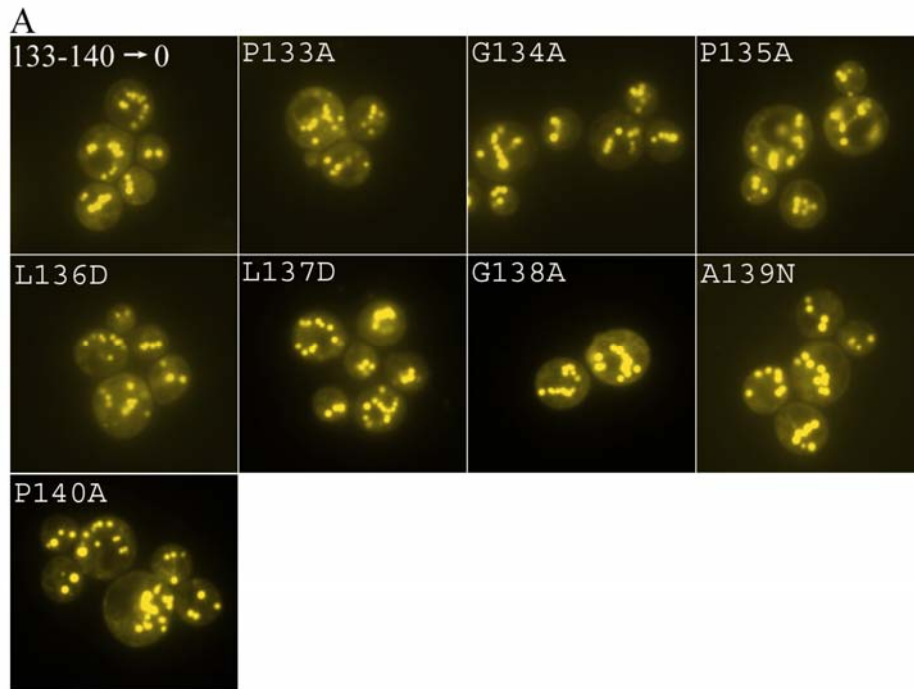
Figure 5-16. The PGPLLGAP motif is not essential for Ylr404wp's function in LD formation. Site-directed mutagenesis was performed using YCplac111-YLR404W-GFP as indicated. Transformed *ylr404w* cells were grown to stationary phase and subjected to Nile red staining (A) or examination of the localization of Ylr404wp-GFP (B).

5.4 Biochemical characterization of *ylr404w* strain

Does the composition of the LDs of the *ylr404w* cells differ from that of the WT cells? With this question in mind, I performed lipid analysis for the mutant as well as lipid and proteomic characterization of the LDs isolated from the *ylr404w* strain and from the WT strain.
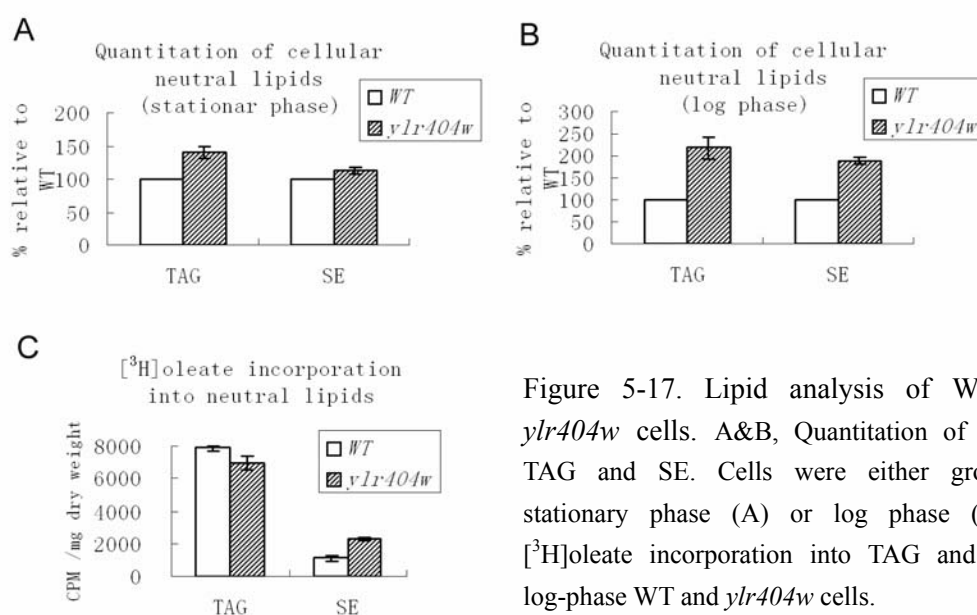
Figure 5-17. Lipid analysis of WT and *ylr404w* cells. A&B, Quantitation of cellular TAG and SE. Cells were either grown to stationary phase (A) or log phase (B). C) [³H]oleate incorporation into TAG and SE in log-phase WT and *ylr404w* cells.

5.4.1 Lipid analysis of the *ylr404w* strain

Total lipid extraction from the lyophilized yeast cells as well as separation and quantitation of neutral lipids was performed as described in Materials and Methods. Both WT and *ylr404w* cells were cultured in synthetic complete medium, harvested, and lyophilized. The dry cell pellets were weighed and subsequently subjected to total lipids extraction. Different components of the cellular lipids were separated using thin layer chromatography (TLC). Neutral lipids were derivatized, followed by densitometric scanning. The result of neutral lipids quantitation is shown in Figure 5-17. When cells

were grown to stationary phase, compared with the WT, *ylr404w* cells synthesized 30% more TAG and 10% more SE (Figure 5-17A). For log phase, ylr404w cells contained 110% more TAG and 90% more SE than WT (Figure 5-17B). This was consistent with the fact that the *ylr404w* strain accumulated fewer but much larger LDs than the WT.

Since the enzyme ACAT catalyzes the synthesis of SE (Yang et al., 1996) and DGAT/PDAT the synthesis of TAG (Sorger and Daum, 2003), to test if the increased synthesis of neutral lipids was caused by elevated enzyme activity, oleate incorporation assay was subsequently performed to compare the rate of incorporation of oleate into neutral lipids between the WT and the mutant. Both strains were refreshed in synthetic complete medium and grown to log phase (OD_{600}~0.8). Then cells were pulsed with 1 µCi of [^{3}H]oleic acid per ml cell culture at 30°C for 30 min with shaking, followed by lipid extraction and separation of lipid components by TLC. Incorporation of label into neutral lipids was determined by scintillation counting. The result is shown in Figure 5-17C. Unexpectedly, *ylr404w* strain incorporated 10% less oleate into TAG than the WT, but two times of oleate into SE as that of the WT. This result suggests that ACAT and DGAT/PDAT activity is uncoupled with the elevated neutral lipids synthesis of the *ylr404w* strain. Therefore, other regulatory pathway(s) should exist in this mutant.

5.4.2 Lipid and protein compositions of the LDs isolated from the *ylr404w* cells

To test whether the compositions of the LDs of the *ylr404w* cells is remarkably different from those of the WT, I isolated the LD-rich fraction from the two strains via

Ficoll gradient centrifugation, extracted lipids and proteins, and made comparisons of their compositions between the LD-rich fractions isolated from the two strains.

Extraction of lipids and solubilization of LD-associated proteins were performed as described in Materials and Methods. Lipid components were subsequently separated via TLC and the plate was stained with iodine vapor. As shown in Figure 5-18, there was no significant difference between the WT strain and the *ylr404w* strain in terms of gross lipid compositions of LDs. Lipids extracted from LD-rich fractions isolated from both strains contained all the major lipid components: TAG, SE, free fatty acids, sterols, and phospholipids.
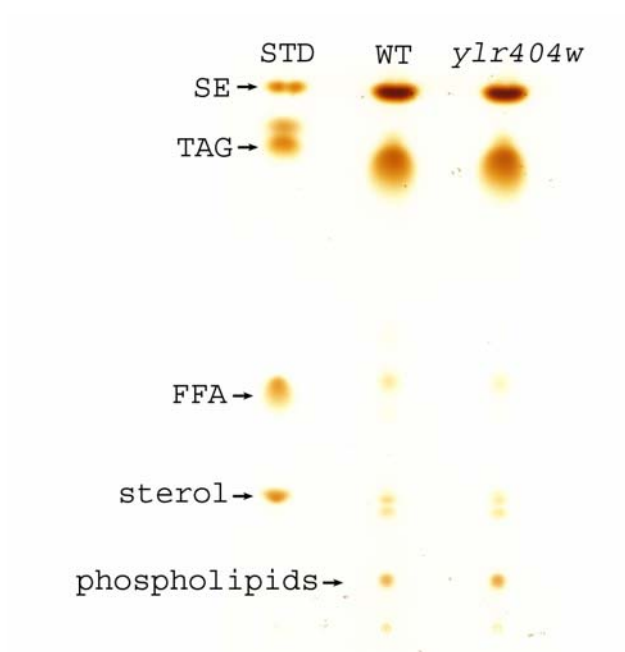
Figure 5-18. Gross profiling of lipids extracted from LDs isolated from WT and *ylr404w* cells via thin layer chromatography (TLC).

To study whether the protein compositions of the LD-rich fraction of the *ylr404w* strain differ greatly from those of the WT strain, solubilized proteins were separated by

SDS-PAGE. I stained the protein bands using an Invitrogen MS-compatible silver stain kit. All the major protein bands were carefully excised and tandem mass spectrometry (MALDI-TOF MS) was subsequently carried out for peptide sequence determination. The protein patterns of LDs isolated from the two strains are shown in Figure 5-19 and proteins identified by MALDI-TOF MS in Table 5-3. Altogether 13 proteins were identified in the LD-rich fraction isolated from the WT cells and 14 proteins from that of the *ylr404w* strain. The presence of ER resident proteins (indicated by letters in italic, Table 5-1), Kar2p, Pdi1p, Cwh41p, and Pmt1p (Rose et al., 1989; Noiva and Lennarz, 1992; Jiang et al., 1996; Strahl-Bolsinger et al., 1993) in the LD-rich fraction could result from the contamination of the ER; it is very unlikely to completely separate ER from LDs by gradient centrifugation because they are closely associated with each other. Among the other proteins, 7 proteins (indicated by letters in bold) could be detected in LD-rich fractions of both strains. These proteins were Tgl4p, Eht1p, Tgl3p, Yim1p, Erg6p, Ayr1p, and Erg27p. Their association with LDs has been previously reported (Athenstaedt et al., 1999; Athenstaedt et al., 2006). Except that the function of Yim1p is yet to be determined, the other 6 proteins are involved in lipid metabolism. Tgl3p and Tgl4p are TAG lipases (Athenstaedt and Daum, 2003; Athenstaedt and Daum, 2005). Eht1p is an acyl-coenzymeA:ethanol O-acyltransferase that plays a role in medium-chain fatty acid ethyl ester biosynthesis (Saerens et al., 2006). Erg6p and Erg27p are ergosterol biosynthetic enzymes (McCammon et al., 1984; Gachotte et al., 1999). Ayr1p is an NADPH-dependent 1-acyl dihydroxyacetone phosphate reductase involved in phosphatidic acid biosynthesis (Athenstaedt and Daum, 2000).

Besides the above-mentioned 7 proteins, Faa1p, Sac1p and Kes1p were also detected in the LD-rich fraction of the WT cells. Their association with LDs has been reported in another yeast strain Yarrowia lipolytica (Athenstaedt et al., 2006). Faa1p is a long chain fatty acyl-CoA synthetase required for fatty acid activation (Duronio et al., 1992). Sac1p is a lipid phosphoinositide phosphatase involved in protein trafficking and secretion (Hughes et al., 2000). Kes1p which is also named Osh4 is an oxysterol binding protein (Fang et al., 1996). The presence of Sac1p and Kes1p suggests that LD has a role in intracellular trafficking.

In contrast, these three proteins were not detected in the LD-rich fraction of the *ylr404w* cells. Instead, another four proteins, Pma1p, Eno2p, Tdh1p, and Tdh2p, were identified. Eno2, Tdh1p, and Tdh2p are enzymes that functions during glycolysis and gluconeogenesis (McAlister and Holland, 1982; McAlister and Holland, 1985). Their association with LDs might suggest that glucose metabolism is altered in the *ylr404w* strain. Pma1p is a plasma membrane H^+-ATPase (Serrano et al., 1986). Previously it has not been reported that Pma1p associates with LDs. The functional relevance of this association in *ylr404w* cells should be characterized in the immediate future.
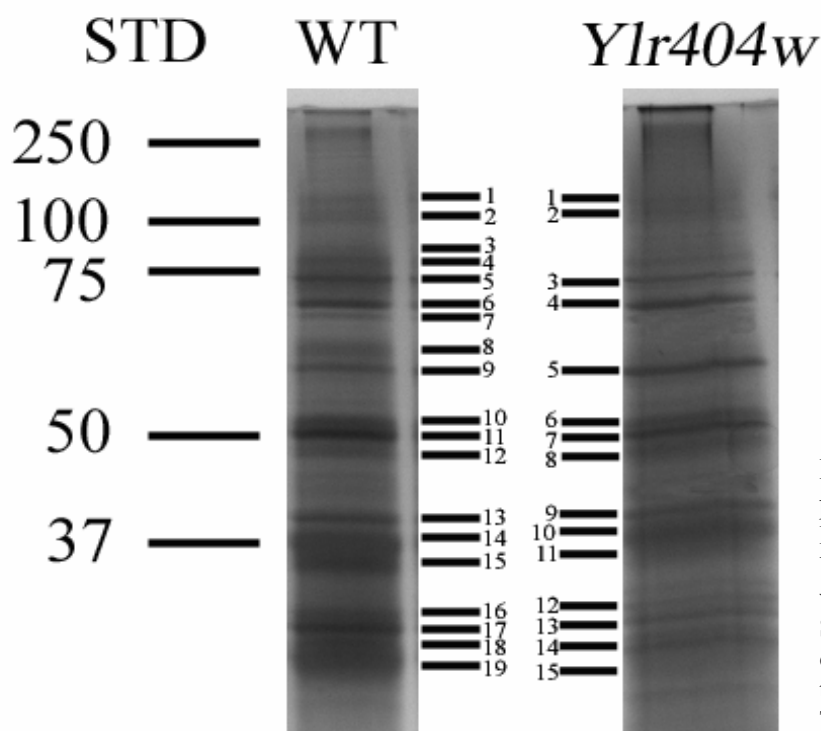
Figure 5-19. Protein pattern of LDs. Proteins isolated from WT and *ylr404w* cells were separated by SDS-PAGE. Numbering of the protein bands is the same as shown in Tables 5-1.

WT			*ylr404w*		
Band(s)	Protein(s)	Mw (KDa)	Band	Protein(s)	Mw (KDa)
1, 2	*Cwh41p*	96	1,2	Pma1p	100
3, 4, 8	Faa1p	78	2	*Pmt1p*	93
5	**Kar2p**	74	3,	**Kar2p**	74
6	**Pdi1p**	58	4	**Pdi1p**	58
7	Sac1p	71	5	**Tgl4p**	102
9	**Tgl4p**	102	6, 8	**Eht1p**	51
10	Kes1p	49	7	**Tgl3p**, Eno2p	74, 47
10, 12	**Eht1p**	51	9	**Yim1p**	42
11	**Tgl3p**	74	9-11	**Erg6p**	43
13	**Yim1p**	42	12	Tdh1p, Tdh2p	36, 36
13-15	**Erg6p**	43	13, 14	**Ayr1p**	33
16-18	**Ayr1p**	33	15	**Erg27p**	40
19	**Erg27p**	40			

Table 5-3. Proteins of LD-rich fractions isolated from the WT and *ylr404w* strains identified by MS (MALDI-TOF MS). Proteins were separated by SDS-PAGE, and protein bands excised and analyzed by MALDI-TOF MS. Letters in bold are proteins identified in LD-rich fractions of both WT and *ylr404w* strains. Letters in italic are ER resident proteins, which may suggest the contamination of ER in the LD-rich fractions.

Chapter 6

Seipin, mammalian functional homolog of Ylr404wp

Congenital generalized lipodystrophy (CGL) is a rare autosomal recessive syndrome characterized by a near complete absence of adipose tissue since birth, acanthosis nigricans, severe insulin resistance, marked hypertriglyceridemia, and early-onset diabetes mellitus (Garg, 2000). Recently, mutations in the 1-acylglycerol-3-phosphate O-acyltransferase 2 (*AGPAT2*) gene linked to chromosome 9q34 were found to be responsible for the CGL1 subtype (Garg et al., 1999; Agarwal et al., 2002), and mutations in the *Seipin* gene (also termed *BSCL2*) linked to chromosome 11q13 for CGL2 subtype (Magre et al., 2001). Both subtypes display marked lack of metabolically active adipose tissue located at most sc, intermuscular, bone marrow, intraabdominal, and intrathoracic regions, but CGL2 shows more severe deficiency of body fat; even mechanical adipose tissues become scarce in the palms, soles, orbits, scalp, and periarticular regions (Simha and Garg, 2003). In addition, CGL2 patients have an increased prevalence of mild mental retardation and cardiomyopathy (Agarwal et al., 2003).

AGPAT2 catalyzes acylation of lysophosphatidic acid to phosphatidic acid, an essential reaction in the biosynthetic pathway of TAG and phospholipids from glycerol-3-phosphate (Agarwal and Garg, 2003). Unlike AGPAT2, the molecular function of seipin remains largely obscure and it does not exhibit sequence homology with AGPAT2. Seipin may have several isoforms because northern blot analysis has shown that *BSCL2* gene gives rise to at least three different mRNAs with sizes ranging from 1.8,

2.0 to 2.4 kb (Magre et al, 2001) and two peptides with 398 or 462 amino acids (Lundin et al., 2006). The 2.0 kb mRNA is exclusively expressed in brain and testis, but the 1.8 and 2.4 kb mRNAs are ubiquitously expressed.

```
Homo_sapiens              1  ---------MVN--DP--------PVPALLWA-QEVGQVL----AGR-------------ARRLLL   29
Mus_musculus              1  ---------MVN--DP--------PVPALLWA-QEVGHVL----AGR-------------ARRLML   29
Rattus_norvegicus         1  ---------MVN--DP--------PVPALLWA-QEVGHVL----AGR-------------ARRLML   29
Xenopus_laevis            1  -------------------------------MGLLM----FLR-------------ARRLFL   14
Danio_rerio               1  --MQSSTEELNSED----------SGVQDVGPQI--RGLVVEILETMSDLLVWMRRKAV   45
Drosophila_melanogaster   1  MNILLRLIVFAL---DPLGLGRRFLIRPAVNLGWNVYDRVRSKADEKVGT--------VRELVL   53
Saccharomyces_cerevisiae  1  ---------MKINVSR--------PLQF-----------------------LQWSSY   17

Homo_sapiens             30  QFGVLFCTILLLLWVSVFLYGSFYYSYMPT-VSHLSPVHFYYRTDCDSSTTSLCSFPVANVSLTK-----   93
Mus_musculus             30  QFGVLFCTILLLLWVSVFLYGSFYYSYMPT-VSHLSPVHFHYRTDCDSSTASLCSFPVANVSLAK-----   93
Rattus_norvegicus        30  QFGVLFCTILLLLWVSVFLYGSFYYSYMPT-VSHLSPVHFYYRTDCDSSTASLCSFPVANVSLTK-----   93
Xenopus_laevis           15  QAAIFLCVLILLLWVSVFLYGSFYYSYMPT-VKYSSPVHYQYSSTCEPPPGILCSFPTANVSLLR-----   78
Danio_rerio              46  EMVIIICVILLVFWVALFLYGSFYYSFMPT-ANFVAPVNFFHRTDCPSPHHPMCSFPMANVSLLK-----  109
Drosophila_melanogaster  54  RLGLIAFAVVLIIWLAVFMYAAFYYVYMPA-ISHTRPVHMQFKTCLET--STPCTFPHAHVSLT-------  114
Saccharomyces_cerevisiae 18  IVVAFLIQLLIILPLSILIYHDFYLRLLPADSSNVVPLN-TFNILNGV--QFGTKFFQSIKSIPVGTDLP   84

Homo_sapiens             94  ----GGRDRVLM--YGQPYRVTLELELPESPV--NQDLGMFLVTI----------SCYTRGGRIISTSS  144
Mus_musculus             94  ----SGRDRVLM--YGQPYRVTLELELPESPV--NQDLGMFLVTV----------SCYTRGGRIISTSS  144
Rattus_norvegicus        94  ----SGRDRVLM--YGQPYRVTLELELPESPV--NQDLGMFLVTV----------SCYTRGGRIISTSS  144
Xenopus_laevis           79  ----NNRDRVLI--HGQPYRISLELQLPESTV--NQDLGMFMVTM----------SCYTRGGKQISYTA  129
Danio_rerio             110  ----NGKHQVMT--YGQPYQITLKLEMPESPT--NQQLGMFLVTI----------TPYSKAGQIIGVSS  160
Drosophila_melanogaster 115  -----KKQQLLM--VGQAYKVIVNIDMPESPQ--NLELGMFMVCA----------EMRDYDSMLRGHSC  164
Saccharomyces_cerevisiae 85  QTIDNGLSQLIPMRDNMEYKLDLNLQLYCQSKTDHLNLDNLLIDVYRGPGPLLGAPGGSNSKDEKIFHTS  154

Homo_sapiens            145  RSVMLHYRSDLLQMLDTLVFSSLLLFGFAEQKQLLEVELYADYRENSYVPTTGAIIEIHSKRIQLYGAYL  214
Mus_musculus            145  RSVMLHYRSQLLQVLDTLLFSSLLLFGFAEQKQLLEVELYSDYRENSYVPTTGAIIEIHSKRIQMYGAYL  214
Rattus_norvegicus       145  RSVMLHYRSQLLQMLDTLVFSSLLLFGFAEQKQLLEVELYSDYRENSYVPTTGAIIEVHSKRVQMYGAYL  214
Xenopus_laevis          130  RSAMLHYKSPLLRTMETLASSPLLLLGFSEQKQSLEVELYPEYREDSYVPTVGAVIQVQSVRIEIYTAEL  199
Danio_rerio             161  RSAMLHYRSSLLQTLGTLVFSPMFLSGMSEQKQSVTVELFSEFKDDSYKPTVGAMLEIHAPNIQIYKANL  230
Drosophila_melanogaster 165  RSAMMRYRSPLIRMISTWVLSPLYVLGWKEEFQQVPVEIFSRYLEERQHPITDVYVEIQSQKIQFYTVTL  234
Saccharomyces_cerevisiae 155  RPIVCLALTDSMSPQEIEQLGPSRLDV-YDEEWLNTIRIEDKISLESSYETISVFLKTEIAQ----RNL  218

Homo_sapiens            215  RIHAH---------FTGLRYLLYNFPMTCAFIGVASNFTFLSVIVLFS-YMQWVWGGIWPRHRFSLQVNI  274
Mus_musculus            215  RIHAH---------FTGLRYLLYNFPMTCAFVGVASNFTFLSVIVLFS-YMQWVWGAVWPRHRFSLQVNI  274
Rattus_norvegicus       215  RIHAH---------FTGLRYLLYNFPMTCAFVGVASNFTFLSVIALFS-YMQWVWGAVWPRHRFSLQVNI  274
Xenopus_laevis          200  RVHAY---------FTGIRYLLYHFPVTSAVIGISSNFIFLSVLVLLS-YLQWGFG----RTRLR---DV  252
Danio_rerio             231  YIFAH---------FTGIRYLYQFPLISALMGVWTNFTFLSLIIVLS-FLQFNLNGRQFRRKARMQQEE  290
Drosophila_melanogaster 235  HIVAD---------FTGLRYIMFNWPVLSAIVAISTNLFFILVVFLLS-WYHWSDAKWLH----SVQIKY  290
Saccharomyces_cerevisiae 219  IIHPESGIKFRMNFEQGLRNLMLRKRFLSYIIGISIFHCIICVLFFITGCTAFIFVRKG---------  277

Homo_sapiens            275  RKRDNSRKEVQRRISA---HQPGPEGGQEESTPQSDVTEDGESPEDPSG---TEGQLSEEEKPDQQPLSGE  338
Mus_musculus            275  RQRDNSHHGAPRRISR---HQPG----QESTQQSDVTEDGESPEDPSG---TEGQLSEEEKPEKRPLNGE  334
Rattus_norvegicus       275  RQRDNSGHGAQRRISR---HQPG----QASTQQSDVTEDGESPEDPSG---TEGQLSEEEKPEKQPLNGE  334
Xenopus_laevis          253  QQRTRNVRGAETRPES---FSQ-----TEDKDQSDTETIGQNDTDSQGAQQTETQVVQNISSD-------  307
Danio_rerio             291  MDEID-------DLFD---DPSEPHDRGIIPENVDTMDCNSADMEES-----IPDVTGEDSDDSRELTKD  345
Drosophila_melanogaster 291  ARLTK-------SLEPGVIHSKASSLRDDDDD-------------------LVAYSDKSDIADVGG-     330
Saccharomyces_cerevisiae

Homo_sapiens            339  EELEPEASDGSGSWEDA-ALLTEANLPAPAPASASAPVLETLGSSEPAGGALRQRPTCSSS----  398
Mus_musculus            335  EEQEPEASD--GSWEDA-ALLTEANPPTSASASALAP-------------ETLGSLRQRPTCSSS-  383
Rattus_norvegicus       335  GEQEPEASD--GSWEDA-ALLTEASTSALAP-------------------ETLGSLRQRQTCSSS-  377
Xenopus_laevis          308  ----------------LDTDSNAQFSA-----------------------LHQRSAQSSSN-     329
Danio_rerio             346  EPICEDGNEETILRRR------------HLSQDSLQAPQVLT--ETTDKNYYRVGVCSSS-  391
Drosophila_melanogaster 331  ----------DTLSDVDADDLVLVKKSRSGK-------------------RESPDALRKRPTKKTTADH  370
Saccharomyces_cerevisiae 278  ---------------------------------------------QEKSKKHS---  285
```

Figure 6-1. Sequence alignment of seipin and Ylr404wp via PROMALS. Amino acids in red are identical and those in blue are highly similar across all seven species. Yellow-shaded amino acids are either identical or highly similar between human and other species besides those in red and blue, including A212P. Orange bars represent two transmembrane domains.

Sequence homology searches show that human seipin has homologs in many species,

including *Drosophila melanogaster* (fly), *Danio rerio* (zebrafish), *Xenopus laevis* (African clawed frog), *Mus musculus* (mouse) and *Rattus norvegicus* (rat). Now sequence analysis of Ylr404wp via Position-Specific Iterated BLAST indicates that Ylr404wp has 12% identity and 27% or 28% similarity with human, rat, and mouse seipin. Sequence alignment of these proteins via PROMALS is shown in Figure 6-1. Apparently seipin is highly conserved from human to rat, and to mouse. The region that covers the first 280 amino acids of human seipin is 88% identical among rat, mouse, chimpanzee and human homologs (Agarwal and Garg, 2004). In addition, like Ylr404wp which is predicted to be a double-pass integral membrane protein, human seipin and its homologs also share this feature (Table 6-1). Consistent with this prediction, localization studies showed that human seipin is an integral membrane protein of the ER (Windpassinger et al., 2004). More recently, a membrane topology study suggests that the N- and C-terminal tails of human seipin are located in the cytosol, while the central loop is in the ER lumen (Lundin et al., 2006).

Although Ylr404wp does not have a strong sequence identity with these proteins, it still appears to belong to the seipin family, given that Ylr404wp and seipins have many similar characteristics: 1) they are all membrane proteins. In addition, they are predicted to have two transmembrane helices. 2) Both Ylr404wp and human seipin localize to the ER. 3) Topology analysis suggests that Ylr404wp and human seipin consists of cytosolically oriented N- and C-terminal tails and a luminal central loop (Figure 6-2). 4) Whereas Ylr404wp is involved in LD dynamics, the loss of function of human seipin leads to lipodystrophy.

Table 6-1, Prediction of transmembrane helices by TMHMM and HMMTOP in human seipin and its homologs. * denotes a weakly predicted transmembrane helix.

protein	Prediction Model	Result		
Human seipin (AAH12140, 398aa)	TMHMM	TMhelix	27	49
		TMhelix	236	258
	HMMTOP	TMhelix	31	55
		TMhelix	238	262
Rat seipin (AAH89942, 377aa)	TMHMM	TMhelix	27	49
		TMhelix	225	247
	HMMTOP	TMhelix	31	55
		TMhelix	235	259
Mouse seipin (NP_032170, 383aa)	TMHMM	TMhelix	27	49
		TMhelix	236	258
	HMMTOP	TMhelix	31	55
		TMhelix	235	259
Frog seipin (LOC734949, 329aa)	TMHMM	TMhelix	12	34
		TMhelix	218	240
	HMMTOP	TMhelix	18	42
		TMhelix	220	244
Zebrafish seipin (AAI52256, 391aa)	TMHMM	TMhelix	48	70
		TMhelix	249	271
	HMMTOP	TMhelix	47	71
		TMhelix	248	271
Fly seipin (NP_570012, 370aa)	TMHMM	TMhelix	58	80
		TMhelix*	175	192
		TMhelix	250	272
	HMMTOP	TMhelix	55	79
		TMhelix	251	275
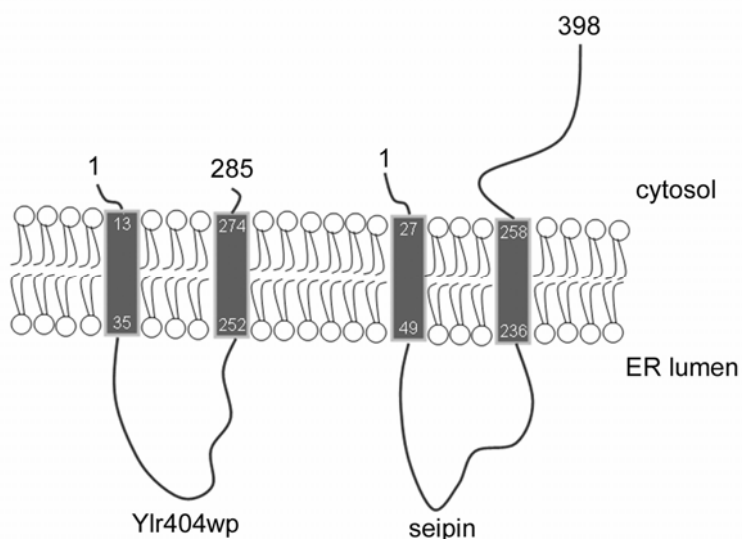
Figure 6-2. Topology model of Ylr404wp and seipin based on the prediction of transmembrane helices by TMHMM.

To verify this possibility, I amplified human seipin from cDNA BC012140 (398 amino acids) and AF052149 (462 amino acids, with 64 amino acids extended at the putative N-terminus) and mouse seipin from cDNA BC061689 (443 amino acids), and inserted them into the YCplac111 vector under the control of yeast MET3 promoter. Remarkably, expression of human and mouse seipin successfully complemented the defect in LD morphology in *ylr404w* cells (Figure 6-3). When *ylr404w* cells were cultured in defined medium, 80% of the cell population contained one or two supsersized LDs with an average diameter of 1.21±0.19 (n=117). After cells were transformed with vectors that expressed human or mouse seipin, the supersized LDs disappeared, and cells synthesized many small LDs with an average diameter of 0.43±0.05 (n=106), resembling the feature of WT cells. This experiment indicates that human and mouse seipin can complement the function of Ylr404wp.
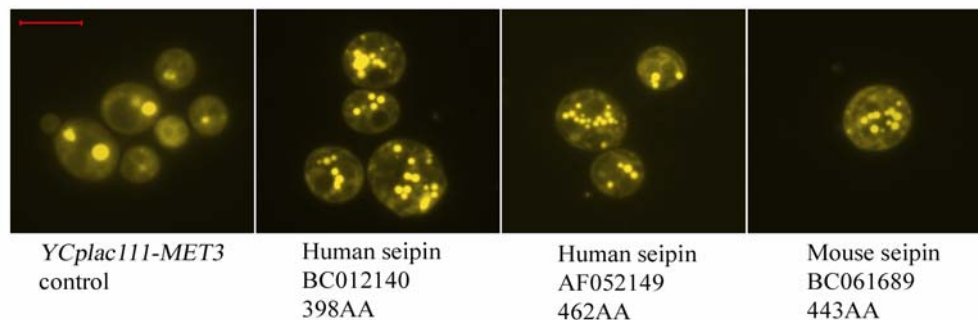
Figure 6-3. Expression of human and mouse seipin in *ylr404w* cells rescues the defect in LD morphology. Gene sequences encoding human and mouse seipin were inserted into YCPlac111 vector under the control of MET3 promoter. *ylr404w* cells carrying vectors that express human or mouse seipin were cultured in defined medium until stationary phase, stained with Nile red and examined by fluorescence microscopy. Bar, 5 μm.

Subsequently, I examined the effects of point mutations in seipin that are implicated in lipodystrophy and motoneuron disorders. A212P has been identified as a missense mutation leading to CGL (Magre et al., 2001), whereas two heterozygous missense

mutations resulting in the amino acid substitutions N88S and S90L are held accountable

for distal hereditary motor neuropathy (dHMN) and silver syndrome (SS). One

speculative mechanism is that N88S and S90L affect the glycosylation of seipin, which

causes aggregates formation leading to neurodegeneration (Windpassinger et al., 2004).

Alternatively, peripheral neuropathy might result from the disturbance in lipid metabolism

of motor neuron cells (Agarwal and Garg, 2004).

Interestingly, expression of N88S and S90L, but not A212P rescued the defects in LD

morphology (Figure 6-4). The fact that the mutant form of human seipin implicated in

lipid metabolism disorder (A212P) could not restore the normal LD morphology in

ylr404w cells gives additional evidence that seipin is a homolog of Ylr404wp. The

finding that N88S and S90L do not affect the function of seipin in regulating LD

morphology might suggest that peripheral neuropathy is probably not a result of

disturbance in lipid metabolism.

Lastly, expression of the highly conserved 280 amino acids region of seipin rescued

the defects in LD morphology (Figure 6-4). This result may provide additional evidence

that the functional domain of Ylr404wp and seipin is located in the ER lumen.
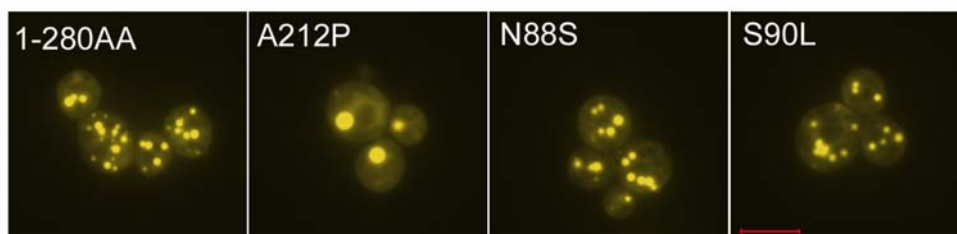
Figure 6-4. Expression of the highly conserved (amino acids 1-280) region of seipin and
various seipin mutants in *ylr404w* cells. Bar, 5 μm

Recently, Ory's group reported that contrary to our expectation, small interference

RNA-mediated knockdown of *AGPAT2* did not reduce the cellular level of phosphatidic

acid (PA); rather phosphatidic acid (PA) was elevated by 3-fold in TAG-depleted

adipocytes with *AGPAT2* knockdown, suggesting that impaired AGPAT2 activity does

not impair overall PA synthesis or utilization of PA for phospholipid synthesis, but only

affects availability of PA for TAG synthesis (Gale et al., 2007). This result prompted a

speculation that AGPAT2 controls adipogenesis through modulation of the synthesis of

phospholipids (Gale et al., 2007). Since mutations in AGPAT2 and BSCL2 cause similar

clinical manifestations, we wondered if aberrant phospholipids metabolism may underlie

the cellular defects for both conditions. Lipid species from WT and *ylr404w* whole cell

extracts were analyzed by ESI tandem mass spectrometry.

A
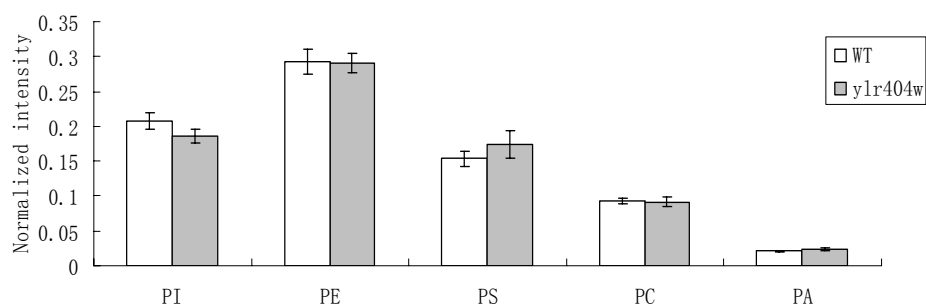
B
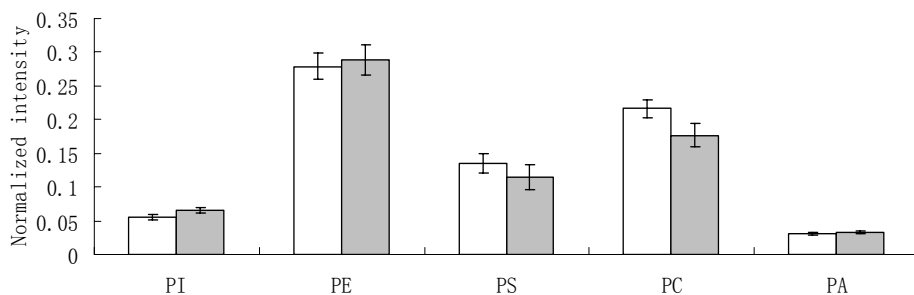
C
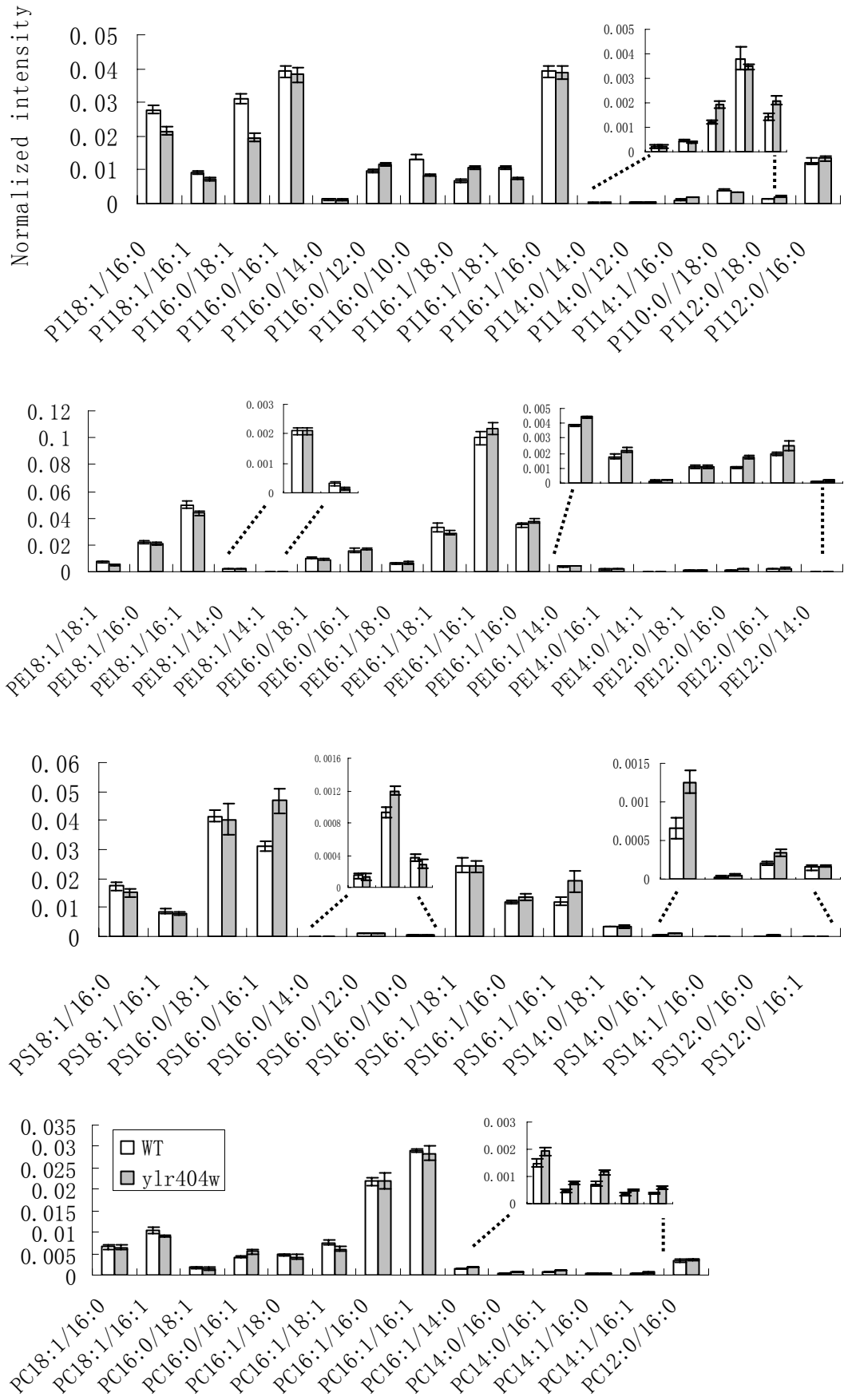
D
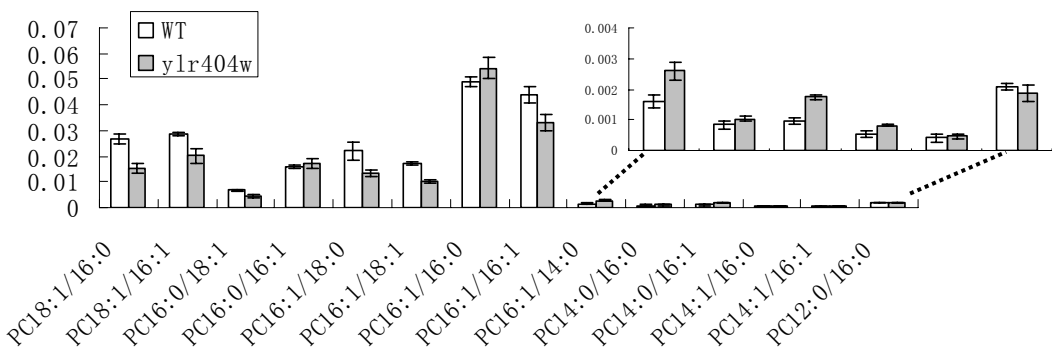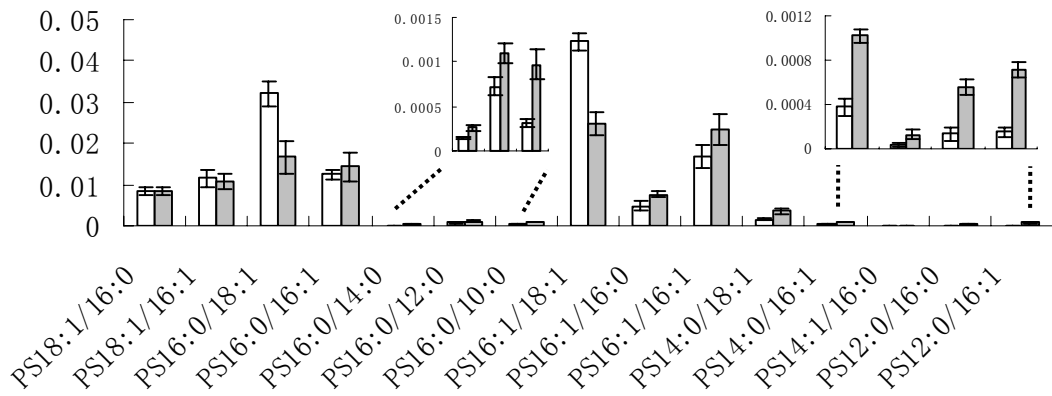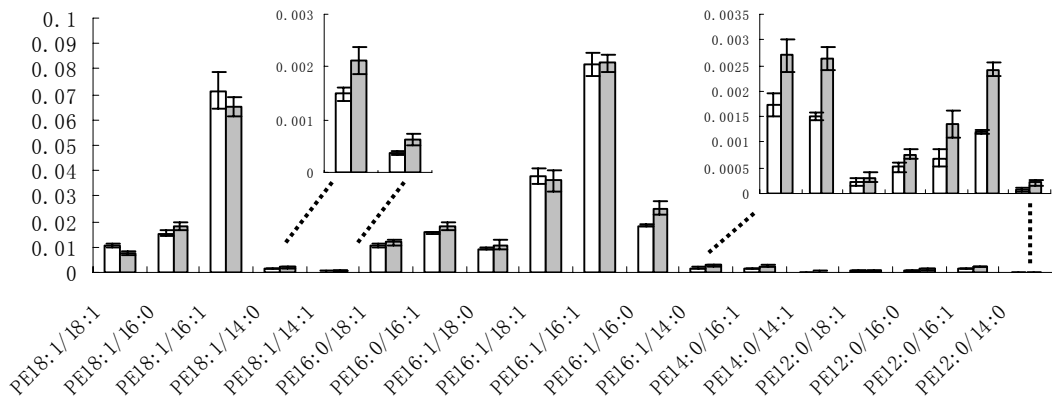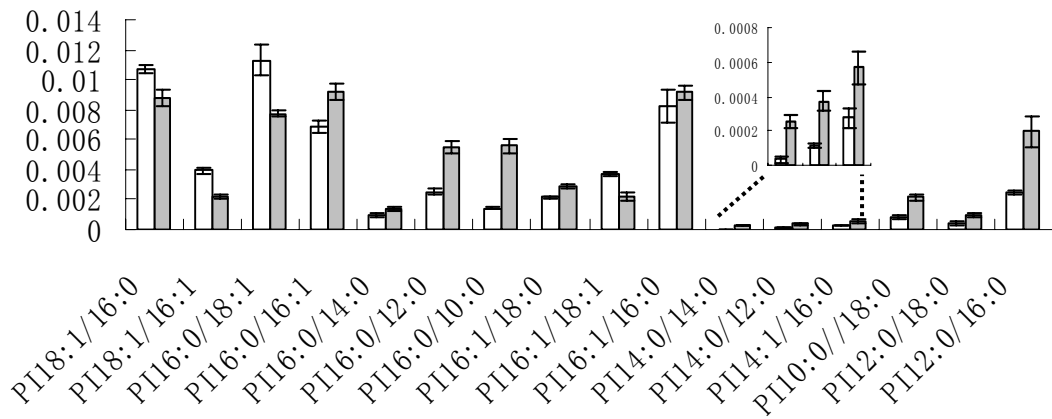
E
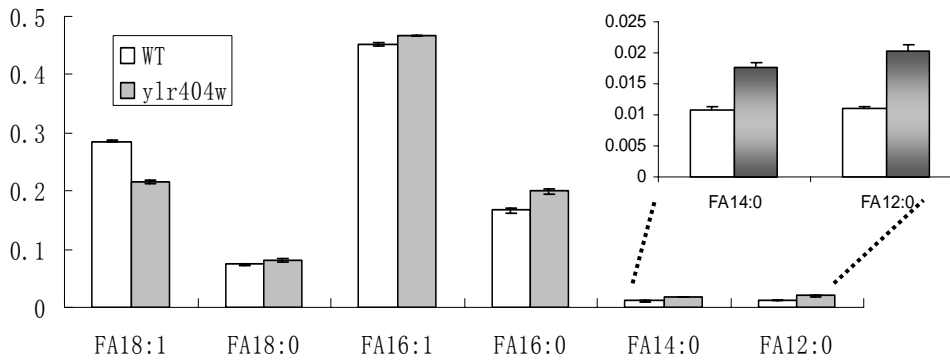
F
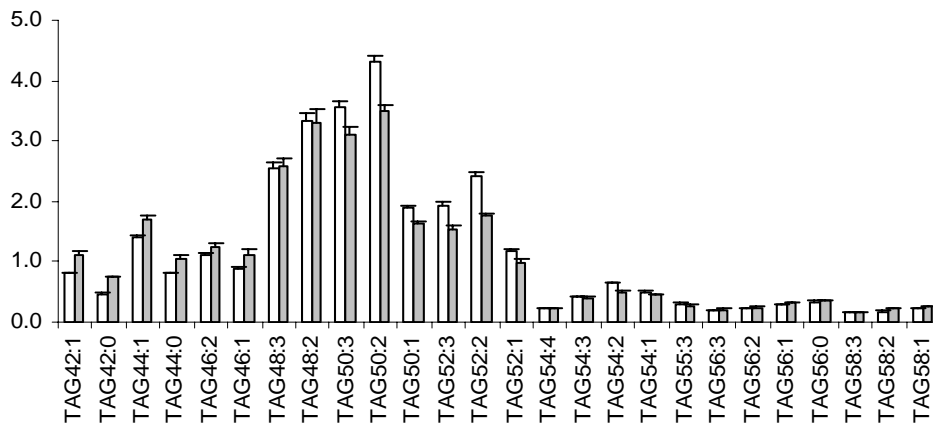
Figure 6-5. Fatty acyl profiling of phospholipids and TAG of WT and *ylr404w* cells. A&B, Relative total amount of phosphatidyl inositol (PI), phosphatidyl ethanolamine (PE), phosphotidyl serine (PS), and phosphatidyl choline (PC), as well as phosphatidic acid (PA) extracted from WT and *ylr404w* cells cultured in YPD medium (A) or SC medium (B). C&D, phospholipid profiles of WT and *ylr404w* cells cultured in YPD medium (C) or SC medium (D). E, Fatty acid profiles of polar lipids of WT and *ylr404w* cells cultured in SC medium. F, TAG profiles of WT and *ylr404w* cells cultured in SC medium. n=4.

As seen in Figure 6-5 A&B, the level of PA only increased slightly in *ylr404w* cells,

no matter cells were cultured in YPD medium (Figure 6-5A) or SC medium (Figure 6-5B).

In addition, there was no significant difference in the cellular levels of four major classes

of phospholipids, i.e., phosphatidyl inositol (PI), phosphatidyl ethanolamine (PE),

phosphotidyl serine (PS), and phosphatidyl choline (PC).

Interestingly, there was a shift from long-chain (18:1) to medium/short-chain (16:0, 14:0, 12:0) fatty acid incorporation into all major phospholipids due to the deletion of *YLR404W* (Figure 6-5 C&D). This change was even more pronounced when cells were cultured in SC medium than in YPD medium. For instance, when cells were cultured in YPD medium, compared with WT, *ylr404w* cells displayed 23%, 18%, 37%, and 30% decrease of PI18:1/16:0, PI18:1/16:1, PI16:0/18:1, and PI16:1/18:1, respectively, together with 17%, 62%, and 46% increase of PI16:0/12:0, PI14:1/16:0, and PI12:0/18:0, respetively (Figure 6-5C). When cells were cultured in SC medium, *ylr404w* cells displayed 18%, 44%, 32%, and 41% decrease of PI18:1/16:0, PI18:1/16:1, PI16:0/18:1, and PI16:1/18:1, respectively, and 116%, 108%, and 136% increase of PI16:0/12:0, PI14:1/16:0, and PI12:0/18:0, respetively (Figure 6-5D and Table 6-2).

Table 6-2. Normalized intensity of seven phosphatidyl inositol (PI) subspecies of *ylr404w* cells relative to WT and their difference. – and + denote decrease and increase, respectively.

Lipid subspecies	YPD medium		SC medium	
	ylr404w cells relative to WT	difference	*ylr404w* cells relative to WT	difference
PI18:1/16:0	77%	-23%	82%	-18%
PI18:1/16:1	82%	-18%	56%	-44%
PI16:0/18:1	63%	-37%	68%	-32%
PI16:1/18:1	70%	-30%	59%	-41%
PI16:0/12:0	117%	+17%	216%	+116%
PI14:1/16:0	162%	+62%	208%	+108%
PI12:0/18:0	146%	+46%	236%	+136%

Fatty acyl profiles of polar lipids confirmed the long-chain to medium/short-chain shift in acyl chain pattern of phospholipids in *ylr404w* cells. When cells were cultured in SC medium, polar lipids of *ylr404w* cells incorporated 24% less FA18:1, but 20% more

FA16:0, 64% more FA14:0, and 85% more FA12:0 than those of WT cells (Figure 6-5 E).

Remarkably, TAG profiles of *ylr404w* cells displayed this long-chain to medium/short-chain shift as well (Figure 6-5 F). In addition, phospholipid and TAG profiles of LDs isolated from *ylr404w* cells also showed this shift in their acyl chain pattern (Figure 6-6 A-C).

A
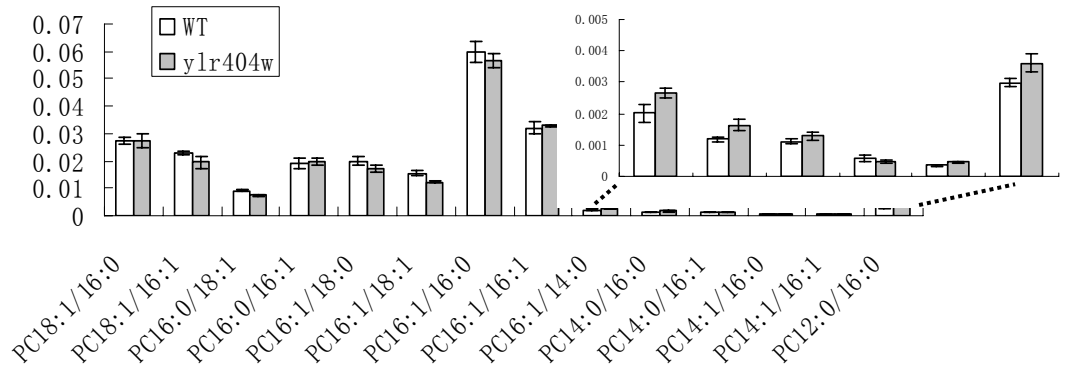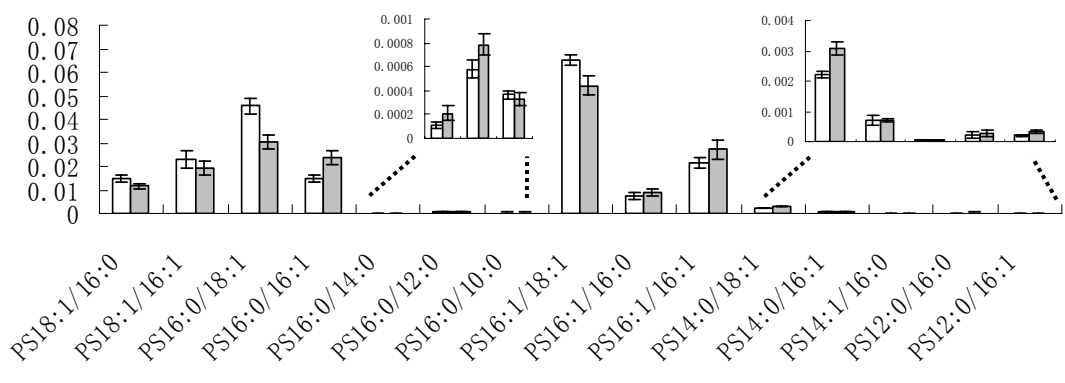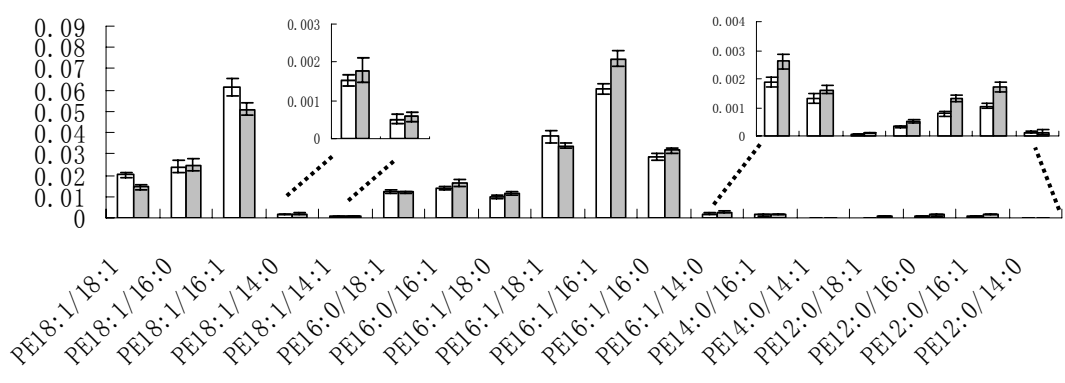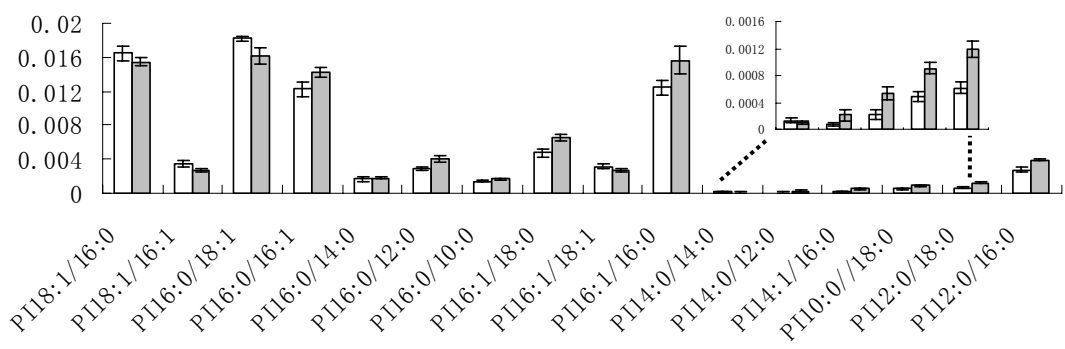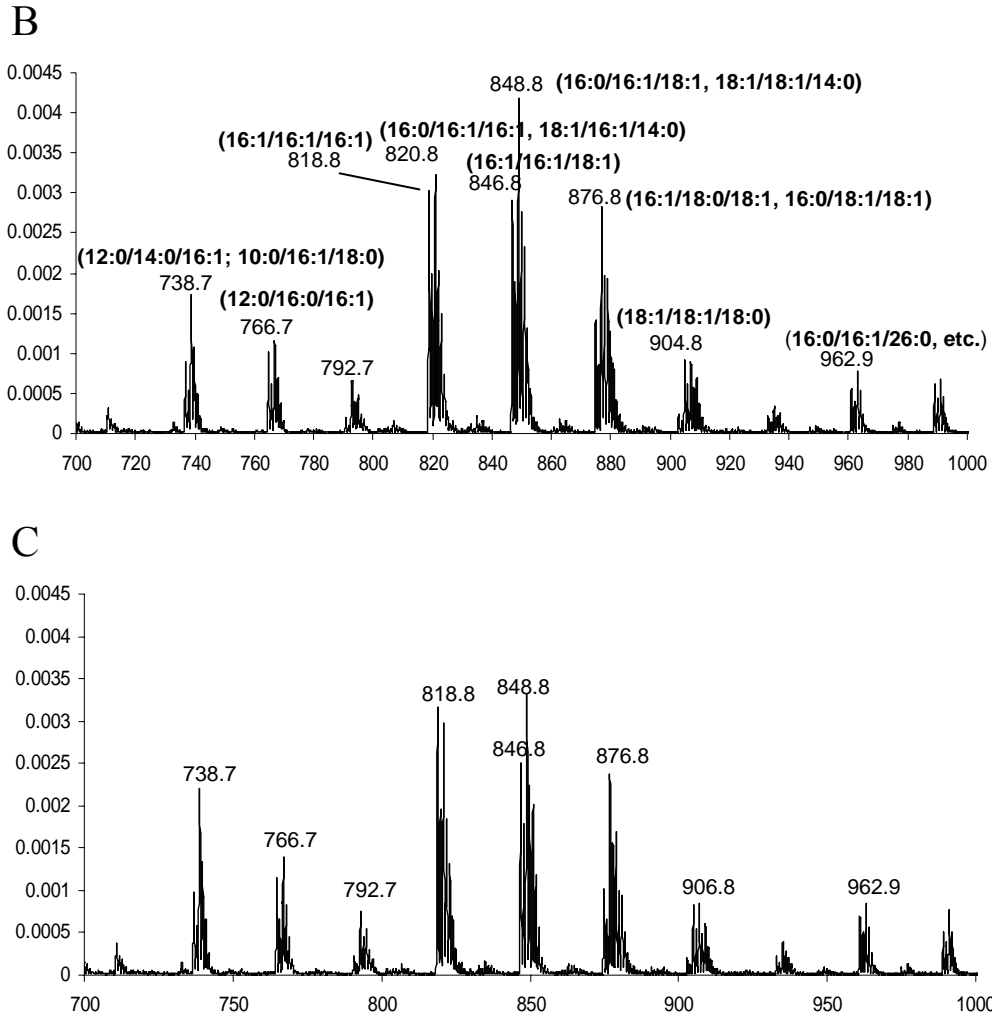
Figure 6-6. Phospholipids and TAG profiles of LDs isolated from WT and *ylr404w* cells cultured in SC medium. A. Phospholipid profiles. B&C, TAG profiles of LDs isolated from WT (B) and *ylr404w* cells (C). n=4.

Chapter 7

Discussion

7.1 Lipid droplets, new discovery of an old cellular component

Studies of LDs carried out in the past 10 years show that LDs exist in all eukaryotic organisms as well as in some prokaryotes. Prokaryotes that have been known to produce LDs include *Rhodococcus* and *Streptomyces* (Alvarez and Steinbüchel, 2002). LDs are distinct from the other cellular organelles. First, while all other organelles are aqueous-cored compartments, LDs consist of a hydrophobic core of neutral lipids. Second, the other organelles are delineated by a phospholipid bilayer, whereas LDs by a monolayer of phospholipids.

In the past, LDs were thought to be inert, storing neutral lipids and providing substrates for synthesis of some specific lipophilic substance. Now we understand that the function of LDs is rather multi-faceted and complicated. They are actively involved in immune response, viral replication, and protein quality control and disposal. We may even imagine that LDs play more roles in cellular processes which will be unveiled in the near future with the advancement in molecular and biochemical techniques.

Very recently, Oloffson and colleagues reported the association of three SNAREs with LDs: VAMP4, syntaxin5 and SNAP-23 (Boström et al., 2007). In their study, a significant amount of VAMP4, syntaxin5 and SNAP-23 was associated with oleic acid-induced LDs. SNAP-23, which lacks a membrane-spanning sequence, required palmitoylation for its association with LDs. Moreover, coimmunoprecipitation experiments showed that VAMP4, syntaxin5 and SNAP-23 form a distinct complex.

Functionally, short interfering RNA (siRNA) and the overexpression of a dominant negative SNAP-23 construct resulted in decreased LD fusion rate and reduced size of LDs, suggesting that VAMP4, syntaxin5 and SNAP-23 are required for LD fusion. This study demonstrates for the first time that homotypic fusion between LDs uses SNAREs, which greatly broadens our understanding of LD cell biology and opens a new research area for LDs.

Furthermore, studies into the pathogenesis of LD-associated devastating human diseases, such as atherosclerosis, type 2 diabetes, and fatty liver, have reached a new level. The emerging concept is that in obesity the TAG storage capacity of adipose tissue overflows, thereby releasing free fatty acids and resulting in accumulation of TAG in non-adipose tissues (Unger et al., 2003).

In summary, recent advances in LD research has tremendously changed our view of LDs. LDs are an independent organelle ubiquitously found in eukaryotic organisms. In addition, LDs are not simple inert storage depots; rather they are actively involved in many cellular processes. Most importantly, LDs are associated with many devastating human diseases. LD research has become urgent and indispensable due to the recent dramatic increase in obesity and diabetes.

7.2 Endoplasmic reticulum, the factory of LD production

In this study, in an effort to identify genes that affect intracellular LD accumulation, I screened the entire collection of yeast viable single gene deletion mutants for changes in

the quantity and morphology of LDs, and identified 16 fld mutants and 117 mld mutants. Genes whose deletions have reduced number of LDs encode: proteins responsible for DNA maintenance and chromatin structure, components of glycosylation machinery, enzymes seated on some metabolic pathways, proteins involved in protein biosynthesis, and miscellaneous proteins (Table 4-1). Genes whose deletions lead to increased quantity of LDs include members of the same groups discussed above; besides, genes whose products serve as channels and transporters, most of which belong to the vacuolar ATPase family, genes of cytoskeleton related proteins, genes encoding proteins responsible for DNA maintenance and chromatin structure, genes whose products involved in protein modification and degradation, genes encoding transcription factors, genes whose products implicated in vesicular trafficking, and some hypothetical or uncharacterized ORFs (Table 4-2).

In terms of function, the scope of the identified genes is very broad and many categories have been discussed in Chapter 4. A very important finding of this study is that a link between ER stress and LD synthesis likely exists. First, mutants defective in protein glycosylation, ERAD, vacuolar H^+-ATPase assembly and vesicular protein trafficking display more LDs than the WT cells; all these mutants cause ER stress. Second, alleviation of ER stress via restoration of glycosylation decreases LD production. Third, Tunicamycin and Brefeldin A, agents that induce ER stress, induce LD synthesis as well. Moreover, the reason that *S. cerevisiae* cells accumulate LDs when they enter stationary phase, particularly in response to nitrogen limitation (Willison and Johnston, 1985), might also be due to ER stress, because nutrient deprivation proves to induce ER stress by

causing protein misfolding, similar to mutations in the genes encoding secretory proteins and differentiation of professional secretory cells (Rutkowski and Kaufman, 2004).

Although *cwh8* cells which exhibit severe underglycosylation of many glycoproteins do not show LD hyperaccumulation, this does not veto the association between ER stress and LD synthesis. It has been shown in Chpater 4 that lack of Cwh8p significantly reduces the intracellular levels of Are1p and Lro1p. Accordingly, we may conclude that deletion of *CWH8* gene on one hand causes protein underglycosylation, leading to ER stress which is supposed to induce LD synthesis; on the other hand, this deletion also leads to insufficient expression of enzymes involved in neutral lipids synthesis, which ultimately affects TAG and SE synthesis and blocks ER stress-induced LD synthesis.

It has been proposed that to cope with ER stress, yeast cells activate both unfolded protein response (UPR) and inositol response (IR), which results in increased synthesis of ER protein-folding factors and of enzymes participating in phospholipid biosynthesis, respectively (Cox et al., 1997). It is generally agreed that UPR requires Ire1p, but evidence suggests that IR is not completely dependent on Ire1p (Stroobants et al., 1999).

In this study, I examined whether elevated LD synthesis in conditions of ER stress was Ire1p dependent. As shown in Chapter 4, deletion of *IRE1* gene from the strains defective in protein glycosylation or ERAD did not reduce the accumulation of LDs. In addition, Tunicamycin that induces ER stress triggered LD synthesis in *ire1* strain as well. These experiments suggest that ER stress-induced LD formation was Ire1p independent. Consistently, I found that enzymes participating in neutral lipids synthesis were not

upregulated in conditions of ER stress, suggesting that ER stress-induced neutral lipids synthesis and LD formation is not necessarily part of UPR. Currently it is still not clear how LD synthesis is induced in conditions of ER stress and what is the signaling pathway(s), but one thing is certain: it is the ER that synthesizes TAG and SE, the LD core components, which are subsequently incorporated into LDs. The link between ER stress and LD synthesis once again signifies the importance of the ER in LD formation.

The ER is central to many essential cellular functions. Contiguous with the nuclear envelope membrane, it forms a membranous network in the cell that is the major site of lipid biosynthesis and is the entry point into the secretory pathway. Being an important calcium store, the ER also functions in cellular signal transduction cascades. Because of its central role in both lipid and protein export, the ER can be considered the common ancestor of all membranes downstream in the secretory pathway, including the Golgi, secretory vesicles, the lysosome, and the plasma membrane. Now evidence is mounting that the ER is also the ancestor of peroxisomes (Kunau, 2005) and LDs (Murphy, and Vance, 1999).

Considering that the ER is the factory of LD production, we may have to pay close attention to the ER in our journey to search for factors that affect LD synthesis, particularly for proteins that are directly involved in LD formation.

7.3 Ylr404wp/Seipin regulates the morphology of LDs

A major finding of this study is the identification of Ylr404wp/seipin as a determinant of the morphology of yeast LDs. LDs of the *ylr404w* cells were morphologically distinct from those of WT cells. When grown in rich medium until stationary-phase, WT cells usually displayed 3 to 6 LDs under the microscope. These LDs were between 0.2-0.4 μm in diameter and were almost spherical in shape, as shown by fluorescence microscopy and electron microscopy. Strikingly, up to thirty percent of the total population of *ylr404w* cells contained one or few "supersized" LDs that were spherical in shape and were about 0.5 to 1.5 μm in diameter. About sixty percent of the *ylr404w* population contained an amorphous aggregation of small- or intermediate-sized LDs. The remaining ~10% of the *ylr404w* cells contained many loosely scattered and weakly stained tiny LDs which had a diameter of less than 0.1 μm. More strikingly, when cultured in synthetic complete medium, the relative ratio of cells accumulating "supersized" LDs to those accumulating amorphous LD clump increased dramatically. More than 80% of the *ylr404w* cells displayed only one or two "supersized" LDs, while amorphous aggregation of many small LDs that were common in cells cultured in YPD media were only observed in about 10% of the cells grown in synthetic complete medium.

The existence of morphologically distinct LDs within the same deletion mutant is intriguing. However, it does suggest enhanced fusion activities of LDs in the mutant cells: the small, discrete LDs may represent the newly synthesized LDs which tend to aggregate before eventually fuse into a "supersized" LD. Consistent with this hypothesis, when *ylr404w* cells were cultured in the synthetic complete medium until mid-log phase (OD_{600}~1.5), fusion of LDs was observed in 10% of the targeted cells in which two or

several LDs lay close together. The fusion process started from the approaching of one LD toward the other, and finished after a new and larger LD appeared. This process was very fast and completed within seconds. No fusion events were observed in WT cells.

Moreover, LDs isolated from *ylr404w* cells demonstrated enhanced fusion activity *in vitro* as well. Purified LDs from both WT and *ylr404w* cells were left in PBS buffer and examined by microscopy before and after 180 minutes. Whereas LDs from WT cells remained scattered and unchanged in size, LDs from *ylr404w* cells formed aggregates or fused into huge lipid inclusions. These experiments clearly show that the lack of Ylr404wp leads to enhanced fusion of LDs in this mutant.

Ylr404wp is a protein of 285 amino acids with two predicted transmembrane domain. Localization studies show that Ylr404wp is an integral ER membrane protein, which again signifies the great importance of the ER in LD formation. Ylr404wp is predicted to span the ER membrane twice by 3 prediction models (TMHMM, HMMTOP, and SOSUI). Moreover, a previous topology study showed that both the N-terminus and C-terminus of Ylr404wp are cytosolically oriented (Kim et al., 2003). Considering that LDs and the ER are closely associated and that the ER has a propensity to enwrap around LDs, I initially thought that Ylr404wp might have direct interaction with LDs, and that by this interaction LDs were held in the vicinity of the ER. When cells were mutated in *YLR404W*, LDs became unstable and displayed tendency to form aggregation. To examine this probability, two truncated Ylr404wp were constructed, which lacked N-terminus and C-terminus respectively. Surprisingly, the result showed that neither terminus is essential for

Ylr404wp's function in maintaining the normal morphology of LDs, which also suggested that the functional domain of this protein is in the ER lumen. Consistent with the prediction, targeted multiple amino acid deletions and single amino acid substitution in the luminal domain completely obliterated the rescue effect of Ylr404wp in the *ylr404w* mutant.

How does Ylr404wp whose functional domain is in the ER lumen affect LD morphology? One probability is that Ylr404wp exerts its effect though a yet-unidentified interaction partner which in turn has direct association with LDs. However, based on our result that LDs isolated from *ylr404w* cells can fuse *in vitro* in the absence of cytosolic proteins and ATP, it is more likely that the physical property of LD components, i.e., phospholipid surface and/or neutral lipids core, has been altered in this mutant, resulting in LD clustering and formation of "supersized" LDs.

Further studies are needed to determine the role of Ylr404wp in LD assembly. In this study sequence homologs of Ylr404wp were sought, so that via comparison we might have some clue to the function of this protein in question. Sequence homology search suggested that four double-pass transmembrane proteins (Kpol_1002p3 of *Vanderwaltozyma polyspora*, a hypothetical protein CAGL0M09933g of *Candida glabrata*, AER072Wp of *Ashbya gossypii*, an unnamed protein product (accession No., CAH02060) of *Kluyveromyces lactis*) are very likely homologs of Ylr404wp. However, none of them have been characterized before. Besides these proteins, Ylr404wp also displays some similarity to mammalian seipins which are also predicted to span the ER membrane twice. A very important finding of this study is that expression of human and

mouse seipin in the *ylr404w* mutant fully rescued its defect in LD morphology, confirming that seipin is an ortholog of Ylr404wp. Since seipin is mutated in type 2 congenital generalized lipodystrophy (CGL2), this result suggests a new link between LD assembly and lipodystrophy.

Sequence alignment of seipin from four species, including human, mouse, rat and chimpanzee, has revealed several interesting features (Agarwal and Garg, 2004). First, the highly conserved region of 280 amino acids begins at the N-terminal end, and is 88% identical across the four species. Second, one isoform of human seipin (AF052149) could extend at least another 64 residues at the putative N-terminus. Third, whereas the C-terminal regions are variable among species, a CAAX-motif sequence (CSSS) at the C-terminus is well preserved. I have shown in this study that expression of the first 280 amino acids of human seipin successfully rescued the defect of LD morphology in *ylr404w* mutant cells. Based on this result as well as sequence alignment, I predict that the functional domain of seipin/Ylr404wp falls within this region. Consistent with the prediction, all the identified seipin mutants that result in CGL are mutated within amino acid 1-280. Among these mutations are F63fsX75, F100fsX111, F105fsX111, F105fsX112, F108fsX113, R138X, ΔV99-S146, A212P, F213fsX232, F224fsX225, and F224ΔY225-Q271fsX288 (Magre et al., 2001), F101fsX111 and F213fsX231 (Van Maldergem et al., 2002), W259X (Heathcote et al., 2002), F53fsX93, F64fsX91, L227X, and G271fsX283 (Agarwal et al., 2003), R275X (Ebihara et al., 2004), and E189X (Jin et al., 2007). Interestingly, one point mutations of human seipin that is implicated in lipodystrophy (A212P) also abolished its rescue effect in *ylr404w* cells, suggesting

defective LD morphology/assembly and CGL2 are connected.

Human seipin mutations are also implicated in the etiology of distal hereditary motor neuropathy and Silver syndrome. Two heterozygous missense mutations resulting in amino acid substitutions N88S and S90L were identified and these two amino acid substitutions were thought to affect glycosylation of seipin and result in protein aggregate formation leading to neurodegeneration (Windpassinger et al., 2004). In this study I showed that these two mutations did not affect the function of seipin in LD assembly, which may suggest that motorneuron disease is not associated with defective lipid metabolism.

7.4 Congenital generalized lipodystrophy and LD formation

Congenital generalized lipodystrophy, a rare autosomal recessive disorder, is characterized by near complete absence of adipose tissue from birth. Affected individuals have marked insulin resistance, hypertriglyceridemia and acanthosis nigricans, and develop early-onset diabetes mellitus. Genetic studies revealed that two genes, when mutated individually, cause CGL. *AGPAT2* linked to chromosome 9q34 is responsible for CGL1 subtype (Agarwal et al., 2002), and *BSCL2* (encoding seipin) linked to chromosome 11q13 is responsible for CGL2 subtype (Magre et al., 2001).

Recently, the gene mutated in fatty liver dystrophy (fld) mice which carry features of human lipodystrophy was isolated and named *Lpin1* (Péterfy et al., 2001). Subsequent studies revealed that the protein product of *Lpin1*, lipin-1, is a phosphatidic acid

phosphatase (PAP-1). Carman's group purified PAP-1 activity from *Saccharomyces cerevisiae* and through amino acid sequencing, identified it as Smp2p, the yeast ortholog of lipin (Han et al., 2006). Subsequently, mammalian lipin-1 and its two isoforms, lipin-2 and lipin-3, were characterized to act as PAP-1 enzymes (Donkor et al., 2007).

AGPATs catalyze acylation of lysophosphatidic acid to phosphatidic acid, and lipins subsequently convert phosphatidic acid to DAG (Figure 7-1). Since both enzymes are extremely important in biosynthesis of TAG, human congenital generalized lipodystrophy caused by *AGPAT2* mutation and mouse fatty liver dystrophy caused by *Lpin1* mutation might be attributed in part to insufficient TAG synthesis. Supporting this speculation, both AGPAT2 and lipin-1 were identified as major isoform of AGPAT and lipin, respectively, in adipose tissue. Human *AGPAT* has five isoforms, namely, *AGPAT1* through *AGPAT5*. Quantitation of mRNA levels of five *AGPAT* isoforms revealed that in adipose tissue *AGPAT2* was expressed twofold more than *AGPAT1*. In liver expression of *AGPAT2* and *AGPAT1* was almost at the same level. In skeletal muscle *AGPAT1* was expressed 1.8-fold more than *AGPAT2*. Expression of the other three isoforms was barely detectable (Agarwal et al., 2002). As for lipin-1, using tissues from fld mice, it was determined that it accounts for all PAP-1 activity in white and brown adipose tissue, and skeletal muscle, the metabolic tissues with the highest levels of lipin-1 expression (Donkor et al., 2007). Activity in liver of fld mice, however, was normal (Donkor et al., 2007) or reduced by 50% (Harris et al., 2007), suggesting compensation by another member(s) of the lipin protein family. Consistent with this possibility, lipin-2 is normally expressed at

substantial levels in liver of WT and fld mice, and lipin-3 is upregulated by fourfold in the liver of fld mice (Donkor et al., 2007).

Furthermore, enhanced lipin expression in adipose tissue promotes obesity (Phan and Reue, 2005). Lipin-1 expression driven by adipocyte fatty acid binding protein (aP2) regulatory element was used to produce transgenic mice with elevated lipin-1 expression in adipose tissue. On a chow diet, adipose-specific transgenic mice had similar body weights to control littermates. On a high-fat diet, however, adipose-specific transgenic mice gained weight much faster than non-transgenic mice, despite equivalent food intake. They displayed a 40% increase in body weight after 6 weeks on the diet; the increase in non-transgenic mice was only 20%. In addition, they had a normal number of adipocytes, but increased TAG storage and increased expression of lipogenic genes, including acetyl-CoA carboxylase and DGAT. In light of these findings that while lipin-1 deficiency produces lipodystrophy, enhanced lipin-1 expression in transgenic mice gives rise to obesity, it appears that lipin-1 levels determines TAG synthesis. Analogously, AGPAT2 activity is also required for TAG mass accumulation in mature adipocytes and lipid accumulation was attenuated by 50% in adipocytes with stable knockdown of AGPAT2 (Gale et al., 2006).

However, lipodystrophy is more than reduced TAG synthesis. Lipodystrophy is characterized by a marked lack of adipose tissue (both cells and lipid cargo). Decreased TAG synthesis only affects lipid loading of adipocytes. Therefore, one question arises, why mutation of *AGPAT2* or *Lpin1* impairs differentiation of preadipocytes into

adipocytes? Here I discuss the latest findings concerning the role of AGPAT2 and lipin-1

in adipogenesis.
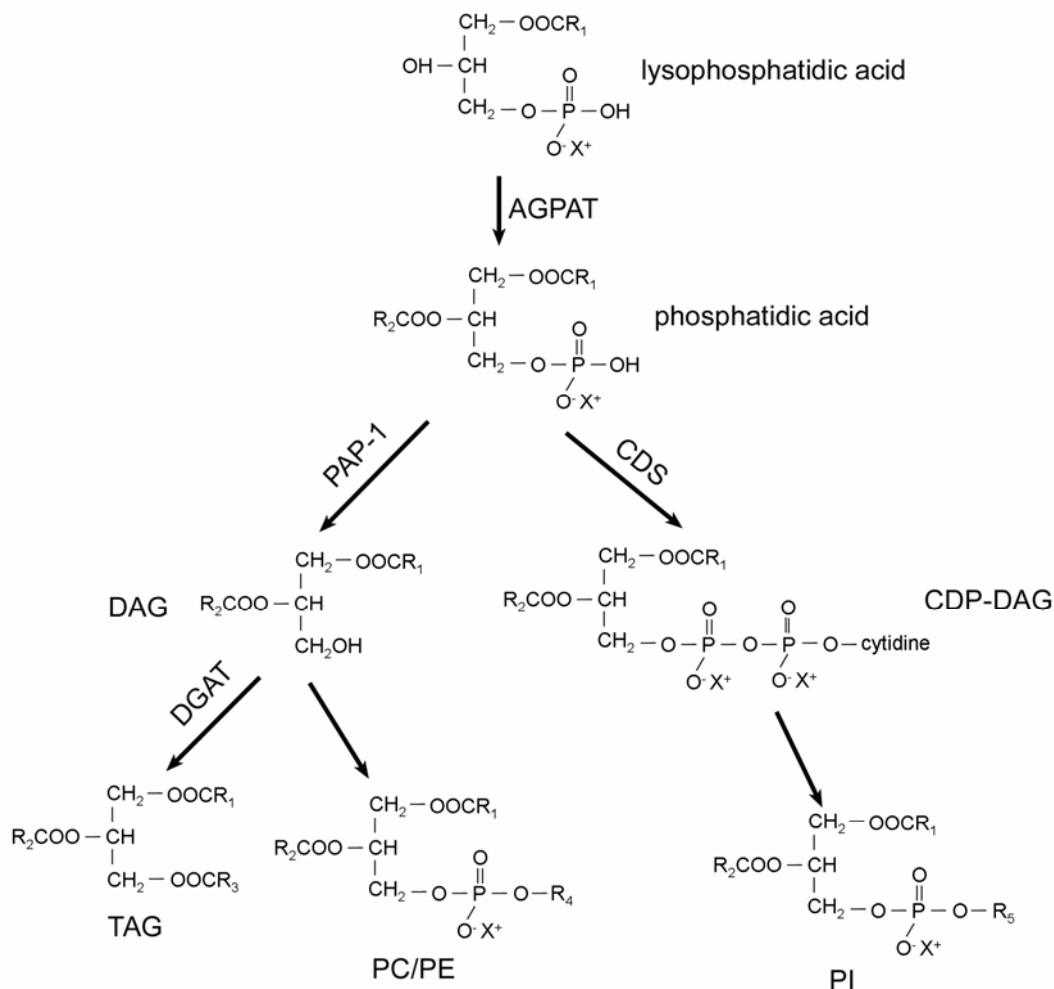
Figure 7-1. The role of AGPAT and PAP-1 in synthesis of phospholipids and TAG. AGPAT, 1-acylglycerol-3-phosphate acyltransferase; PAP-1, phosphatidic acid phosphatase; DGAT, sn-1,2-diacylglycerol acyltransferase; CDS, CDP-DAG synthase. R_1, R_2, and R_3 are acyl chains. R_4 represents a choline or ethanolamine group. R_5 is an inositol group. X=H, Na, K, Ca, etc.

During adipogenesis (differentiation of preadipocytes into adipocytes), a cascade of

transcriptional factors coordinate this process. Over the past two decades, attention has

centered on the nuclear receptor peroxisome proliferator-activated receptor γ (PPARγ)

and CCAAT-enhancer binding proteins (C/EBPs). PPARγ, the 'master regulator' of

adipogenesis, is necessary for adipogenesis, and crucial signalling pathways in adipogenesis, both pro-adipogenesis and anti-adipogenesis, converge on the regulation of PPARγ expression or activity (Rosen and MacDougald, 2007). C/EBP family members are also very important for adipogenesis. The temporal expression of C/EBPs indicates that early induction of C/EBPβ and C/EBPδ leads to induction of C/EBPα. Knockdown of C/EBPα resulted in near-complete loss of white adipose tissue in mice (Linhart et al., 2001), indicating a key role for this factor in adipose tissue development. However, C/EBPs cannot function independently in the absence of PPARγ. First, C/EBPβ cannot induce expression of C/EBPα in the absence of PPARγ (Zuo et al., 2006). In addition, ectopic expression of C/EBPα cannot rescue adipogenesis in $Pparg^{-/-}$ fibroblasts (Rosen et al., 2002).

Evidence suggested that lipin expression preceding PPARγ is critical for adipogenesis (Phan et al., 2004). Using primary mouse embryonic fibroblasts isolated from fld mice, lipin deficiency was shown to prevent induction of key adipogenic genes, including PPARγ and C/EBPα. In 3T3-L1 preadipocytes, prior to the induction of PPARγ and C/EBPα, transient lipin expression was detected at 10 h into the differentiation program. Similarly, AGPAT2 mRNA expression is induced 30-fold during adipocyte differentiation, and small interference RNA-mediated knockdown of AGPAT2 expression prevents appropriate early induction of PPARγ and C/EBPβ, and delays expression of multiple adipocyte-related genes, including genes involved in glucose uptake (GLUT4), fatty acid metabolism (ACSL1 and AP2), TAG storage (perilipin), and energy homeostasis (adiponectin) (Gale et al., 2006). Based on these data, AGPAT2 and lipin-1

may on one hand contribute to TAG synthesis, on the other hand promote adipogenesis by activating PPARγ and C/EBPs.

How does *BSCL2* mutation lead to lipodystrophy? This remains an open question. Human *BSCL2* is most highly expressed in brain and testes (Magre et al., 2001), similar to its mouse homolog *Gng3lg* (Downes et al., 1998). High expression of *BSCL2* mRNA in the brain led to speculation that lack of body fat in patients with *BSCL2* mutation might be due to hypothalamopituitary dysfunction (Magre et al., 2001). However, an alternative hypothesis proposed that lipodystrophy in patients with BSCL2 mutations is due to the direct disruption of adipocyte differentiation, based on semiquantitative reverse-transcription PCR results that *BSCL2* mRNA level in adipose tissue is twofold greater than that in liver, and that skeletal muscle poorly expresses *BSCL2*. Accordingly, the activity of PPARγ and/or C/EBPs should be impaired in *BSCL2* mutation as in *AGPAT2* mutation and *Lpin1* mutation.

Phenotypic study disclosed that CGL2 (due to *BSCL2* mutation) not only had marked lack of metabolically-active adipose tissue from subcutaneous areas, intraabdominal and intrathoracic regions, and bone marrow, but also displayed paucity of mechanical adipose tissue in the orbits, palms, soles, scalp, and peri-articular regions; in contrast, CGL1 (due to *AGPAT2* mutation) only displayed paucity of metabolically-active adipose tissue (Simha and Garg, 2003). In addition, CGL2 patients had an earlier onset of diabetes, and higher prevalence of mild mental retardation compared with CGL1 (Agarwal et al., 2003). These differences indicate that the influence of seipin on adipogenesis is even more

profound than that of AGPAT2. Considering that the differentiation of preadipocytes in humans to white adipocytes could proceed either towards metabolically-active or mechanical adipocytes (Klaus, 1997), the *BSCL2* mutation should affect the process of differentiation more proximally compared with *AGPAT2* mutation.

In *S. cerevisiae*, *SMP2* (homolog of *Lpin1*) mutation caused reduced levels of PAP-1 enzyme activity, leading to increased accumulation of phosphatidic acid and reduced production of DAG and its derivative TAG (Han et al., 2006). Deletion of *SLC1* (yeast *AGPAT*) does not greatly affect TAG synthesis due to the presence of a redundant *SLC4* (Athenstaedt and Daum, 1997; Benghezal et al., 2007). In contrast, deletion of *YLR404W*, the yeast ortholog of *BSCL2*, resulted in a significant increase of neutral lipids synthesis (30% increase of TAG and 10% increase of SE when cultured in YPD medium till stationary phase). This raises a possibility that seipin mutation mainly impairs differentiation of preadipocytes into adipocytes without reducing TAG synthesis. To test this possibility, a genetic *BSCL2* knockout mice/rats model is desired for future research.

Intriguingly, we observed that there is a shift from long-chain (18:1) to medium/short-chain (16:0, 14:0, 12:0) fatty acid incorporation into all major phospholipids as well as TAG due to the deletion of *YLR404W*. Although it is yet to be determined whether this shift accounts for fusion of LDs, the role of Ylr404wp in phospholipid metabolism itself is worth investigating, considering the great importance of phospholipids in a variety of cellular processes.

Fatty acyl chain pattern of phospholipids and TAG could be affected by many factors

along their synthesis pathways, including 1) availability of fatty acids which is determined by *de novo* fatty acid synthesis and fatty acid supplementation, 2) conversion of fatty acids to acyl-CoA, 3) stepwise acylation of sn-glycerol-3-phosphate/1,3-dihydroxyacetone phosphate and sn-1-acyl-glycerol-3-phosphate, as well as acylation of DAG (into TAG), 4) remodeling of acyl chain pattern of phospholipids (Given that phosphatidic acid is the key intermediate in phopholipid synthesis as well as in TAG synthesis, phospholipid remodeling can also affect acyl chain pattern of TAG).

Phospholipid remodeling by acyl chain exchange mainly proceeds via deacylation to a lysophospholipid intermediate, followed by acyl-CoA dependent reacylation with an acyltransferase. Recently Slc4p (also named Lpt1p, Ale1p, and Lca1p) was identified as the major lysophospholipid acyltransferase in yeast, which prefers incorporating unsaturated acyl chains into phospholipids *in vitro* (Jain et al., 2007; Riekhof et al., 2007; Tamaki et al., 2007). However, deletion of *SLC4* did not lead to a shift of acyl chains from long-chain to medium/short-chain in all major phospholipids (Benghezal et al., 2007). Therefore, phenotypic acyl chain pattern of phospholipids and TAG due to *YLR404W* deletion may not result from phospholipid remodeling.

The sn-1 position of phospholipids and TAG is acylated by Gat1p and Gat2p in yeast using sn-glycerol-3-phosphate/1,3-dihydroxyacetone phosphate as substrate. Subsequently, the sn-2 postion is acylated by Slc1p and Slc4p using sn-1-acyl-glycerol-3-phosphate (lysophosphatidic acid) as substrate. Preference for unsaturated fatty acids has been reported for Gat1p and Gat2p (Zheng and Zou, 2001),

and for Slc4p, but none of the single gene deletion mutants, *gat1*, *gat2*, *slc1*, and *slc4*, displays a major change in the fatty acyl pattern of phospholipids and TAG (Zheng and Zou, 2001; Benghezal et al., 2007). Therefore, if there is probability that the change from long-chain to medium/short-chain fatty acyls of phospholipids and TAG is due to defective acylation, Ylr404wp must have direct or indirect interaction with at least two acyltransferases.

Conversion of fatty acids to acyl-CoA is catalyzed by acyl-CoA synthases (ACS). The yeast *S. cerevisiae* has 6 ACS enzymes, Faa1p through Faa4p, Fat1p and Fat2p. Faa1p is quite abundant and accounts for most of the long chain ACS activity (Faergeman et al., 2001). The presence of Faa1p is detected on the plasma membrane, mitochondria, as well as LDs (Black and DiRusso, 2007). In this study, however, proteomics of LDs isolated from *ylr404w* cells suggested that Faa1p might be missing from this fraction. If this result is reproducible, the dissociation of Faa1p from LDs might contribute to the shift from long-chain to medium/short-chain of acyl chain pattern of phospholipids and TAG.

De novo fatty acid synthesis needs to be considered as a possible cause as well, in light of the fatty acyl profiles of polar lipids extracted from *ylr404w* cells (Figure 6-5 E). Many factors could be involved in this process. For instance, the expression level and activity of stearoyl-CoA 9-desaturase (Ole1) could affect the synthesis of FA18:1 (Stukey et al., 1990).

7.5. Future studies

During the same period of this study, Goodman's group independently found that Ylr404wp is a homolog of human seipin and it modulates LD assembly in the budding yeast (Szymanski et al., 2007). Combining their study and ours, we should be able to draw a conclusion that the function of seipin is well conserved from yeast to human, indicating a fundamental role for this protein. Since seipin mutation is implicated in lipodystrophy and Ylr404wp plays a key role in regulating LD assembly and phospholipid homeostasis, it is very necessary to explore their molecular functions.

YLR404W deletion leads to fusion of LDs, producing 'supersized' LDs. It remains to be established whether the change of acyl chain pattern of phospholipids/TAG accounts for the phenotype and how Ylr404wp regulates phospholipids/TAG metabolism. Specifically, in order to show whether the shift from long-chain to medium/short-chain fatty acid incorporation into phospholipids/TAG is due to defective acylation, the expression level of acyltransferases, including Gat1p, Gat2p, Slc1p, and slc4p, requires to be examined in *ylr404w* mutant and WT strain. Second, the missing of Faa1p from the LD-rich fraction isolated from *ylr404w* cells remains to be confirmed. If Faa1p is really dissociated from LDs due to lack of Ylr404wp, the cause of dissociation should be investigated. In addition, whether dissociation of faa1p from LDs attributes to acyl chain pattern of phospholipids/TAG in *ylr404w* cells needs to be addressed. Third, the acyl chain pattern of phospholipids/TAG after fatty acid complementation should be probed in order to show whether de novo fatty acid synthesis is responsible for the phenotypic change of phospholipids/TAG. Fourth, previously I have shown that *ylr404w* cells displayed a faster incorporation of oleate into SE but a slower incorporation of oleate into

TAG than WT cells (Figure 5-17C). It remains to be determined whether this is specific for oleate and if *ylr404w* cells could incorporate C14:0 and C16:0 much faster than C18:1 (oleate) into phospholipids/TAG.

Since a lack of Ylr404wp results in a change in acyl chain pattern of phospholipids, which might be the cause of LD fusion, it is of great interest to examine other organelles, since acyl chain pattern of phospholipids might have detrimental effect on membrane thickness, intrinsic curvature, and fluidity, which ultimately affects the physical properties of membranes and dynamic processes such as membrane fusion and fission.

It is also of interest to look for the interaction partner(s) of Ylr404wp. In addition, as I have shown that LD fusion in *ylr404w* cells is actin-dependent, effort is needed to determine how actin plays a role in LD fusion and which actin-related proteins are involved in this process.

In contrast to the missing of Faa1p, I detected the presence of Pma1p in the LD-rich fraction of *ylr404w* cells but not of WT cells. Experiments should be carried out to confirm this result. If this turns out to be reproducible, this means Pma1p, the plasma membrane P-type H^+-ATPase that pumps protons out of the cell (Serrano et al., 1986), can be relocated to LDs. physiological relevance of this relocation should be investigated.

In addition to necessary Ylr404wp research in the *S. cerevisiae*, seipin-centered studies should also be carried out in animals and human. First of all, a genetic seipin knockout mice model is desired. Using this model, the role of seipin in adipogenesis will be explored. In addition, understanding the role of seipin in the assembly of mammalian LDs is desirable.

7.6. Summary

In order to identify genes that affect LD dynamics in *S. cerevisiae*, I screened the

entire collection of viable yeast single-gene deletion mutants and identified 16 strains

with decreased accumulation of LDs and 117 strains with increased accumulation of LDs.

The scope of the identified genes is very broad, but a link between ER stress and LD

synthesis likely exists.

A novel yeast protein (Ylr404wp) was identified which appears to be a key regulator

of the cellular dynamics of LDs. Deletion of *YLR404W* causes increased level of neutral

lipids, clustering of LDs and formation of enlarged (supersized) LDs. Increased neutral

lipids in WT cells often lead to a (dramatic) increase in the number but not the size of

LDs. Therefore, the appearance of "supersized" LDs in *ylr404w* cells are unlikely to be

caused by a moderate increase in neutral lipids. Rather, the physical property of the

surface of LDs might have been altered in *ylr404w* cells due to changes in phospholipids,

which may facilitate the clustering and fusion of LDs. In support of this, LDs isolated

from *ylr404w* cells can aggregate and fuse without the supply of ATP and cytoplasmic

proteins. Our data also highlight the role of Ylr404wp in determining the size of LDs. The

average size of LDs in adipocytes is much larger than that in liver or muscle cells under

normal physiological conditions. It would be interesting to see if seipin is involved in the

regulation of the size of LDs in mammallian cells.

Results described herein show for the first time that seipin and its homologues

modulate the formation and especially fusion of the LDs. Importantly, our data suggest

that changes in phospholipid metabolism may be the unifying theme for both CGL1 and

CGL2. This study identified a key regulator for the formation of LDs and provided novel

insights into the molecular function of an important disease protein. Furthermore, it will

open up new avenues of research for uncovering the molecular mechanisms underlying

LD fusion and adipogenesis.

References

Abell BM, Holbrook LA, Abenes M, Murphy DJ, Hills MJ, Moloney MM. (1997). Role of the proline knot motif in oleosin endoplasmic reticulum topology and oil body targeting. Plant Cell. 9, 1481-93.

Adams AE, Pringle JR. (1984). Relationship of actin and tubulin distribution to bud growth in wild-type and morphogenetic-mutant Saccharomyces cerevisiae. J Cell Biol. 98, 934-45.

Agarwal AK, Arioglu E, De Almeida S, Akkoc N, Taylor SI, Bowcock AM, Barnes RI, Garg A. (2002). AGPAT2 is mutated in congenital generalized lipodystrophy linked to chromosome 9q34. Nat Genet. 31, 21-3.

Agarwal AK, Garg A. (2003). Congenital generalized lipodystrophy: significance of triglyceride biosynthetic pathways. Trends Endocrinol Metab. 14, 214-21.

Agarwal AK, Garg A. (2004). Seipin: a mysterious protein. Trends Mol Med. 10, 440-4.

Agarwal AK, Simha V, Oral EA, Moran SA, Gorden P, O'Rahilly S, Zaidi Z, Gurakan F, Arslanian SA, Klar A, Ricker A, White NH, Bindl L, Herbst K, Kennel K, Patel SB, Al-Gazali L, Garg A. (2003). Phenotypic and genetic heterogeneity in congenital generalized lipodystrophy. J Clin Endocrinol Metab. 88, 4840-7.

Alvarez HM, Steinbüchel A. (2002). Triacylglycerols in prokaryotic microorganisms. Appl Microbiol Biotechnol. 60, 367-76.

Andersson L, Boström P, Ericson J, Rutberg M, Magnusson B, Marchesan D, Ruiz M, Asp L, Huang P, Frohman MA, Borén J, Olofsson SO. (2006). PLD1 and ERK2 regulate cytosolic lipid droplet formation. J Cell Sci. 119, 2246-57.

Athenstaedt K, Daum G. (1997). Biosynthesis of phosphatidic acid in lipid particles and endoplasmic reticulum of Saccharomyces cerevisiae. J Bacteriol. 179, 7611-6.

Athenstaedt K, Daum G. (2000). 1-Acyldihydroxyacetone-phosphate reductase (Ayr1p) of the yeast Saccharomyces cerevisiae encoded by the open reading frame YIL124w is a major component of lipid particles. J Biol Chem. 275, 235-40.

Athenstaedt, K., and Daum, G. (2003). YMR313C/TGL3 encodes a novel triacylglycerol lipase located in lipid particles of Saccharomyces cerevisiae. J Biol Chem. 278, 23317-23.

Athenstaedt K, Daum G. (2005). Tgl4p and Tgl5p, two triacylglycerol lipases of the yeast Saccharomyces cerevisiae are localized to lipid particles. J Biol Chem. 280, 37301-9.

Athenstaedt K, Jolivet P, Boulard C, Zivy M, Negroni L, Nicaud JM, Chardot T. (2006). Lipid particle

composition of the yeast Yarrowia lipolytica depends on the carbon source. Proteomics. 6, 1450-9.

Athenstaedt, K., Zweytick, D., Jandrositz, A., Kohlwein, S.D., and Daum, G. (1999). Identification and characterization of major lipid particle proteins of the yeast Saccharomyces cerevisiae. J Bacteriol. 181, 6441-8.

Ausubel, F. M., Brent, R., Kingston, R. E., Moore, D. D., Seidman, J. G., Smith, J. A., and Struhl, K. (2003). Current Protocols in Molecular Biology. John Wiley & Sons, Inc. New York.

Ayscough KR, Stryker J, Pokala N, Sanders M, Crews P, Drubin DG. (1997).High rates of actin filament turnover in budding yeast and roles for actin in establishment and maintenance of cell polarity revealed using the actin inhibitor latrunculin-A. J Cell Biol. 137, 399-416.

Baker D, Wuestehube L, Schekman R, Botstein D, Segev N. (1990). GTP-binding Ypt1 protein and Ca2+ function independently in a cell-free protein transport reaction. Proc Natl Acad Sci U S A. 87, 355-9.

Barba G, Harper F, Harada T, Kohara M, Goulinet S, Matsuura Y, Eder G, Schaff Z, Chapman MJ, Miyamura T, Brechot C. (1997). Hepatitis C virus core protein shows a cytoplasmic localization and associates to cellular lipid storage droplets. Proc Natl Acad Sci U S A. 94, 1200-5.

Barlowe C. (2002). COPII-dependent transport from the endoplasmic reticulum. Curr Opin Cell Biol. 14, 417-22.

Baudin A, Ozier-Kalogeropoulos O, Denouel A, Lacroute F, Cullin C. (1993). A simple and efficient method for direct gene deletion in Saccharomyces cerevisiae. Nucleic Acids Res. 21, 3329-30.

Bell, R. M., Ballas, L. M., and Coleman, R. A. (1980). Lipid topogenesis. J Lipid Res. 22, 391-403

Bell, R.M., and Coleman, R.A. (1980). Enzymes of glycerolipid synthesis in eukaryotes. Annu Rev Biochem. 49, 459-87.

Benghezal M, Roubaty C, Veepuri V, Knudsen J, Conzelmann A. (2007). SLC1 and SLC4 encode partially redundant acyl-coenzyme A 1-acylglycerol-3-phosphate O-acyltransferases of budding yeast. J Biol Chem. 282, 30845-55.

Bergfeld R, Hong YN, Kühnl T, and Schopfer P. (1978). Formation of oleosomes (storage lipid bodies) during embryogenesis and their breakdown during seedling development in cotyledons of Sinapis alba L. Planta. 1978, 297-307.

Beyenbach KW, Wieczorek H. (2006). The V-type H+ ATPase: molecular structure and function, physiological roles and regulation. J Exp Biol. 209, 577-89.

Binns D, Januszewski T, Chen Y, Hill J, Markin VS, Zhao Y, Gilpin C, Chapman KD, Anderson RG,

Goodman JM. (2006). An intimate collaboration between peroxisomes and lipid bodies. J Cell Biol. 173, 719-31.

Black PN, DiRusso CC. (2007). Yeast acyl-CoA synthetases at the crossroads of fatty acid metabolism and regulation. Biochim Biophys Acta. 1771, 286-98.

Blanchette-Mackie, E.J., Dwyer, N.K., Barber, T., Coxey, R.A., Takeda, T., Rondinone, C.M., Theodorakis, J.L., Greenberg, A.S., and Londos, C. (1995). Perilipin is located on the surface layer of intracellular lipid droplets in adipocytes. J Lipid Res. 36, 1211-26.

Bligh EG, Dyer WJ. (1959). A rapid method of total lipid extraction and purification. Can J Biochem Physiol. 37, 911-7.

Bonifacino, J. S., Dasso, M., Harford, J. B., Lippincott-Schwartz, J., and Yamada, K. M. (2003). Current Protocols in Cell Biology. John Wiley & Sons, Inc. New York.

Boström P, Andersson L, Rutberg M, Perman J, Lidberg U, Johansson BR, Fernandez-Rodriguez J, Ericson J, Nilsson T, Borén J, Olofsson SO. (2007). SNARE proteins mediate fusion between cytosolic lipid droplets and are implicated in insulin sensitivity. Nat Cell Biol. 9, 1286-93.

Bostrom P, Rutberg M, Ericsson J, Holmdahl P, Andersson L, Frohman MA, Boren J, Olofsson SO. (2005). Cytosolic lipid droplets increase in size by microtubule-dependent complex formation. Arterioscler Thromb Vasc Biol. 25, 1945-51.

Boulant S, Targett-Adams P, McLauchlan J. (2007). Disrupting the association of hepatitis C virus core protein with lipid droplets correlates with a loss in production of infectious virus. J Gen Virol. 88, 2204-13.

Bozza PT, Melo RC, Bandeira-Melo C. (2007). Leukocyte lipid bodies regulation and function: contribution to allergy and host defense. Pharmacol Ther. 113, 30-49.

Bozzola, J.J. and Russell, L.D. (1992). Electron microscopy. Jones and Bartlett publishers, pp.471.

Bradford, MM. (1976). A rapid and sensitive for the quantitation of microgram quantitites of protein utilizing the principle of protein-dye binding. Anal Biochem. *72,* 248-254.

Brasaemle, D.L., Barber, T., Wolins, N.E., Serrero, G., Blanchette-Mackie, E.J., and Londos, C. (1997). Adipose differentiation-related protein is an ubiquitously expressed lipid storage droplet-associated protein. J Lipid Res. 38, 2249-63.

Brasaemle DL, Dolios G, Shapiro L, Wang R. (2004). Proteomic analysis of proteins associated with lipid droplets of basal and lipolytically stimulated 3T3-L1 adipocytes. J Biol Chem. 279, 46835-42.

Brasaemle DL, Hansen JC. (2006). Developmental biology: holding pattern for histones.Curr Biol. 16,

R918-20.

Brasaemle DL, Rubin B, Harten IA, Gruia-Gray J, Kimmel AR, Londos C. (2000). Perilipin A increases triacylglycerol storage by decreasing the rate of triacylglycerol hydrolysis. J Biol Chem. 275, 38486-93.

Bretscher, M. S. (1972). Asymmetric lipid bilayer structure for biological membranes. Nature (New Biol.). 236, 11–12.

Budd ME, Campbell JL. (1997). A yeast replicative helicase, Dna2 helicase, interacts with yeast FEN-1 nuclease in carrying out its essential function. Mol Cell Biol. 17, 2136-42.

Buhman, K.F., Accad, M., and Farese, R.V.Jr. (2000). Mammalian acyl-CoA:cholesterol acyltransferases. Biochim Biophys Acta. 1529, 142-154

Bussell R Jr, Eliezer D. (2003). A structural and functional role for 11-mer repeats in alpha-synuclein and other exchangeable lipid binding proteins. J Mol Biol. 329, 763-78.

Camadro JM, Labbe P. (1996). Cloning and characterization of the yeast HEM14 gene coding for protoporphyrinogen oxidase, the molecular target of diphenyl ether-type herbicides. J Biol Chem. 271, 9120-8.

Carlson M. (1999). Glucose repression in yeast. Curr Opin Microbiol. 2, 202-7.

Cases, S., Novak, S., Zheng, Y-W., Myers, H.M., Lear, S.R., Sande, E., Welch, C.B., Lusis, A.J., Spencer, T.A., Krause, B.R., Erickson, S.K., and Farese, R.V.Jr. (1998). ACAT-2, A second mammalian acyl-CoA:cholesterol acyltransferase, its cloning, expression, and characterization. J Biol Chem. 273, 26755-26764.

Cases, S., Smith, S.J., Zheng, Y.W., Myers, H.M., Lear, S.R., Sande, E., Novak, S., Collins, C., Welch, C.B., Lusis, A.J., Erickson, S.K., and Farese, R.V. Jr. (1998). Identification of a gene encoding an acyl CoA:diacylglycerol acyltransferase, a key enzyme in triacylglycerol synthesis. Proc Natl Acad Sci U S A. 95,13018-23

Cases, S., Stone, S.J., Zhou, P., Yen, E., Tow, B., Lardizabal, K.D., Voelker, T., and Farese, R.V. Jr. (2001). Cloning of DGAT2, a second mammalian diacylglycerol acyltransferase, and related family members. J Biol Chem. 276, 38870-6

Cermelli S, Guo Y, Gross SP, Welte MA. (2006). The lipid-droplet proteome reveals that droplets are a protein-storage depot. Curr Biol. 16, 1783-95.

Chang BH, Li L, Paul A, Taniguchi S, Nannegari V, Heird WC, Chan L. (2005). Protection against fatty liver but normal adipogenesis in mice lacking adipose differentiation-related protein. Mol Cell Biol. 26, 1063-76.

Chang, C.C.Y., Huh, H.Y., Cadigan, K.M., and Chang, T.Y. (1993). Molecular cloning and functional expression of human acyl-coenzyme A:cholesterol acyltransferase cDNA in mutant chinese hamster ovary cells. J Biol Chem. 268, 20747-20755.

Chavez S, Beilharz T, Rondon AG, Erdjument-Bromage H, Tempst P, Svejstrup JQ, Lithgow T, Aguilera A. (2000). A protein complex containing Tho2, Hpr1, Mft1 and a novel protein, Thp2, connects transcription elongation with mitotic recombination in Saccharomyces cerevisiae. EMBO J. 19, 5824-34.

Chen JC, Lin RH, Huang HC, Tzen JT. (1997). Cloning, expression and isoform classification of a minor oleosin in sesame oil bodies. J Biochem (Tokyo). 122, 819-24.

Cho SY, Shin ES, Park PJ, Shin DW, Chang HK, Kim D, Lee HH, Lee JH, Kim SH, Song MJ, Chang IS, Lee OS, Lee TR. (2007). Identification of mouse Prp19p as a lipid droplet-associated protein and its possible involvement in the biogenesis of lipid droplets. J Biol Chem. 282, 2456-65.

Choo QL, Kuo G, Weiner AJ, Overby LR, Bradley DW, Houghton M. (1989). Isolation of a cDNA clone derived from a blood-borne non-A, non-B viral hepatitis genome. Science. 244, 359-62.

Christiansen K, Jensen PK. (1972). Membrane-bound lipid particles from beef heart. Chemical composition and structure. Biochim Biophys Acta. 260, 449-59.

Clifford GM, Londos C, Kraemer FB, Vernon RG, Yeaman SJ. (2000). Translocation of hormone-sensitive lipase and perilipin upon lipolytic stimulation of rat adipocytes. J Biol Chem. 2275, 5011-5.

Coe JG, Lim AC, Xu J, Hong W. (1999). A role for Tlg1p in the transport of proteins within the Golgi apparatus of Saccharomyces cerevisiae. Mol Biol Cell. 10, 2407-23.

Cohen AW, Razani B, Schubert W, Williams TM, Wang XB, Iyengar P, Brasaemle DL, Scherer PE, Lisanti MP. (2004). Role of caveolin-1 in the modulation of lipolysis and lipid droplet formation. Diabetes. 53, 1261-70.

Cole NB, Murphy DD, Grider T, Rueter S, Brasaemle D, Nussbaum RL. (2002). Lipid droplet binding and oligomerization properties of the Parkinson's disease protein alpha-synuclein. J Biol Chem. 277, 6344-52.

Coleman, R., and Bell, R.M. (1976). Triacylglycerol synthesis in isolated fat cells. Studies on the microsomal diacylglycerol acyltransferase activity using ethanol-dispersed diacylglycerols. J Biol Chem. 251, 4537-43.

Coleman, R. A., and Lee, D. P. (2004). Enzymes of triacylglycerol synthesis and their regulation. Prog Lipid Res. 43, 134-176

Cote J, Quinn J, Workman JL, Peterson CL. (1994). Stimulation of GAL4 derivative binding to nucleosomal DNA by the yeast SWI/SNF complex. Science. 265, 53-60.

Cox JS, Chapman RE, Walter P. (1997). The unfolded protein response coordinates the production of endoplasmic reticulum protein and endoplasmic reticulum membrane. Mol Biol Cell. 8, 1805-14.

Cumsky MG, Ko C, Trueblood CE, Poyton RO. (1985). Two nonidentical forms of subunit V are functional in yeast cytochrome c oxidase. Proc Natl Acad Sci U S A. 82, 2235-9.

Dahlqvist, A., Stahl, U., Lenman, M., Banas, A., Lee, M., Sandager, L., Ronne, H., and Stymne, S. (2000). Phospholipid:diacylglycerol acyltransferase: an enzyme that catalyzes the acyl-CoA-independent formation of triacylglycerol in yeast and plants. Proc Natl Acad Sci U S A. 97, 6487-92.

Daum G, Bohni PC, Schatz G. (1982). Import of proteins into mitochondria. Cytochrome b2 and cytochrome c peroxidase are located in the intermembrane space of yeast mitochondria. J Biol Chem. 257, 13028-33.

D'Amours D and Jackson SP (2002) The Mre11 complex: at the crossroads of dna repair and checkpoint signalling. Nat Rev Mol Cell Biol 3, 317-27

De Francesco R. (1999). Molecular virology of the hepatitis C virus. J Hepatol. 31 Suppl 1, 47-53.

Diaz, E., and Pfeffer, S.R. (1998). TIP47: a cargo selection device for mannose 6-phosphate receptor trafficking. Cell. 93, 433-43.

Donkor J, Sariahmetoglu M, Dewald J, Brindley DN, Reue K. (2007). Three mammalian lipins act as phosphatidate phosphatases with distinct tissue expression patterns. J Biol Chem. 282, 3450-7.

Doolittle, G.M., and Chang, T.Y. (1982). Solubilization, partial purification, and reconstitution in phosphatidylcholine-cholesterol liposomes of acyl-CoA:cholesterol acyltransferase. Biochemistry 21, 674–79

Downes GB, Copeland NG, Jenkins NA, Gautam N. (1998). Structure and mapping of the G protein gamma3 subunit gene and a divergently transcribed novel gene, gng3lg. Genomics. 53, 220-30.

Duronio RJ, Knoll LJ, Gordon JI. (1992). Isolation of a Saccharomyces cerevisiae long chain fatty acyl:CoA synthetase gene (FAA1) and assessment of its role in protein N-myristoylation. J Cell Biol. 117, 515-29.

Dürr, G., Strayle, J., Plemper, R., Elbs, S., Klee, S.K., Catty, P., Wolf, D.H. and Rudolph, H.K. (1998) The medial-Golgi ion pump Pmr1 supplies the yeast secretory pathway with Ca2+ and Mn2+ required for glycosylation, sorting, and endoplasmic reticulum-associated protein degradation. Mol. Biol. Cell.

9, 1149-1162.

Ebihara K, Kusakabe T, Masuzaki H, Kobayashi N, Tanaka T, Chusho H, Miyanaga F, Miyazawa T, Hayashi T, Hosoda K, Ogawa Y, Nakao K. (2004). Gene and phenotype analysis of congenital generalized lipodystrophy in Japanese: a novel homozygous nonsense mutation in seipin gene. J Clin Endocrinol Metab. 89, 2360-4.

Faergeman NJ, Black PN, Zhao XD, Knudsen J, DiRusso CC. (2001). The Acyl-CoA synthetases encoded within FAA1 and FAA4 in Saccharomyces cerevisiae function as components of the fatty acid transport system linking import, activation, and intracellular Utilization. J Biol Chem. 276, 37051-9.

Fang M, Kearns BG, Gedvilaite A, Kagiwada S, Kearns M, Fung MK, Bankaitis VA. (1996). Kes1p shares homology with human oxysterol binding protein and participates in a novel regulatory pathway for yeast Golgi-derived transport vesicle biogenesis. EMBO J. 15, 6447-59.

Farrell GC. (2004). Probing Prometheus: fat fueling the fire? Hepatology. 40, 1252-5.

Fernandez F, Rush JS, Toke DA, Han GS, Quinn JE, Carman GM, Choi JY, Voelker DR, Aebi M, Waechter CJ. (2001). The CWH8 gene encodes a dolichyl pyrophosphate phosphatase with a luminally oriented active site in the endoplasmic reticulum of Saccharomyces cerevisiae. J Biol Chem. 276, 41455-64.

Fernández MA, Albor C, Ingelmo-Torres M, Nixon SJ, Ferguson C, Kurzchalia T, Tebar F, Enrich C, Parton RG, Pol A. (2006). Caveolin-1 is essential for liver regeneration.Science. 313, 1628-32.

Fujimoto Y, Itabe H, Sakai J, Makita M, Noda J, Mori M, Higashi Y, Kojima S, Takano T. (2004). Identification of major proteins in the lipid droplet-enriched fraction isolated from the human hepatocyte cell line HuH7. Biochim Biophys Acta. 1644, 47-59.

Fujimoto T, Kogo H, Ishiguro K, Tauchi K, Nomura R. (2001). Caveolin-2 is targeted to lipid droplets, a new "membrane domain" in the cell. J Cell Biol. 152, 1079-85.

Fujimoto T, Ohsaki Y. (2006). Cytoplasmic lipid droplets: rediscovery of an old structure as a unique platform. Ann N Y Acad Sci. 1086, 104-15.

Gachotte D, Sen SE, Eckstein J, Barbuch R, Krieger M, Ray BD, Bard M. (1999). Characterization of the Saccharomyces cerevisiae ERG27 gene encoding the 3-keto reductase involved in C-4 sterol demethylation. Proc Natl Acad Sci U S A. 96, 12655-60.

Gadal O, Labarre S, Boschiero C, Thuriaux P. (2002). Hmo1, an HMG-box protein, belongs to the yeast ribosomal DNA transcription system. EMBO J. 21, 5498-507.

Gale SE, Frolov A, Han X, Bickel PE, Cao L, Bowcock A, Schaffer JE, Ory DS. (2006). A regulatory role for 1-acylglycerol-3-phosphate-O-acyltransferase 2 in adipocyte differentiation. J Biol Chem. 281,

11082-9.

Gao J, Serrero G. (1999). Adipose differentiation related protein (ADRP) expressed in transfected COS-7 cells selectively stimulates long chain fatty acid uptake. J Biol Chem. 274, 16825-30.

Garg A. (2000). Lipodystrophies. Am J Med. 108, 143-52.

Garg A, Wilson R, Barnes R, Arioglu E, Zaidi Z, Gurakan F, Kocak N, O'Rahilly S, Taylor SI, Patel SB, Bowcock AM. (1999). A gene for congenital generalized lipodystrophy maps to human chromosome 9q34. J Clin Endocrinol Metab. 84, 3390-4.

Gietz RD, Woods RA. (2002). Transformation of yeast by lithium acetate/single-stranded carrier DNA/polyethylene glycol method. Methods Enzymol. 350, 87-96.

Gilliquet V, Legrain M, Berben G, Hilger F. (1990). Negative regulatory elements of the Saccharomyces cerevisiae PHO system: interaction between PHO80 and PHO85 proteins. Gene. 96, 181-8.

Glomset, J.A. (1962). The mechanism of the plasma cholesterol esterification reaction: plasma fatty acid transferase. Biochim Biophys Acta. 65, 128-135.

Goffeau A, Barrell BG, Bussey H, Davis RW, Dujon B, Feldmann H, Galibert F, Hoheisel JD, Jacq C, Johnston M, Louis EJ, Mewes HW, Murakami Y, Philippsen P, Tettelin H, Oliver SG. (1996). Life with 6000 genes. Science. 274, 546-567.

Gollub EG, Liu KP, Dayan J, Adlersberg M, Sprinson DB. (1977). Yeast mutants deficient in heme biosynthesis and a heme mutant additionally blocked in cyclization of 2,3-oxidosqualene. J Biol Chem. 252, 2846-54.

Goodman, D.S., Deykin, D., and Shiratori, T. (1964). The formation of cholesterol esters with rat liver enzymes. J Biol Chem. 239,1335–45

Greenspan, P., and Fowler, S.D. (1985). Spectrofluorometric studies of the lipid probe, nile red. J Lipid Res. 26, 781-9.

Greenspan, P., Mayer, E.P., Fowler, S.D. (1985). Nile red: a selective fluorescent stain for intracellular lipid droplets. J Cell Biol. 100, 965-73.

Gronke S, Beller M, Fellert S, Ramakrishnan H, Jackle H, Kuhnlein RP. (2003). Control of fat storage by a Drosophila PAT domain protein. Curr Biol. 13, 603-6.

Guan XL, He X, Ong WY, Yeo WK, Shui G, Wenk MR (2006). Non-targeted profiling of lipids during kainate-induced neuronal injury. FASEB J. 20, 1152-61.

Hall DB, Wade JT, Struhl K. (2006). An HMG protein, Hmo1, associates with promoters of many ribosomal protein genes and throughout the rRNA gene locus in Saccharomyces cerevisiae. Mol Cell Biol. 26, 3672-9.

Hänisch J, Wältermann M, Robenek H, Steinbüchel A. (2006). Eukaryotic lipid body proteins in oleogenous actinomycetes and their targeting to intracellular triacylglycerol inclusions: Impact on models of lipid body biogenesis. Appl Environ Microbiol. 72, 6743-50.

Han GS, Wu WI, Carman GM. (2006). The Saccharomyces cerevisiae Lipin homolog is a Mg2+-dependent phosphatidate phosphatase enzyme. J Biol Chem. 281, 9210-8.

Hanson PK, Grant AM, Nichols JW. (2002). NBD-labeled phosphatidylcholine enters the yeast vacuole via the pre-vacuolar compartment. J Cell Sci. 115, 2725-33.

Hardie DG, Carling D, Carlson M. (1998). The AMP-activated/SNF1 protein kinase subfamily: metabolic sensors of the eukaryotic cell? Annu Rev Biochem. 67, 821-55.

Harris TE, Huffman TA, Chi A, Shabanowitz J, Hunt DF, Kumar A, Lawrence JC Jr. (2007). Insulin controls subcellular localization and multisite phosphorylation of the phosphatidic acid phosphatase, lipin 1. J Biol Chem. 282, 277-86.

Hashimoto, S., and Fogelman, A.M. (1980). Smooth microsomes. a trap for cholesteryl ester formed in hepatic microsomes. J Biol Chem. 255, 8678–84

Heathcote K, Rajab A, Magré J, Syrris P, Besti M, Patton M, Délépine M, Lathrop M, Capeau J, Jeffery S. (2002). Molecular analysis of Berardinelli-Seip congenital lipodystrophy in Oman: evidence for multiple loci. Diabetes. 51, 1291-3.

Henneberry, A. L., Wright, M. M., and McMaster, C. R. (2002). The Major sites of cellular phospholipid synthesis and molecular determinants of fatty acid and lipid head group specificity. Mol Biol Cell. 13, 3148-3161.

Hicke L, Yoshihisa T, Schekman R. (1992). Sec23p and a novel 105-kDa protein function as a multimeric complex to promote vesicle budding and protein transport from the endoplasmic reticulum. Mol Biol Cell. 3, 667-76.

Hickenbottom SJ, Kimmel AR, Londos C, Hurley JH. (2004). Structure of a lipid droplet protein; the PAT family member TIP47.Structure. 12, 1199-207.

Hirokawa T, Boon-Chieng S, Mitaku S. (1998). SOSUI: classification and secondary structure prediction system for membrane proteins. Bioinformatics. 14, 378-9.

Hong W. (2005). SNAREs and traffic. Biochim Biophys Acta. 1744, 493-517.

Hope RG, McLauchlan J. (2000). Sequence motifs required for lipid droplet association and protein stability are unique to the hepatitis C virus core protein.J Gen Virol. 81, 1913-25.

Hope RG, Murphy DJ, McLauchlan J. (2002). The domains required to direct core proteins of hepatitis C virus and GB virus-B to lipid droplets share common features with plant oleosin proteins. J Biol Chem. 277, 4261-70.

Hughes WE, Woscholski R, Cooke FT, Patrick RS, Dove SK, McDonald NQ, Parker PJ. (2000). SAC1 encodes a regulated lipid phosphoinositide phosphatase, defects in which can be suppressed by the homologous Inp52p and Inp53p phosphatases. J Biol Chem. 275, 801-8.

Huh, W.K., Falvo, J.V., Gerke, L.C., Carroll, A.S., Howson, R.W., Weissman, J.S., and O'Shea, E.K. (2003). Global analysis of protein localization in budding yeast. Nature. 425, 686-91.

Ikonen E, Heino S, Lusa S. (2004). Caveolins and membrane cholesterol. Biochem Soc Trans. 232, 121-3.

Imamura M, Inoguchi T, Ikuyama S, Taniguchi S, Kobayashi K, Nakashima N, Nawata H. (2002). ADRP stimulates lipid accumulation and lipid droplet formation in murine fibroblasts. Am J Physiol Endocrinol Metab. 283, E775-83.

Jain S, Stanford N, Bhagwat N, Seiler B, Costanzo M, Boone C, Oelkers P. (2007). Identification of a novel lysophospholipid acyltransferase in Saccharomyces cerevisiae. J Biol Chem. 282, 30562-9.

Jenkins GM, Frohman MA. (2005). Phospholipase D: a lipid centric review. Cell Mol Life Sci. 62, 2305-16.

Jiang B, Sheraton J, Ram AF, Dijkgraaf GJ, Klis FM, Bussey H. (1996). CWH41 encodes a novel endoplasmic reticulum membrane N-glycoprotein involved in beta 1,6-glucan assembly. J Bacteriol. 178, 1162-71.

Jiang H, He J, Pu S, Tang C, Xu G. (2007). Heat shock protein 70 is translocated to lipid droplets in rat adipocytes upon heat stimulation.Biochim Biophys Acta. 1771, 66-74.

Jiang HP, Serrero G. (1992). Isolation and characterization of a full-length cDNA coding for an adipose differentiation-related protein. Proc Natl Acad Sci U S A. 89, 7856-60.

Jiang R, Carlson M. (1996). Glucose regulates protein interactions within the yeast SNF1 protein kinase complex. Genes Dev.10, 3105-15.

Jimeno S, Rondon AG, Luna R, Aguilera A. (2002). The yeast THO complex and mRNA export factors link RNA metabolism with transcription and genome instability. EMBO J. 21, 3526-35.

Jin J, Cao L, Zhao Z, Shen S, Kiess W, Zhi D, Ye R, Cheng R, Chen L, Yang Y, Luo F. (2007). Novel

BSCL2 gene mutation E189X in Chinese congenital generalized lipodystrophy child with early onset diabetes mellitus. Eur J Endocrinol. 157, 783-787.

Kaiser, C., S. Michaelis, and A. Mitchell. 1994. Methods in yeast genetics: a laboratory course manual. Cold Spring Harbor Laboratory Press, Cold Spring Harbor, NY.

Kaiser CA, Schekman R. (1990). Distinct sets of SEC genes govern transport vesicle formation and fusion early in the secretory pathway. Cell. 61, 723-33.

Kamisaka Y, Noda N, Tomita N, Kimura K, Kodaki T, Hosaka K. (2006). Identification of genes affecting lipid content using transposon mutagenesis in Saccharomyces cerevisiae. Biosci Biotechnol Biochem. 70, 646-53.

Kim H, Melen K, von Heijne G. (2003). Topology models for 37 Saccharomyces cerevisiae membrane proteins based on C-terminal reporter fusions and predictions. J Biol Chem. 278, 10208-13.

Klaus S. (1997). Functional differentiation of white and brown adipocytes. Bioessays. 19, 215-23.

Kolling R, Hollenberg CP. (1994). The ABC-transporter Ste6 accumulates in the plasma membrane in a ubiquitinated form in endocytosis mutants. EMBO J. 13, 3261-71.

Krogh A, Larsson B, von Heijne G, Sonnhammer EL. (2001). Predicting transmembrane protein topology with a hidden Markov model: application to complete genomes. J Mol Biol. 305, 567-80.

Kuivenhoven, J.A., Pritchard, H., Hill, J., Frohlich, J., Assmann, G., and Kastelein, J. (1997). The molecular pathology of lecithin:cholesterol acyltransferase (LCAT) deficiency syndromes. J Lipid Res. 38, 191-205.

Kunau WH. (2005). Peroxisome biogenesis: end of the debate. Curr Biol. 15, R774-6.

Kurzchalia TV, Parton RG. (1999). Membrane microdomains and caveolae. Curr Opin Cell Biol. 11, 424-31.

Laemmli UK. (1970). Cleavage of structural proteins during the assembly of the head of bacteriophage T4. Nature. 227, 680-5.

Lange, Y., Strebel, F., and Steck, T.L. (1993). Role of the plasma membrane in cholesterol esterification in rat hepatoma cells. J Biol Chem. 268,13838–43

Lardizabal, K.D., Mai, J.T., Wagner, N.W., Wyrick, A., Voelker, T., and Hawkins, D.J. (2001). DGAT2 is a new diacylglycerol acyltransferase gene family: purification, cloning, and expression in insect cells of two polypeptides from Mortierella ramanniana with diacylglycerol acyltransferase activity. J Biol Chem. 276, 38862-9

Leber R, Zinser E, Zellnig G, Paltauf F, Daum G. (1994). Characterization of lipid particles of the yeast, Saccharomyces cerevisiae. Yeast. 10, 1421-8.

Lee, R.G., Willingham, M.C., Davis, M.A., Skinner, K.A., and Rudel, L.L. (2000). Differential expression of ACAT1 and ACAT2 among cells within liver, intestine, kidney, and adrenal of nonhuman primates. J Lipid Res. 41, 1991-2001.

Lehner R., an6 Kuksis A. (1993). Triacylglycerol synthesis by an sn-1,2(2,3)-diacylglycerol transacylase from rat intestinal microsomes. J Biol Chem. 268, 8781-8786

Lehner, R., and Kuksis, A. (1996). Biosynthesis of triacylglycerols. Prog Lipid Res. 35, 169-201.

Leung DW. (2001). The structure and functions of human lysophosphatidic acid acyltransferases. Front Biosci. 6, D944-53.

Li M, Smith LJ, Clark DC, Wilson R, Murphy DJ. (1992). Secondary structures of a new class of lipid body proteins from oilseeds. J Biol Chem. 267, 8245-53.

Linhart HG, Ishimura-Oka K, DeMayo F, Kibe T, Repka D, Poindexter B, Bick RJ, Darlington GJ. (2001). C/EBPalpha is required for differentiation of white, but not brown, adipose tissue. Proc Natl Acad Sci U S A. 98, 12532-7.

Litvak V, Shaul YD, Shulewitz M, Amarilio R, Carmon S, Lev S. (2002). Targeting of Nir2 to lipid droplets is regulated by a specific threonine residue within its PI-transfer domain.Curr Biol. 12, 1513-8.

Liu P, Ying Y, Zhao Y, Mundy DI, Zhu M, Anderson RG. (2004). Chinese hamster ovary K2 cell lipid droplets appear to be metabolic organelles involved in membrane traffic. J Biol Chem. 279, 3787-92.

Lu J, Kobayashi R, Brill SJ. (1996). Characterization of a high mobility group 1/2 homolog in yeast. J Biol Chem. 271, 33678-85.

Lum PY, Wright R. (1995). Degradation of HMG-CoA reductase-induced membranes in the fission yeast, Schizosaccharomyces pombe. J Cell Biol. 131, 81-94.

Lundin C, Nordstrom R, Wagner K, Windpassinger C, Andersson H, von Heijne G, Nilsson I. (2006). Membrane topology of the human seipin protein. FEBS Lett. 580, 2281-4.

Mager WH, Planta RJ, Ballesta JG, Lee JC, Mizuta K, Suzuki K, Warner JR, Woolford J. (1997) A new nomenclature for the cytoplasmic ribosomal proteins of Saccharomyces cerevisiae. Nucleic Acids Res. 25, 4872-5.

Magnusson B, Asp L, Bostrom P, Ruiz M, Stillemark-Billton P, Linden D, Boren J, Olofsson SO. (2006). Adipocyte differentiation-related protein promotes fatty acid storage in cytosolic triglycerides

and inhibits secretion of very low-density lipoproteins. Arterioscler Thromb Vasc Biol. 26, 1566-71.

Magre J, Delepine M, Khallouf E, Gedde-Dahl T Jr, Van Maldergem L, Sobel E, Papp J, Meier M, Megarbane A, Bachy A, Verloes A, d'Abronzo FH, Seemanova E, Assan R, Baudic N, Bourut C, Czernichow P, Huet F, Grigorescu F, de Kerdanet M, Lacombe D, Labrune P, Lanza M, Loret H, Matsuda F, Navarro J, Nivelon-Chevalier A, Polak M, Robert JJ, Tric P, Tubiana-Rufi N, Vigouroux C, Weissenbach J, Savasta S, Maassen JA, Trygstad O, Bogalho P, Freitas P, Medina JL, Bonnicci F, Joffe BI, Loyson G, Panz VR, Raal FJ, O'Rahilly S, Stephenson T, Kahn CR, Lathrop M, Capeau J; BSCL Working Group. (2001). Identification of the gene altered in Berardinelli-Seip congenital lipodystrophy on chromosome 11q13. Nat Genet. 28, 365-70.

Marchesan D, Rutberg M, Andersson L, Asp L, Larsson T, Boren J, Johansson BR, Olofsson SO. (2003). A phospholipase D-dependent process forms lipid droplets containing caveolin, adipocyte differentiation-related protein, and vimentin in a cell-free system. J Biol Chem. 278, 27293-300.

Martin S, Driessen K, Nixon SJ, Zerial M, Parton RG. (2005). Regulated localization of Rab18 to lipid droplets: effects of lipolytic stimulation and inhibition of lipid droplet catabolism. J Biol Chem. 280, 42325-35.

Martinez-Botas J, Anderson JB, Tessier D, Lapillonne A, Chang BH, Quast MJ, Gorenstein D, Chen KH, Chan L. (2000). Absence of perilipin results in leanness and reverses obesity in Lepr(db/db) mice. Nat Genet. 26, 474-9.

McAlister L, Holland MJ. (1982). Targeted deletion of a yeast enolase structural gene. Identification and isolation of yeast enolase isozymes. J Biol Chem. 257, 7181-8.

McAlister L, Holland MJ. (1985). Differential expression of the three yeast glyceraldehyde-3-phosphate dehydrogenase genes. J Biol Chem. 260, 15019-27.

McCammon MT, Hartmann MA, Bottema CD, Parks LW. (1984). Sterol methylation in Saccharomyces cerevisiae. J Bacteriol. 157, 475-83.

McLauchlan J, Lemberg MK, Hope G, Martoglio B. (2002). Intramembrane proteolysis promotes trafficking of hepatitis C virus core protein to lipid droplets. EMBO J. 21, 3980-8.

McLean, J., Fielding, C., Drayna, D., Dieplinger, H., Baer, B., Kohr, W., Henzel, W. and Lawn, R. (1986). Cloning and expression of human lecithin-cholesterol acyltransferase cDNA. Proc Natl Acad Sci USA. 83, 2335-2339.

Mersmann HJ, Goodman JR, Brown LJ (1975). Development of swine adipose tissue: morphology and chemical composition. J Lipid Res. 16, 269-79.

Meiner, V., Tam, C., Gunn, M.D., Dong, L.M., Weisgraber, K.H., Novak, S., Myers, H.M., Erickson, S.K., and Farese, R.V. Jr. (1997) Tissue expression studies of mouse acyl CoA : cholesterol

acyltransferase gene (Acact): findings supporting the existence of multiple cholesterol esterification enzymes in mice. J Lipid Res. 38, 1928-1933.

Milla, P., Athenstaedt, K., Viola, F., Oliaro-Bosso, S., Kohlwein, S.D., Daum, G., and Balliano, G. (2002). Yeast oxidosqualene cyclase (Erg7p) is a major component of lipid particles. J Biol Chem. 277, 2406-12.

Millichip M, Tatham AS, Jackson F, Griffiths G, Shewry PR, Stobart AK. (1996). Purification and characterization of oil-bodies (oleosomes) and oil-body boundary proteins (oleosins) from the developing cotyledons of sunflower (Helianthus annuus L.) Biochem J. 314, 333-7.

Miyanari Y, Atsuzawa K, Usuda N, Watashi K, Hishiki T, Zayas M, Bartenschlager R, Wakita T, Hijikata M, Shimotohno K. (2007). The lipid droplet is an important organelle for hepatitis C virus production. Nat Cell Biol. 9, 1089-97.

Miyoshi H, Souza SC, Zhang HH, Strissel KJ, Christoffolete MA, Kovsan J, Rudich A, Kraemer FB, Bianco AC, Obin MS, Greenberg AS. (2006). Perilipin promotes hormone-sensitive lipase-mediated adipocyte lipolysis via phosphorylation-dependent and -independent mechanisms. J Biol Chem. 281, 15837-44.

Moradpour D, Englert C, Wakita T, Wands JR. (1996). Characterization of cell lines allowing tightly regulated expression of hepatitis C virus core protein. Virology. 222, 51-63.

Murphy DJ. (1993). Structure, function and biogenesis of storage lipid bodies and oleosins in plants. Prog Lipid Res. 32, 247-80.

Murphy, D.J. (2001). The biogenesis and functions of lipid bodies in animals, plants and microorganisms. Prog Lipid Res. 40, 325-438.

Murphy, D.J., and Vance, J. (1999). Mechanisms of lipid-body formation. Trends Biochem Sci. 24, 109-15.

Nakamura N, Akashi T, Taneda T, Kogo H, Kikuchi A, Fujimoto T. (2004). ADRP is dissociated from lipid droplets by ARF1-dependent mechanism. Biochem Biophys Res Commun. 322, 957-65.

Nakamura, N., Banno, Y. Tamiya-Koizumi, K. (2005). Arf1-dependent PLD1 is localized to oleic acid-induced lipid droplets in NIH3T3 cells. Biochem. Biophys. Res. Commun. 335, 117–123.

Nakano A, Muramatsu M. (1989). A novel GTP-binding protein, Sar1p, is involved in transport from the endoplasmic reticulum to the Golgi apparatus. J Cell Biol. 109, 2677-91.

Noiva R, Lennarz WJ. (1992). Protein disulfide isomerase. A multifunctional protein resident in the lumen of the endoplasmic reticulum. J Biol Chem. 267, 3553-6.

Novikoff AB, Novikoff PM, Rosen OM, Rubin CS. (1980). Organelle relationships in cultured 3T3-L1 preadipocytes. J Cell Biol. 87, 180-96.

Oelkers, P., Behari, A., Cromley, D., Billheimer, J.T., and Sturley, S.L. (1998). Characterization of two human genes encoding acyl coenzyme A:cholesterol acyltransferase-related enzymes. J Biol Chem. 273, 26765-71.

Oelkers, P., Tinkelenberg, A., Erdeniz, N., Cromley, D., Billheimer, J.T., and Sturley, S.L. (2000). A lecithin cholesterol acyltransferase-like gene mediates diacylglycerol esterification in yeast. J Biol Chem. 275, 15609-12.

Oelkers, P., Cromley, D., Padamsee, M., Billheimer, J.T., and Sturley, S.L. (2002). The DGA1 gene determines a second triglyceride synthetic pathway in yeast. J Biol Chem. 277, 8877-81.

Ogden CL, Carroll MD, Curtin LR, McDowell MA, Tabak CJ, Flegal KM (2006). Prevalence of overweight and obesity in the United States, 1999-2004. JAMA. 295, 1549-55.

Ohsaki Y, Cheng J, Fujita A, Tokumoto T, Fujimoto T. (2006) Cytoplasmic lipid droplets are sites of convergence of proteasomal and autophagic degradation of apolipoprotein B.Mol Biol Cell. 17, 2674-83.

Ostermeyer AG, Paci JM, Zeng Y, Lublin DM, Munro S, Brown DA. (2001). Accumulation of caveolin in the endoplasmic reticulum redirects the protein to lipid storage droplets. J Cell Biol. 152, 1071-8.

Ozeki S, Cheng J, Tauchi-Sato K, Hatano N, Taniguchi H, Fujimoto T. (2005). Rab18 localizes to lipid droplets and induces their close apposition to the endoplasmic reticulum-derived membrane. J Cell Sci. 118, 2601-11.

Patel RT, Soulages JL, Hariharasundaram B, Arrese EL. (2005). Activation of the lipid droplet controls the rate of lipolysis of triglycerides in the insect fat body. J Biol Chem. 280, 22624-31.

Patil, C. and Walter P. (2001). Intracellular signaling from the endoplasmic reticulum to the nucleus: the unfolded protein response in yeast and mammals. Curr. Opin. Cell Biol. 13, 349-355.

Pei J, Grishin NV. (2007). PROMALS: towards accurate multiple sequence alignments of distantly related proteins. Bioinformatics. 23, 802-8.

Péterfy M, Phan J, Xu P, Reue K. (2001). Lipodystrophy in the fld mouse results from mutation of a new gene encoding a nuclear protein, lipin. Nat Genet. 27, 121-4.

Phan J, Péterfy M, Reue K. (2004). Lipin expression preceding peroxisome proliferator-activated receptor-gamma is critical for adipogenesis in vivo and in vitro. J Biol Chem. 279, 29558-64.

Phan J, Reue K. (2005). Lipin, a lipodystrophy and obesity gene. Cell Metab. 1, 73-83.

Ploegh HL. (2007). A lipid-based model for the creation of an escape hatch from the endoplasmic reticulum. Nature. 448, 435-8.

Pol A, Luetterforst R, Lindsay M, Heino S, Ikonen E, Parton RG. (2001). A caveolin dominant negative mutant associates with lipid bodies and induces intracellular cholesterol imbalance. J Cell Biol. 152, 1057-70.

Pol A, Martin S, Fernandez MA, Ferguson C, Carozzi A, Luetterforst R, Enrich C, Parton RG. (2004). Dynamic and regulated association of caveolin with lipid bodies: modulation of lipid body motility and function by a dominant negative mutant.Mol Biol Cell. 15, 99-110.

Prattes S, Horl G, Hammer A, Blaschitz A, Graier WF, Sattler W, Zechner R, Steyrer E. (2000). Intracellular distribution and mobilization of unesterified cholesterol in adipocytes: triglyceride droplets are surrounded by cholesterol-rich ER-like surface layer structures. J Cell Sci. 113, 2977-89.

Pringle, J.R., Preston, R.A., Adams, A.E.M., Stearns, T., Drubin, D.G., Haarer, B.K., and Jones, E.W. (1989). Fluorescence microscopy methods for yeast. *Methods Cell Biol.* 31:357–435.

Puri V, Konda S, Ranjit S, Aouadi M, Chawla A, Chouinard M, Chakladar A, Czech MP. (2007). Fat-specific Protein 27, a Novel Lipid Droplet Protein That Enhances Triglyceride Storage. J Biol Chem. 282, 34213-8.

Ramirez-Zacarias JL, Castro-Munozledo F, Kuri-Harcuch W (1992). Quantitation of adipose conversion and triglycerides by staining intracytoplasmic lipids with Oil red O. Histochemistry. 97, 493-7.

Riekhof WR, Wu J, Jones JL, Voelker DR. (2007). Identification and characterization of the major lysophosphatidylethanolamine acyltransferase in Saccharomyces cerevisiae. J Biol Chem. 282, 28344-52.

Reinhart, M.P., Billheimer, J.T., Faust, J.R., and Gaylor, J.L. (1987). Subcellular localization of the enzymes of cholesterol biosynthesis and metabolism in rat liver. J Biol Chem. 262, 9649–55

Robenek H, Hofnagel O, Buers I, Robenek MJ, Troyer D, Severs NJ. (2006). Adipophilin-enriched domains in the ER membrane are sites of lipid droplet biogenesis. J Cell Sci. 119, 4215-24.

Roberts MR, Hodge R, Ross JH, Sorensen A, Murphy DJ, Draper J, Scott R. (1993). Characterization of a new class of oleosins suggests a male gametophyte-specific lipid storage pathway. Plant J. 3, 629-36.

Rose MD, Misra LM, Vogel JP. (1989). KAR2, a karyogamy gene, is the yeast homolog of the mammalian BiP/GRP78 gene. Cell. 57, 1211-21.

Rosen ED, Hsu CH, Wang X, Sakai S, Freeman MW, Gonzalez FJ, Spiegelman BM. (2002). C/EBPalpha induces adipogenesis through PPARgamma: a unified pathway. Genes Dev. 16, 22-6.

Rosen ED, MacDougald OA. (2007). Adipocyte differentiation from the inside out. Nat Rev Mol Cell Biol. 7, 885-96.

Rudolph, H.K., Antebi, A., Fink, G.R., Buckley, C.M., Dorman, T.E., LeVitre, J., Davidow, L.S., Mao, J.I. and Moir, D.T. (1989) The yeast secretory pathway is perturbed by mutations in PMR1, a member of a Ca2+ ATPase family. Cell. 58, 133-145.

Rutkowski DT, Kaufman RJ (2004) A trip to the ER: coping with stress. Trends Cell. Biol. 14, 20-28.

Saerens SM, Verstrepen KJ, Van Laere SD, Voet AR, Van Dijck P, Delvaux FR, Thevelein JM. (2006). The Saccharomyces cerevisiae EHT1 and EEB1 genes encode novel enzymes with medium-chain fatty acid ethyl ester synthesis and hydrolysis capacity. J Biol Chem. 281, 4446-56.

Saito I, Miyamura T, Ohbayashi A, Harada H, Katayama T, Kikuchi S, Watanabe Y, Koi S, Onji M, Ohta Y, et al. (1990).Hepatitis C virus infection is associated with the development of hepatocellular carcinoma. Proc Natl Acad Sci U S A. 87, 6547-9.

Sakashita, N., Miyazaki, A.. Takeya, M., Horiuchi, S., Chang, C.C.Y., Chang, T.-Y., and Takahashi, K. (2000). Localization of human acyl-coenzyme A: cholesterol acyltransferase-1 (ACAT-1) in macrophages and in various tissues. Am J Pathol. 156, 227-236.

Salama NR, Chuang JS, Schekman RW. (1997). Sec31 encodes an essential component of the COPII coat required for transport vesicle budding from the endoplasmic reticulum. Mol Biol Cell. 8, 205-17.

Saltzgaber-Muller J, Schatz G. (1978). Heme is necessary for the accumulation and assembly of cytochrome c oxidase subunits in Saccharomyces cerevisiae. J Biol Chem. 253, 305-10.

Sandager, L., Gustavsson, M.H., Stahl, U., Dahlqvist, A., Wiberg, E., Banas, A., Lenman, M., Ronne, H., and Stymne, S. (2002). Storage lipid synthesis is non-essential in yeast. J Biol Chem. 277, 6478-82.

Sanger F, Nicklen S, Coulson AR. (1977). DNA sequencing with chain-terminating inhibitors. Proc Natl Acad Sci U S A. 74, 5463-7.

Schatz G, Kovac L. (1974). Isolation of promitochondria from anaerobically grown Saccharomyces cerevisiae. Methods Enzymol. 31(Pt A), 627-32.

Schrader M. (2001). Tubulo-reticular clusters of peroxisomes in living COS-7 cells: dynamic behavior and association with lipid droplets. J Histochem Cytochem. 49, 1421-29.

Serrano R, Kielland-Brandt MC, Fink GR. (1986). Yeast plasma membrane ATPase is essential for

growth and has homology with (Na+ + K+), K+- and Ca2+-ATPases. Nature. 319, 689-93.

Serrero G, Frolov A, Schroeder F, Tanaka K, Gelhaar L. (2000). Adipose differentiation related protein: expression, purification of recombinant protein in Escherichia coli and characterization of its fatty acid binding properties. Biochim Biophys Acta. 1488, 245-54.

Servetnick DA, Brasaemle DL, Gruia-Gray J, Kimmel AR, Wolff J, Londos C. (1995). Perilipins are associated with cholesteryl ester droplets in steroidogenic adrenal cortical and Leydig cells. J Biol Chem. 14, 270,16970-3.

Shavinskaya A, Boulant S, Penin F, McLauchlan J, Bartenschlager R. (2007). The lipid droplet binding domain of hepatitis C virus core protein is a major determinant for efficient virus assembly. J Biol Chem. 282, 37158-37169.

Shelness, G.S., and Sellers, J.A. (2001). Very-low-density lipoprotein assembly and secretion. Curr Opin Lipidol. 12, 151-157

Shui G, Bendt AK, Pethe K, Dick T, Wenk MR (2007). Sensitive profiling of chemically diverse bioactive lipids. J Lipid Res. 48, 1976-84.

Simha V, Garg A. (2003). Phenotypic heterogeneity in body fat distribution in patients with congenital generalized lipodystrophy caused by mutations in the AGPAT2 or seipin genes. J Clin Endocrinol Metab. 88, 5433-7.

Smith, C.G. (1974). The ultrastructural development of spherosomes and oil bodies in the developing embyro of *Crambe abyssinica*. Planta. 119, 125-142.

Sorger, D., and Daum, G. (2001) Synthesis of triacylglycerols by the acyl-coenzyme A:diacyl-glycerol acyltransferase Dga1p in lipid particles of the yeast Saccharomyces cerevisiae. J Bacteriol. 84, 519-24.

Sorger D, Daum G. (2003). Triacylglycerol biosynthesis in yeast. Appl Microbiol Biotechnol. 61, 289-99.

 Stobart AK, Stymne S, and Höglund, S. (1986). Safflower microsomes catalyse oil accumulation in vitro: A model system. Planta. 1986, 33-37.

Strahl-Bolsinger S, Immervoll T, Deutzmann R, Tanner W. (1993). PMT1, the gene for a key enzyme of protein O-glycosylation in Saccharomyces cerevisiae. Proc Natl Acad Sci U S A. 90, 8164-8.

Stroobants AK, Hettema EH, van den Berg M, Tabak HF. (1999). Enlargement of the endoplasmic reticulum membrane in Saccharomyces cerevisiae is not necessarily linked to the unfolded protein response via Ire1p. FEBS Lett. 453, 210-4.

Stukey JE, McDonough VM, Martin CE. (1990). The OLE1 gene of Saccharomyces cerevisiae

encodes the delta 9 fatty acid desaturase and can be functionally replaced by the rat stearoyl-CoA desaturase gene. J Biol Chem. 265, 20144-9.

Sztalryd C, Xu G, Dorward H, Tansey JT, Contreras JA, Kimmel AR, Londos C. (2003). Perilipin A is essential for the translocation of hormone-sensitive lipase during lipolytic activation. J Cell Biol. 161, 1093-103.

Szymanski KM, Binns D, Bartz R, Grishin NV, Li WP, Agarwal AK, Garg A, Anderson RG, Goodman JM. (2007). The lipodystrophy protein seipin is found at endoplasmic reticulum lipid droplet junctions and is important for droplet morphology. Proc Natl Acad Sci U S A. 104, 20890-5.

Taggart AK, Zakian VA. (2003). Telomerase: what are the Est proteins doing? Curr Opin Cell Biol. 15, 275-80.

Tamaki H, Shimada A, Ito Y, Ohya M, Takase J, Miyashita M, Miyagawa H, Nozaki H, Nakayama R, Kumagai H. (2007). LPT1 encodes a membrane-bound O-acyltransferase involved in the acylation of lysophospholipids in the yeast Saccharomyces cerevisiae. J Biol Chem. 282, 34288-98.

Tansey JT, Sztalryd C, Gruia-Gray J, Roush DL, Zee JV, Gavrilova O, Reitman ML, Deng CX, Li C, Kimmel AR, Londos C. (2001). Perilipin ablation results in a lean mouse with aberrant adipocyte lipolysis, enhanced leptin production, and resistance to diet-induced obesity. Proc Natl Acad Sci U S A. 98, 6494-9.

Tauchi-Sato K, Ozeki S, Houjou T, Taguchi R, Fujimoto T. (2002). The surface of lipid droplets is a phospholipid monolayer with a unique Fatty Acid composition. J Biol Chem. 277, 44507-12.

Timblin BK, Tatchell K, Bergman LW. (1996). Deletion of the gene encoding the cyclin-dependent protein kinase Pho85 alters glycogen metabolism in Saccharomyces cerevisiae. Genetics. 143, 57-66.

Ting, J.T., Balsamo, R.A., Ratnayake, C., and Huang, A.H. (1996). Oleosin of plant seed oil bodies is correctly targeted to the lipid bodies in transformed yeast. J Biol Chem. 272, 3699-706.

Towbin H, Staehelin T, Gordon J. (1979). Electrophoretic transfer of proteins from polyacrylamide gels to nitrocellulose sheets: procedure and some applications. Proc Natl Acad Sci U S A. 76, 4350-4.

Traber MG, Kayden HJ. (1987). Tocopherol distribution and intracellular localization in human adipose tissue. Am J Clin Nutr. 46, 488-95.

Tusnady GE, Simon I. (1998). Principles governing amino acid composition of integral membrane proteins: application to topology prediction. J Mol Biol. 283, 489-506.

Tusnady GE, Simon I. (2001). The HMMTOP transmembrane topology prediction server. Bioinformatics. 17, 849-50.

Tzen JT, Lai YK, Chan KL, Huang AH. (1990). Oleosin Isoforms of High and Low Molecular Weights Are Present in the Oil Bodies of Diverse Seed Species. Plant Physiol. 94, 1282-1289.

Umlauf E, Csaszar E, Moertelmaier M, Schuetz GJ, Parton RG, Prohaska R. (2004). Association of stomatin with lipid bodies. J Biol Chem. 279, 23699-709.

Unger RH. (2003). Lipid overload and overflow: metabolic trauma and the metabolic syndrome. Trends Endocrinol Metab. 14, 398-403.

van Berkel MA, Rieger M, te Heesen S, Ram AF, van den Ende H, Aebi M, Klis FM. (1999). The Saccharomyces cerevisiae CWH8 gene is required for full levels of dolichol-linked oligosaccharides in the endoplasmic reticulum and for efficient N-glycosylation. Glycobiology. 9, 243-53.

Van Maldergem L, Magré J, Khallouf TE, Gedde-Dahl T Jr, Delépine M, Trygstad O, Seemanova E, Stephenson T, Albott CS, Bonnici F, Panz VR, Medina JL, Bogalho P, Huet F, Savasta S, Verloes A, Robert JJ, Loret H, De Kerdanet M, Tubiana-Rufi N, Mégarbané A, Maassen J, Polak M, Lacombe D, Kahn CR, Silveira EL, D'Abronzo FH, Grigorescu F, Lathrop M, Capeau J, O'Rahilly S. (2002). Genotype-phenotype relationships in Berardinelli-Seip congenital lipodystrophy. J Med Genet. 39, 722-33.

van Meer G. (2001). Caveolin, cholesterol, and lipid droplets? J Cell Biol. 152, F29-34.

Vida TA, Emr SD. (1995). A new vital stain for visualizing vacuolar membrane dynamics and endocytosis in yeast. J Cell Biol. 128, 779-92.

Weller PF, Ackerman SJ, Nicholson-Weller A, Dvorak AM. (1989). Cytoplasmic lipid bodies of human neutrophilic leukocytes. Am J Pathol. 135, 947-59.

Welte MA. (2007). Proteins under new management: lipid droplets deliver. Trends Cell Biol. 17, 363-9.

Welte MA, Cermelli S, Griner J, Viera A, Guo Y, Kim DH, Gindhart JG, Gross SP. (2005). Regulation of lipid-droplet transport by the perilipin homolog LSD2. Curr Biol. 15, 1266-75.

Willison JH, Johnston GC. (1985). Ultrastructure of Saccharomyces cerevisiae strain AG1-7 and its responses to changes in environment. Can J Microbiol. 31, 109-18.

Windpassinger C, Auer-Grumbach M, Irobi J, Patel H, Petek E, Horl G, Malli R, Reed JA, Dierick I, Verpoorten N, Warner TT, Proukakis C, Van den Bergh P, Verellen C, Van Maldergem L, Merlini L, De Jonghe P, Timmerman V, Crosby AH, Wagner K. (2004). Heterozygous missense mutations in BSCL2 are associated with distal hereditary motor neuropathy and Silver syndrome. Nat Genet. 36, 271-6.

Winzeler, E.A., Shoemaker, D.D., Astromoff, A., Liang, H., Anderson, K., Andre, B., Bangham, R.,

Benito, R., Boeke, J.D., Bussey, H., Chu, A.M., Connelly, C., Davis, K., Dietrich, F., Dow, S.W, El Bakkoury, M., Foury, F., Friend, S.H., Gentalen, E., Giaever, G., Hegemann, J.H., Jones, T., Laub, M., Liao, H., Liebundguth, N., Lockhart, D.J., Lucau-Danila, A., Lussier, M., M'Rabet, N., Menard, P., Mittmann, M., Pai, C., Rebischung, C., Revuelta, J.L., Riles, L., Roberts, C.J., Ross-MacDonald, P., Scherens, B., Snyder, M., Sookhai-Mahadeo, S., Storms, R.K., Veronneau, S., Voet, M., Volckaert, G., Ward, T.R., Wysocki, R., Yen, G.S., Yu, K., Zimmermann, K., Philippsen, P., Johnston, M., and Davis RW. (1999). Functional characterization of the S. cerevisiae genome by gene deletion and parallel analysis. Science. 285, 901-6.

Wolins NE, Brasaemle DL, Bickel PE. (2006). A proposed model of fat packaging by exchangeable lipid droplet proteins. FEBS Lett. 580, 5484-91.

Wolins NE, Quaynor BK, Skinner JR, Schoenfish MJ, Tzekov A, Bickel PE. (2005). S3-12, Adipophilin, and TIP47 package lipid in adipocytes. J Biol Chem. 280, 19146-55.

Wolins NE, Rubin B, Brasaemle DL. (2000). TIP47 associates with lipid droplets. J Biol Chem. 276, 5101-8.

Wolins NE, Skinner JR, Schoenfish MJ, Tzekov A, Bensch KG, Bickel PE. (2003). Adipocyte protein S3-12 coats nascent lipid droplets. J Biol Chem. 278, 37713-21.

Yamada M, Blaner WS, Soprano DR, Dixon JL, Kjeldbye HM, Goodman DS. (1987). Biochemical characteristics of isolated rat liver stellate cells. Hepatology. 7, 1224-9.

Yamaguchi T, Matsushita S, Motojima K, Hirose F, Osumi T. (2006). MLDP, a novel PAT family protein localized to lipid droplets and enriched in the heart, is regulated by peroxisome proliferator-activated receptor alpha. J Biol Chem. 281, 14232-40.

Yang, H., Bard, M., Bruner, D.A., Gleeson, A., Deckelbaum, R.J., Aljinovic, G., Pohl, T.M., Rothstein, R., and Sturley, S.L. (1996). Sterol esterification in yeast: a two-gene process. Science. 272, 1353-6.

Yatsu LY, Jacks TJ. (1972). Spherosome Membranes: Half Unit-Membranes. Plant Physiol. 49, 937-943.

Zhang Q, Chieu HK, Low CP, Zhang S, Heng CK, Yang H. (2003). Schizosaccharomyces pombe cells deficient in triacylglycerols synthesis undergo apoptosis upon entry into the stationary phase. J Biol Chem. 278, 47145-55.

Zheng Z, Zou J. (2001). The initial step of the glycerolipid pathway: identification of glycerol 3-phosphate/dihydroxyacetone phosphate dual substrate acyltransferases in Saccharomyces cerevisiae. J Biol Chem. 276, 41710-6.

Zuo Y, Qiang L, Farmer SR. (2006). Activation of CCAAT/enhancer-binding protein (C/EBP) alpha expression by C/EBP beta during adipogenesis requires a peroxisome proliferator-activated

receptor-gamma-associated repression of HDAC1 at the C/ebp alpha gene promoter. J Biol Chem. 281, 7960-7.

Zweytick, D., Athenstaedt, K., and Daum, G. (2000). Intracellular lipid particles of eukaryotic cells. Biochim Biophys Acta. 1469, 101-20.

Zweytick D, Leitner E, Kohlwein SD, Yu C, Rothblatt J, Daum G. (2000). Contribution of Are1p and Are2p to steryl ester synthesis in the yeast Saccharomyces cerevisiae. Eur J Biochem. 267, 1075-82.

Appendix

Abstracts of two published papers

1.

Fei W, Shui G, Gaeta B, Du X, Kuerschner L, Li P, Brown AJ, Wenk MR, Parton RG and Yang H. (2008). Fld1p, a functional homologue of human seipin, regulates the size of lipid droplets in yeast. Journal of Cell Biology. In press.

Lipid droplets (LDs) are emerging cellular organelles that are of crucial importance in cell biology and human diseases. We present here our screen of ~4700 *Saccharomyces cerevisiae* mutants for abnormalities in the number and morphology of LDs; we identify 17 *fld* (for few lipid droplets) and 116 *mld* (for many lipid droplets) mutants. One of the *fld* mutants (*fld1)* is due to deletion of *YLR404W*, a previously uncharacterized open reading frame. Cells lacking *FLD1* contain strikingly enlarged ("supersized") LDs, and LDs from *fld1*Δ cells demonstrate significantly enhanced fusion activities both *in vivo* and *in vitro*. Interestingly, expression of human seipin, mutations in which are associated with Berardinelli-Seip Congenital Lipodystrophy and motoneuron disorders, rescues LD-associated defects in *fld1*Δ cells. Lipid profiling reveals alterations in acyl chain compositions of major phospholipids in *fld1*Δ cells. These results suggest that an evolutionarily conserved function of seipin in phospholipid metabolism and LD formation may be functionally important in human adipogenesis.

2.

 Fei W, Alfaro G, Muthusamy BP, Klaassen Z, Graham TR, Yang H, Beh CT. (2007).

Genome-Wide Analysis of Sterol-Lipid Storage and Trafficking in Saccharomyces

cerevisiae. Eukaryotic Cell doi:10.1128/EC.00386-07.

The pandemic of lipid-related disease necessitates a determination of how cholesterol

and other lipids are transported and stored within cells. The first step in this determination

is the identification of the genes involved in these transport and storage processes. Using

genome-wide screens, we identified 56 yeast genes involved in sterol-lipid biosynthesis,

intracellular trafficking, and/or neutral-lipid storage. Direct biochemical and cytological

examination of mutant cells revealed an unanticipated link between secretory protein

glycosylation and triacylglycerol (TAG)/steryl ester (SE) synthesis for the storage of

lipids. Together with the analysis of other deletion mutants, these results suggested at

least two distinct events for the biogenesis of lipid storage particles: a step affecting

neutral lipid synthesis, generating the lipid core of storage particles, and another step for

particle assembly. In addition to the lipid storage mutants, we identified mutants that

affect the localization of unesterified sterols, which are normally concentrated in the

plasma membrane. These findings implicated phospholipase C and the protein

phosphatase Ptc1p in the regulation of sterol distribution within cells. This study

identified novel sterol-related genes that define several distinct processes maintaining

sterol homeostasis.